DISSERTATION ZUR ERLANGUNG DES DOKTORGRADES DER FAKULTÄT FÜR CHEMIE UND PHARMAZIE DER LUDWIG-MAXIMILIANS-UNIVERSITÄT MÜNCHEN

DEVELOPMENT AND CHARACTERIZATION OF ENVIRONMENTALLY BENIGN LIGHT AND SMOKE-PRODUCING PYROTECHNICAL FORMULATIONS

JOHANN GLÜCK

aus

Trostberg, Deutschland

2018

Erklärung

Diese Dissertation wurde im Sinne von § 7 der Promotionsordnung vom 28.November 2011 von Herrn Professor Dr. Thomas M. Klapötke betreut.

Eidesstattliche Versicherung

Diese Dissertation wurde eigenständig und ohne unerlaubte Hilfe erarbeitet.

München, 03.05.2018 ……………………………………………………………

Johann Glück

Dissertation eingereicht am	11.05.2018
1. Gutachter:	Professor Dr. Thomas M. Klapötke
2. Gutachter:	Professor Dr. Konstantin Karaghiosoff
Mündliche Prüfung am	21.06.2018

Acknowledgement

Mein Dank gilt zuallererst meinem Doktorvater Herrn Prof. Dr. Thomas M. Klapötke für die Aufnahme in den Arbeitskreis, die konstante Unterstützung von der Bachelor-/Masterarbeit, meines Auslandsaufenthalts bis hin zu meiner Promotion. Darüber hinaus möchte ich mich für die spannende und interessante Themenstellung, die finanzielle Unterstützung meiner häufigen Konferenzreisen, sowie die erhaltene wissenschaftliche Freiheit bedanken.

Herrn Prof. Dr. Konstantin Karaghiosoff möchte ich für die häufig fachlichen und interessanten Diskussionen in der Kaffeeküche danken. Seine stets gut gelaunte Art und das jederzeit offene Ohr für alle Anliegen werden mir immer in Erinnerung bleiben. Zudem bedanke ich mich recht herzlich für die freundliche Übernahme des Zweitgutachtens meiner Dissertation, gemessene Kristallstrukturen, sowie der NMR Spektren.

Bei Herrn Dr. Jörg Stierstorfer AOR bedanke ich mich für die gute Zusammenarbeit über die letzten 3 Jahre, die Hilfe bei dem Lösen der Kristallstrukturen, dem Korrekturlesen mancher Publikationen, sowie seinen fortwährenden Bestrebungen Gruppenaktivitäten zu organisieren. Sei es sportlicher oder feuchtfröhlicher Natur, im Sommer wie im Winter. Für seine Habilitation wünsche ich Ihm alles Gute und viel Erfolg.

Herrn Dr. Burkhard Krumm AOR möchte ich meinen Dank für die Betreuung der NMR Geräte und seiner akribischen Art als Sicherheitsbeauftragter aussprechen. Besonders in Erinnerung bleiben wird mir seine Leidenschaft und Leidensfähigkeit für Fußball. Nach der Wahl seines Lieblingsvereins zu urteilen, wird sich daran in absehbarer Zeit auch nichts ändern.

Ein besonderer Dank gilt Frau Irene Scheckenbach, der besten Sekretärin, die man sich nur wünschen kann. Sie ist nicht nur ein Ruhepol, sondern auch entscheidend dass der „Laden läuft“.

Stefan Huber möchte ich für seine einzigartige Art als Typ, seine stets gut informierten Geschichten über Klatsch, Tratsch, Fußball und Politik bedanken. Seine Neigung zu alternativen Fakten und dem kategorischen Missachten politischer Korrektheit hat viele gute Sprüche hervorgebracht. Vielen Dank auch für die unzähligen Sensitivitätsmessungen.

Meinen Kooperationspartnern in Übersee, Jesse J. Sabatini und Anthony P. Shaw danke ich recht herzlich für die erfolgreiche Zusammenarbeit während meiner Masterarbeit und Promotion.

Erwähnt seien auch die übrigen Mitglieder meiner Doktorprüfungs-Kommission, Prof. Dr.-Ing. Robert Schmucker, Prof. Dr. Andreas Kornath, Prof. Dr. Wolfgang Beck und Prof. Dr. Ingo-Peter Lorenz.

Dem DAAD, der GDCh und der International Pyrotechnics Society danke ich für die finanzielle Unterstützung meiner internationalen Konferenzreisen.

Der gesamten Gruppe danke ich für die gute Atmosphäre und schönen Zeit mit euch. Langweilig war es eigentlich nie. Besonders in Erinnerung bleiben werden mir die Freitagabende, BBQs, Weissbiertastings, Skiausflüge, der Gewinn des Campus Turniers, sowie die Klassenfahrt nach Pardubice.

Meinen aktuellen und ehemaligen D3.107er, insbesondere Ivan Gospodinov, Marcel Holler, Benedikt Stiasny, Martin Härtel, Anne Friedrichs, Stefanie Heimsch und Greta Bikelyte waren eine große Unterstützung währen dieser Zeit und die ersten, die meine Laune am Morgen abbekommen haben.

Meinen Freunden Ivan Gospodinov, Marc Bölter, Marcel Holler, Anne Friedrichs, Cornelia Unger und Teresa Küblböck (Kücken) möchte ich mich nicht nur für die immer politisch korrekten oder anständigen Diskussionen beim Mittagessen danken, sondern auch für die gemeinsamen Bergtouren, Kochabende, Prag Ausflüge (Let it go!), Biertastings, Stadionbesuche, Bowling Wettkämpfe und vieles mehr. Die von Ivan organisierten, unvergesslichen, oder doch nie stattgefundenen Ausflüge, beispielsweise zum Go-Kart fahren, Abendessen beim All-you-can-eat Mongolen oder Hot-Pot Essen bilden dabei ein Spezialkategorie. Mit euch hat alles mehr Spaß gemacht. Ihr seid einsame Spitze, bleibt so verrückt wie jetzt.

Danke auch für das Korrektur lesen der Arbeit an Marcel, Ivan, Nadja und Teresa.

Die Promotion und was ich heute bin, hätte ich niemals ohne die wichtigsten Personen in meinem Leben erreichen können. Meine Familie, meine Eltern Johann und Marion Glück, meine Geschwister Lisa und Martina, und meine Nadja. Danke für alles und was noch kommt.

Contents

1. Introduction

1.1 History and Classification of Energetic Materials

Every year on the 10th of December, a small number of pioneers are awarded the Nobel Prize in Stockholm (Sweden) for their outstanding life time achievements on their respective area. Since 1901, this annually announced prize is closely linked to the founder Alfred Nobel. For those, who are interested in the area of energetic or explosive materials, his name is a synonym for one of the world's most famous explosive composition, the so-called *dynamite.* But it was by far not the first commercial available material. According to Conkling and Mocella, "*black powder granules are the first commercial energetic material and have remained an article of commerce for over one thousand years. This unique blend of potassium nitrate (saltpeter), charcoal, and sulfur (brimstone) has served as an explosive, a propellant, and a component in pyrotechnic devices such as safety fuse and squibs*."[1] Upon combustion of blackpowder, hot gasses and particles are produced which are able to accelerate e.g. projectiles or are applied for *"smooth"* cutting off of marble and granite in the mining industry.[2] Nowadays, formulations containing either sodium nitrate or missing sulfur might also be assigned to the family of black powder. Even though black powder was already discovered in ancient China around 220 B.C., it was Roger Bacon to became the first person in Europe to study gunpowder.[3] For centuries, it should be the only commercially available explosive. In the 19th century, the number of new explosives in Europe increased with the discovery of nitrocellulose (NC), nitroglycerin (NG) and 2,4,6-trinitrotoluene (TNT) to name only a few.[4]

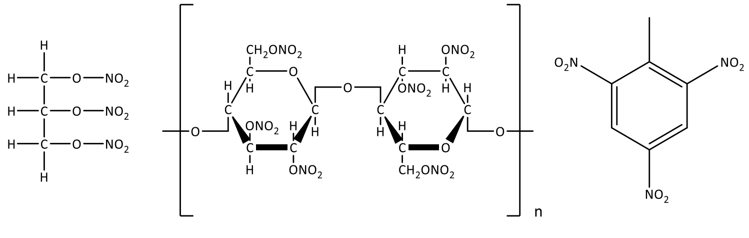

NG NC TNT

Figure 1. Nitroglycerine (NG), nitrocellulose (NC) and trinitrotoluene (TNT).

Finally in 1867, Alfred Nobel patented the NG-based *dynamite* (75% NG, 25% Kieselgur) providing a reliable and safer method for handling NG. The improved safety aspect facilitated the wide application also in mining and tunnelling, which made NG-based *dynamite* the second commercially successful explosive.[5] With the increasing number of existing energetic materials and to some extent fundamentally different behaviour, there was an urgent need for a more precise categorization. A basic differentiation suggested by Klapötke, reveals four different main branches (Figure 2): primary explosives, secondary or high explosives, propellants, and pyrotechnics.[3b]

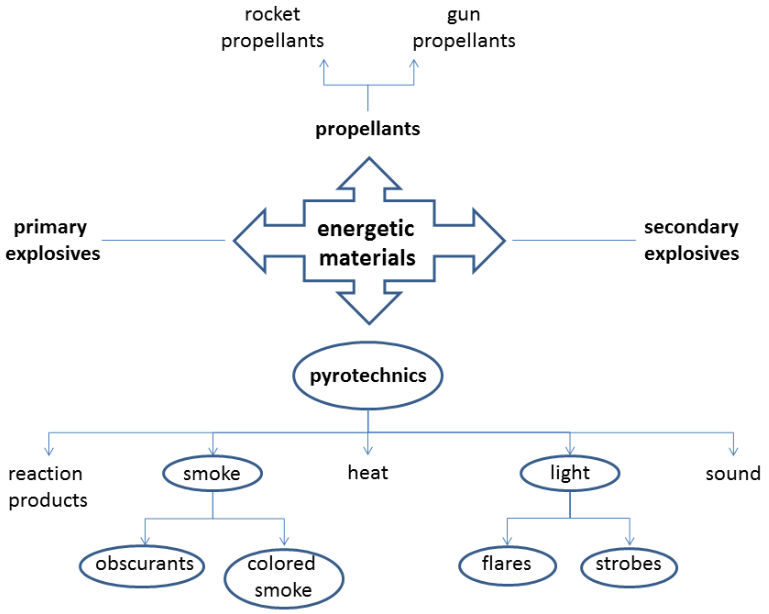

Figure 2. Classification of energetic materials; encircled topics were studied in this thesis.

Primary Explosives: Primary explosives show a fast deflagration-to-detonation-transition (DDT) and can easily be initiated by external stimuli such as heat, friction, impact, electric spark or light radiation.[3b] The resulting shock wave is able to initiate a second, main explosive charge. For this reason, primary explosives are for example applied in detonators. As a rule of thumb, the explosive performance (mainly the heat of explosion Q, detonation pressure p, detonation velocity D) is lower compared to secondary explosives. Typical representatives of this compound class are lead azide $Pb(N_3)_2$ and lead styphnate (LS). Lead-free and therefore assumed environmentally benign alternatives are diazodinitrophenol (DDNP), copper(I) 5-nitrotetrazolate (DBX-1) and the recently reported potassium 1,1'-dinitramino-5,5'-bistetrazolate (K_2DNABT).[3b, 6]

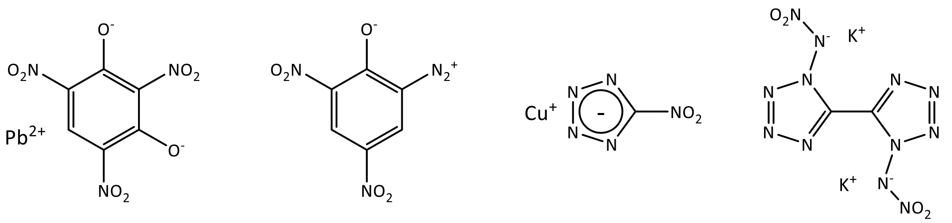

LS **DDNP** **DBX-1** **K_2DNABT**

Figure 3. Selected primary explosives.

Secondary Explosives: In contrast to primary explosives, this compound class is ideally less sensitive towards external stimuli and therefore safer to handle from a practical point of view. At the same time, the explosive performance is usually significantly higher compared to primary explosives. Serving as the main charge in explosive devices, they predominantly rely on the initiation capabilities of primary explosives. Depending on their application purpose, different properties such as a high decomposition temperature or moderate melting temperature are favoured. Traditional representatives of this compound class are TNT, 1,3,5-triamino-2,4,6-trinitrobenzene (TATB), octogen (HMX), hexogen (RDX), and 2,2',4,4',6,6'-hexanitrostilbene (HNS).[7] More recent compounds include bis(hydroxylammonium) 5,5' bis-(tetrazolate-1*N*-oxide) (TKX-50) and 5-nitro-1,2,4-triazol-3-one (NTO).[8]

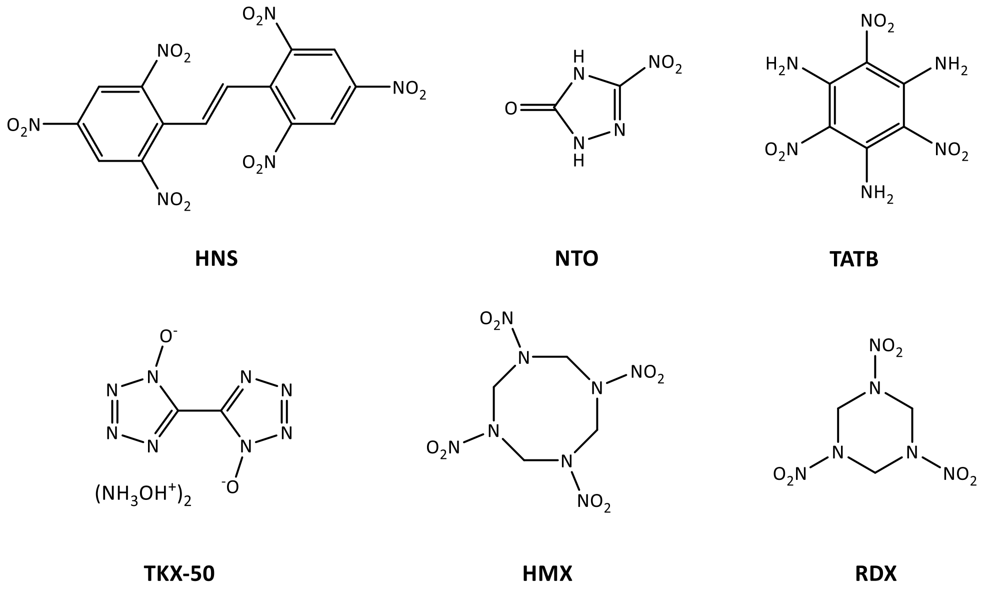

HNS **NTO** **TATB**

TKX-50 **HMX** **RDX**

Figure 4. Selected secondary explosives.

Propellants: Propellants produce large quantities of hot gases to accelerate projectiles, missiles or rockets. In contrast to primary and secondary explosives, the burning behaviour is characterized by a controlled burn-off or deflagration. A detonation is not intended and would result in an immediate destruction of the rocket. Depending on their application purposes, the class of propellants may be classified into gun and rocket propellants. Rocket propellants can be further subclassified into solid and liquid propellants with their adherent subgroups. The specific impulse I_{sp} is one of the key parameters of rocket propellants and describes the effectiveness of the applied propellant system. For example, the applied composite propellant system in the European Ariane 5 rocket consists of ammonium perchlorate (AP), aluminium, hydroxyl terminated polybutadiene (HTPB) and additives achieving an I_{sp} of 262 s.[9] Current research goals are for example the application of nano-Al and the replacement of AP by more environmentally benign alternatives such as ammonium dinitramide (ADN).

Pyrotechnics: The group of pyrotechnics can be divided into different sections regarding their observed effect such as light, sound, smoke, heat and specific product-generating pyrotechnics.[1a, 10] In contrast to secondary explosives such as TNT, the redox pair (oxidizer and reducing agent/nitro groups and carbon backbone) in pyrotechnics is usually not combined in one molecule. Typically a mixture of several solid compounds, in detail a separated oxidizer, reducing agent (= fuel), and various other additives, is applied to give the desired pyrotechnical effect. The redox reaction itself is self-sustaining and in most cases does not rely on an external oxygen supply. Since most of the redox reactions in pyrotechnical systems take place in the solid state, the homogeneity of the mixture is crucial for the performance. According to Conkling and Mocella, a more homogenous composition should enhance the reactivity and might as well enhance its sensitivity.[1a] The nature of a mixture itself provides a high diversity and endless modification options. Pyrotechnical formulations may consist of 2–7 or even more ingredients. There are numerous variables which affect the actual performance such as the particle size, humidity, homogeneity, surface area, thermal conductivity, outside container material for actual devices, loading pressure and degree of confinement.[1a] Since most compositions are designed for a specific purpose, the reproducibility is the most important part and also the biggest issue. Small deviations may result in too short burn times of illuminant signals. As a consequence, these mixtures or devices would not fulfil the requirements of their respective application anymore. An example for a life-threatening deviation involving fatal consequences would be too short delay times in hand grenades. A more detailed view of the pyrotechnical subgroups is given in the following section 1.2.

1.2 Classification of Pyrotechnics

Since it is usually not a single component which creates the observed pyrotechnical effect, but a formulation of different compounds and various other parameters (sample preparation, humidity, and grain sizes to name only a few), the following classification focuses on the resulting phenomena.

1.2.1 Product-Generating Pyrotechnics

Whereas most pyrotechnic compositions produce a vast mixture of different combustion products, there is a smaller number of pyrotechnical exothermic reactions producing pure metals or compounds, alloys, or specific gases, so Ellern.[10] An example of a pyrotechnic composition producing solid materials is the thermite process.

$$2\ Al + Fe_2O_3 \rightarrow Al_2O_3 + 2\ Fe,\ \Delta_R H = -851\ \text{kJ mol}^{-1} \qquad (1)^{[11]}$$

The general procedure, also referred to as an alumino-thermic process, was patented by Goldschmidt and provides access to numerous amounts of metals such as chromium, manganese and cobalt.[12] In detail, the metal oxides are mixed with magnesium or aluminium; after starting the self-sustaining reaction, aluminium oxide and the corresponding metals are produced. Until today, this process is applied for thermite welding and cutting of rails.[13] Gas-producing compositions yielding pure oxygen are referred to as so-called *oxygen candles*. The application area covers the emergency oxygen system in the International Space Station (ISS), submarines as well as airplanes.[14]

$$2\ NaClO_3 \rightarrow 2\ NaCl + 3\ O_2,\ \Delta_R H = -28\ \text{kJ mol}^{-1} \qquad (2)^{[11]}$$

Upon thermal decomposition of sodium chlorate which serves as the oxygen source, sodium chloride and oxygen are produced. Catalytic agents, like iron powder, barium peroxide as well as glass powder and fibers, are added.[10, 15] The big advantage compared to liquefied or compressed gases is the relatively small volume and at the same time higher weight of released gases. Serious disadvantages like the high temperature of the delivered gas, the heating of the canister and the contamination of the gas stream by other combustion products have to be addressed properly to prevent accidental fires.[10] Besides that, the most prominent example for gas generators is the application of NTO in vehicle airbags.[16]

1.2.2 Sound-Producing Pyrotechnics

The two basic audible effects produced by pyrotechnic formulations especially designed for sound generation are a loud noise (firecracker) or a whistling sound (in selected rockets or fountains).[1a] So-called *flash powder* compositions generate a bright light flash followed by a loud explosive noise. Black powder under strong confinement also produces a loud noise but does not display a bright light emission. In general, flash formulations consist of at least one oxidizer (potassium perchlorate, potassium chlorate or barium nitrate), fine metal powder (aluminium, magnesium or magnalium) with a grain size smaller than 53 µm and sometimes, additional fuels (Table 1).

Table 1. Selected flash formulations.

Flash compositions[1a]	wt%				
	$KClO_4$	**Sb_2S_3**	**Mg**	**Al**	**S**
Military simulator	50.0	33.0	17.0	-	-
M-80 firecracker for military training	64.0	3.5	-	22.5	10.0

As a result of the small metal particle size, the sensitivity towards mechanical stimuli increases making those highly energetic compositions very difficult to handle. Some additives such as Sb_2S_3 are also known to promote the detonation inclination in chlorate and perchlorate-containing flash formulations.[17] To prevent bigger accidents around New Year´s Eve, the net weight of *"explosive mass"* in German firecrackers (category 2 fireworks, minimum age 18 years of the buyer) is limited to 6 g of blackpowder per firecracker; flash formulations are forbidden for private consumers.[18]

Table 2. Selected whistle compositions.

Whistle compositions[17]	wt%		
	$KClO_4$	**Potassium benzoate**	**Sodium salicylate**
A	70.0	30.0	-
B	75.0	-	25.0

The whistling sound is produced by firmly pressed binary composition applying potassium perchlorate and potassium benzoate as oxidizer-fuel pair (Table 2).[17, 19] Only a few other formulations showing the same effect are known and the general knowledge is far from understanding the underlying phenomena.[1a] According to Whelan and Elischer, the whistling sound should result from rapid, periodic variations in very fast competing chemical reactions.[19b] However, these conditions are not unique to whistling formulations. As a consequence, research efforts in the past focused on applying a third compound to tailor the acoustic output as well as the burn rate of the known whistling compositions.[20] Despite the non-understanding of the mechanism, this type of formulation has found a wide application in civilian fireworks as well as simulating sounds in military practice (e.g. Ml 19 Whistling Booby Trap Simulator).[1a, 10]

1.2.3 Smoke-Generating Pyrotechnics

A brief introduction to smoke formulations, both obscurants (= white smoke for deception purposes) and coloured smoke, is given in the corresponding papers in chapter 3.

1.2.4 Heat-Producing Pyrotechnics

The exothermic energy released by heat producing pyrotechnics is usually applied to produce colour, smoke or noise. In this chapter, the heat itself will be the topic. A pyrotechnical delay element is favoured if a safety time interval between deployment and start of the reaction is needed like the detonation of hand grenades.[21] The shape of such a device is typically like a column (Figure 5). Ignited on only one side, the reaction front travels to the other end of the column providing a time range of several ms–s cm^{-1} of the column and actually transfers the heat to a propellant or explosive charge.[1a, 10, 22]

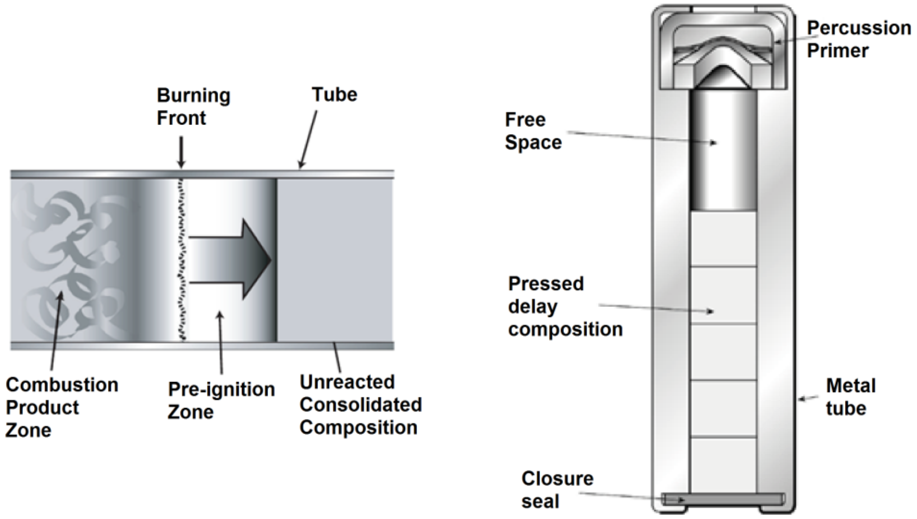

Figure 5. Schematic burning of the ignited delay composition within the tube (left) and delay element scheme (right).[21]

Within the delay systems, a general distinction is made between gassy and gasless delay systems (Table 3).[10] Gassy delay systems such as black powder produce a large volume of gaseous combustion products. Contrary, gasless systems typically of the thermite type generate no significant amount of gas volume.[1a] Due to the high temperature, certain metal oxides might be vaporized even in thermite composition, but recondensate fast and allow the sealing in a closed compartment.[21] This fact has to be considered, since the delay time shows a high-pressure dependency. An increase in pressure leads to an increased burn rate and further, will result in shorter delay times.[21] For this reason, black powder delays require a ventilation system to provide reliable delay times. For other applications, it might be possible to pack the delay column in a pressure canister, which withstands high pressure as well as vacuum at high altitudes.[21]

Table 3. Selected delay compositions.

Delay compositions [21]	wt%						
	Mn	**$BaCrO_4$**	**$PbCrO_4$**	**MnO_2**	**B_4C**	**$NaIO_4$**	**PTFE**
Gassy[23]	-	-	-	-	17.5	72.5	10.0
Gasless[24]	40.0	-	-	60.0	-	-	-
Self-sealing[21]	34.0	30.0	36.0	-	-	-	-

A special type of delay systems is the so-called *"self-sealing"* type which produces a quick solidifying slack. According to Wilson and Hancox, the slack is impermeable to gas flow and isolates the burning front from external factors affecting the burn rate.[21] This specific property makes it suitable for underwater applications. In times of cheap electronic timing systems, the application of pyrotechnical delay systems could be mistaken as out-of-date. In fact, the application until today is justified by the simplicity, a high degree of inherent safety, reliability, and ruggedness.[1b, 25] A power source is not needed, for hand-held devices, a friction-igniter activated by mechanical friction may be applied. Typically, the heat transfer within a pyrotechnical system is not based on just one unique heat transfer, but rather on a cascade of several steps until the intended reaction starts afterward. When it comes to the design of a pyrotechnic system, security issues such as an unintended ignition has to be prevented, but at the same time, the ignition system has to be reliable. For this reasons, usually a physical separation (free space) between the igniter (e.g. percussion primer) or first-fire is applied (Figure 5, right). The igniter is the first source of heat. The heat transfer is achieved by either hot gases or hot glowing sparks bridging the free space and igniting a propellant or other pyrotechnical charges. In the case of delay columns or aerial flare systems, the charge may be additionally coated with a special layer of a pyrotechnical mixture. The ignition surface of charges is treated with these so-called *"primer compositions"* to enhance the probability of a successful ignition, so Kosanke.[21] The heat output occurs in a short time interval, so it does not interfere with the delay times. The released energy output is higher than the required ignition energy of the main charges and therefore, guarantees an uniform ignition. Due to their high sensitivity, the amount of primer material should be smaller in comparison to the main charge. Formulations starting a fire for destructive or non-destructive purposes are referred to as incendiaries or fire-starting respectively.

1.2.5 Light-Generating Pyrotechnics

The group of light-producing pyrotechnics may be categorized into tracers, strobes, flares, photoflashes, near-infrared (NIR) and countermeasure munition in decoy flares. A brief introduction to flare (= constant burning) and strobe (= oscillating burning) formulations is given in the corresponding papers in chapter 4. Flare formulations are for example applied in illumination rounds to light up the battlefield and in tracer munitions, at the back of a projectile (Figure 6). The burning of a light-generating composition provides an optical trace, which allows the shooter to follow the flight path based on the ballistic result.

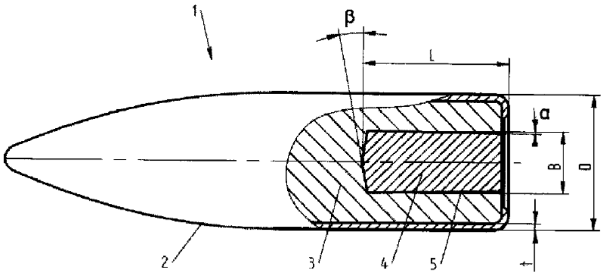

Figure 6. Scheme of tracer ammunition for small- and medium-calibre weapons. (1 = jacketed tracer projectile; 2 = bullet; 3 = metal core; 4 = tracer device;, 5 = cavity for the tracer ammunition which is usually pressed in an additional sleeve).[26]

Unfortunately, tracers can be tracked back to the gunner revealing his position. Recent results by Csernica proposed the application of strobe formulations in tracer ammunition.[27] The oscillating flashlight is detected much faster by the human eye in comparison to a constant burning. As a consequence, the amount of pyrotechnical payload may be reduced. More important, the oscillating behaviour impedes the detection of the shooter, since no direct line can be drawn back to the gun muzzle. For best visual detection in day and night time, a green burning formulation based on boron carbide (B_4C) is applied.[27] Green light is chosen since the human eye´s visual response to light is at its highest in the green region (λ_{max} = 555 nm).[28]

Photoflash formulations are applied for photographic purposes and should produce a very powerful illumination for a short duration.[29] Typically, potassium perchlorate ($KClO_4$) or barium nitrate ($Ba(NO_3)_2$) are used as oxidizers. Fine magnesium, aluminium flakes or fine magnalium (an alloy of magnesium and aluminium) are the fuels of choice. A combination of photoflash and sound formulations is applied in so-called *stun grenades*, such as the *“MK13 Mod 0 BTV-EL Sound & Flash grenade”* sold by *Rheinmetall*.[30] The MK13 grenade generates blinding flashes and deafening noise levels sufficient to daze and disorientate the target. This non-lethal effect allows security and law enforcement agencies the application in urban terrain and hostage rescue operations.

Near-infrared (NIR) illuminants show a characteristic emission in the range of 700–1000 nm and find application in mostly military clandestine night operations.[31] Potassium as well as caesium nitrate are the traditional oxidizers, since both not only show the main emission in the NIR region, but also provide low emission in the visible spectrum (380–780 nm). The standard formulation *"Black Nite"* applied by the U.S. Army usually consists of silicon as metallic fuel.[32] Additives such as hexamine, nitrocellulose and binders may be applied as well.[33] A more recent approach by Fischer *et al*. investigated the use of high-nitrogen compounds and the potassium or caesium salts thereof in NIR formulations showing comparable performance.[31] The non-luminous flame and the clear burning behaviour should contribute to the overall performance.

Decoy flares are a passive countermeasure to lure away heat-seeking missiles.[34] Upon combustion of so-called *MTV* (magnesium, teflon, viton) formulations, magnesium fluoride (l), magnesium (g), soot and radiation are produced to mimic the plume signature of an airplane and mislead the IR-seeker of the rocket (Figure 7).[35]

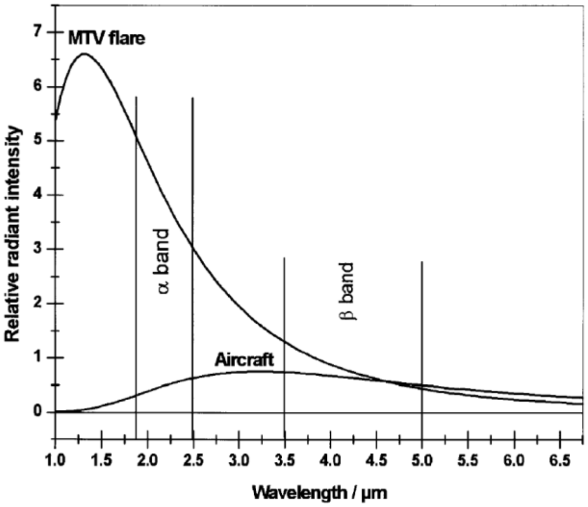

Figure 7. Comparison of relative magnitude of both MTV and target radiant intensity.[34]

While older IR seekers possess a single element photoconductive IR detector (α-band = 2–3 µm or β-band = 3–5 µm), modern IR seekers, such as applied in the German *"IRIS-T Air-to-Air missile"*, evaluate the ratio of intensity $\theta_{\alpha/\beta}$ between the α- and β-band emission (MTV: $\theta_{\alpha/\beta} \approx 1.33$; true targets $0.5 \leq \theta_{\alpha/\beta} \leq 0.8$). Therefore, this seekers can better distinguish between a decoy flare and an airplane signature.[36] A more detailed overview of improved MTV formulations is given by Koch and Brusnahan.[37]

1.3 Motivation and Objectives

Most of nowadays existing pyrotechnical formulations are the results of extensive trial and error procedure in the past. They are applied to serve their purpose, which ironically does not guarantee the complete understanding of the underlying mechanisms such as in the case of strobe or whistling formulations (Table 2).[19a, 38] As a result, some components are historically applied because they are working the appropriate way.

The growing trend towards safer and more environmentally benign energetic materials, while at the same time keeping or even improving the existing performance values, is a very challenging endeavour.[39] More restrictive environmental regulations create the need for *"greener"* replacement of single compounds such as lead azide or even whole formulations (hexachloroethane based obscurants).[40] Usually no adequate, non-toxic alternative is available yet. As a consequence, new pyrotechnic formulations can be characterized by a performance-toxicity trade-off. For example, there is still no suitable chlorine-free oxidizer available to serve as a replacement candidate for potassium chlorate in low temperature smoke formulations. The toxicity issues arising from the application of chlorine-containing compounds will be discussed in the following chapters.
In October 2017, the *Strategic Environmental Research and Development Program* (SERDP) by the *U.S. Department of Defence* (DoD) released a *"Statement of Need"* (SON) program to develop the next generation of pyrotechnics (SON number.: WPSON-19-C4).[41] These novel developed pyrotechnical systems and manufacturing processes should significantly reduce the environmental impact of pyrotechnics. The outlined specific objectives fit this thesis and are listed below:

- Smoke-producing pyrotechnics: Focus on new dyes and fuels; *"tunable"* signal flares which could be used for multi-colour purposes.

- Light-producing pyrotechnics: Multi-colour signals producing minimal smoke; highly efficient combustion; high spectral purity/colour quality; reduced amount of metal colourant; perchlorate-free.
- Minimize production time/cost; reduce multi-step processes/solvent use; reduce solvents and other wastes in flare manufacturing.
- Higher cost pyrotechnics may be evaluated for speciality applications or smaller hand held signals.

Typically, the main ingredient in coloured smoke formulations is the dye with an amount of 40–60 wt%.[42] However, most of the today's in-service smoke formulations by the U.S. Army still contain antraquinone based dyes which are known or at least under suspicion to cause cancer.[42b, 43] To find suitable replacement candidates guaranteeing both a satisfying colour impression and meeting the latest environmental regulations, several green and blue completely antraquinone-free formulations were developed.[44] Surprisingly there is no published information about the yield (produced aerosol compared to the pellet mass) of in-use and literature known coloured smoke formulations.[45] To study this property, an experimental setup was developed and successfully applied to investigate this key characteristic. In addition, efforts were undertaken to further improve the yield of white and coloured smoke formulations by applying 5-amino-1*H*-tetrazole as additive as well as main fuel.[44, 46] The metrics of the yield does not distinguish between the occurring combustion products such as soot, water, dye or burned dye. To obtain more information about the actually dispersed dye, high pressure liquid chromatography (HPLC) measurements were performed to quantify the dye present in the aerosol. In this context, the term *"transfer rate"* was introduced. Up to now, usually every applied coloured smoke signal requires its own optimized specific pyrotechnical system resulting in higher number of stored smoke signals. To reduce costs and at the same time providing a higher degree of safety, so-called *fuel mixes* were developed as a multi-colour approach. These pre-mixed formulations are based on the same pyrotechnical system, which is later combined with the desired dye to produce a variety of colours.

In the case of pyrotechnically disseminated light, the options of emitting species for each desired colour are limited.[17, 47] Strontium salts are traditionally applied for red illuminating formulations in combination with perchlorates or in general chlorine sources to form the metastable emitter Sr(I)Cl.[48] The negative health effects of perchlorates and chlorinated combustion products are literature-known for years.[40a, 49] Recently it was shown, that chlorine-free formulations based on the emitter Sr(I)OH also reveal a good colour performance providing at least a solution to the chlorine-issue.[48] In contrast to this long time tolerated health issues, a new awareness may arise dealing with the application of strontium salts in general. According to the *U.S. Environmental Protection Agency* (EPA), strontium is potentially dangerous to human health affecting the bone growth and stability.[50] To provide solutions for potential future regulations, several lithium-based chlorine-free compositions meeting the optical requirements of the U.S. Army for red light (dominant wavelength = 620±20 nm; spectral purity ≥ 76%) were developed.[51] In this case, the red light is emitted by atomic lithium at 670 nm and 610 nm with decreasing intensity.[51] Furthermore, a pyrotechnical system, which can act either as red flare or red strobe was discovered.[52] The change of the oxidizer lithium nitrate to sodium nitrate provided an analogous yellow strobe system consisting only of environmentally benign ingredients.[53] Here again, the yellow light is produced by the atomic emission of sodium.

Blue light is thought to be the most challenging colour to produce. Up to now, there is no other satisfying blue light emitter known in the literature, which is free of copper and halogen atoms.[54] Good performing blue colourants such as $Cu(CH_3COO)_2 \cdot 3\,Cu(AsO_2)_2$ (Paris green) or $CuHAsO_3$ (Scheele´s green) were completely ruled out for this study due to their high toxicity arising from the arsenic content.[55] In addition, soluble copper salts often show aqueous toxicity, which is accepted due to the lack of existing alternatives.[56] In order to develop the best-performing formulations to this date (dominant wavelength = 465±20 nm; spectral purity ≥ 65%), the focus was on improving the existing copper bromate system by the introduction of high-nitrogen additives.[54b] This method was already applied to other pyrotechnically disseminated colours before.[48, 57] Based on the report of the discovery of indium in 1863 and the reported observation of blue-light emission when burned with hydrochloric acid, the flame chemistry of this element was investigated as a possible emitter for blue light, however, the price and availability prohibit any future application.[58]

1.4 Experimental Procedure

1.4.1 Optical Emission Spectroscopy

The experimental setup to determine the performance of novel light-producing compositions with respect to the colour emission was previously described by Glück *et al.*[54] In detail, the main characteristics include the dominant wavelength (DW), luminous intensity (LI) and spectral purity (SP). A short explanation of the physical and chemical background related to the light emission in the visible spectrum was given by Rusan in 2014.[55] The procedure of frequency measurements carried out during the investigation of strobe formulations is explained in chapter 4.3 and chapter 4.4 in the supporting information section.

1.4.2 Smoke Characterization

Both the newly installed smoke chamber and the newly developed small-scale aerosol collecting setup are explained in detail in chapter 3.1. Transmittance measurements over time were performed to evaluate the smoke persistence as well as the spectroscopic properties. The obtained information was used to calculate the so-called *Figure of merit* (FM_m). The aerosol collecting setup was applied to determine the yield and the transfer rate of tested smoke compositions. The quantification of the smoke dye present in the collected aerosol was performed using high pressure liquid chromatography (HPLC) in cooperation with the *"CBRN Defense, Safety and Environmental Protection School"* of the German *Bundeswehr* (CDSEP-School), Sonthofen/Germany. A Thermo^{TM} Scientific^{TM} DIONEX^{TM} Ultimate^{TM} 3000 HPLC System (accucore RP-MS column (3.0 x 150.0 mm, particle size 2.6 µm) with a DAD-3000 photometer was used to quantify the amount of coloured dyes. The determination of copper content was performed at the internal university ICP-AES instrument.

1.4.3 Sample Preparation and Sensitivity Measurements

To secure the reproducibility of pyrotechnical formulations, a strict sample preparation protocol has to be followed. Therefore, each preparation protocol is provided in the specific chapters. The applied equipment to determine the sensitivity measurements towards mechanical stimuli and electric spark discharge is given in the corresponding experimental sections.

1.5 References

[1] a)J. A. Conkling, C. Mocella, *Chemistry of Pyrotechnics: Basic Principles and Theory*, 2nd ed., Taylor & Francis, **2010**; b)Fuse Blasting Time, http://www.pica.army.mil/pmccs/supportmunitions/demolitionsys/fuseblastingtime.html, March 2018.

[2] G. Girmscheid, *Bauprozesse und Bauverfahren des Tunnelbaus*, 3rd ed., Ernst & Sohn, **2013**.

[3] a)About blackpowder, http://www.rsc.org/Education/Teachers/Resources/Contemporary/student/pop_blackpowder.html, Jan 2018; b)T. M. Klapötke, *Chemistry of High-Energy Materials*, 4th ed., De Gruyter, Berlin, Boston, **2017**.

[4] J. P. Agrawal, in *High Energy Materials: Propellants, Explosives and Pyrotechnics*, Wiley-VCH Verlag GmbH & Co. KGaA, **2010**, pp. 1-67.

[5] a)J. Köhler, R. Meyer, A. Homburg, *Explosivstoffe: Zehnte, vollstandig überarbeitete Auflage*, Wiley-VCH, Weinheim · New York · Chichester · Brisbane · Singapore · Toronto, **2012**; b)150 Jahre Patent auf Dynamit - Erfindung mit Sprengkraft, http://www.deutschlandfunk.de/150-jahre-patent-auf-dynamit-erfindung-mit-sprengkraft.871.de.html?dram:article_id=385561, Sept 2017.

[6] a)D. Fischer, T. M. Klapötke, J. Stierstorfer, *Angew. Chem. Int. Ed.* **2014**, *53*, 8172-8175; b)J. P. Agrawal, R. Hodgson, *Organic Chemistry of Explosives*, John Wiley & Sons, West Sussex, United Kingdom, **2010**; c)J. W. Fronabarger, M. D. Williams, W. B. Sanborn, J. G. Bragg, D. A. Parrish, M. Bichay, *Propellants, Explos., Pyrotech.* **2011**, *36*, 541-550.

[7] a)C. L. Jackson, J. F. Wing, *Amer. Chem. J.* **1888**, *10*; b)B. M. Dobratz, *The Insensitive High Explosive Triaminotrinitrobenzene (TATB): Development and Characterization - 1888 to 1994*, LA-13014-H*,* Los Alamos, NM, **1995**.

[8] a)N. Fischer, D. Fischer, T. M. Klapotke, D. G. Piercey, J. Stierstorfer, *J. Mater. Chem.* **2012**, *22*, 20418-20422; b)A. T. Nielsen, A. P. Chafin, S. L. Christian, D. W. Moore, M. P. Nadler, R. A. Nissan, D. J. Vanderah, R. D. Gilardi, C. F. George, J. L. Flippen-Anderson, *Tetrahedron* **1998**, *54*, 11793-11812.

[9] Boosters (EAP), http://www.esa.int/Our_Activities/Space_Transportation/Launch_vehicles/Boosters_EAP, Sept 2017.

[10] H. Ellern, *Military and Civilian Pyrotechnics*, Chemical Publishing Company, New York, USA, **1968**.

[11] NIST Chemistry WebBook, https://webbook.nist.gov/, March 2018.

[12] H. Goldschmidt, (Ed.: Kaiserliches Patentamt), **1895**, *DE 96317*.

[13] Alu-Thermit Schweißen, https://www.gleisbau-welt.de/lexikon/gleisbau-und-instandhaltung/maschineller-gleisbau/schweisstechnologie/alu-thermit-schweissen/, March 2018.

[14] a)Space Station Crew to Ignite First Oxygen-Generating Candles, https://www.space.com/1099-space-station-crew-ignite-oxygen-generating-candles.html, Sept 2017; b)Sodium Chlorate: Providing Emergency Oxygen, https://chlorine.americanchemistry.com/Science-Center/Chlorine-Compound-of-the-Month-Library/Sodium-Chlorate-Providing-Emergency-Oxygen/, ; c)When your airplane emergency mask deploys, the oxygen you need doesn't come from a tank, https://www.techly.com.au/2015/04/18/when-your-airplane-emergency-mask-deploys-the-oxygen-you-need-doesnt-come-from-a-tank/, Sept 2017; d)Chemical Oxygen Generators, https://www.skybrary.aero/index.php/Chemical_Oxygen_Generators, Sept 2017.

[15] a)T. T. Lewis, **1972**, *US3702305A*; b)D. S. P. L. Chartier, R. Geffroy, **1956**, *US2775511A*.

[16] S. Zeuner, R. Schropp, U. Reimann, K.-H. Rödig, TRW Airbag Systems GmbH, DE, **2004**, *DE102004057770A1*.

[17] T. Shimizu, *Fireworks-The Art Science and Technique*, Pyrotechnica Publications, Austin, Texas (USA), **1996**.

[18] Buy fireworks in Germany!, https://www.bam.de/Content/EN/Press-Releases/2015/2015-12-18-firework.html, Sept 2017.

[19] a)W. R. Maxwell, *Proceedings of the Fourth International Symposium on Combustion*, Williams and Wilkins, **1953**, 906-914; b)D. J. Whelan, P. P. Elischer, *Propellants, Explos., Pyrotech.* **1984**, *9*, 45-47; c)J. Akhavan, *The Chemistry of Explosives*, Royal Society of Chemistry, **2015**.

[20] a)J. A. Domanico, G. V. Tracy, M. N. Gerber, *22nd Int. Pyrotech. Sem., Proc.*, IPSUSA Seminars, Inc., Fort Collins, Colorado, USA, July 15-19, **1996**, 489-496; b)J. Akhavan, C. M. E.,

20th Int. Pyrotech. Sem., Proc., IPSUSA, Inc., Colorad Springs, Colorado, USA, July 25-29, **1994**, 1-10.

[21] B. Kosanke, K. Kosanke, B. Sturman, T. Shimizu, M. A. Wilson, I. von Maltitz, R. J. Hancox, N. N. Kubota, C. Jennings-White, D. Chapman, D. R. Dillehay, T. Smith, M. Podlesak, *Pyrotechnic chemistry, Pyrotechnic Reference Series No. 4*, Journal of Pyrotechnic, Inc., **2014**.

[22] Y. C. Montgomery, W. W. Focke, C. Kelly, *Propellants, Explos., Pyrotech.* **2017**, *42*, 1289-1295.

[23] A. P. Shaw, J. C. Poret, H. A. Grau, R. A. Gilbert, *ACS Sustainable Chem. Eng.* **2015**, *3*, 1558-1563.

[24] E. J. Miklaszewski, A. P. Shaw, J. C. Poret, S. F. Son, L. J. Groven, *ACS Sustainable Chem. Eng.* **2014**, *2*, 1312-1317.

[25] S. M. Tichapondwa, W. W. Focke, O. Del Fabbro, C. Kelly, *Propellants, Explos., Pyrotech.* **2015**, *40*, 518-525.

[26] Å. Andersson, A. Bjärstätt, H. Johansson, L. Norum, **2016**, *WO2016/159855*.

[27] C. M. Csernica, *42nd Int. Pyrotech. Sem., Proc.*, IPSUSA Seminars, Inc., Grand Junction, Colorado, USA, July 10-15, **2016**.

[28] S. J. Robinson, J. T. Schmidt, *Mater. Eval.* **1984**, *42*, 1029-1034.

[29] J. P. Agrawal, in *High Energy Materials: Propellants, Explosives and Pyrotechnics*, Wiley-VCH Verlag GmbH & Co. KGaA, **2010**, pp. 331-412.

[30] MK13 Mod 0 BTV-EL Flash Bang, https://www.rheinmetall-defence.com/en/rheinmetall_defence/company/divisions_and_subsidiaries/american_rheinmetall_munitions/mk13.php, Sept 2017.

[31] N. Fischer, M. Feller, T. M. Klapötke, M. Kowalewski, S. Scheutzow, J. Stierstorfer, *Propellants, Explos., Pyrotech.* **2014**, *39*, 166-172.

[32] E.-C. Koch, D. Clément, *Propellants, Explos., Pyrotech.* **2007**, *32*, 205-212.

[33] P. L. Farnell, R. Broad, S. Nemiroff, **1998**, *WO 1998002712*.

[34] E. C. Koch, *Propellants, Explos., Pyrotech.* **2001**, *26*, 3-11.

[35] E. C. Koch, A. Dochnahl, *Propellants, Explos., Pyrotech.* **2000**, *25*, 37-40.

[36] IRIS-T air-to-air guided missile, http://www.diehl.com/de/diehl-defence/produkte/lenkflugkoerper/iris-t-familie/iris-t.html, Sept 2017.

[37] a)E.-C. Koch, *Propellants, Explos., Pyrotech.* **2009**, *34*, 6-12; b)E.-C. Koch, in *Metal-Fluorocarbon Based Energetic Materials*, 10.1002/9783527644186.ch10, Wiley-VCH Verlag GmbH & Co. KGaA, **2012**, pp. 151-196; c)J. S. Brusnahan, M. Fitzgerald, M. Morgan, R. Pietrobon, *Propellants, Explos., Pyrotech.* **2014**, *39*, 133-137.

[38] J. M. L. Corbel, J. N. J. van Lingen, J. F. Zevenbergen, O. L. J. Gijzeman, A. Meijerink, *Angew. Chem. Int. Ed.* **2013**, *52*, 290-303.

[39] a)K. J. Graham, *Insensitive Munitions – US Problems and Solutions*, NATO, STO-EN-AVT-214, **2013**; b)I. J. Powell, *Propellants, Explos., Pyrotech.* **2016**, *41*, 409-413; c)T. M. Klapötke, T. G. Witkowski, *Propellants, Explos., Pyrotech.* **2016**, *41*, 470-483.

[40] a)Health and Ecological Criteria Division, Office of Science and Technology, Office of Water, U.S. Environmental Protection Agency, *Interim Drinking Water Health Advisory for Perchlorate,*, EPA 822-R-08-025*,* Washington, DC, **2008**; b)K. Sellers, K. Weeks, W. R. Alsop, S. R. Clough, M. Hoyt, B. Pugh, *Perchlorate Environmental Problems and Solutions*, Taylor & Francis, Boca Raton, FL (USA), **2007**; c)European Chemicals Agency (ECHA), *Inclusion of substances of very high concern in the candidate list*, ED/77/2011*,* Helsinki, Finnland, **2011**; d)A. P. Shaw, J. C. Poret, R. A. Gilbert, J. A. Domanico, E. L. Black, *Propellants, Explos., Pyrotech.* **2013**, *38*, 622-628; e)J. J. Cichowicz, *Programmatic Life Cycle Environmental Assessment for Smoke/Obscurants, HC Smoke, Vol. 4*, **1983**; f)J. C. Eaton, R. J. Lopinto, W. G. Palmer, *Health Effects of Hexachloroethane (HC) Smoke*, ADA277838*,* Fort Belvoir, VA, **1994**, 1-60.

[41] Strategic Environmental Research and Development Program (SERDP), *Novel Pyrotechnics that Reduce Environmental Impact*, SON Number: WPSON-19-C4*,* Alexandria, VA, USA, **2017**.

[42] a)J. D. Moretti, J. J. Sabatini, A. P. Shaw, G. R. Chen, A. J. Gilbert, K. D. Oyler, *ACS Sustainable Chem. Eng.* **2013**, *1*, 673-678; b)National Research Council (US) Subcommittee on Military Smokes and Obscurants, *Toxicity of Military Smokes and Obscurants, Vol. 3*, National Academies Press (US), Washington DC, **1999**.

[43] T. C. Marrs, H. F. Colgrave, P. Rice, J. A. G. Edginton, B. Morris, *J. Hazard. Mater.* **1989**, *21*, 73-88.

[44] J. Glück, T. M. Klapötke, M. Rusan, A. P. Shaw, *Propellants, Explos., Pyrotech.* **2017**, *42*, 131-141.

[45] a)J. D. Moretti, J. J. Sabatini, A. P. Shaw, R. Gilbert, *ACS Sustainable Chem. Eng.* **2014**, *2*, 1325-1330; b)S. R. Chakraborty, *16th Int. Pyrotech. Semin., Proc.*, IPSUSA Seminars, Inc., Jonköping, Sweden, June 24-28, **1991**, *16*, 665-674; c)M. L. Springer, T. Rush, H. M. Beardsley, K. Watts, J. Bergmann, *Final Report, Demonstration of the Replacement of the Dyes and Sulfur in the M18 Red and Violet Smoke Grenades*, ESTCP Project WP-0122, **2008**; d)G. Raibeck, G. Chen, *35th Int. Pyrotech. Semin., Proc.*, IPSUSA Seminars Inc., Fort Collins, Colorado, USA, July 13-18, **2008**, 103-112; e)J. A. Domanico, *35th Int. Pyrotech. Sem., Proc.*, IPSUSA Seminars Inc., Fort Collins, Colorado, USA, July 13-18, **2008**, 75-81; f)G. Diviacchi, *35th Int. Pyrotech. Sem., Proc.*, IPSUSA Seminar Inc., Fort Collins, Colorado, USA, July 13-18, **2008**, 491-497; g)N. J. Caldwell, N. E. Hutslar, T. W. Clements, *20th Int. Pyrotech. Sem., Proc.*, IPSUSA Sem. Inc., Colorado Springs, Colorado, USA, July 25-29, **1994**, 139-151.

[46] J. Glück, T. M. Klapötke, A. P. Shaw, *Cent. Eur. J. Energ. Mater.* **2017**, *14*, 489-500.

[47] B. E. Douda, *Theory of Colored Flame Production, ADA951815, ,* RDTN No. 71*,* NSWC Crane, Indiana, USA, **1964**.

[48] J. J. Sabatini, E.-C. Koch, J. C. Poret, J. D. Moretti, S. M. Harbol, *Angew. Chem. Int. Ed.* **2015**, *54*, 10968-10970.

[49] a)K. Sellers, K. Weeks, W. Slsop, S. R. Clough, W. Hoyt, B. Pugh, J. Robb, *Perchlorate Environmental Problems and Solutions*, CRC Press – Taylor & Francis Group, Boca Raton, FL, USA, **2007**; b)J. J. Sabatini, in *Green Energetic Materials* (Ed.: T. Brinck), John Wiley & Sons, Ltd, West Sussex, United Kingdom, **2014**, pp. 63-102; c)G. Steinhauser, T. M. Klapötke, *Angew. Chem., Int. Ed.* **2008**, *47*, 3330-3347.

[50] a)Wisconsin strontium levels among highest in U.S. drinking water supplies, http://wisconsinwatch.org/2016/03/wisconsin-strontium-levels-among-highest-in-u-s-drinking-water-supplies/, Oct 2017; b)A. J. O'Donnell, D. A. Lytle, S. Harmon, K. Vu, H. Chait, D. D. Dionysiou, *Water Res.* **2016**, *103*, 319-333; c)U.S. Environmental Protection Agency (EPA) Makes Preliminary Determination to Regulate Strontium in Drinking Water, https://yosemite.epa.gov/opa/admpress.nsf/6427a6b7538955c585257359003f0230/327f339e63facb5a85257d77005f4bf9!OpenDocument, Oct 2017; d)G. Steinhauser, J. H. Sterba, M. Foster, F. Grass, M. Bichler, *Atmos. Environ.* **2008**, *42*, 8616-8622.

[51] J. Glück, T. M. Klapötke, M. Rusan, J. J. Sabatini, J. Stierstorfer, *Angew. Chem., Int. Ed.* **2017**, *56*, 16507.

[52] J. Glück, T. M. Klapötke, J. J. Sabatini, *Chem. Commun.* **2018**, *54*, 821-824.

[53] J. Glück, T. M. Klapötke, T. Küblböck, *ACS Sustainable Chem. Eng.* **2018**, *6*, 4400-4404.

[54] J. Glück, T. M. Klapötke, M. Rusan, J. Stierstorfer, *Chem. - Eur. J.* **2014**, *20*, 15947-15960.

[55] M. Rusan, Dissertation, LMU München thesis, **2014**.

2. Summary and Conclusion

Chapters 3–4 have been published in peer-reviewed scientific journals if not stated otherwise. The content of these chapters is consistent with the respective publications; however, the layout of the articles has been modified in order to fit this thesis. A brief summary of the results presented in this thesis is given in this chapter.

2.1 Anthraquinone-Free Blue and Green Coloured Pyrotechnical Smoke Formulations

An environmentally friendly and less toxic alternative to the in-use U.S. military M18 green smoke grenade is presented. The developed blue and green coloured smoke formulations do not apply anthraquinone dyes, which are known or at least under suspicion to be toxic and carcinogenic. In this context, copper(II) phthalocyanine (CuPc) served as the blue dye, a 1:1 mixture with the food dye Solvent Yellow 33 (SY33) produced green smoke.

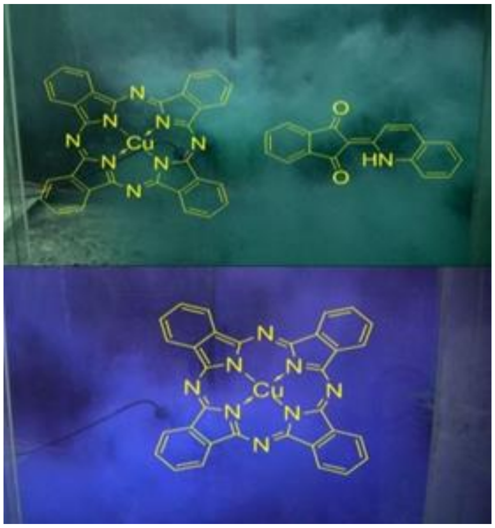

Figure 8. Copper(II) phthalocyanine (bottom) and Solvent Yellow 33 (top right) applied in new green and blue smoke formulations.

In general, coloured smoke formulations are expected to suffer from a low efficiency. Low efficiency refers to the fact, that not all of the dye present in the pyrotechnical formulations is actually dispersed. However, there is no sufficient information provided in the literature. To face this issue, a laboratory-scale aerosol collecting setup was designed and used to study the new formulations. A smoke chamber was installed to measure the transmittance over time. Since a higher efficiency would not only result in an improved smoke cloud, but also reduce the actually needed dye, the effect of adding additional gas generators was studied. 5-Amino-1*H*-tetrazole (5-AT) proved to increase the efficiency of the novel smokes and might serve as a starting point for both high-performance as well as reduced ecological impact formulations.

2.2 Modified U.S. Army Terephthalic Acid White Smoke Composition

Traditionally, military visible obscuration compositions (obscurants, smokes) are applied for screening or signaling purposes. This study presents the exploration of modified terephthalic acid (TA) white smoke formulations such as applied in the U.S. M18 TA white smoke grenade. In 1990, this cool-burning, less toxic, but also low-efficiency white smoke composition replaced the previously used AN-M8 hexachloroethane (HC) smoke grenade due to toxicity reasons. The consequences for soldiers were dramatic, as the effective carry-on weight increased. Three TA grenades are needed to achieve a similar smoke cloud obtained from just one AN-M8 grenade on a dry day.

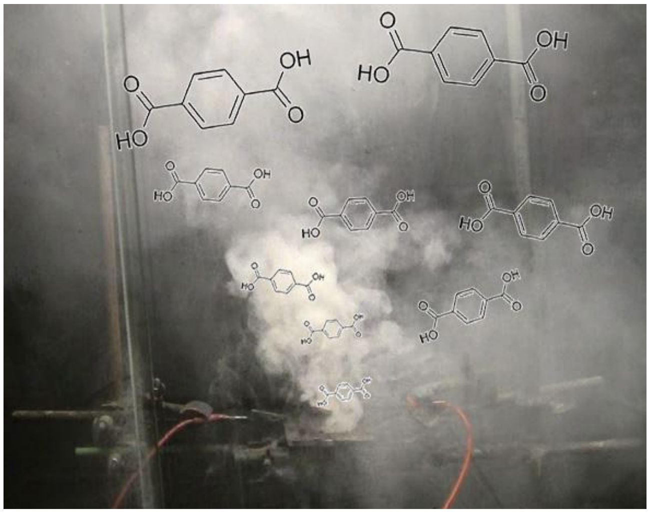

Figure 9. TA-based white smoke applying 5-AT.

Since the sublimation-condensation mechanism is similar to coloured smoke formulations, 5-AT was applied to the TA-based compositions as well. Remarkably, it has been found that sugar is not necessarily required in the formulations, which has implications for the future improvement of sublimation-condensation smoke compositions. It was shown, that formulations containing 5-AT as the main fuel, and no sucrose, displayed the lowest transmittance values over time, and remained stable over the entire measurement period.

2.3 5-Amino-1*H*-Tetrazole-Based Multi-Coloured Smoke Signals Applying the Concept of Fuel Mixes

The next logical step was to apply 5-AT as main fuel to other coloured smoke dyes applied in the U.S. M18 smoke grenades. Finally, three different fuel mixes for each coloured smoke compositions (yellow, green, red and violet) based on 5-AT were obtained. Essentially, fuel mixes are combinations of certain components such as the oxidizer ($KClO_3$), fuel, coolant (carbonates) and other additives. These ingredients are pre-mixed to give the respective fuel mix, which is later combined with the corresponding final ingredients (in this case the dye). This serves two purposes. First, producers and big consumers can reduce the amount of in-stock pyrotechnical signals serving each colour. Upon request, the desired smoke signals can be prepared by combining the fuel mix and dye A, dye B or dye C without the need for storing signal A, signal B or signal C in huge amounts over a longer period of time. Second, the number of materials applied for different coloured smoke signals is dramatically reduced as all formulations rely on the same ingredients. This benefit reduces cost and simplifies the supply chain management.

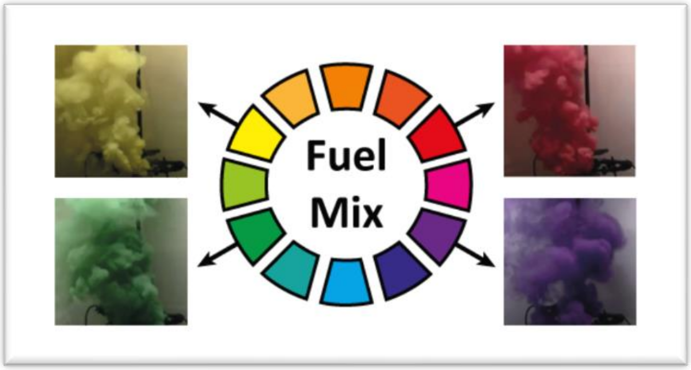

Figure 10. The variety of colours produced by one fuel-mix.

The analysis of the aerosol revealed similar yields compared to sugar-based reference formulations. A closer look at the dye percentage present in the aerosol for yellow and red coloured smoke formulations revealed the superiority of the sugar-based formulations. Sugar-based formulations achieved at least 10% higher transfer rates compared to 5-AT based formulations. The highest detected value was obtained for the red reference formulation **Ref-R** with 86% transfer rate. However, these results provide the necessary information and baseline for future investigations.

2.4 Metal Salts of 3,3'-Diamino-4,4'-Dinitramino-5,5'-Bi-1,2,4-Triazole in Pyrotechnic Compositions

The synthesis and characterization of seven alkaline and earth alkaline salts of 3,3'-diamino-4,4'-dinitramino-5,5'-bi-1,2,4-triazole (H_2ANAT) is presented. The compounds were synthesized by reaction of 1,3-diaminoguanidine hydrochloride with oxalic acid in polyphosphoric acid. After nitration and an additional saltification step, the corresponding sodium, potassium, caesium, rubidium, calcium, strontium and barium salts were prepared.

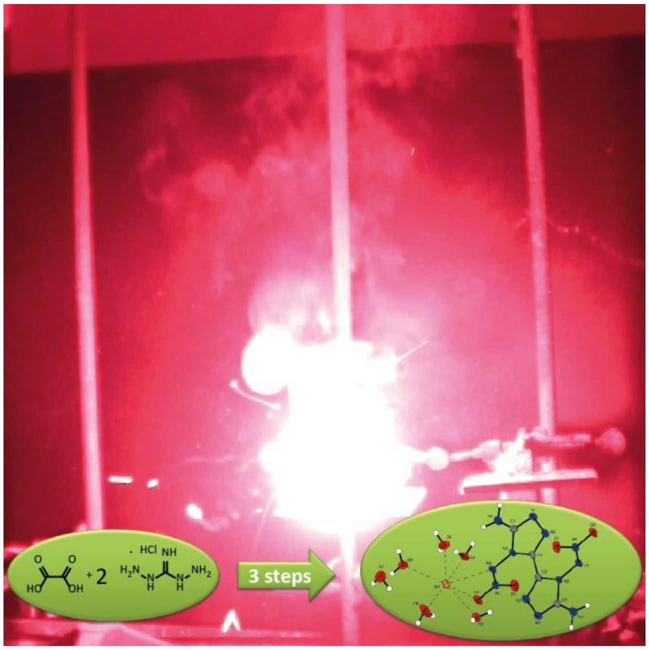

Figure 11. Red pyrotechnical formulation based on SrANAT· $6H_2O$.

The focus of this work was on chlorine and nitrate-free pyrotechnical formulations based on SrANAT · 6H_2O. Optical measurements revealed a dominant wavelength DW = 616 nm and spectral purity SP = 75%, which are in close range to the U.S. military requirement for red light. Besides the presence of crystal water, no hygroscopicity issues were observed. To reduce the potential contamination arising from nitrate based illuminant signals, the presented SrANAT· 6H_2O might serve as a potential alternative.

2.5 A Strontium- and Chlorine-Free Pyrotechnic Illuminant of High Colour Purity

The first strontium- and halogen-free pyrotechnical illuminant meeting the U.S. military requirement for red light (dominant wavelength (DW) = 620 ± 20 nm; spectral purity (SP) ≥ 76%) is described. The best working formulations applying dilithium 3,3'-diamino-4,4'-dinitramino-5,5'-bi-1,2,4-triazolate trihydrate (Li_2ANAT), magnesium, NC, 5-AT and an epoxy binder system achieved a DW = 606 nm and SP = 88%. Li_2ANAT, which serves as both oxidizer and colourant in one molecule, can be obtained in a simple three steps synthesis without the need for an organic solvent. These so-prepared formulations achieved a good colour quality comparable to those of chlorine-free strontium-based compositions. Traditional red-light-emitting pyrotechnical formulations suffer from two disadvantages, they contain strontium salts as well as chlorinated materials. Usually, compounds such as perchlorates or polyvinyl chloride (PVC) are applied to work as oxidizer and chlorine source. Upon combustion, these formulations form the metastable Sr(I)Cl as the red-light-emitting species and, to some extent, highly toxic polychlorinated organic compounds. Recently, chlorine-free compositions based on Sr(I)OH as red-light emitter were reported and therefore, offer a solution to the chlorine issue. Whereas the negative, but reversible health effect of the perchlorate anion interfering with the proper function of the thyroid gland is literature-known for years, the health concerns correlated to strontium were first mentioned by the United States Environmental Protection Agency (U.S. EPA) in 2014.

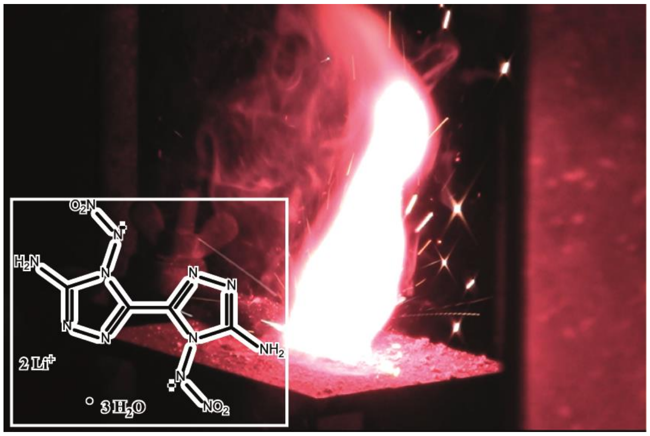

Figure 12. The first halogen-free lithium-based flare formulations meeting the U.S. military requirement (DW/SP).

According to the U.S. EPA, strontium is potentially harmful to human health and replaces calcium in the bones. As a consequence, U.S. EPA started regulating the strontium concentrations in the drinking water. The naturally occurring element strontium has been detected at the level of concerns in 7% of all public water systems in the USA. Military training grounds were not included in this study; however, due to the presence of strontium in red-illuminating signals, these areas may show elevated strontium concentrations as well. Moreover, lithium-based illumination formulations were investigated to meet potential future regulations and prevent live fire-stops at military training grounds.

2.6 Flare or Strobe: A Tunable Chlorine-Free Pyrotechnic System Based on Lithium Nitrate

The herein presented pyrotechnical system is the first of its kind serving either as red-light-emitting flare or strobe formulation. Lithium served as atomic emitter revealing a DW = 598 nm and SP = 75% in the best working flare composition. To obtain constant burning, a mixture of lithium nitrate, Mg, hexamine, NC and an epoxy binder system was applied. The same behaviour is observed if NC is replaced by 5-AT; however, formulations applying NC as additional binder suffered less from hygroscopicity issues. Surprisingly, some formulations applying solely hexamine and Mg as fuel revealed oscillatory burning with periodically alternating dark (no or almost no light output) and flash (bright light) phase reactions. Time dependant high-speed video recordings and frequency analysis proofed a comparable peak separation to literature-known strobe formulations. Next to the colour quality of strobe formulations, the flash separation as well as a constant frequency is important. Changing the Mg/hexamine ratio allowed the regulation of observed frequencies in the range from 3–12 Hz.

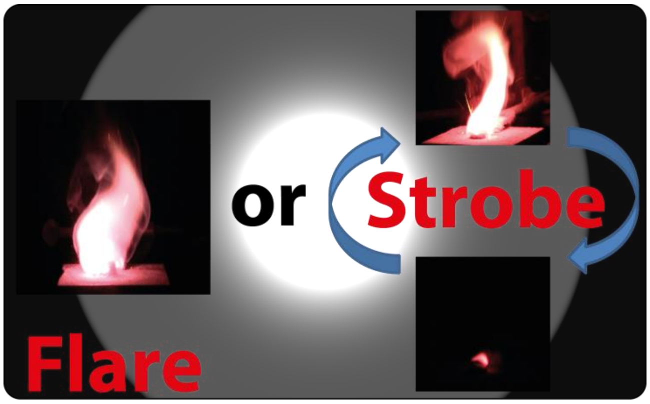

Figure 13. Red-light-emitting flare or strobe based on lithium nitrate.

In contrast to most literature-known strobe compositions, usually applied frequency modifiers such as copper-chrome oxide, hexachlorobenzene and potassium dichromate are not needed. Moreover, all developed formulations are additionally chlorine-free and safe to handle.

2.7 Development of a Sustainable Perchlorate-Free Yellow Pyrotechnical Strobe Formulation

Yellow strobe formulations applying sodium nitrate, hexamine, Mg, nitrocellulose and an epoxy binder system are reported. Analogue to the previous described red strobe formulations based on lithium nitrate, the frequency was controlled by altering the Mg/hexamine ratio to cover the range from $7 \text{ Hz} \leq x \leq 20 \text{ Hz}$. Only environmentally benign materials were applied. The developed formulations fulfil both the requirement of the U.S. EPA and European Regulation Law REACH (Registration, Evaluation, Authorization and Restriction of Chemicals). In addition, no hygroscopicity issues were observed. All tested formulations were insensitive towards friction and only moderate sensitive towards impact.

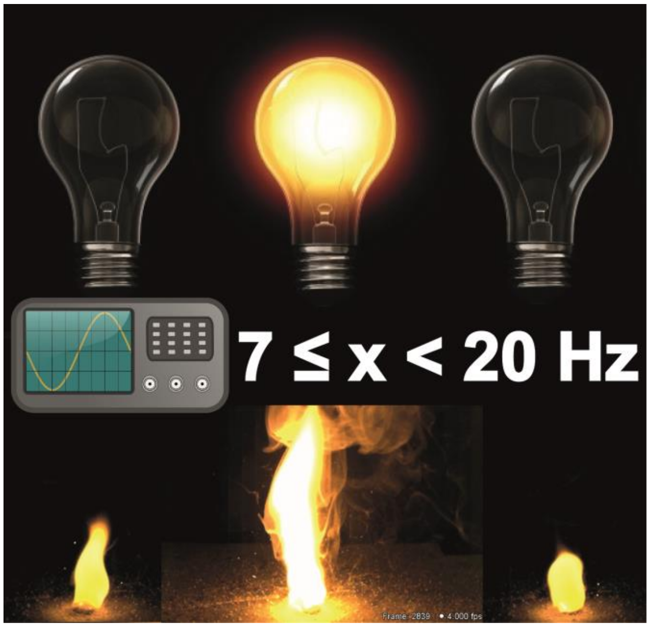

Figure 14. Yellow strobe formulations based on sodium nitrate.

Besides relying on environmentally benign materials, these new compositions have three out of five ingredients in common with a proposed replacement candidate for the U.S. Mk 144 yellow marine smoke and illumination signal. This fact and the resulting synergies may enhance the chance for future application in both the military and civilian sectors.

3. Smoke-Generating Pyrotechnics

3.1 Improved Efficiency by Adding 5-Aminotetrazole to Anthraquinone-Free New Blue and Green Colored Pyrotechnical Smoke Formulations

Published in *Propellants, Explos., Pyrotech.* **2017**, *42*, 131-141. (DOI: 10.1002/prep.201600136)

Abstract: Pyrotechnical smoke formulations are predominantly used in the military sector for obscuring or signalling purposes. For decades, the performance was the only point of interest and no toxicity issues have been considered. Although fuels like sulfur have already been replaced in colored smoke formulations, the main ingredient still remains the dye. In the past few years certain highly toxic anthraquinone dyes, e.g. benzanthrone and vat yellow 4 have successfully been replaced by Solvent Yellow 33 (SY33). Additionally, colored smoke formulations suffer from a low efficiency and there is no published information about the yield like the amount of produced aerosol of in-use formulations. To face this issue, we designed several new blue and green smoke formulations containing 5-aminotetrazole (5-AT) as additional gas generator to increase the efficiency. Maintaining the environmental risks in an acceptable range, we applied copper(II) phthalocyanine (CuPc) for blue and a mixture of CuPc/SY33 for green formulations. A self-developed aerosol collecting setup was used to investigate the formulations.

1 Introduction

Pyrotechnical smoke compositions play an important role in today´s warfare. To keep up with more complex operation scenarios, the military forces have to be provided with suitable materials providing a good performance while dealing with safety and health issues. Regarding the huge diversity of application purposes, the authors will focus on obscurants and signaling munitions.[1] Obscurants, for example, serve for screening, blinding, deception and training purposes.[2] An obscurant device creates an aerosol cloud brought into the line of sight between the observer and the target. This tactical advantage can be used to hide or to change position on the battlefield. Colored smoke compositions however are used for both ground and ground-to-air signaling. These formulations usually consist of an oxidizer/fuel pair which produces the heat to vaporize the dye.

The coolant keeps the temperature in the desired range, additives may be used to modify the mechanical stability or burning properties. The big benefit of smoke signals is the high visibility over greater distances when employed against a terrain background of contrasting color.[3] Smoke is therefore valuable for marking unit flanks, positions of lead elements, locations of targets, drop zones, tactical landing areas, and medical evacuation landing sites. Whereas white obscurants have been studied extensively for decades regarding their total amount of produced aerosol (=yield) and optical performance like smoke thickness and smoke color, there is a lack of such information about colored smoke formulations.[4]

In the case of the U.S. Army M18 yellow smoke grenade, there is no information provided about the yield or the percentage of other combustion products, like soot or water. The efficiency is assumed to be relatively low since the oxidizer/fuel pair constitutes a large proportion of the composition.[5] To face this issue, we designed a cheap and easy laboratory-scale aerosol collecting setup which gives better insight in the performance regarding the yield factor. The collected aerosol was further analyzed to calculate the percentage of dye in the aerosol. To obtain a higher degree of dispersion, we applied 5-aminotetrazole (5-AT) as additional gas generator.

In the past few years, the major focus was to tackle the toxicity problems which comes along with the use of anthraquinone based dyes, like Disperse Red 9, Vat Yellow 4 or Disperse Blue 180.[6] Some representatives of this substance class have been reported as toxic and carcinogenic substances.[6a] A list of current dyes used in the *U.S. Army* are presented in Figure 1 and discussed with regards to health associated risks.[7]

Most of the dyes shown above belong to the anthraquinone group. The toxicity is influenced by the substituents and their position on the tricyclic molecular skeleton. Especially the position of the hydroxyl group on the molecule is important for the toxicity.[8] The majority of the anthraquinone dyes that give active response in the Ames mutagenicity test contain amino, nitro or hydroxyl moieties.[8-9]

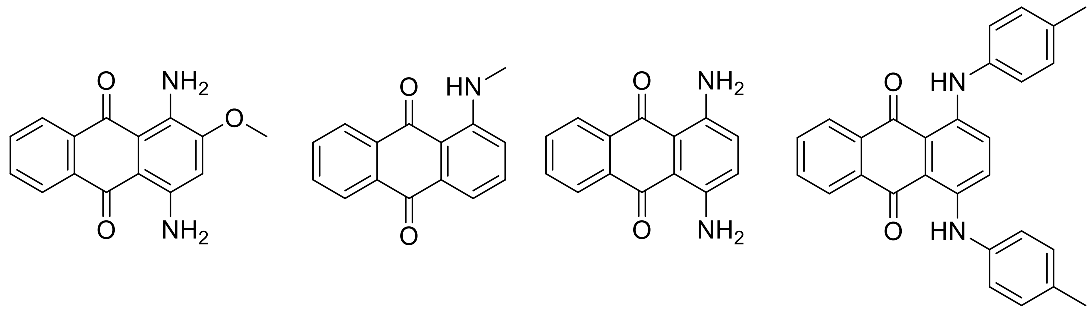

Disperse Red 11 Disperse Red 9 Solvent Violet 47 Solvent Green 3

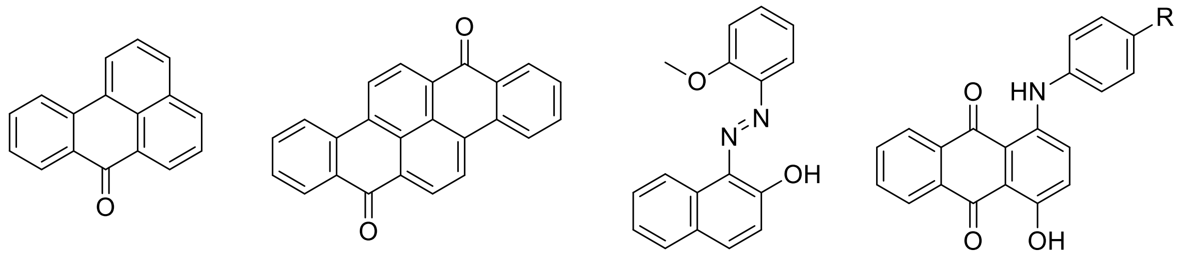

Benzanthrone Vat Yellow 4 Solvent Red 1 Disperse Blue 180: mixture of three dyes;
with R = H, CH_3 + Solvent Green 3

Figure 1. List of current dyes used in *U.S. Army* + Disperse Blue 180 [7a].

Disperse Red 9 has been assigned a toxicity ranking of 1 when inhaled or swallowed. The rating of 1 is defined as a slightly toxic material whose effects are temporarily and disappear upon termination of exposure.[10] When combusted, the dye is subjected to oxidative and pyrolytic reactions, which can result in a variety of reaction byproducts. Rubin *et al.* indicated that during combustion, Disperse Red 9 (1-(methyl-amino)anthraquinone) is mainly converted to 1-aminoanthraquinone and 2-aminoanthraquinone.[11] 2-Aminoanthraquinone has been found to be carcinogenic in a rat and mouse bioassay.[12] In todays in-use formulation, Disperse Red 9 is replaced by a mixture of Solvent Red 1 and Disperse Red 11.[7b] According to the U.S. military subcommittee, the experimental data are insufficient to assess the toxic effects of Solvent Red 1.[7c] Solvent Red 1 is reported to be both genotoxic and carcinogen.[13]

The *U.S. Army´s* M194 yellow smoke hand-held signal consisted of two toxic yellow dyes, benzanthrone and Vat Yellow 4.[6b] Benzanthrone is reported to cause an itching and burning sensation, erythema, dermatitis, and skin pigmentation.[7c] Vat Yellow 4 is classified as a “Group 3” material by the International Agency for Research on Cancer (IARC) because the carcinogenity of this compound remains undetermined, but there is limited evidence for carcinogenity of Vat Yellow in experimental animals.[14] A possible replacement candidate is Solvent Yellow 33.[6b] This dye is widely used in the EU as a food additive (E 104). Studies, including several long-term carcinogenity studies at dose levels up to 2500 mg/kg/day in the rat and 7500 mg/kg/day in the mouse revealed no evidence of carcinogenity, including subcutaneous injections. [10, 15]

The former violet dye mix is a mixture of Solvent Violet 47 (80 wt%) and Disperse Red 9 (20 wt%).[7b] Due to the previously mentioned concerns of Disperse Red 9, the current in-use compositions contain Disperse Red 11 and terephthalic acid to give a violet smoke.[7b]

The M18 green smoke mix is based on a mixture of three dyes: benzanthrone (24 wt%), Vat Yellow 4 (13 wt%) and Solvent Green 3 (62 wt%).[7c] Carcinogenity and mutagenicity tests reported by Brown *et al.* and Epler *et al.* showed contradictory results, so the U.S. military subcommittee officially announced the major concern related to this dye is the poorly solubility in the lungs and accumulation with repeated exposures to high concentrations of the material.[7c, 16]

Marrs *et al.* conducted an animal study on the repeated dose of a smoke containing Disperse Blue 180 back in 1989.[7a] The smoke is similar to the in-use formulation of the SASR (Australian Army) “L” series grenades, except for the absence of kaolin colloidal, zinc stearate and gum acacia powder.[17] The authors of the study reported that among the surviving mice, there was a significantly high frequency of alveolic carcinoma.[7a] The other important result was alveolar and peribronchial infiltration with macrophages containing granules. Disperse Blue 180 was also tested in the Ames salmonella typhimurium test. To show the complexity of this test result, the results for the single strains (certain genetic variant) of the bacteria are listed: the dye was mutagenic for the strain TA 153R+, but non-mutagenic for strains TA1535, TA1537, TA1538, TA98 and TA100.[7a]

Beside the toxicity profile of the formulations ingredients, it is very important to identify potential toxic combustion products and their particle size. If those are smaller than 2 µm, they are capable of penetrating deep into the lung alveoli when inhaled.[8]

To address the need for more environmentally friendly compositions, we developed anthraquinone-free formulations and combined them with the Solvent Yellow 33 system published by Moretti *et al*.[6b] In the Solvent Yellow 33 system potassium chlorate/sucrose is the oxidizer/fuel pair, magnesium carbonate hydroxide pentahydrate (MCHP) is the coolant, SY33 is the dye and stearic acid is used as additive. Copper (II) phthalocyanine (CuPc) showed the best results for blue formulations, a 1:1 mixture of CuPc and Solvent Yellow 33 (SY33) performed best producing green colored smoke (Figure 2). Literature research revealed CuPc as a non-toxic/-mutagenic/-carcinogenic dye used for food packaging.[18] The ß-modification is used as the cyan standard in the 3 color printing ink (C.I.Pigment Blue 15:3) and in colored lacquer. CuPc was also tested in the Ames salmonella typhimurium test for the following strains: TA97, TA98, TA100, TA102, TA1535, TA1538. In contrast to Disperse Blue 180, all variants of the test for CuPc were negative for mutagenicity, both with and without metabolic activation.[18-19] Impurities of CuPc, like the starting materials phthalonitrile and other copper salts may cause a positive Ames bacterial test.[18, 20] Additionally the mammalian cell gene mutation assay with mouse lymphoma cell line L5178Y TK +/- showed now evidence for mutations or chromosome damage caused by CuPc.[19] Further investigations on rat hepatocytes did not report unscheduled DNA synthesis, as well as the standard method of the C3H/1oT1/2 CL8 cell transformation assay gave no evidence for a carcinogenic effect.[21] An animal study on rabbits apparently reported no irritating effect with acute exposure of CuPc to the skin and eyes. There was no evidence of sensitization in this animal study, whereas it is assumed to be slightly irritating to humans.[18, 22] Animal studies showed only low biological activity and no resorption of CuPc in the stomach. The observed oral LD_{50} value in rabbits is 16000 mg/kg and >15000 mg/kg for rats.[19] If released into the environment, CuPc binds to surfaces or sediments to the ground since it is not soluble in water.[23]

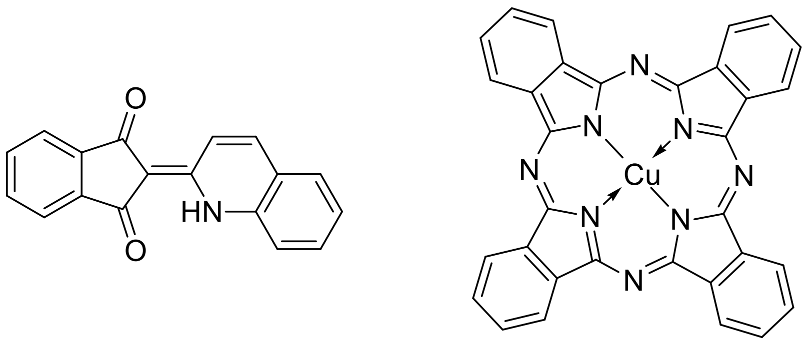

Figure 2. Solvent yellow 33 (left) and Copper (II) phthalocyanine (right).

This paper describes the developed laboratory scale aerosol collecting setup and reports the increased efficiency by adding gas generators to blue and a new green smoke formulation. The percentage of dye in the aerosol was determined by ICP-AES. All formulations were investigated regarding their combustion behavior as well as their energetic and thermal properties. Optical measurements of the transmittance were performed using a smoke chamber.

2 Experimental Section

Materials. Potassium chlorate (≥99%), sucrose (≥99%), sodium hydrogen carbonate, Solvent Yellow 33 (95%) and magnesium carbonate hydroxide pentahydrate were purchased from Sigma-Aldrich. 5-Aminotetrazole (98%) was purchased from abcr chemicals. Stearic acid was purchased from Grüssing GmbH. Copper (II) phthalocyanine (approx. 95%) was purchased from ACROS Organics.

For initial testing, small mixtures (2 g) were carefully mixed manually for 5 min in a mortar by combining the dry compounds. If those tests were successful, bigger mixtures (40 g) were prepared by combining the dry components in a cylindrical rubber barrel and rolling for 120 min. The rotatory rock tumbler (model 67631) was built by “Chicago Electric power tools” and operated with steel balls. To remove any clumps, the compositions were passed through a 800 µm screen. 2 g of this so prepared composition were pressed into a cylindrical steel compartment (diameter 2.0 cm), with the aid of a tooling die and a hydraulic press. The used consolidation dead load of 2000 kg was applied for 3 s, if not stated otherwise. These pellets were used for the aerosol determination and the optical measurements. For each composition, five pellets were tested and the results were averaged. An electrical resistance wire (“Kanthal”, 0.6 mm diameter, 5.25 Ohm/m) was used to ignite the pellets.

Burn rate. Compositions were pressed into cardboard tube for burning rate studies. The cardboard rolls, cylindrical and open on both ends, had a 2.50 cm inner diameter, 4.0 cm height, and a 1.6 mm wall thickness. The compositions (10 g) were pressed with a consolidation dead load of 2000 kg for 10s. The pellets were ignited at the bottom using a bended electrically heated "Kanthal A1" (FeCrAl) wire. Digital video recordings were used to determine burning times. The length of the pellets was divided by the burning times to obtain the linear burning rates.

Optical measurements. Optical measurements were performed in a 80 cm x 80 cm x 180 cm smoke chamber, which was designed by Poret and suggested by Shaw (Figure 3).[24] The pellets were placed on the top of the wire and ignited by a bended electrically heated "Kanthal wire". A broadband light source (halogen lamp 75 W) combined with a spectrometer ("Ocean optics HR2000+ES) with an ILX511B linear silicon CCD-array detector (range 190–1100 nm)") was used as experimental setup to determine transmittance as a function of wavelength in the visible spectrum. The aspheric condenser lens (Edmund Optics, "75 mm Diameter x 50 mm FL") is used for the parallel adjustment of the scattered radiation of the light source. The aligned light passes through the glass windows, the chamber, the ND filter and is detected by the spectrometer. The ND filter is used to reduce the incoming intensity to the spectrometers operating range. But it is also possible to reduce the incoming intensity manually by changing the angle of the optical fiber.

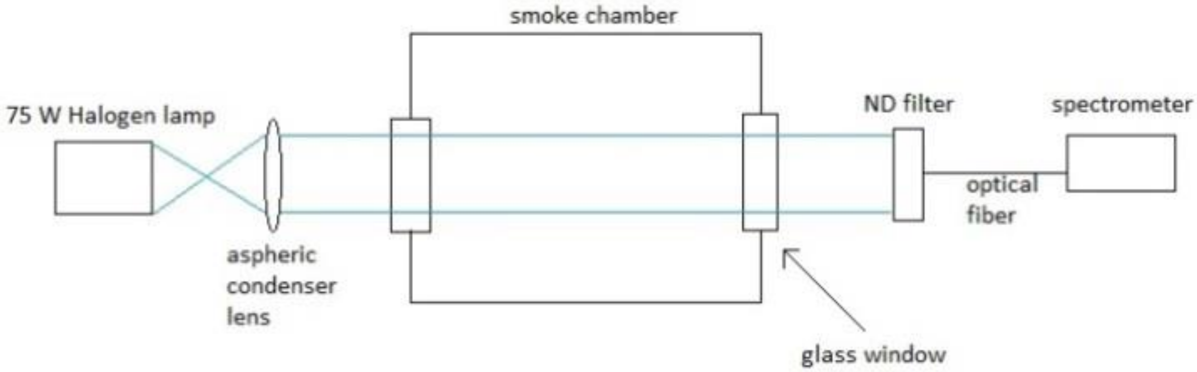

Figure 3. Setup for optical measurement designed by Poret and suggested by Sha*w* [24].

To compare different obscurant formulations of the same pellet size to each other, the mass-based composition figure of merit (FM_m) is used. Shaw described these smoke metrics in the appendix of his 2014 IPSUSA Paper by using an equation based on the Lambert-Beer law, however it is also possible to obtain the FM_m from a very simple chamber.[24]

All that must be known is: pellet mass, chamber volume, path length of the light and the transmittance (Equation 1: mass based figure of merit (FM_m)).

Equation 1*:*

$$FM_m = \boldsymbol{\alpha \cdot Y} = \left(\frac{-V \cdot lnT}{m_a \cdot L}\right) \cdot \left(\frac{m_a}{m_c}\right) = \frac{-V \cdot lnT}{m_c \cdot L}$$

Annotation: α = extinction coefficient, Y = yield factor, m(a) = mass aerosol, m(c) = mass composition, V = volume of the chamber, T = transmittance, L = pathway of the light beam.

At the beginning of each measurement, a spectrum of the empty chamber was recorded. Afterwards the pellet was ignited and the smoke was vented in the chamber until it was equilibrated. The point of equilibration was indicated by a constant, not further decreasing transmittance value. At this point, the fan was turned off and a spectrum in the visible region was recorded at the equilibrium state and every 20 s for the next 6 min. The wavelength at 678 nm was chosen for FM_m calculation as this is the literature known maximum absorption of CuPc in the blue smoke formulations.

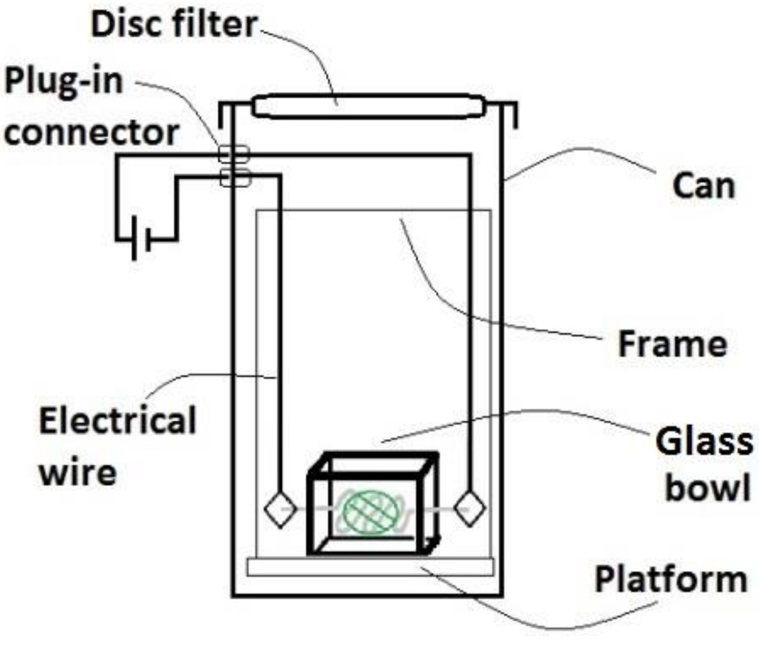

Figure 4. Scheme aerosol collecting setup.

FM_m was calculated by averaging the values at 678 nm over 6 min for the transmittance. In the case of the green smoke formulations, the values at 555 nm, the wavelength of peak photopic response of the human eye, was used for calculation of FM_m.

Aerosol collecting setup. The compartment of the aerosol collecting setup is a tin can (11 cm diameter, 20 cm height) with a plug-in type separable connector (Figure 4). The cap is a tin loop with a centered hole (8 cm diameter) which fixes a LLG-Plain disc filter (diameter 15 cm).

The gap between the overlapping filter paper, the cap and the can is sealed by an adhesive tape. The removable platform inside is attached to a frame for better handling (Figure 5).

Figure 5. Aerosol collecting setup 1.

A carved glass bowl is placed at the platform and contains a lowered bended Kanthal A1 (FeCrAl) wire for ignition (Figure 6). The pellet is placed on top of the wire. Due to the lowered wire, the pellet is fenced by the glass bowl edge and cannot get out of place.

Figure 6. Aerosol collecting setup 2.

The bended wire is connected to the plug-in connectors via electrical wires and to an electrical source outside the tin compartment. The idea was to ignite the smoke pellet inside the can with closed and sealed cap. The gaseous products should leave through the filter disc which at the same time keeps the smoke particles inside, theoretically the whole residue drops through the bended wire to the ground of the glass bowl. With this setup, the total amount of produced aerosol can be easily determined by subtracting of the remaining residue (Equation 2: Calculation of aerosol).

Equation 2:

$$m\,(aerosol) = \Delta m\,\big(can(loaded) - can(combustion)\big)\ - |\Delta m(bowl(combustion) - bowl(empty)|$$

Regarding the fact, that not all collected aerosol is the dispersed dye, further analysis were done. To quantify the percentage of blue dye in the aerosol, ICP-AES was the method of choice.

Sensitivity measurements. The impact and friction sensitivity was determined using a BAM drophammer and a BAM friction tester. The sensitivities of the compounds were indicated according to the UN Recommendations on the Transport of Dangerous Goods (+): impact: insensitive >40 J, less sensitive >35 J, sensitive >4 J, very sensitive 4< J; friction: insensitive >360 N, less sensitive = 360 N, sensitive <360 N>80 N, very sensitive <80 N, extreme sensitive <10 N. Additionally all formulations were tested for sensitivity towards electrical discharge using an Electric Spark Tester ESD 2010 EN.

Thermal stability measurements. Decomposition points were measured with a OZM Research DTA 552-Ex Differential Thermal Analyzer. Measurements were performed at a heating rate of 5 °C/min.

3 Results and Discussion

Obscurants and colored smoke formulations have different quality criteria. For obscurants, a higher FM_m as well as a higher yield, is desired.[2] Since white and grey are the dominating colours of obscurants, other combustion products like soot or water increase the total amount of produced aerosol and at the same time are beneficial to their optical performance (smoke color, smoke thickness) which result in a bigger FM_m value. In order to investigate, if this parameter is also suitable for colored smoke formulations and to compare different colored smoke formulations to each other, the authors calculated the FM_m values for selected blue and green colored smoke formulations. Since the obtained FM_m values did not correlate with the observed optical performance, like smoke color and smoke thickness, the authors decided that the calculation of FM_m based on these results is an improper tool to evaluate the performance of colored smoke formulations. The most important part for colored smoke is to be reliably recognized as the intended colored smoke by the receiver.[3] For this reasons, the sole consideration of the yield as a performance criteria fails, too. Soot or other colored combustion products falsify the intended color. So the authors introduce the term “transfer rate” to describe the ratio of the dye in the aerosol compared to the amount of dye in the pyrotechnical payload. This parameter is considered to be more important than the yield. In this context the term “efficiency” includes both yield and transfer rate.

Blue smoke formulations based on copper(II) phthalocyanine (CuPc)

The known toxicity issues with Disperse Blue 180 lead to the idea of developing a more environmentally friendly composition without anthraquinone based dyes. Shimizu and Ledgard reported similar blue smoke formulations consisting of potassium chlorate (32.1 wt%), milk sugar (26.2 wt%), rice starch (2.9 wt%) and CuPc (38.8 wt%).[25] Chakraborty reported a formulation containing potassium chlorate (20.0 wt%), lactose (18.0 wt%), CuPc (60.0 wt%) and magnesium carbonate (2.0 wt%).[26] Unfortunately this formulation consumed the dye and produced grey soot on a 2 g scale. Even after varying the oxidizer (ammonium nitrate, ammonium dinitramide) no colored smoke was observed. So the dye was applied to Moretti´s Solvent Yellow 33 system with variable amounts of 5-AT to increase the efficiency.[6b] It was very important to keep the burning temperature below 350 °C as this is the dyes point of self-ignition.[27] Fuels like boron or azodicarbonamide provided too high temperatures and are therefore not suitable for these low temperature formulations.

Formulations using the dye CuPc were investigated and the content is shown in Table 1. All formulations **B1** - **B4** produced blue smoke with comparable smoke thickness and volume (Figure 7).

Table 1. Blue compositions **B1–B4**.

	$KClO_3$ [wt%]	Sucrose [wt%]	MCHP [wt%]	Stearic acid [wt%]	5-AT [wt%]	CuPc [wt%]
B1	26.0	14.5	14.0	1.0	7.0	37.5
B2	26.0	16.5	12.0	1.0	7.0	37.5
B3	27.4	14.2	11.8	1.0	8.8	36.8
B4	26.9	12.0	13.5	1.0	10.6	36.0

To prevent the production of a naked flame, as observed in Chakraborty´s blue formulation, the amount of coolant was increased in formulations **B1**–**B4**. The oxidizer content is varying from 26.0–27.4 wt%, sucrose from 12.0–16.5 wt% and 5-AT from 7.0–10.6 wt%.

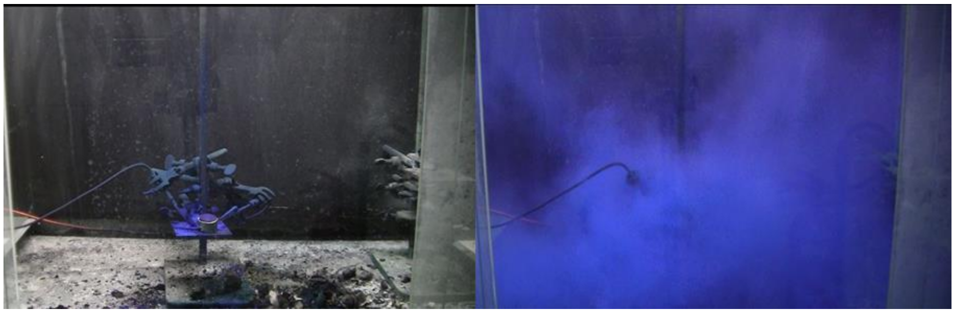

Figure 7. B1 before (left) and after (right) ignition.

The burn times of **B1**–**B4** are in the range of 17–26 s with **B4** showing the fastest burning (Table 2). The burn rates therefore show the same trend. Formulations **B1**–**B4** are insensitive towards friction and only **B3** is moderate sensitive towards impact. Regarding the decomposition temperatures, all formulations showed a melting-decomposition transition between 148 °C to 153 °C. The sensitivities of **B1**–**B4** towards electrostatic discharge increased with increasing amounts of 5-AT from 1.25 J in **B1**/**B2** to 1.1 J for **B3**. Formulation **B4** was most sensitive towards electrostatic discharge with 1.0 J.

Table 2. Properties of **B1**–**B4**.

	Burn time [s]	Burn rate [gs^{-1}]	Impact [J]	Friction [N]	ESD$^{a)}$ [J]	$T_{dec}$$^{b)}$ [°C]
B1	19	0.526	40	>360	1.25	149
B2	26	0.385	40	>360	1.25	148
B3	20	0.500	30	>360	1.1	153
B4	17	0.588	40	>360	1.0	152

Annotation: a) Electrostatic discharge. b) Decomposition temperature.

The total amount of produced aerosol (Y) is shown in Table 3. The values are averaged over at least five pellets, standard deviation (SD) (for calculation see supporting information) and relative humidity (RH) are listed, too. The performance of hygroscopic compounds is heavily influenced by the humidity. An increased humidity results in a higher yield. For comparison reasons, the measurements have to be accompanied by the RH value since even minor hygroscopic combustion products may have an effect.[28]

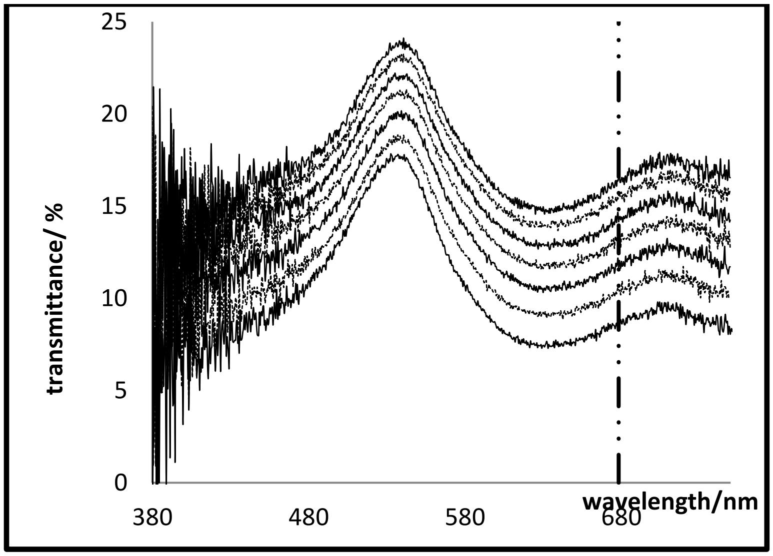

Figure 8. B1 Transmittance [%] **-** wavelength [nm] for 6 min.

Figure 8 shows an extract of the transmittance (in %) as a function of wavelength in the visible spectrum of **B1**. For clearness reasons the number of depicted functions was limited to one function per minute, the function of the empty chamber was cut off, too. The visible part of the spectrum depicted (380–750 nm) shows two peaks at approximately 540 nm and 711 nm. The vertical line at 678 nm marks the literature known maximum absorption of CuPc. Following the expected trend, the transmission values decrease to the lowest values (function at the bottom) at the time of starting the measurement (t = 0 s) and constantly increase with additional time. After 6 min of recording spectra, the experiment was stopped.

Table 3. Quantification of **B1–B4**.

	RH[a)]	**Y**[b)]	**SD(Y)**[c)]
B1	24.4	13.7	1.4
B2	18.3	16.0	2.6
B3	26.0	10.5	5.4
B4	28.2	14.4	2.1

Annotation: a) relative humidity [%]; b)Yield (Mass of aerosol/mass of pellet)[%]; mass of pellet = 1.8 - 2.3g; c) standard deviation of Y.

B1 and **B2** are compared to each other since they only differ in the sucrose/coolant ratio. **B2**, having more sucrose and less MCHP than **B1**, showed a higher yield while measured at lower RH values. The observations are in agreement with the idea of increasing the yield by introducing more gas generators. In **B3** the amount of sucrose was reduced and compensated by a higher 5-AT percentage compared to **B2**. The amount of potassium chlorate was increased and the percentage of used dye was slightly reduced, too. In this case we did not observe an increase of dispersed aerosol, quite contrary we observed a decrease which is higher than the amount of reduced dye. **B4** produced the second highest amount of aerosol in this series having the highest amount of 5-AT and the lowest amount of dye. This may have several reasons. **B4** has less sucrose which not only serves as a gas generator, but also produces solid combustion products like soot. The reduction of sucrose in **B4** therefore diminishes the yield and at the same time cannot be compensated by adding more 5-AT. The main combustion product of 5-AT is nitrogen gas, which is applied to increase the yield by producing more gaseous products and do not produce solid combustion materials.

To study the effect of dramatically increased amount of fuels, further formulations based on potassium chlorate (30.0 wt%), sucrose (21.5 wt%), MCHP (8.0 wt%), stearic acid (3.0 wt%), 5-AT (10.0 wt%) and CuPc (27.5 wt%) were developed using an overall amount of fuel (sucrose and 5-AT) between 31.5–46.5 wt% compared to the 26.2 wt% Shimizu used. The amount of 5-AT was increased step-wise by 5.0 wt% from 10.0 wt% up to 25.0 wt% with at the same time reducing the amount of used dye. Unfortunately the color purity and smoke thickness of these formulations decreased too far to be considered for further investigations.

Green smoke formulations based on CuPc and Solvent Yellow 33 (SY33)

Since the blue formulations **B1**–**B4** by now were developed using Moretti´s Solvent Yellow 33 system, the next step was to combine CuPc and Solvent Yellow 33 (SY33) according to the subtractive color mixing scheme to obtain green smoke.[29] Unlike pyrotechnic flares which rely on the spectrum emitted to determine color, colored smokes are generated from the light spectrum absorbed by the particles suspended in the air.[30] The absence of colored particles is white and the presence of all primary colors (cyan, magenta and yellow) is black. The presence of only two of them, cyan and yellow colored dyes, results in green smoke as shown in the experiments. Similar approaches were done by the authors to use a mixture of the dyes curcumin or (–)riboflavin (yellow) with CuPc (blue), resulting in poor performance regarding the smoke color, smoke volume and smoke thickness. SY33 is a literature reported non-toxic quinophthalone dye which is allowed to be used as food additive in the European Union (EU).[15] Moretti *et al.* reported 2013 the successful prototype testing of a novel yellow smoke formulation based on the environmentally benign dye SY33.[6b] The older, in-use *U.S. Army* green smoke formulation consists of potassium chlorate (24.5 wt%), sucrose (16.5 wt%), magnesium carbonate monohydrate (17.0 wt%), SY33 (12.5 wt%) and Solvent Green 3 (SG3) (29.5 wt%).[31] The green dye, SG3 or 1,4-Bis(p-tolyl-amino)anthraquinone, is an anthraquinone based dye used e.g. in the M18 smoke grenade. Unfortunately the tested M18 green smoke formulation consumed the dye and produced grey soot on a 2 g scale. No colored smoke was observed.

Formulations using both dyes CuPc and SY33 were investigated and the content is shown in Table 4 and Table 5. All formulations **G1**–**G8** produced green smoke with comparable smoke thickness and volume (Figure 9).

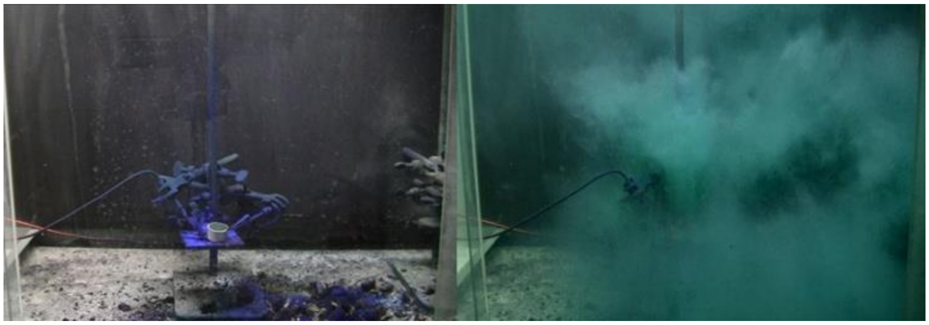

Figure 9. Burning of **G8** before (left) and after ignition (right).

Formulations **G1**–**G8** were developed to compare the effect of varying amounts of 5-AT to the efficiency and provide an alternative green smoke producing system. In **G1**–**G8** the amount of coolant (sodium hydrogen carbonate) was decreased with respect to the U.S. Army M18 green smoke formulation. The oxidizer content is varying from 28.5–34.5 wt%, sucrose from 13.5–21.5 wt% and 5-AT from 0.0–10.0 wt%.

Table 4. Green smoke formulations **G1–G7**.

	$KClO_3$ [wt%]	**Sucrose [wt%]**	**$NaHCO_3$ [wt%]**	**Stearic acid [wt%]**	**5-AT [wt%]**	**CuPc [wt%]**	**SY33 [wt%]**
G1	32.5	21.5	8.0	1.0	0	18.5	18.5
G2	30.5	21.5	10.0	1.0	0	18.5	18.5
G3	28.5	21.5	12.0	1.0	0	18.5	18.5
G4	34.5	19.5	6.0	1.0	2.0	18.5	18.5
G5	32.5	17.5	8.0	1.0	4.0	18.5	18.5
G6	30.5	15.5	10.0	1.0	6.0	18.5	18.5
G7	28.5	13.5	12.0	1.0	8.0	18.5	18.5

Formulation **G8** contains the overall highest amount of fuel used in the series **G1**–**G8** with 31.4 wt% in total (Table 5). The coolant used is magnesium carbonate hydroxide pentahydrate (MCHP) which is a weaker coolant in comparison to sodium bicarbonate. The amount of used dye is significantly lower than in **G1**–**G7**.

Table 5. Green composition **G8**.

	$KClO_3$ [wt%]	Sucrose [wt%]	MCHP [wt%]	Stearic acid [wt%]	5-AT [wt%]	CuPc [wt%]	SY33 [wt%]
G8	32.0	21.4	8.0	1.0	10.0	13.8	13.8

The burn times of formulations **G1**–**G8** are in the range of 16–46s, with **G8** showing the shortest one (Table 6). The calculated burn rates are in the range of 0.303 gs^{-1} to 0.909 gs^{-1}. **G1**–**G3** are insensitive towards impact, **G4–G6** are less sensitive towards impact and **G7**/**G8** are characterized as sensitive. The prepared formulations **G1**–**G8** are insensitive towards friction and show melting-decomposition transitions in the range of 145–202 °C with **G5** showing the lowest one. All formulations are insensitive towards electrostatic discharge up to the instruments maximum of 1.5 J.

Table 6. Properties of **G1**–**G8**.

	Burn time [s]	Burn rate [gs^{-1}]	Impact [J]	Friction [N]	ESD[a] [J]	T_{dec}[b] [°C]
G1	22	0.455	40	>360	>1.5	202
G2	21	0.909	40	>360	>1.5	170
G3	26	0.385	40	>360	>1.5	174
G4	20	0.455	35	>360	>1.5	167
G5	18	0.556	35	>360	>1.5	145
G6	23	0.435	35	>360	>1.5	170
G7	33	0.303	25	>360	>1.5	165
G8	13	0.769	25	>360	>1.5	171

Annotation: a) Electrostatic discharge. b) Decomposition temperature.

Figure 10 shows the transmittance (in %) as a function of wavelength spectrum of **G8**. For clearness reasons the number of depicted functions was limited to one function per minute. Since we were not interested in the NIR region, only the visible part of the spectrum is depicted (380–750 nm). The vertical lines at 439 nm (SY33) and 678 nm (CuPc) marks the literature known maximum absorption of the two dyes. The third vertical line at 555 nm is the peak of highest sensitivity of the human eye during daylight and was therefore chosen for the mass-based composition figure of merit (FM_m) calculation (see supporting information). The function with the lowest transmittance value at the bottom describes the behavior of the smoke after ignition and equilibration (t = 0 s). From the bottom to the top the next functions are 120 s, 180 s, 240 s, 300 s and 360 s (approximately 70% transmittance at 555 nm). The function at the very top shows the empty chamber before igniting the pellet.

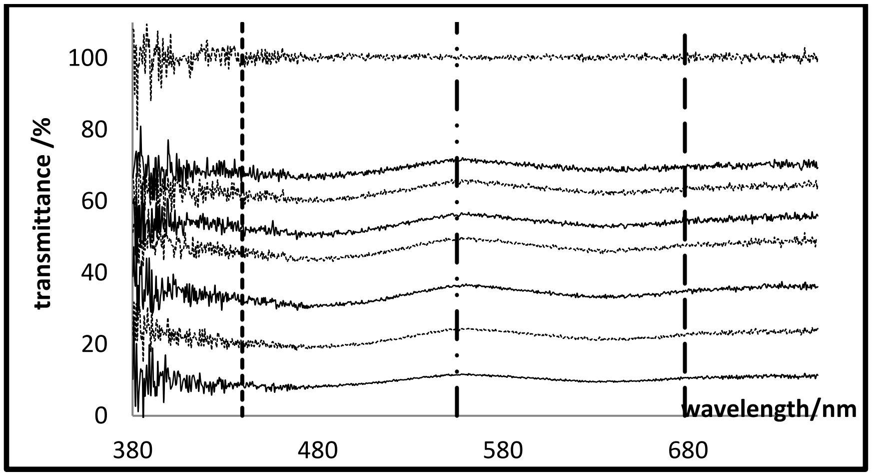

Figure 10. G8 Transmittance [%] - wavelength [nm] for 6 min.

In the case of obscurants, the calculation of FM_m is a widely accepted method to compare the performance of different formulations to each other.[24] The calculation takes the total amount of produced aerosol, the molar extinction coefficient and a certain time period into account (see optical measurement). We calculated the FM_m the first time for colored formulations **G1**–**G8** and compared the values to the optical performance and the determined amount of CuPc. According to these FM_m values, formulations **G1/G7** performed best and **G8** performed worst (Table 7). **G2–G6** are in the range of 0.351 to 0.486. As there are no other literature known values for FM_m of colored smoke formulations, we decided to verify the results and determined the yield and the CuPc content in the aerosol separately.

Table 7. FM_m calculation.

	FM_m[a)]	SD[b)]
G1	0.835	0.084
G2	0.351	0.010
G3	0.392	0.023
G4	0.486	0.077
G5	0.424	0.059
G6	0.418	0.088
G7	0.861	0.058
G8	0.295	0.005

Annotation: a) FM_m = mass-based composition figure of merit; b) SD = Standard deviation of Y.

The yield of formulations **G1**–**G8** was determined using the self-developed aerosol collecting setup (see Experimental Section). The yield is the quotient of the total amount of produced aerosol and the pyrotechnical payload. As the total amount of aerosol does not distinguish between combustion products, like soot, water or the dye, it is more precisely to determine the amount of dispersed dye. In contrast to white obscuring smokes where other combustion products like soot have a positive effect on the shielding effect (higher FM_m values), it is not favoured for colored smoke formulations. Large amounts of white combustion products can weaken the color purity and falsify the color impression which is a major concern with visible signalling devices. Therefore the FM_m calculation was found to be an improper tool for the evaluation of colored smoke formulations. Since CuPc is a salt, we determined the copper content in the collected aerosol using "inductively coupled plasma atomic emission spectroscopy (ICP-AES) to calculate the percentage of dispersed blue dye in the aerosol. The authors call this the transfer rate.

The effect of changing the oxidizer/coolant ratio can be seen in **G1–G3**. All three formulations do not contain any 5-AT and therefore served as baseline for formulations **G4**–**G8** (Table 8). With a decreasing oxidizer/coolant ratio, the total amount of produced aerosol decreased, too. The effect of possible hygroscopic combustion products can be neglected as the RH values are almost identical. **G1** produced the largest amount of total aerosol with a calculated 38 wt% transfer rate of CuPc. **G4** contains more oxidizer, less coolant and for the first time 5-AT (2 wt%) as additional gas generator compared to **G1**. The yield and calculated Cu content is better than **G3**, but worse than **G1**.

Table 8. Quantification of aerosol of **G1–G8**.

	RH[a]	**Y**[b]	**SD(Y)**[c]	**Cu content**[d]
G1	25.8	15.2	2.9	38.0
G2	26.1	10.6	2.3	24.3
G3	24.7	7.9	2.6	24.1
G4	25.2	9.9	1.8	26.6
G5	31.5	15.0	2.6	26.9
G6	34.0	13.0	1.5	20.6
G7	34.0	6.6	1.0	15.0
G8	27.0	21.5	1.4	59.8

Annotation: a) RH = relative humidity [%]; b) Y = yield (Mass of aerosol/mass of pellet)[wt%]; mass of pellet = 1.8–2.3g; c) SD(Y) = Standard deviation; d) Determined via ICP-AES [%].

In **G5**–**G7** the amount of 5-AT was increased stepwise up to 8 wt%, while the amount of sucrose was reduced. The oxidizer/coolant ratio decreased, too. Regarding the yield, **G5** performed better than **G2**/**G3** and similar to **G1,** but shows a lower transfer rate than **G1**. An explanation is the increased RH value compared to the **G1** measurement. Even weak hygroscopic materials may have a positive effect on the yield and lead to a reduced calculated transfer rate. The results of **G5**–**G7** showed, that a decreasing oxidizer/coolant ratio and at the same time increasing amount of 5-AT do not result in a better performance regarding the yield or transfer rate of CuPc.

G8 is one example of a series of good performing formulations using MCHP, which is a weaker coolant compared to sodium hydrogen carbonate and was used by Moretti *et al.* earlier.[5] **G8** was measured at almost identical RH conditions like **G1** and shows both a higher yield (6 wt% higher) as well as a dramatically increased transfer rate (22 wt% higher) of CuPc (Table 8). **G8** dispersed more dye than any of formulations **G1–G7** while having 5 wt% less CuPc in the pyrotechnical payload.

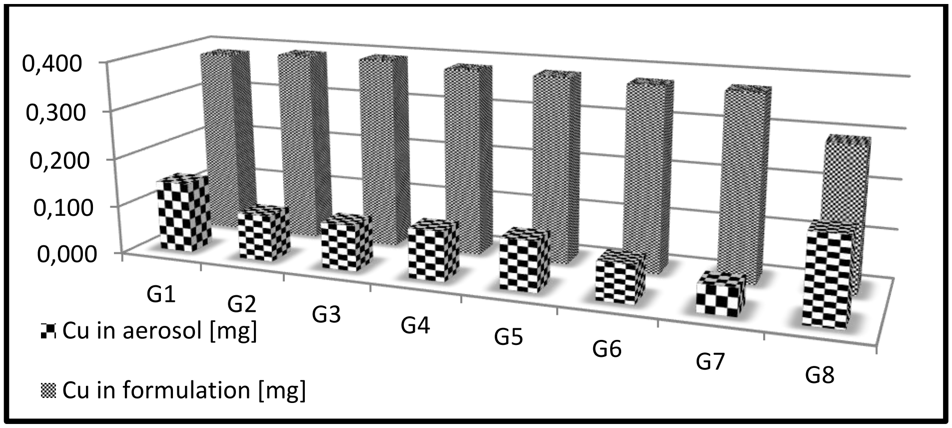

Figure 11. Comparison of CuPc transfer rates.

Figure 11 compares the amount of CuPc in 2 g pellets to the calculated amount of CuPc in the aerosol. As discussed, **G8** has the highest transfer rate. According to our results, it is possible to increase the amount of dispersed dye by adding gas generators in the case of our developed green smoke formulations. In the case of **G8**, the reduction of CuPc was more than compensated by increasing the amount of 5-AT.

4 Conclusions

New blue and green anthraquinone-free smoke formulations applying 5-AT as additional gas generator were developed. The yield and the ICP-AES measurements of **G8** proofed a higher degree of dispersion for CuPc compared to 5-AT free formulations. To determine the yield of our formulations, an inexpensive and simple laboratory-scale aerosol collecting setup was developed. This prototype setup is adjusted for low-temperature formulations and gives the yield with repeatedly standard deviations in the range of 1.0–5.4 %. The optical performance for selected formulations was characterized by measuring the transmittance as a function of wavelength in the visible region. The FM_m calculations, which are generally used for white obscurants, were calculated the first time for colored smoke formulations and were found to be an improper tool to evaluate the performance. In the case of green smoke formulations, SG3, an anthraquinone based dye was successfully replaced by the more environmentally benign dyes CuPc and SY33. These formulations are promising alternatives to the in-use U.S. Army M18 green smoke formulation. For an appropriate evaluation, the characterization of the gaseous combustion products/aerosol, as well as particle size and distribution still has to be done. The detection and quantification of possible CO, HCl, HCN and nitrogen oxide species may be achieved using fourier transform infrared spectroscopy (FTIR). A scanning mobility particle size spectrometer (SMPS) could be used to determine the particle size and distribution of the aerosol. All used materials can be readily purchased and do not pose environmental risks. The burn rate tests show the compatibility with cardboard tubes casing, which is advantageous in terms of biodegradability, cost and reducing the carry-on weight for soldiers. The low sensitivity towards physical stimuli is a promising fact for safe handling and manufacturing.

References

[1] T. M. Klapötke, *Chemistry of High-energy Materials*, 3rd ed., De Gruyter, **2015**.

[2] E.-C. Koch, *Propellants, Explos., Pyrotech.* **2008**, *33*, 165-176.

[3] Headquarters, *Field manual 21-60, Visual Signals* (Ed.: Department of the Army), Washington, DC, USA, **1987**.

[4] a)N. Sordoni, W. Heard, W. Rouse, *ERDEC-TR-129*, Aberdeen Proving Ground, Maryland,USA, **1993**, *1*, 25; b)G. A. Lane, W. A. Smith, E. M. Jankowiak, *1st Int. Pyrotech. Semin., Proc.*, IPSUSA Seminars, Inc., Estes Park, Colorado, USA, August 12–17, **1968**.

[5] J. D. Moretti, J. J. Sabatini, A. P. Shaw, R. Gilbert, *ACS Sustainable Chem. Eng.* **2014**, *2*, 1325-1330.

[6] a)WHO, *Some Pharmaceutical Drugs, IARC Monographs on the Evaluation of the carcinogenic risk of chemicals to man, Vol. 50*, WHO, Geneva, **1990**; b)J. D. Moretti, J. J. Sabatini, A. P. Shaw, G. R. Chen, A. J. Gilbert, K. D. Oyler, *ACS Sustainable Chem. Eng.* **2013**, *1*, 673-678.

[7] a)T. C. Marrs, H. F. Colgrave, P. Rice, J. A. G. Edginton, B. Morris, *Journal of Hazardous Materials* **1989**, *21*, 73-88; b)M. L. Springer, T. Rush, H. M. Beardsley, K. Watts, J. Bergmann, *Final Report, Demonstration of the Replacement of the Dyes and Sulfur in the M18 Red and Violet Smoke Grenades*, ESTCP Project WP-0122, **2008**; c)National Research Council (US) Subcommittee on Military Smokes and Obscurants, *Toxicity of Military Smokes and Obscurants, Vol. 3*, National Academic Press, Washington DC, **1999**.

[8] M. Hemmilä, M. Hihkiö, K. Linnainmaa, *Propellants, Explos., Pyrotech.* **2007**, *32*, 415-422.

[9] G. S. Bondy, C. L. Armstrong, B. A. Dawson, C. Héroux-Metcalf, G. A. Neville, C. G. Rogers, *Toxicol. In Vitro* **1994**, *8*, 329-335.

[10] P. A. Parent, *Bilogical effects of colored smoke ingredients,CRDL Special Publications*, AD A003827*,* Edgewood Arsenal, Aberdeen Proving ground, Edgewood, **1964**, *4-9*.

[11] a)M. V. Buchanan, I. B. Rubin, J. H. Moneyhun, *Compositional Changes in Red and Violet Smoke Mixes after Combustion*, Oak Ridge National Laboratory, Oak Ridge, TN, **1983**, *CONF8304591*; b)I. B. Rubin, M. V. Buchanan, J. H. Moneyhun, *Chemical Characterization and Toxicologic Evaluation of Airborne Mixtures: Chemical Characterization of Combusted Inventory Red and Violet Smoke Mixes*, ORNL/TM-8810, AD A131527*,* Oak Ridge, TN, USA, **1982**.

[12] National Cancer Institute, *Bioassay of 2-Aminoanthraquinone for Possible Carcinogenicity*, National Institute of Health, NCI, Bethesda **1987**.

[13] EFSA, *EFSA J.* **2005**, *263*, 1-71.

[14] IARC Monographs on the Evaluation of Carcinogenic Risks to Humans, http://monographs.iarc.fr/ENG/Classification/index.php, Feb 2015.

[15] EFSA ANS Panel, *EFSA J.* **2009**, *7*.

[16] a)J. L. Epler, *U.S. Army Project Order No. 9600*, Oak Ridge National Laboratory, Oak Ridge, TN, **1979**; b)J. P. Brown, R. J. Brown, *Mutat. Res.* **1976**, *40*, 203-224.

[17] S. A. Army, *Final report of the Expert Panel to review SAS Veterans´ Health Concern*, Perth, Australia, **2003**.

[18] http://gestis.itrust.de/nxt/gateway.dll/gestis_de/013930.xml?f=templates$fn=default.htm$3.0, April 2015.

[19] Organization for Economic Cooperation and Development (OECD), *Screening Information Data Set for Copper phthalocyanine* CAS 147-14-8, **1993**, 139-140.

[20] http://www.bibra-information.co.uk/downloads/toxicity-profile-for-phthalocyanine-blue-2005/, April 2016.

[21] European Commission, *ESIS; IUCLID Dataset, Tetrabenzo-5,10,15,20-diazaporphyrinephthalocyanine (147-14-8) p.35 (2000 CD-ROM edition). Available from, as of April 27, 2010: http://esis.jrc.ec.europa.eu/*, **2010**.

[22] *Toxicity Profile: Phthalocyanine Blue* (Ed.: The British Industrial Biological Research Association), **1988**, 3.

[23] G. L. Baughman, T. A. Perenich, *Investigating the Fate of Dyes in the Environment,Amer Dyestuff Reporter* (Ed.: U.S. Environmental Protection Agency (EPA)), EPA/600/M-88/013, **1988**.

[24] A. P. Shaw, G. Diviacchi, E. L. Black, *40th Int. Pyrotech. Semin., Proc.*, IPSUSA Seminars, Inc., Colorado Spings, Colorado, USA, **2014**, 170-191.

[25] a)J. Ledgard, *The preparatory of Black Powder and Pyrotechnics, Version 1.4*, Jared Ledgard, **2007**; b)T. Shimizu, *Fireworks-The Art Science and Technique*, Pyrotechnica Publications, Austin, Texas (USA), **1996**.

[26] S. R. Chakraborty, *16th Int. Pyrotech. Semin., Proc.*, IPSUSA Seminars, Inc., Jonköping, Sweden, June 24-28, **1991**, *16*, 665-674.

[27] *Clariant GPS Product safety Summary Pigment Blue 15,Clariant GPS Product safety Summary Pigment Blue 15*, **2012**.

[28] N. Sordoni, W. Heard, W. Rouse, *Pyrotechnical Smoke Analysis Volume 1,Defense Technical Information Center (DTIC): Fort Belvoir, VA*, ERDEC-TR-129*,* Aberdeen Proving Ground, Maryland, USA, **1993**.

[29] H. Naumann, G. Schröder, M. Löffler-Mang, *Handbuch Bauelemente der Optik: Grundlagen, Werkstoffe, Geräte, Messtechnik*, Carl Hanser Verlag GmbH & Company KG, **2014**.

[30] J. A. Conkling, C. Mocella, *Chemistry of Pyrotechnics: Basic Principles and Theory*, 2nd ed., Taylor & Francis, **2010**.

[31] M. D. Smith, F. M. Stewart, *8th Int. Pyrotech. Semin., Proc.*, IPSUSA Seminars, Inc., Steamboat Springs, Colorado, USA, July 12-16, **1982**, 623-635.

Supporting Information

1. Calculation Standard deviation (SD):

SD was calculated using the “Microsoft Excel 2013” software and the “STABW” function.

2. Description of Smoke Figures of Merit and Measurement Technique

This section is taken from A. Shaw´s 2014 IPSUSA Appendix:

[1] A. P. Shaw, G. D. Chen, Advanced boron carbide-based visual obscurants for military smoke grenades, *Proc. Int. Pyrotech. Semin.(40th)*, Colorado Springs, Colorado, USA, 13-18 July, **2014**, 170-191.

Table A1. Smoke measurement variables,definitions, and units.

Variable	**Definition**	**Units**
T	transmittance, I/I_0	
L	path length	m
V	cloud or chamber volume	m^3
c	concentration	g/m^3
α_m	mass-based composition figure	m^2/g
FM_m	mass-based composition figure of merit	m^2/g
FM_V	volume-based composition figure of merit	m^2/cm^3
FM_{md}	mass-based device figure of merit	m^2/g
FM_{vd}	volume-based device figure of merit	m^2/cm^3
m_a	mass of aerosol	g
m_c	mass of composition	g
m_d	mass of device	g
v_c	volume of composition	cm^3
v_d	volume of device	cm^3
ρ_c	density of composition, m_c/v_c	g/cm^3
Y	composition yield factor, m_a/m_c	
F_m	mass fill fraction, m_c/m_d	
F_v	volume fill fraction, v_c/v_d	

Visual screening smokes may be quantitatively assessed in a suitably-sized aerosol chamber. In atypical experiment, the total attenuation of visible light from both scattering and absorption is measured by determining transmittance (T), the ratio of transmitted light intensity (I) to that of the incident beam (I_0). The Beer-Lambert law (Equation 1) relates T to the aerosol concentration(c), the path length the light travels through (L), and the extinction coefficient (α).

Equation 1:

$$T = {}^{I}\!/_{I_0} = e^{-cL\alpha}$$

The extinction coefficient, which is independent of concentration and path length, determines the effectiveness of an aerosol as an obscurant. [A1] The units of α are such that the term $cL\alpha$ (the optical depth) is dimensionless. Therefore, when L is measured in meters and c is defined as the mass of aerosol particles divided by the volume of the chamber (g/m^3), the units of α are m^2/g. This is a mass-based extinction coefficient (α_m). Rearranging the terms and substituting m_a/V for c, where m_a is the aerosol mass and V is the chamber volume, gives Equation 2.

Equation 2:

$$\alpha_m = \frac{-\ln(T)}{cL} = \frac{-V \ \cdot \ln(T)}{m_a L}$$

Since α_m is only a characteristic of the aerosol, it does not account for the properties of the initial smoke-producing material. Two practical factors, unaccounted for by α_m, are the composition/device efficiency and whether or not the volatilized materials absorb atmospheric constituents. Various *figures of merit* have been used to account for these factors with the goal of quantifying actual smoke composition performance. In 1968, Lane and co-workers described “total obscuring power” (TOP) which was intended to represent the area in square feet that could be obscured by a pound of smoke composition. This figure of merit incorporated a factor to account for the “discrimination capability of the human eye”.[A2] A figure of merit more closely related to the Beer-Lambert law may be obtained by multiplying α_m by the yield factor (Y). Here, Y is the ratio of aerosol mass (m_a) to the mass of initial composition (m_c). Equation 3 shows how the resulting mass-based figure of merit, FM$_m$, is related to the initial smoke composition mass. Like α_m, the units of FM$_m$ are m^2/g.

Equation 3:

$$FM_m = \alpha_m Y = \left(\frac{-V \cdot \ln(T)}{m_a L}\right)\left(\frac{m_a}{m_c}\right) = \frac{-V \cdot \ln(T)}{m_c L}$$

If all the smoke from the composition is kept in the chamber, the technique is greatly simplified as only T must be measured to determine $\mathrm{FM_m}$ (V, L, and m_c are known). In practice, the cloud generated by just one smoke grenade is too thick even for large smoke chambers and smoke must be partially vented to obtain a reasonable measurement of T (usually in the 0.1-0.5 range). In this case, aerosol sampling to determine m_a must be performed before and after the venting step. The first determination is used to calculate Y. The second is used to calculate α_m at the time of optical measurement. These two values are then multiplied to give $\mathrm{FM_m}$ (as shown in equation 3). It is assumed that the aerosol does not change during the process. Even if it is possible to determine $\mathrm{FM_m}$ without chamber venting and aerosol sampling, α_m and Y are still quite informative. A yield factor greater than unity indicates with certainty, that the smoke has absorbed mass from the air (usually water). In actual devices, the amount of smoke composition is often limited by the device *volume*. Thus, for different compositions with comparable $\mathrm{FM_m}$ values, the one with greater density is preferable provided a heavier device is acceptable. A volume-based figure of merit that accounts for this is obtained by multiplying $\mathrm{FM_m}$ by the composition density (ρ_c, g/cm^3). The units of $\mathrm{FM_v}$ are m^2/cm^3 (Equation 4). This figure of merit, which is related to the initial volume of smoke composition (v_c), has been used since the 1980s if not earlier.[A3,A4]

Equation 4:

$$FM_v = FM_m \rho_c = \alpha_m Y \rho_c = \frac{-V \cdot \ln(T)}{v_c L}$$

Figures of merit suitable for direct device-to-device comparison are obtained by incorporating fill fractions, F_m or F_v, the ratio of composition mass or volume to that of the device.[A5] Multiplying $\mathrm{FM_m}$ or $\mathrm{FM_v}$ by F_m or F_v, respectively, gives device-based figures of merit that are related to the total device mass or volume (Equations 5 and 6).

Equation 5:

$$FM_{md} = FM_m F_m = \alpha_m Y F_m = \frac{-V \cdot \ln(T)}{m_d L}$$

Equation 6:

$$FM_{vd} = FM_v F_v = \alpha_m Y \rho_c F_v = \frac{-V \cdot \ln(T)}{v_d L}$$

A broadband light source (tungsten-halogen bulb or xenon arc lamp) combined with a spectrometer as the detector is the most flexible experimental setup. Measurements of *T* may be obtained at specific wavelengths, averaged across the visible spectrum, or weighted to the photopic response of the human eye.[A6] Any reported α or FM value should therefore be accompanied by the wavelength, wavelength range, or weighting operation that was used to calculate it. The behavior of many pyrotechnic smoke compositions depends on device configuration, although some are less configuration-sensitive than others. Information about the test containers and sample sizes should be noted. Additionally, performance (as determined by a figure of merit) can depend on humidity. Compositions that aerosolize hygroscopic compounds perform better as humidity and yield factor increase. In such cases, the extinction coefficient also varies, but not nearly as much as the yield factor does.[A7,A8] Yield factors for nonhygroscopic smokes are governed by aerosolization efficiency.

3. References

[A1] C. F. Bohren, D.R. Huffman, *Absorption and Scattering of Light by Small Particles*; Wiley-VCH: Weinheim, Germany, **2004**, Section 3.4, pp 69-81.

[A2] G. A. Lane, W. A. Smith, E. M. Jankowiak, Novel Pyrotechnic Compositions for Screening Smokes*, Proc. Int. Pyrotech. Semin. (1st)*, Estes Park, Colorado, August 12–17, **1968**, 25-39.

[A3] A. L. Turetsky, G. P. Young, Advances in Pyrotechnically Based Visual Smoke Systems. *Proc. Int. Pyrotech.Semin. (13th),* Grand Junction, CO, U.S.A., July 11-15, **1988**, pp 805-810.

[A4] J. F. Embury, D. Walker, C. J. Zimmermann, *Screening Smoke Performance of Commercially Available Powders. II. Visible Screening by Titanium Dioxide*, Accession Number ADA284072, Defense Technical Information Center (DTIC): Fort Belvoir, VA, **1994**, pp 1-30.

[A5] B. De Lacy, D. Redding, J. Matthews, Mass Extinction Coefficients of Surface Modified Titanium Dioxide, *2011 Obscurants Symposium*, Baltimore, MD, U.S.A., May 10-12, **2011**.

[A6] The 1931 CIE standard luminosity function is often used. Many slight modifications have since been suggested: L. T. Sharpe, A. Stockman, W. Jagla, H. Jägle, A Luminous Efficiency Function, $V^*(\lambda)$, For Daylight Adaptation, *J. Vis.* **2005**, *5*, 948-968.

[A7] M. E. Milham, D. H. Anderson, *Obscuration Sciences Smoke Data Compendium – Standard Smokes*, Accession Number CBRNIAC-CB-153496, Defense Technical Information Center (DTIC): Fort Belvoir, VA, **1983**, pp 1-56.

[A8] N. Sordoni, W. Heard, W. Rouse, *Pyrotechnic Smoke Analysis Volume I*, Accession Number CBRNIAC-CB-027023, Defense Technical Information Center (DTIC): Fort Belvoir, VA, **1993**, pp 1-49.

3.2 Effect of Adding 5-Aminotetrazole to a Modified U.S. Army Terephthalic Acid White Smoke Composition

Published in *Cent. Eur. J. Energ. Mater.* **2017**, *14,* 489-500. (DOI: 10.22211/cejem/76843)

Abstract: Military visible obscuration compositions (obscurants, smokes) play an important role on today's battlefield. For many years, the known toxicity or ageing problems of established formulations were commonly accepted since there was a lack of alternatives. Since the U.S. Army stopped producing the AN-M8 hexachloroethane (HC) smoke grenade, the M83 terephthalic acid (TA) smoke grenade has been used in its place. This cool-burning, less toxic, but also low efficiency white smoke formulation cannot compete with HC-based formulations in terms of obscuration performance. In this context, we have explored the use of 5-aminotetrazole (5-AT) as an additive and fuel in the known TA system. Remarkably, it has been found that sugar is not necessarily required in the formulations, which has implications for the future improvement of sublimation-condensation smoke compositions, including coloured smoke compositions. In small-scale tests, it was found that replacing sucrose with 5-AT in the formulations resulted in significantly improved smoke persistence.

Introduction

Military smoke or obscurant formulations are used on the battlefield for signaling, marking targets and screening troop movements [1]. The earliest reported application in Europe dates from 1701, but the development of modern smoke technology was launched later, with the introduction of the Berger mixture during WWI [2]. The American (type C) HC (hexachloroethane) smoke (as used in the AN-M8 smoke grenade), traces its origins to the Berger mixture, and was used by the U.S. Army until it was largely replaced by terephthalic acid-based (TA) compositions in the 1990s and 2000s. Combustion of formulations containing hexachloroethane, zinc oxide and aluminium produce volatilized metal chlorides which undergo further reactions with moisture from the atmosphere to give the desired aerosol [3]. In addition to the desired hygroscopic combustion products, in reality the smoke emitted by HC compositions contained as much as 10% of highly toxic chlorinated compounds such as CCl_4, C_2Cl_4, C_6Cl_6 and polychlorinated dibenzodioxins [4]. Since hexachloroethane is itself toxic, and several injuries and deaths were correlated to HC smoke exposure, there was a need for less toxic alternatives [5]. The requirements for potential new compositions are not only limited to performance issues, they also include toxicity issues, ageing, sensitivities and burning properties [1, 6]. It is obvious that such an ideal composition is not yet available and that smoke compositions are generally characterized by a safety/performance trade-off.

Compositions based on for example white and red phosphorus, rely on atmospheric burning to generate phosphorus pentoxide, which is further hydrolyzed to give the aerosol cloud [7]. Such formulations have been used since WWI and WWII respectively and are superior to any other smoke material in terms of yield factor (Y) [7a]. Y is the quotient of the total amount of aerosol produced and the pyrotechnical payload. Yield may be expressed as a ratio or as a percentage (wt.%), although the term “yield factor” almost always refers to a ratio. It is therefore important to distinguish between hygroscopic and non-hygroscopic aerosols. Lane *et al.* and Sordoni *et al.* [8] reported the influence of various relative humidities (RH) on the performance of red phosphorus and HC containing formulations. Y increased from 3.73 (20% RH) to 5.77 (80% RH) for red phosphorus and from 1.25 (20% RH) to 2.77 (80% RH) for HC compositions [8]. All experimental measurements should therefore be accompanied by RH values, as even minor hygroscopic combustion products could influence the observed obscuring properties.

Whereas white phosphorus is toxic and incendiary, most compositions containing red phosphorus have serious ageing and sensitivity issues [1, 9]. Red phosphorus suffers from hydrolytic degradation, which leads to the formation of highly toxic and flammable phosphine gas, as well as phosphoric acid [10]. This problem has been known for decades and drives the search for alternatives. In 2016 Shaw *et al.* [11] predicted boron phosphide, BP, to be a suitable candidate after theoretically studying a system based on BP/KNO_3. BP is resistant to hydrolysis, which might solve the degradation problems correlated with red phosphorus containing formulations [11]. However, the compound BP is not yet commercially available and this currently hinders further experimental investigations [12]. In a recent publication by Koch *et al.* [9], phosphorus(V) nitride, P_3N_5, was suggested as a replacement candidate for red phosphorus. P_3N_5 is stable towards moisture and is reportedly safe to handle in combination with a range of oxidants, including nitrates, chlorates and perchlorates. Koch and coworkers did not detect any phosphine release from the compositions, while at the same time demonstrating smoke performance competitive with red phosphorus-based compositions [9a]. Unfortunately, the alpha form of P_3N_5 (crystalline density = 2.77 g·cm^{-3}, phosphorus density = 1.58 g·cm^{-3}), which is the phase stable at atmospheric pressure, has a low phosphorus density compared to white phosphorus (1.82 g·cm^{-3}), red phosphorus (2.0-2.4 g·cm^{-3}), and BP (crystalline density = 2.97 g·cm^{-3}, phosphorus density = 2.20 g·cm^{-3}). [9a, 12-13]

Earlier in 2013, new boron carbide (B_4C) smoke formulations were reported by Shaw and coworkers [14]. These formulations used B_4C/KNO_3 as a pyrotechnic fuel/oxidizer pair, KCl as a diluent, and calcium stearate as a burning rate modifier. In field and smoke chamber tests, these prototype smoke grenades outperformed the U.S. Army M83 TA grenade by a wide margin. The best prototypes were functionally equivalent to nearly two M83 TA smoke grenades and have been considered as possible replacement candidates [1]. However, as with HC smoke grenades, the B_4C-based compositions burn at a high temperature, so unintended incendiary effects would not be mitigated.

The original TA white smoke composition consists of potassium chlorate, sucrose, terephthalic acid, magnesium carbonate, polyvinyl alcohol and stearic acid [15]. Since it was developed in the 1990s, it has replaced the HC composition within the U.S. Army white smoke grenade due to the toxicity concerns mentioned previously [16]. The consequences for soldiers were dramatic, as the effective carry on weight increased. To obtain an obscuring cloud similar to one AN-M8 HC grenade, a soldier nowadays has to use three M83 TA grenades instead [1]. However, a major benefit of the TA system is the low burning temperature, which makes it less likely to be incendiary. In general, the TA system is very similar to coloured smoke formulations, *e.g.* the yellow smoke system published by Moretti *et al.* in 2014 [17]. The organic dye is vaporized through a sublimation/recondensation mechanism. In 2008, Chen *et al.* [18] described the urgent need to replace sulfur as the main fuel in the M18 red and violet coloured smoke grenades. The resulting SO_2 produced upon combustion is toxic and highly irritating to inhale, and is therefore undesirable.

Sugar was considered as a less toxic alternative, which resulted in a complete reformulation of the previously mentioned formulations. However, there may be possible replacements for sugar that could improve smoke dispersal, efficiency, and persistence. In our previous work, we reported on the application of 5-aminotetrazole (5-AT) as an additive and additional gas generator in green and blue coloured smoke formulations [19]. Taking this as a starting point, we have developed completely sugar-free white smoke formulations based on TA.

To tackle the above mentioned problems with TA smoke, the authors studied the effect of adding 5-AT to a baseline TA formulation as a gas generator, with the intention of increasing the relatively low aerosolization and dispersal efficiency. Several working formulations were developed with varying burning times. Two formulations using 5-AT *instead* of sucrose were developed and compared to each other. This paper describes the results of the optical measurements performed using a convenient small-scale smoke chamber.

2 Experimental Section

2.1 Materials

Potassium chlorate (≥99%), sucrose (≥99%), sodium bicarbonate, poly(vinyl alcohol) hydrolyzed (99+%), terephthalic acid (98%) and magnesium carbonate hydroxide pentahydrate (BioXtra) were purchased from Sigma-Aldrich. 5-AT (98%) was purchased from abcr chemicals. Stearic acid was purchased from Grüssing GmbH. Sodium carbonate was purchased from Brenntag GmbH. For initial testing, small mixtures (2 g) were carefully mixed manually for 5 min in a mortar by combining the dry compounds. If these tests were successful, larger mixtures (40 g) were then prepared by combining the dry components in a cylindrical rubber barrel and rolling for 120 min. The rotatory rock tumbler (model 67631) was built by "Chicago Electric Power Tools" and operated with steel balls. To remove any clumps, the compositions were passed through a 800 µm screen. 2 g of this thus prepared composition was pressed into a cylindrical steel compartment (diameter 2.0 cm), with the aid of a tooling die and a hydraulic press. Unless stated otherwise a consolidation dead load of 2000 kg was applied for 3 s. For each composition, four pellets were tested and the results were averaged. An electrical resistance wire ("Kanthal A1" (FexCrAl), 0.6 mm diameter, 5.25 Ohm·m^{-1}) was used to ignite the pellets.

2.2 Optical measurements

Transmittance data were recorded in a smoke chamber fully described in a previous investigation on coloured smoke formulations [19]. The starting time (t = 0 s) for recording the transmittance values at 555 nm over a period of time was determined by the time needed to fully equilibrate the smoke. A fully equilibrated smoke cloud was indicated by a constant transmittance value. If the transmittance value remained constant for a period of 5 s, data recording was started. In our experiments, we experienced a total time period of 13-18 s to be suitable for equilibration. At this point the cloud was evenly dispersed within the smoke chamber. As the compositions are intended for visual obscuration, we chose the peak photopic response of the human eye at 555 nm for recording all of the transmittance values. The recorded spectra were normalized with a recorded spectrum of the empty chamber before each measurement.

2.3 Thermal and energetic properties

The impact and friction sensitivities were determined using a BAM drophammer and a BAM friction tester. The sensitivities of the compositions are indicated according to the UN Recommendations on the Transport of Dangerous Goods (+): impact: insensitive >40 J, less sensitive >35 J, sensitive >4 J, very sensitive <4 J; friction: insensitive >360 N, less sensitive = 360 N, sensitive 360>N>80 N, very sensitive <80 N, extremely sensitive <10 N. Thermal stability measurements: the onset temperatures were measured with a OZM Research DTA 552-Ex Differential Thermal Analyzer at a heating rate of 5 °C/min.

3 Results and Discussion

The baseline TA white smoke composition in Table 1 was the starting point for our studies [15]. TA (terephthalic acid) was applied as the white pigment. The molecular structure, especially the electron-withdrawing carboxy groups, makes it highly deactivated and therefore more resistant to oxidation. By contrast, dyes containing for example azo- or amino-groups are more likely to be oxidized to the azoxy or N-oxide species, respectively [20]. Based on this formulation, we examined varying coolants, including magnesium carbonate hydroxide pentahydrate (MCHP), sodium bicarbonate ($NaHCO_3$) and sodium carbonate (Na_2CO_3), to give formulations **A**, **B** and **C** respectively (Table 1). Unfortunately all three formulations burned with an open flame after ignition and no further white smoke production was observed. This behaviour indicated that excessively high temperatures were produced and might be explained by the difference in configuration compared to a full scale smoke grenade. The thermal environment within a conductive steel grenade canister is quite different to a bare pellet. Another reason might be the chemicals themselves. Fish and Chen [21] reported a study performed on six samples of magnesium carbonate received from different suppliers. One of the samples was identified as magnesite, while the other five were identified as hydromagnesite. Within those five similar samples, three were morphologically different. Fish and Chen proposed that these differences can affect pyrotechnic performance. For these reasons, in the work presented here, we were only able to compare the performance of the developed formulations with each other.

Table 1. Baseline TA formulation with varying coolants[a]

	$KClO_3$ [wt.%]	Sucrose [wt.%]	TA [wt.%]	$MgCO_3$ [wt.%]	MCHP [wt.%]	$NaHCO_3$ [wt.%)	Na_2CO_3 [wt.%]	Stearic acid [wt.%]
base-line mix	23	14	57	3	-	-	-	3
A	23	14	57	-	3	-	-	3
B	23	14	57	-	-	3	-	3
C	23	14	57	-	-	-	3	3

a) In these formulations, 1 wt.% PVA was added in excess to all formulations, making the total to 101 wt.%.

All four reference formulations (Table 1) only differ in the coolant applied. $KClO_3$/sucrose is the oxidizer/fuel pair and generates the necessary heat to vaporize the TA. The coolant is applied to keep the burning temperature in the desired range and prevents thermal degradation of TA. Stearic acid is used as a processing aid, burning rate modifier and dry binder. PVA serves as a binder that can optionally be used to granulate the compositions if it is applied as a concentrated aqueous solution. However, in these studies, all the components were prepared and mixed in a dry state.

Table 2. Developed TA formulations containing 5-AT[a]

	$KClO_3$ [wt.%]	Sucrose [wt.%]	TA [wt.%]	MCHP [wt.%]	$NaHCO_3$ [wt.%]	Stearic acid [wt.%]	5-AT [wt.%]
1	22.8	13.8	41.6	3.0	-	3.0	14.8
2	22.8	4.9	56.4	3.0	-	3.0	8.9
3	22.8	-	56.4	-	3.0	3.0	13.8
4	22.1	-	51.9	-	5.8	2.9	16.3

a) In these formulations, 1 wt % PVA was added in excess to all formulations, making the total to 100 wt.%.

5-AT was applied as an additional fuel and gas generator with the intention of improving smoke dispersion and efficiency. This strategy was successfully applied in previous work dealing with coloured smoke formulations [19]. Both the mentioned coloured smoke formulations and the TA smoke composition rely on the same sublimation/recondensation mechanism. Formulations **1-4** used 5-AT in different amounts, in the range of 9–16 wt.% (Table 2). Additionally formulations **3** and **4** contained 5-AT as the main fuel, in place of sucrose. Two different coolants, MCHP and $NaHCO_3$, were applied.

For smoke devices with similar burning times, differences in the visual obscuration performance depend on the properties and the amount of smoke (aerosol) produced [1]. White pigments with high refractive indices would provide the best obscuring properties, however it is very difficult to effectively disperse TiO_2, for example, to achieve a long-duration aerosol cloud [22].

Table 3. Energetic properties of the developed TA smoke compositions

	FS [N]	IS [J]	ESD [J]	T_{onset} [°C]
A	360	40	1.5	178
B	360	35	1.0	174
C	360	35	0.9	175
1	360	35	1.0	164
2	360	40	1.0	158

3	360	35	1.0	172
4	360	40	0.9	175

Legend: FS = friction sensitivity, IS = impact sensitivity, ESD = electrostatic discharge sensitivity, T_{onset} = thermal decomposition given as the onset point.

All of the tested formulations were insensitive towards friction and only slightly sensitive towards impact (Table 3). Regarding the ESD sensitivity, all formulations were in the range of 0.9–1.5 J, with formulation C having 0.9 J. The onset temperature of all of the formulations was in the range of 158–178 °C (see supporting information for DTA evaluation of the formulations, as well as single components). The observed burning times of formulations **1**–**4** were in the range of 26–33 s (Table 4). With the exception of formulation **2** (33 s), all of the other formulations had similar burning times.

Table 4. Visual obscuration data for 2 g pellets

	BT [s][a]	Average transmittance (555 nm) over time[b]	SD (555 nm)[c]	RH [%][d]
1	28	0.585	0.026	26.6
2	33	0.531	0.041	25.0
3	28	0.216	0.023	23.1
4	26	0.228	0.011	23.0

a) burning time; b) average of collected transmittance values at 555 nm over time for all pellets; c) standard deviation; d) relative humidity.

For the reasons described earlier, it was only possible to compare the formulations with each other and not to the intended reference formulations.

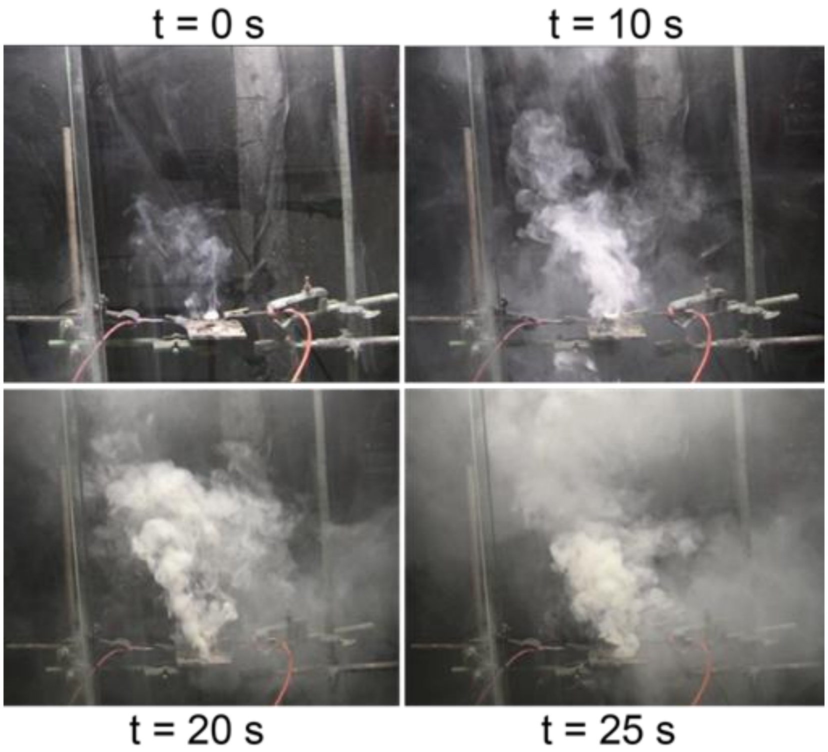

Figure 1. Burning of a 2 g pellet of formulation **4**

In formulations **1** and **2**, both 5-AT and sucrose were applied as fuels, with **1** having the higher 5-AT content but less TA. Alternatively, 5-AT was applied as the main fuel in place of sucrose in formulations **3** and **4** (Figure 1). These formulations differ in the 5-AT/coolant/TA content ratio, but showed nearly the same burning time.

The transmittance (555 nm) over time of formulations **1** and **2** changed dramatically (Figure 2). We observed a steady increase of transmittance from 18 to 87% (**1**) and 23 to 75% (**2**) over 6 min of measurement. By contrast, the transmittance over time for formulations **3** and **4** remained quite constant (15–23% and 19–25% respectively). In general, the average transmittance over time of **3** and **4** was the lowest observed in all of our tests (Table 4).

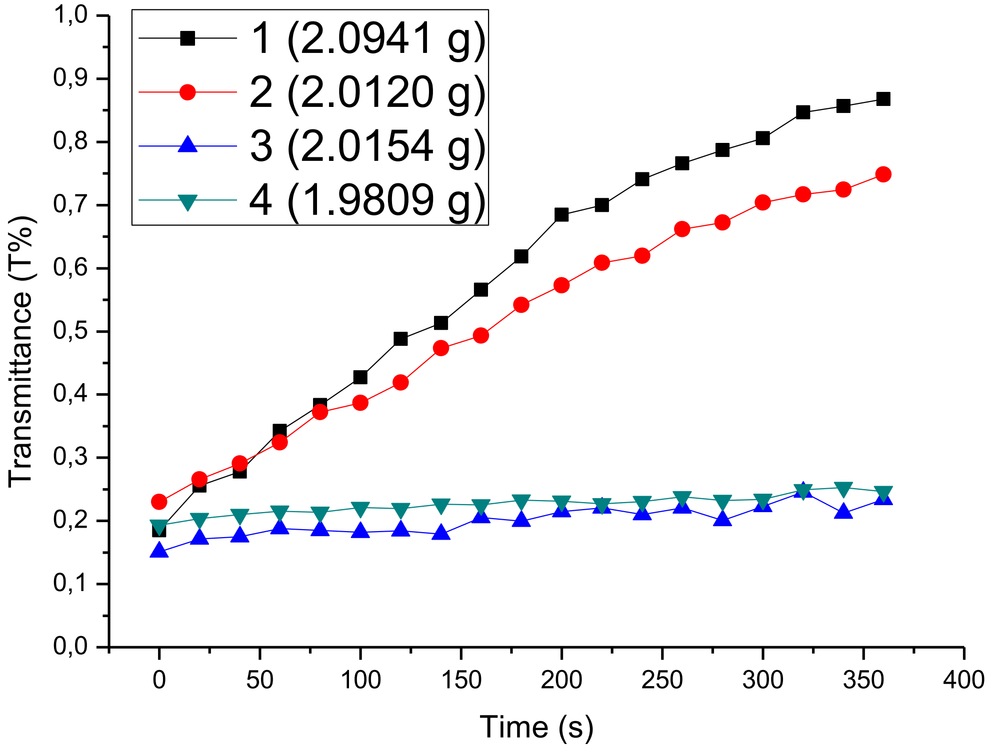

Figure 2. Transmittance (555 nm) over time for a representative pellet of each composition

These results have important implications regarding the effective dispersal and persistence of pyrotechnically generated smoke. Surprisingly, relatively minor changes to the compositions can markedly influence the measured opacity of the resulting smoke clouds over time. This is despite the fact that the initial equilibrated transmittance values are quite similar in several cases. Steadily increasing transmittance values indicate sedimentation of smoke particles. This may be due to larger particles having been formed initially, or to agglomeration of the particles over time. Notably, the compositions containing 5-AT as the main fuel, and no sucrose, displayed the lowest transmittance values over time, and remained stable over the entire measurement period. This suggests that certain formulations containing 5-AT are able to produce a thick, yet well-dispersed aerosol that is quite persistent and resistant to sedimentation.

Interestingly, measurements of the yield factor (Y) indicate that formulations **3** and **4** do not produce a larger amount of aerosol (see additional aerosol quantification in the supporting information section). This implies that the improved performance, in this case, is the result of other aerosol properties, the investigation of which is beyond the scope of this particular report. It is also apparent that the performance of the compositions is not directly related to, or controlled by, the TA content (as a comparison of formulations **2** and **4** demonstrates). However, it is clear that sucrose is not required in the compositions and 5-AT can be used instead, in similar amounts. Finally, the behaviour of formulations **3** and **4** suggests that in future work, 5-AT should be investigated as the main fuel in a variety of sublimation/condensation-type smoke systems.

4 Conclusions

The development of four new white smoke formulations based on TA was reported. All formulations were characterized by means of IS/FS/ESD/T_{onset} as well as their obscuration properties (transmittance). The low sensitivity towards physical stimuli is a promising fact for safe handling and manufacturing. In two out of the four formulations, a fuel mixture of 5-AT and sucrose was applied. Applying 5-AT as the main fuel resulted in the two best performing formulations, **3** and **4,** in terms of transmittance values and this provides a reason to explore 5-AT as the main fuel in other smoke formulations. Furthermore the behaviour of these two formulations suggests that a higher amount of 5-AT can compensate for a reduced amount of TA, resulting in the same transmittance values. Firm answers regarding the performance in actual devices can only be obtained once the compositions are tested on a larger scale in representative configurations. This includes a comparison to the M83 TA white smoke grenade in a full-scale test. In future work, the characterization of the aerosols produced by selected compositions, as well as determination of the aerosol particle size distribution should be performed. A scanning mobility particle size spectrometer (SMPS) may be appropriate for these investigations.

References

[1] Shaw, A. P.; Diviacchi, G.; Black, E. L. Advanced Boron Carbide-based Visual Obscurants for Military Smoke Grenades. *International Pyrotechnics Seminar*, *40th*, Colorado Springs, CO, USA, 13-18 July, **2014**, 170-191.

[2] a) Koch, E.-C. 1916-2016: The Berger Smoke Mixture Turns 100. *Propellants Explos. Pyrotech*. **2016**, *41*, 779.; b) Turetsky, A. L.; Young, G. P. Advances in Pyrotechnically Based

Visual Smoke Systems. *International Pyrotechnics Seminar*, *13th*, Grand Junction, CO, USA **1988**, 805-811.

[3] a) Conkling, J. A.; Mocella, C. *Chemistry of Pyrotechnics: Basic Principles and Theory*. 2nd ed., Taylor & Francis, New York **2010**; ISBN 978-1-4200-1809-7; b) Freiwald, H.; Preahauser, G.; Schießl, A. Improvements with Pyrotechnical Smoke. *International Pyrotechnics Seminar*, *6th*, Estes Park, CO, USA **1978**, 185-208.

[4] a) Cichowicz, J. J. *Programmatic Life Cycle Environmental Assessment for Smoke/Obscurants, HC Smoke*, Vol. 4, National Academy Press, Washington D.C **1983**; b) Holmes, P. S. Pneumomediastinum Associated with Inhalation of White Smoke. *Mil. Med*. **1999**, *164*: 751-752.

[5] a) Eaton, J. C.; Lopinto, R. J.; Palmer, W. G. *Health Effects of Hexachloroethane (HC) Smoke*. Accession Number ADA277838, Defense Technical Information Center (DTIC), Fort Belvoir, VA, **1994**, 1-60; b) Agency for Toxic Substances and Disease Registry, *Toxicological Profile for Hexachloroethane*, Accession Number CBRNIAC-CB-069808, Defense Technical Information Center (DTIC), Fort Belvoir, VA, USA **1994**, 1-60.

[6] Sabatini, J. J. *Advances Toward the Development of "Green" Pyrotechnics, in Green Energetic Materials*. John Wiley & Sons, Ltd, Chichester, United Kingdom **2014**; ISBN 9781119941293.

[7] a) Koch, E.-C. Special Materials in Pyrotechnics: V. Military Applications of Phosphorus and its Compounds. *Propellants Explos. Pyrotech.* **2008**, *33*: 165-176; b) Koch, E.-C.; Schneider, J. Reactions in Phosphorus based IR-screening Smoke – An Investigation of the Underlying Phenomena. *Proceedings of Smoke and Obscurants Symposium*, *20th*, Aberdeen Proving Ground, Maryland, USA, April **1998**, 3.

[8] a) Sordoni, N.; Heard, W.; Rouse, W. *Pyrotechnical Smoke Analysis*, Volume 1, Defense Technical Information Center (DTIC), Fort Belvoir, VA, **1993**; b) Lane, G. A.; Smith, W. A.; Jankowiak, E. M. Novel Pyrotechnic Compositions for Screening Smokes. *International Pyrotechnics Seminar*, *1st*, Estes Park, CO, USA, **1968**, 25-39.

[9] a) Koch, E.-C.; Cudziło, S. Safer Pyrotechnic Obscurants Based on Phosphorus(V) Nitride *Angew. Chem*. *Int. Ed.* **2016**, *55*: 15439; b) Fisher, K.; Montgomery, F.; Phipps, A.; Nugent, T.; Hubble, R. An Evaluation of Using Microencapsulated Red Phosphorus in Marine Location

Marker Pyrotechnic Compositions. *International Pyrotechnics Seminar*, *28th*, Adelaide, Australia **2001**, 273-282.

[10] Hemmilä, M.; Hihkiö, M.; Kasanen, J.-P.; Turunen, M.; Järvelä, M.; Suhonen, S.; Pasanen, A.-L.; Norppa, H. Cytotoxicity and Genotoxicity in vitro and Irritation Potency in vivo of Two Red Phosphorus-based Pyrotechnic Smokes. *Mutat. Res., Genet. Toxicol. Environ. Mutagen.* **2010**, *701*(2): 137-144.

[11] Shaw, A. P.; Brusnahan, J. S.; Poret, J. C.; Morris, L. A. Thermodynamic Modeling of Pyrotechnic Smoke Compositions. *ACS Sustainable Chem. Eng*. **2016**, *4*: 2309-2315.

[12] Shaw, A. P.; Poret, J. C.; Gilbert, R. A.; Domanico, J. A.; Black, E. L. Development and Performance of Boron Carbide-Based Smoke Compositions. *Propellants Explos. Pyrotech*. **2013**, *38*: 622-628.

[13] Muse, W. T.; Anthony, J. S.; Bergmann, J. D.; Burnett, D. C.; Crouse, C. L.; Gaviola, B. P.; Thomson, S. A. Chemical and Toxicological Evaluation of Pyrotechnically Disseminated Terephthalic Acid Smoke. *Drug Chem. Toxicol.* **1997**, *20*: 293-302.

[14] a) Hemmilä, M.; Hihkiö, M.; Kasanen, J.-P.; Turunen, M.; Hautamäki, M.; Pasanen, A.-L.; Linnainmaa, K. In Vivo and In Vitro Evaluation of the Acute Toxicity, the Genotoxicity, and the Irritation Potency of Two Hexachloroethane-based Pyrotechnic Smokes. *J. Toxicol. Environ. Health*, Part A **2007**, *70*: 1167-1181; b) van Hulst, M.; Langenberg, J.; de Klerk, W.; Alblas, M. Acute Toxicity Resulting from Human Exposures to Military Smokes. *Propellants Explos. Pyrotech*. **2017**, *42*: 17.

[15] Moretti, J. D.; Sabatini, J. J.; Shaw, A. P.; Gilbert, R. Promising Properties and System Demonstration of an Environmentally Benign Yellow Smoke Formulation for Hand-Held Signals. *ACS Sustainable Chem. Eng*. **2014**, *2*: 1325-1330.

[16] Chen, G.; Showalter, S.; Raibeck, G.; Wejsa, J. *Enivronmentally Benign Battlefield Effects Black Smoke Simulator*. Accession Number ADA481520, U.S. ARMY RDECOM-ARDEC, Picatinny, NJ 07806-5000, USA **2006**.

[17] Glück, J.; Klapötke, T. M.; Rusan, M.; Shaw, A. P. Improved Efficiency by Adding 5-Aminotetrazole to Anthraquinone-Free New Blue and Green Colored Pyrotechnical Smoke Formulations. *Propellants Explos. Pyrotech*. **2017**, *42:* 131.

[18] Oakes, J; Gratton, P. Kinetic Investigations of the Oxidation of Methyl Orange and Substituted Arylazonaphthol Dyes by Peracids in Aqueous Solution. *J. Chem. Soc., Perkin Trans. 2*, **1998**, 2563-2568.

[19] Fish, C.; Chen, G. Characterization of Magnesium Carbonate for Use in Pyrotechnic Smoke Composition as a Thermal Regulator. *International Pyrotechnics Seminar*, *35th*, Fort Collins, CO, USA **2008**, 83-93.

[20] Embury, J. F.; Walker, D.; Zimmermann, C. J. *Screening Smoke Performance of Commercially Available Powders, II, Visible Screening by Titanium Dioxide*. Accession Number ADA284072, Defense Technical Information Center (DTIC), Fort Belvoir, VA, USA **1994**, 1-30.

Supporting Information

The transmittances (555 nm) over time values are presented for each formulation (Fig. 1 – 4). For each formulation at least 4 pellets were tested (Table 1). The data points were recorded starting from t = 0 s every 20 s for 6 min. For every pellet, the average of recorded data points is calculated and further averaged with all pellets from one formulation. The obtained value is called "average transmittance (555 nm) over time" and used for comparison of the different smoke formulations.

Table 1. Transmittance (555 nm) over time for each formulation

	Pellet 1	Pellet 2	Pellet 3	Pellet 4	Average transmittance (555 nm) over time[a]	Standard deviation
1 (79)	0.56257	0.62138	0.56954	0.5848	0.585	0.026
2 (82)	0.51710	0.55267	0.57401	0.48019	0.531	0.041
3 (347)	0.20015	0.19131	0.23536	0.23591	0.216	0.023
4 (350)	0.23167	0.22645	0.21456	0.24005	0.228	0.011

Annotation: a = average of collected transmittance values at 555 nm over time for all pellets

The plots show the transmittance (555 nm) over time for each formulation. The y-axis shows the transmittance [%], the x-axis gives the time [s]. The exact mass of each pellet [g] is depicted in each graph (e.g. 1.9913 g, 2.0350 g, 2.0800 g, 2.0941 g in Fig. 1).

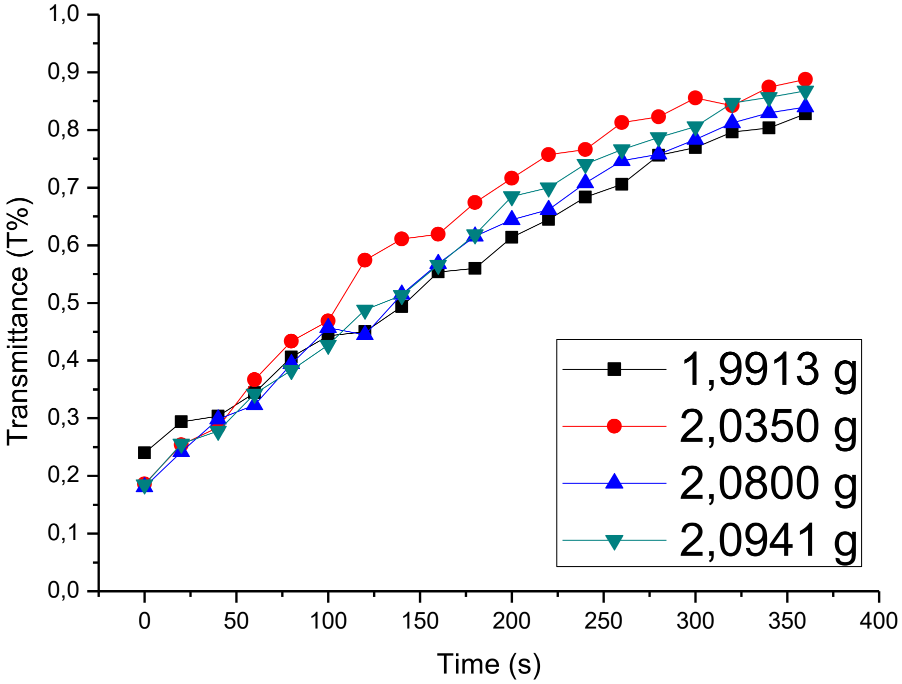

Figure 1. Transmittance (555 nm) over time of formulation 1

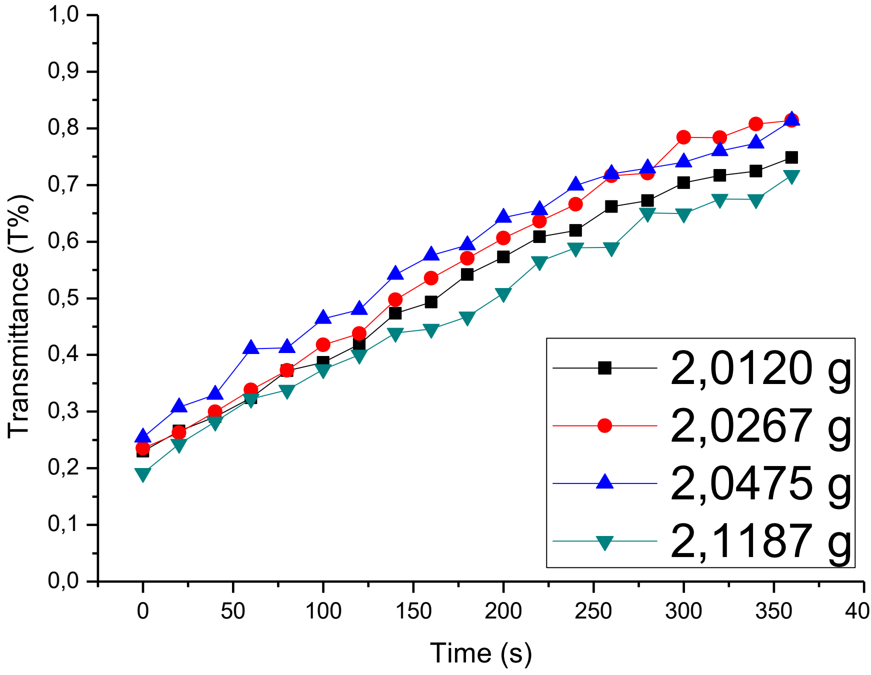

Figure 2. Transmittance (555 nm) over time of formulation 2

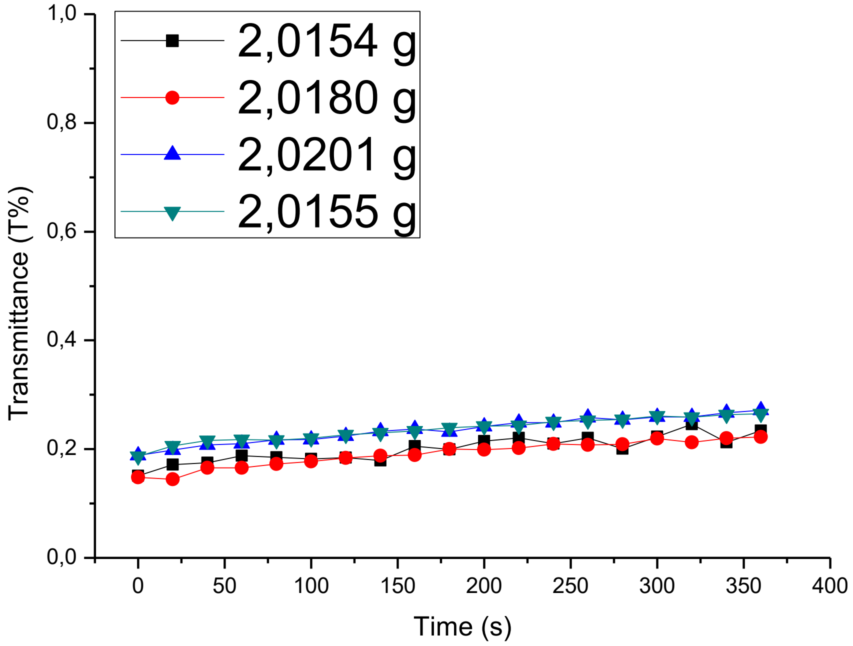

Figure 3. Transmittance (555 nm) over time of formulation 3

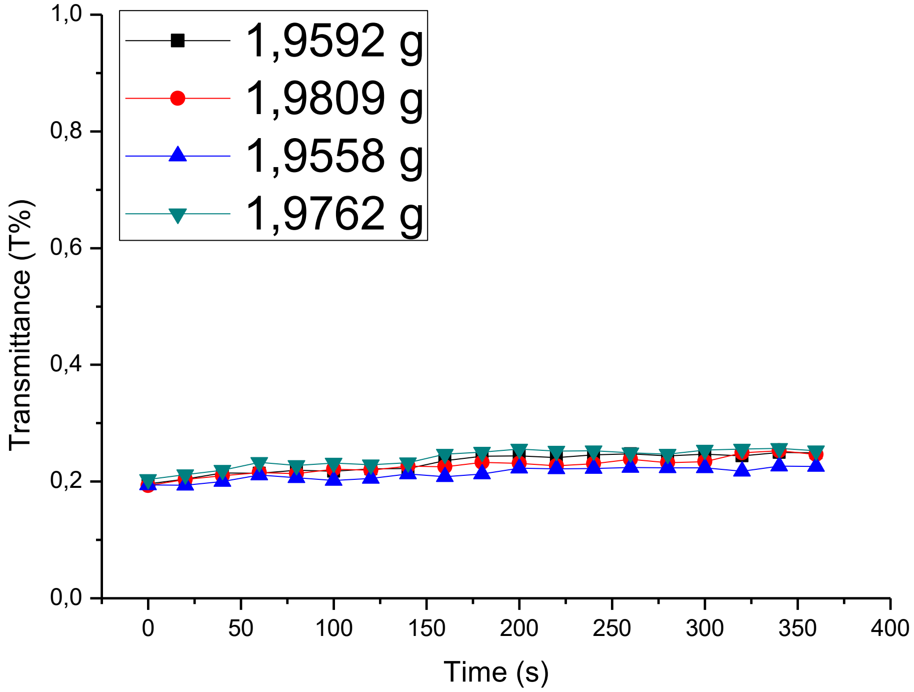

Figure 4. Transmittance (555 nm) over time of formulation 4

Table 2. Averaged burning time of tested formulations

Formulation	Burning time [s]	Standard deviation [s]
1	28	1
2	33	3
3	28	1
4	26	1

Determination of the yield factor

The experimental setup was described earlier in following journal [A]:

[A] J. Glück, T. M. Klapötke, M. Rusan, A. P. Shaw, *Propellants., Explos., Pyrotech.* **2017**, *42*, 131-141.

Table 3. Yield factor of tested formulations

Formulation	Yield factor	Standard deviation	Relative humidity [%]
1	0.274	0.028	66
2	0.309	0.053	61
3	0.237	0.014	61
4	0.229	0.039	63

Annotation: Yield factor = mass of aerosol/mass of pyrotechnical payload

The quantification of the aerosol revealed that formulation **1** and **2** produced more aerosol compared to the sugar-free formulations. Since the recorded transmittance values show a better performance for formulation **3** and **4**, it may be concluded that the either a higher degree of dispersion or different resulting combustion products are responsible for this behavior. A higher amount of aerosol, neglecting the resulting particle size or degree of dispersion, is therefore no guarantee for a better performance.

Differential Thermal Analysis (DTA) of tested formulations (Fig. 5 -8):

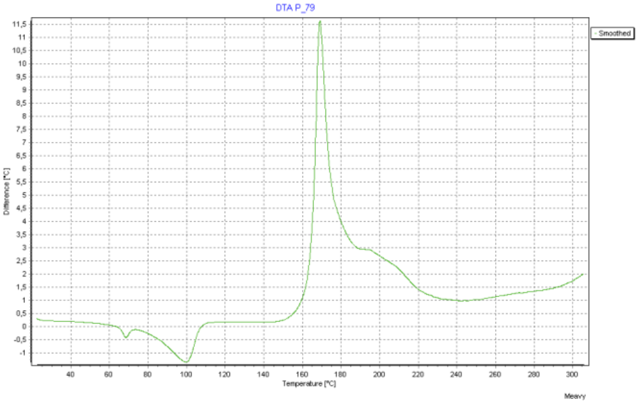

Figure 5. DTA (5°C/min) of formulation 1

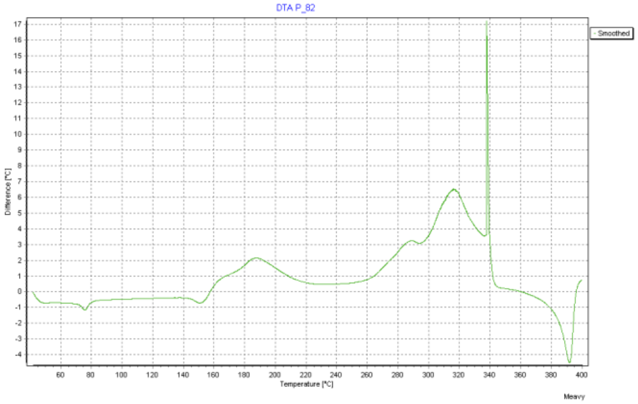

Figure 6. DTA (5°C/min) of formulation 2

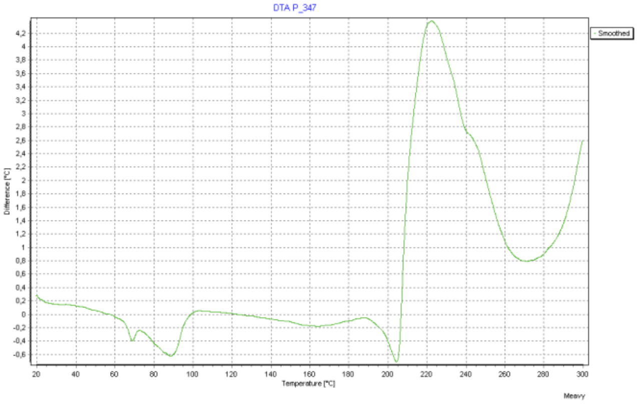

Figure 7. DTA (5°C/min) of formulation 3

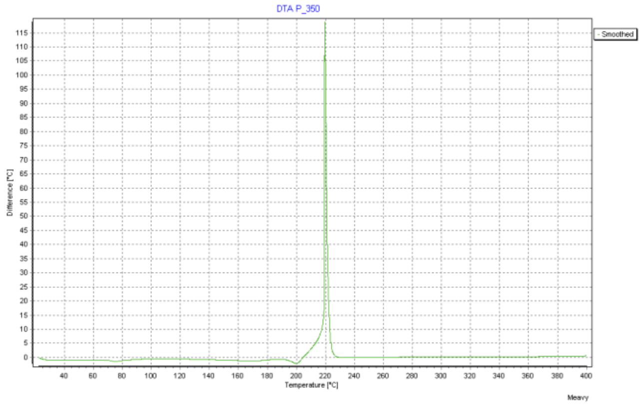

Figure 8. DTA (5°C/min) of formulation 4

All DTA graphs showed an endothermic peak in the range of 60 – 80°C which might be correlated to stearic acid (see Fig. 14). Formulation **1** and **2** (see Fig. 5/6) showed an exothermic peak for sucrose in the range of 160 – 200 °C. In contrast, formulation **3** and **4** (see Fig. 7/8) did not conatin this peak. The exothermic peak at 220 °C can be correlated to 5-aminotetrazole (see Fig. 10). The DTA of terephthalic acid (TA) showed no decomposition point, but a strong endothermic behavior starting from 330 °C (see Fig. 12).

Differential Thermal Analysis (DTA) of single components (Fig. 9 – 16):

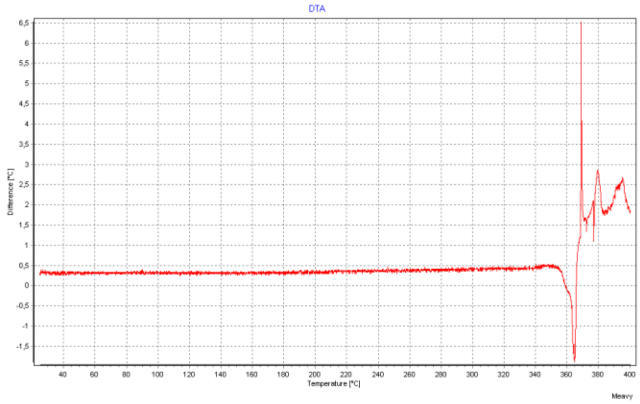

Figure 9. DTA (5°C/min) of $KClO_3$

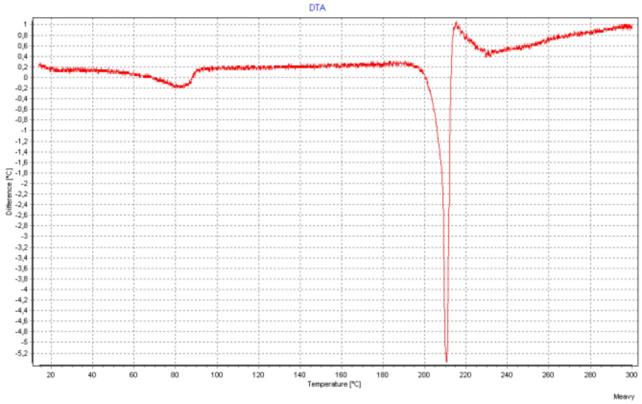

Figure 10. DTA (5°C/min) of 5-aminotetrazole

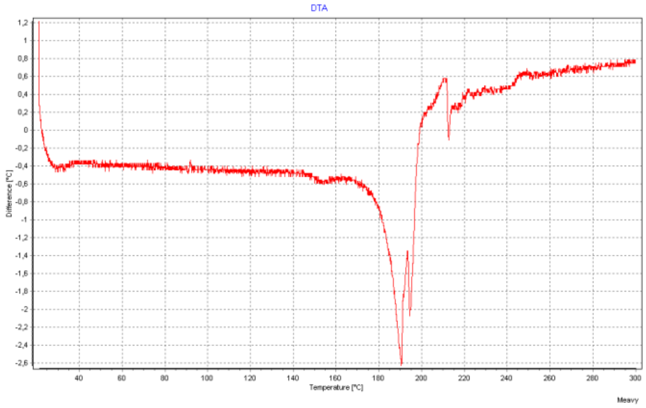

Figure 11. DTA (5°C/min) of sucrose

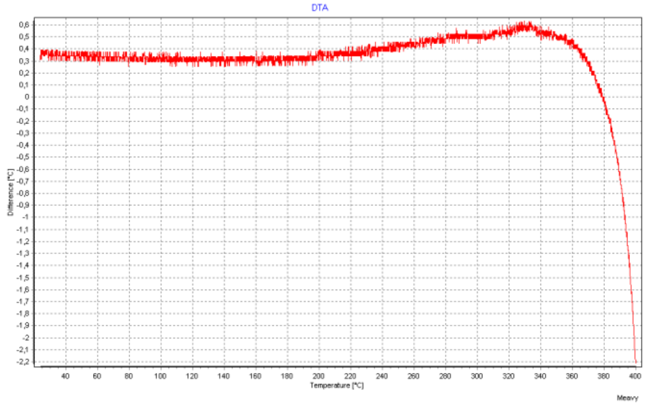

Figure 12. DTA (5°C/min) of terephthalic acid

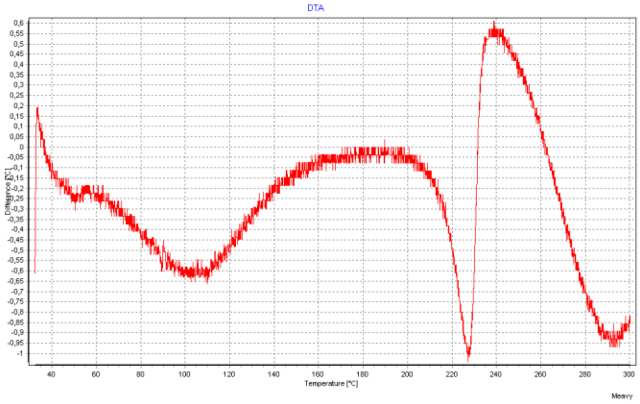

Figure 13. DTA (5°C/min) of PVA

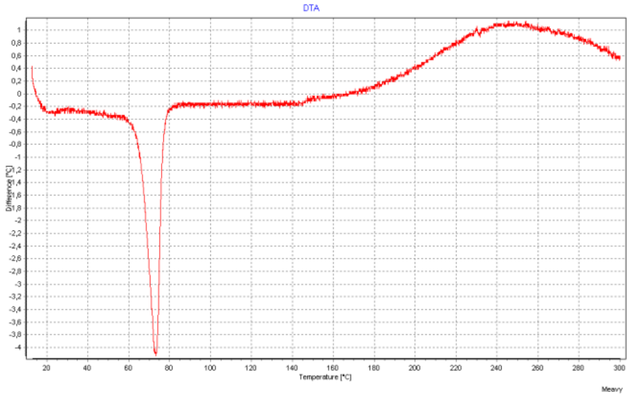

Figure 14. DTA (5°C/min) of stearic acid

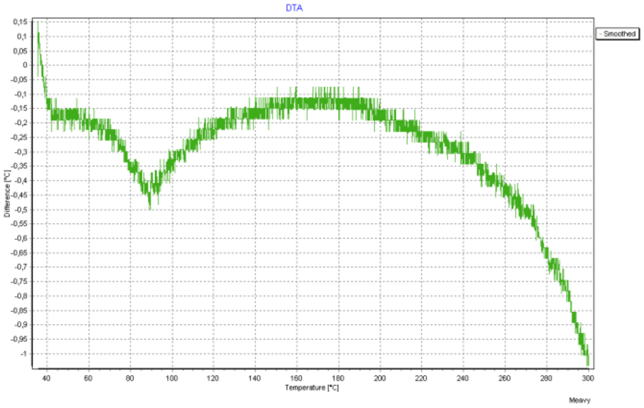

Figure 15. DTA (5°C/min) of MCHP

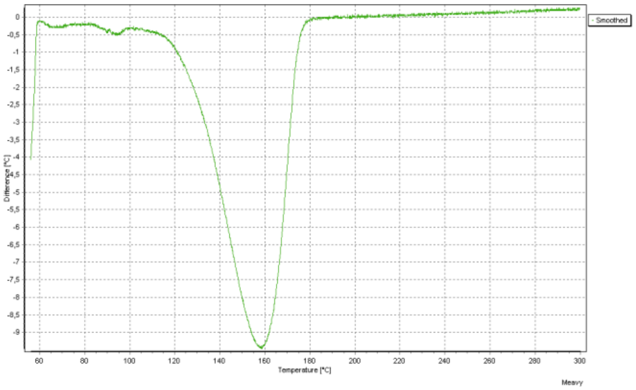

Figure 16. DTA (5°C/min) of $NaHCO_3$, measurement started at elevated temperatures (60 °C), no decomposition before 60 °C

3.3 5-Amino-1*H*-Tetrazole-Based Multi-Coloured Smoke Signals Applying the Concept of Fuel Mixes

Published in *New. J. Chem.* **2018**, *42,* 10670-10675. (DOI: 10.1039/C8NJ01786G) - *Reproduced by permission of The Royal Society of Chemistry (RSC) on behalf of the Centre National de la Recherche Scientifique (CNRS) and the RSC*

The development of sugar-free multi-coloured smoke formulations, so-called *fuel mixes* is reported. These simple four ingredient-based mixtures of dye, potassium chlorate, 5-amino-1*H*-tetrazole and a magnesium carbonate derivative are able to produce a variety of colours by applying the same pyrotechnical system. All components except the dye are pre-mixed; the dye is added in the final step. Based on previous results which indicated an overall higher smoke performance in terms of efficiency and persistence by applying 5-amino-1*H*-tetrazole as fuel in smoke formulations, we developed new coloured smoke formulations. For big producers as well as consumers, the concept of fuel mixes is an effective way to reduce costs and provide a higher degree of safety. In this article, the focus was on dyes applied in the U.S. M18 coloured smoke grenades

Introduction

Coloured smoke signals are a non-electronic communication tool for both ground as well as ground-to-air signalling.[1] During daytime, the big benefit compared to light-emitting signals is the high visibility over greater distances, when employed against a terrain background of contrasting colour.[1b] In this context, the most perceptible colour contrast displaying optimum visibility at a considerable distance is offered by red, green, yellow and violet, thereby creating great research interest.[2] A rather new segment in the market for coloured smokes is the so-called *daylight firework*.[3] Similar to classical firework displays at night, these formulations create visible effects such as smoke trails or fountains at daytime. Daylight fireworks might be used for any daytime events like sport competitions, religious celebrations and cultural events like museum openings.[3] So far, the biggest consumer of smoke signals still remains the military sector. For decades, coloured smoke signals are valuable in the military for marking unit flanks, target locations, drop zones, and medical evacuation landing sites.[1b, 1c, 4] This also includes marine distress signals, which are an essential part of any safety equipment inventory in the shipping industry as well as sport activities.[5] For both civilian and military application, the formulation compounds remain the same. Typically, smoke-generating compositions consist of an oxidizer/fuel pair providing the heat to vaporize the dye.[6] The coolant keeps the reaction temperature in the desired range, while other additives may be used to modify the mechanical or burning properties.[7] Historically, the old M18 coloured smoke grenades contained an anthraquinone-based dye mixed with sulfur, potassium chlorate and sodium bicarbonate. Further, an optional amount of refined kerosene and tricalcium phosphate for control of dusting and caking could be added.[8]

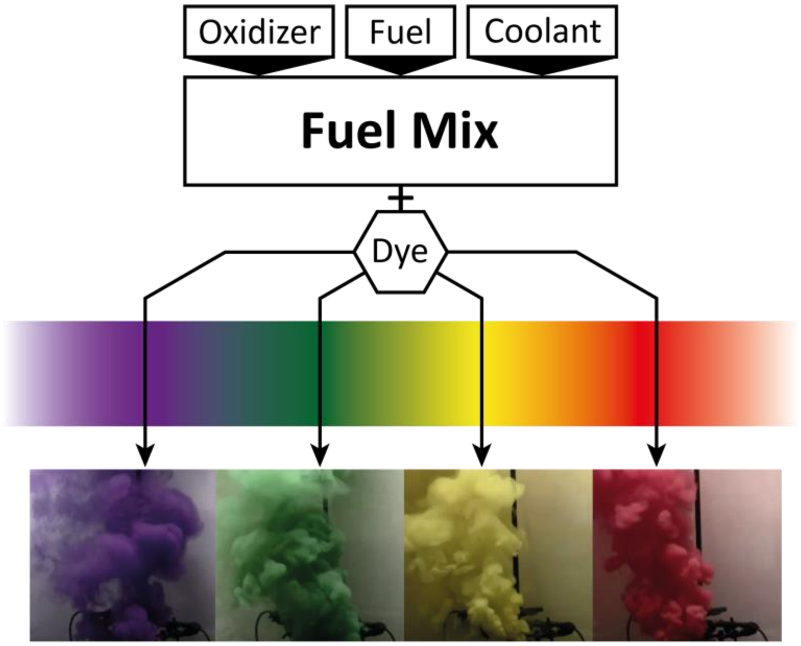

Figure 1: The concept of fuel mixes.

However, due to toxicity and health issues, these smoke compositions are no longer produced, since they are suspected to release hazardous SO_2 during combustion. An indication for this is provided by soldiers perceiving a burning sensation in their lungs when inhaling such smoke.**[4c]**

For this reason, these early smoke signals, which were already applied during the World War II era, do not meet today's environmental demands anymore and are therefore under constant evaluation for reformulation.[4c, 9] Sugar was considered as a less toxic alternative to the widely applied sulfur-containing formulations.[9a, 10] Compared to the former produced sulfoxides, the now resulting combustion products derived from sugars contain only harmless H_2O and CO_2.[4c]

A look in the literature revealed, that there is only a limited number of information provided about the percentage of dye actually sublimed upon combustion of the signal.**[11]** The question arises, whether it is possible to apply alternative fuels, which might improve the smoke dispersal, efficiency, and persistence. As a consequence, the amount of hazardous dyes could be reduced to its minimum, while providing the same colour impression. Unfortunately, each coloured smoke dye has a different enthalpy of sublimation affecting the resulting behaviour and performance of a coloured smoke formulation.**[4c]** For this reason, up to now every single dye needs its own optimized pyrotechnical formulation to meet the requirements for burn time and colour quality. A possible solution to this circumstance might be the development of so-called *fuel mixes* (Fig. 1).**[4b]** Essentially, fuel mixes are combinations of certain components such as the oxidizer/fuel pair and further, other additives like coolant or minor fuels. These ingredients are pre-mixed and subsequently combined with a smoke dye.

The great benefit for producers and consumers is that the need to have a certain number of different smoke formulations in stock serving each colour is gone. In comparison to the conventional smoke signals, the quick-mixing of only two pre-mixed powders (fuel mix + dye) with known quality produces the desired smoke colour. As a result, not only the required space for safe storage is reduced dramatically, but also the total amount of energetic materials stored in the same place drops accordingly. Based on previous work carried out within our group, we investigated the effect of applying 5-amino-1*H*-tetrazole (5-AT) as main fuel in so-called *fuel mixes*.[11] Hereby, the main combustion product of the fuel would be N_2.[12] The slightly higher decomposition temperature compared to sucrose allowed the application as alternative fuel. The small temperature difference itself might be partially explained by the existence of non-oxidized bonds in 5-AT. $KClO_3$ in combination with 5-AT served as the oxidizer/fuel pair; magnesium carbonate hydroxide pentahydrate (MCHP) was the coolant. Most of the applied dyes belong to the anthraquinone group. Disperse Red 9 ((1-methylamino) anthraquinone) was applied for red, Solvent Green 3 (1,4-di-*p*-toluidino-9,10-anthraquinone) for green and Solvent Yellow 33 (2-(2-quinolyl)-1,3-indandione) for yellow. Moreover, to obtain a violet smoke signal the Violet Smoke Dye Mix consisting of the two dyes Disperse Red 9 and Solvent Violet 47 (1,4-diamino-2,3-dihydroxyanthraquinone) were applied.[4b]

In a first step different ratios of the pre-mixed powders (oxidizer + fuel + coolant = fuel mix) and the dye were tested to give a coloured smoke cloud. The second step focused on adapting the colour. Diviacchi stated earlier, that the actual colour impression of the emerging smoke may be different from the labelled colour.**[4b]** To overcome this issue, we applied a dye mixture in case the colour was too dark or brighter than intended. The focus of the herein presented results was on the dyes applied in the U.S. M18 coloured smoke grenades and mixtures thereof.**[13]** At this point, we were not interested in investigating the toxicity issues arising from the dyes or resulting combustion products.**[4b, 8b, 13-14]** Instead, we developed three different 5-AT-based fuel mixes (**FM1**, **FM2**, **FM3**) and compared them towards a sucrose-based reference formulation (**Ref-FM**) of the same dye in terms of performance and smoke persistence. HPLC measurements were carried out to quantify the effective amount of dye present in the collected aerosol.

Experimental

Chemicals and Sample Preparation. Sucrose (≥ 99 %), and magnesium carbonate hydroxide pentahydrate (BioXtra) were purchased from Sigma-Aldrich. 5-AT (98 %) was purchased from abcr chemicals. Potassium chlorate (≥ 99 %) was purchased from Grüssing GmbH. Disperse Red 9, Solvent Green 3, Solvent Yellow 33 and the Violet Mix Smoke Dye were purchased by Nation Ford Chemical. For initial testing, small mixtures (2 g) were carefully mixed manually for 5 min in a mortar by combining the dry compounds. If those tests were successful, larger mixtures (40 g) were prepared by combining the dry components in a cylindrical rubber barrel and rolling for 120 min. The rotatory rock tumbler (model 67631) was built by "Chicago Electric Power Tools" and operated with steel balls. To remove any clumps, the compositions were passed through an 800 µm screen. 2 g of this so prepared composition was pressed into a cylindrical steel compartment (diameter 2.0 cm), with the aid of a tooling die and a hydraulic press. The used consolidation dead load of 3000 kg was applied for 3 s, if not stated otherwise. Each pellet was ignited using a resistance heating Kanthal® A1 wire (FeCrAl, 0.8 mm diameter, 2.9 Ω m^{-1}). For each composition, three pellets were tested and the results were averaged.

Aerosol Quantification. The experimental setup to collect the aerosol was described previously.[11] A Thermo Scientific™ DIONEX™ UltiMate™ 3000 HPLC System (accucore RP-MS column (3.0 x 150.0 mm, particle size 2.6 µm) with a DAD-3000 photometer and Chromeleon® 7.2 Chromatography Management Software was used to quantify the amount of dye (see ESI for exact method). The measurements were performed in cooperation with the *CBRN Defense, Safety and Environmental Protection School* of the German *Bundeswehr* (CDSEP-School), Sonthofen (Germany).

Burn Rate. The testing protocols as well as pellet sizes are given in the ESI. However, we were facing serious problems to determine the burn rate at different pellet sizes. Some formulations which produced smoke on a rather small height/diameter ratio burned with an open flame at higher height/diameter ratios. The collected data for two different pellet sizes is provided in the ESI.

Sensitivities and Thermal Stability. The impact and friction sensitivities were determined using a BAM Drophammer and a BAM Friction Tester (method 1 of 6). The sensitivities of the compositions are indicated according to the UN Recommendations on the Transport of Dangerous Goods (+): impact: insensitive > 40 J, less sensitive ≥ 35 J, sensitive > 4 J, very sensitive < 4 J; friction: insensitive > 360 N, less sensitive = 360 N, sensitive 360 N > x > 80 N, very sensitive < 80 N, extreme sensitive < 10 N.[16] Thermal stability measurements. Onset temperatures were measured with an OZM Research DTA 552-Ex Differential Thermal Analyzer at a heating rate of 5 °C min^{-1}. Electrostatic discharge was measured with an OZM small-scale electrostatic spark X SPARK 10. ESD: sensitive < 0.1 J, insensitive > 0.1 J.

Results and Discussion

Development of Coloured Smokes. A suitable starting point to fulfil the concept of fuel mixes is an exactly stated testing protocol as outlined by Domanico (see ESI).[4a] Due to the existing differences in terms of physical behaviour and chemical stability, a screening of several different fuel mix ratios was performed. Therefore, the amount of dye (30 %) was fixed, while the remaining 70 % was the respective fuel mix. The first step of this presented study was the investigation of working smoke compositions for each dye separately. Subsequently, the optical performance evaluation included the emerging colour impression, smoke thickness as well as burning behaviour. The most advanced formulations were selected for further testing and evaluation, such as yield, burn time and rate, transfer rate and sensitivity towards mechanical stimuli as well as thermal stability (Table 1). A fuel mix might be more sensitive than the final coloured smoke formulation. To ensure safe handling in every single manufacturing step, e.g. the mixing and grinding of fuel mixes starting from the single components or the final coloured smoke formulations, the sensitivities have to be determined also for all intermediate steps.

The most promising fuel mixes for further characterization are illustrated within a ternary diagram (Fig. 2). The first fuel mix **FM1** consisted of 50 wt% 5-AT, 30 wt% $KClO_3$ and 20 wt% MCPH and therefore, contained the highest amount of oxidizer. **FM2** had a ratio of 50 wt% 5-AT to 20 wt% $KClO_3$ to 30 wt% MCPH and **FM3** had the highest amount of the fuel 5-AT (60 wt%) and equal contents of $KClO_3$ and MCPH (20 wt%). The reference fuel mix **Ref-FM** contained 40 wt% sucrose, 40 wt% $KClO_3$ and 20 wt% MCPH (see ESI for a complete listing of formulation ingredients and weight percentages). Further, the properties of the resulting coloured smoke formulations based on these fuel mixes are summarized in Table 1.

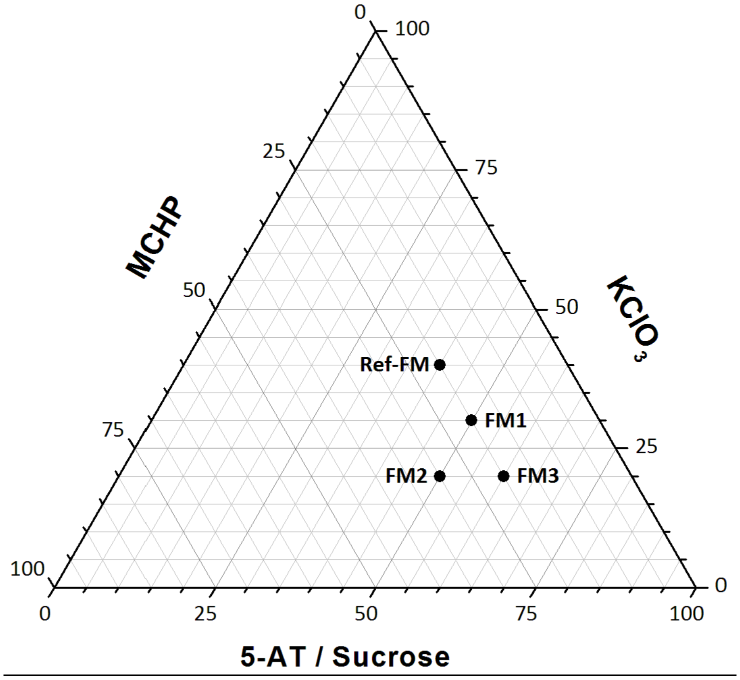

Figure 2: Developed fuel mixes. **FM1** = 5-AT (50 wt%), $KClO_3$ (30 wt%), MCHP (20 wt%); **FM2** = 5-AT (50 wt%), $KClO_3$ (20 wt%), MCHP (30 wt%); **FM3** = 5-AT (60 wt%), $KClO_3$ (20 wt%), MCHP (20 wt%); **Ref-FM** = sucrose (40 wt%), $KClO_3$ (40 wt%), MCHP (20 wt%). See Table 2 and Table 3 for a complete listing of formulation ingredients, weight percentages and the ESI for brief explanation of the triangle diagram.

Properties of Coloured Smoke Formulations. In this context, formulations **Y1**, **G1**, **R1** and **V1** were referred to **FM1**, while **FM2** was the basis for **Y2**, **G2**, **R2** and **V2**. The compositions **Y3**, **G3**, **R3** and **V3** were based on **FM3** and fuel mix **Ref-FM** resulted in coloured reference formulations.

Table 1: Properties of yellow-, green-, red- and violet-coloured smoke formulations based on fuel mixes **FM1**, **FM2**, **FM3** and **Ref-FM**.

	BT /s	**Y** /%	**T%** /%	m_{HPLC} /mg	**ESD** /J	T_{onset} /°C
Y1	15	29	59	354	1.0	184
Y2	26	21	56	233	0.4	189
Y3	29	30	49	292	0.5	187
Ref-Y	13	33	73	435	0.3	178
G1	20	36	–	–	0.4	192
G2	45	24	–	–	0.2	198
G3	31	31	–	–	0.5	194
Ref-G	19	32	–	–	0.2	172
R1	20	29	76	457	0.5	184
R2	75	25	58	351	0.7	182
R3	41	28	72	432	0.5	189
Ref-R	21	36	86	514	0.6	172
V1	23	29	–	–	0.2	182
V2	27	26	–	–	0.3	186
V3	27	29	–	–	0.3	180
Ref-V	15	32	–	–	0.7	178

Annotation: measured for 2.0 g pellet; BT = burn time; Y = yield; T% = transfer rate; m_{HPLC} *= dye content present in aerosol; ESD = electric discharge sensitivity;* T_{onset} *= onset temperature of decomposition; impact sensitivity = 40 J for all measured formulations (only Ref-G/Ref-V = 30 J); friction sensitivity = 360 N for all measured formulations; see ESI for summary of all determined properties.*

In detail, **FM1**- and **Ref-FM**-based formulations resulted in rapid, strong smoke generation, while **FM2**- and **FM3**-based compositions produced smoke continuously over a longer period of time. This trend was also reflected in terms of burn time (**FM1** or **Ref-FM**: 12–23 s compared to **FM2** or **FM3**: 26–45 s) as well as burn rate. An exception was **R2** with the overall longest burn time of 75 s. All tested coloured smoke formulations were insensitive towards impact and friction except of **Ref-G** and **Ref-V**, which were classified as less sensitive. Moreover, all compositions were insensitive towards electrostatic discharge. The decomposition temperatures were in the range of 172–198 °C.

Table 2: Yellow- and green-colored smoke formulations based on fuel mixes **FM1**, **FM2**, **FM3** and **Ref-FM** in weight percent [wt%].

	Y1	Y2	Y3	G1	G2	G3	Ref-Y	Ref-G
$KClO_3$	21	14	14	21	14	14	28	28
5-AT	35	35	42	35	35	42	–	–
MCHP	14	21	14	14	21	14	14	14
Sucrose	–	–	–	–	–	–	28	28
Solvent Yellow 33	30	30	30	10	10	10	30	10
Solvent Green 3	–	–	–	20	20	20	–	20

Table 3: Red- and violet-colored smoke formulations based on fuel mixes **FM1**, **FM2**, **FM3** and **Ref-FM** in weight percent [wt%].

	R1	R2	R3	V1	V2	V3	Ref-R	Ref-V
$KClO_3$	21	14	14	21	14	14	28	28
5-AT	35	35	42	35	35	42	–	–
MCHP	14	21	14	14	21	14	14	14
Sucrose	–	–	–	–	–	–	28	28
Disperse Red 9	30	30	30	–	–	–	30	–
Violet Smoke Dye Mix	–	–	–	30	30	30	–	30

The measurements of all coloured smoke formulations and their references were carried out on approximately similar humidities (see ESI). More precisely, the performance and in particular the yield *Y* of hygroscopic smoke mixtures is strongly dependent on the relative humidity, since at higher humidity levels higher yields are obtained.[11a] It is noticeable, that the yield of **FM2** was significantly worse for all tested dyes in the range of 21–26 %. In contrast, formulations based on **FM3** were approximately as efficient as **FM1** (28–31 %) with the exception of **G1** (36 %). However, the yield of **Ref-FM**-based smoke compositions was slightly higher for yellow, red and violet smoke in the range of 32–33 %.

It has to be stated, that not all produced aerosol disseminated by coloured smoke formulations is in fact the implemented dye. More precisely, the term *aerosol* describes the total amount of produced non-gaseous reaction products including soot, water, dye and all other resulting combustion products. Whereas the information about the collected aerosol is sufficient for obscurants to calculate the yield (quotient between the amount of collected aerosol divided by the pyrotechnical payload), we were interested in the exact amount of dye present in the aerosol. The so-obtained values were used for the calculation of the previously introduced term of the *"transfer rate"* by the authors (quotient between the amount of actually dispersed dye divided by the amount of dye in the pellet).**[11a]** Dye which remains in the pyrotechnical device or is consumed by the flames does not contribute to the optical performance. The optimized ratio between the amount of applied dye and successfully dispersed dye would contribute to a more sustainable material life-circle, since less unburned material is spread into the environment. Due to the high solubility in organic solvents, HPLC analysis of the collected aerosol was performed and revealed the dye concentration in the aerosol (Table 1).

Discussion Transfer Rate / HPLC

HPLC measurements revealed a transfer rate of 49–73 % for the yellow smoke formulations. **Ref-Y** based on sucrose achieved the highest transfer rate, followed by **Y1** with 59 %.

Compared to the yellow smoke compositions, an increase of the transfer rate was observed for the red dye. Formulations **R1**–**R3** and **Ref-R** displayed transfer rates in the range of 58–86 %. Here again, the sucrose-based fuel mix achieved the best value followed by **R1**.

A change of the solution colour was observed for the violet dye mix in acetonitrile upon measurement. Re-running the measurements in darkened glass showed the same result displaying additional peaks. It was concluded, that the dye mix is not stable in solution and was therefore excluded from the HPLC measurements. The green formulations applying a mixture of two dyes proofed to be more difficult than expected and will be addressed in the future.

Properties of Fuel Mixes. The characterization of sensitivity data is mandatory for producers as well as consumers, since the handling, preparing and in particular storing of such fuel mixes need to be safe. Therefore, the sensitivities were determined additionally for the novel fuel mixes (Table 4).

Table 4. Sensitivity data of fuel mixes **FM1**, **FM2**, **FM3** and **Ref-FM**.

	IS /J	**FS** /N	**ESD** /J	**T_{onset}** /°C
FM1	6	252	1.5	331
FM2	20	360	0.3	342
FM3	20	360	0.1	337
Ref-FM	20	360	1.5	172

Annotation: IS = impact sensitivity; FS = friction sensitivity; ESD = electric discharge sensitivity; T_{onset} *= onset temperature of decomposition.*

In detail, the tested fuel mixes were sensitive towards impact, where the impact sensitivity of **FM1** was comparatively higher with 6 J. It is literature known that higher amounts of $KClO_3$ lead to higher sensitivities. Besides that, the exothermic decomposition process of $KClO_3$ causes an acceleration to the rate of reaction.[15] In contrast to this, **FM2**, **FM3** and **Ref-FM** were classified as insensitive towards friction, while **FM1** was sensitive. All samples were insensitive towards electrostatic discharge except of FM3 reaching the transition between sensitive and insensitive material. The onset temperatures of decomposition of 5-AT-based fuel mixes were significantly higher in the range of 331–342 °C in comparison with the sucrose-based reference **Ref-FM** (172 °C). Therefore, these fuel mixes are potentially sensitive energetic materials and must be handled with care and caution.[16]

Conclusions

The successful demonstration of 5-AT-based fuel mixes to produce green, yellow, red and violet smoke is presented. The developed formulations revealed that non-traditional high-nitrogen fuels can produce smoke of high colour quality. More precisely, **FM1**-based mixtures resulted in a rapid, strong smoke generation in a short time, while **FM3**-based compositions were characterized by a slow, continuous smoke generation over a much longer period of time. 5-AT is only one of the potential candidates, which should be considered for future investigations. Sensitivity measurements revealed that all developed formulations are insensitive towards friction. In addition, all developed 5-AT-based coloured smoke formulations are completely insensitive towards impact. The fuel mixes were more sensitive towards mechanical stimuli. A comparison of the collected aerosol revealed similar yields for **FM1**-based and sugar-based formulations. The superiority of prepared sugar-based reference formulations was displayed by the measured transfer rates. The obtained baseline (yield, transfer rate) are the first literature-reported values for sugar- and 5-AT-based coloured smoke formulations. Future investigations in our group will focus on providing even more coloured smoke formulations, e.g. blue and black, applying the same fuel mixes. To secure a proper evaluation, new strategies to characterize aerosol produced by a mixture of two dyes (e.g. green dye mix) has to be established.

Notes and references

[1] a)T. M. Klapötke, *Chemistry of High-Energy Materials*, 4th ed., De Gruyter, Berlin, Boston, **2017**; b)Headquarters, *Field manual 21-60, Visual Signals* (Ed.: Department of the Army), Washington, DC, USA, **1987**; c)C. H. Sterling, *Military Communications: From Ancient Times to the 21st Century*, ABC-CLIO, Santa Barbara, California, USA, **2008**; d)H. A. Webster III, *8th Int. Pyrotech. Sem., Proc.*, IPUSA Seminars Inc., Steamboat Springs, Colorado, USA, July 12-16, **1982**, 718-727.

[2] U. S. Army Material Command, *Engineering Design Handbook: Design of Ammunition for Pyrotechnic Effects*, Military Pyrotechnics Series, Part Four, Washington, DC, USA, **1974**.

[3] Holy smoke! Chinese artist creates fireworks display for the DAYTIME, http://www.dailymail.co.uk/news/article-2072514/Cai-Guo-Qiang-Chinese-artist-creates-fireworks-display-DAYTIME.html, Nov 2017.

[4] a)J. A. Domanico, *35th Int. Pyrotech. Sem., Proc.*, IPSUSA Seminars Inc., Fort Collins, Colorado, USA, July 13-18, **2008**, 75-81; b)G. Diviacchi, *35th Int. Pyrotech. Sem., Proc.*, IPSUSA Seminar Inc., Fort Collins, Colorado, USA, July 13-18, **2008**, 491-497; c)J. J. Sabatini, in *Green Energetic Materials* (Ed.: T. Brinck), John Wiley & Sons, Ltd, West Sussex, United Kingdom, **2014**, pp. 63-102; d)H. Ellern, *Military and Civilian Pyrotechnics*, Chemical Publishing Company, New York, USA, **1968**.

[5] a)http://www.safety-marine.co.uk/, Nov 2017; b)Boating Handbook, http://www.rms.nsw.gov.au/maritime/safety-rules/safety-equipment/index.html, Nov 2017.

[6] a)J. A. Conkling, C. Mocella, *Chemistry of Pyrotechnics: Basic Principles and Theory*, 2nd ed., Taylor & Francis, **2010**; b)J. A. Conkling, in *Kirk-Othmer Encyclopedia of Chemical Technology*, John Wiley & Sons, Inc., **2000**.

[7] B. Kosanke, K. Kosanke, B. Sturman, T. Shimizu, M. A. Wilson, I. von Maltitz, R. J. Hancox, N. N. Kubota, C. Jennings-White, D. Chapman, D. R. Dillehay, T. Smith, M. Podlesak, *Pyrotechnic chemistry, Pyrotechnic Reference Series No. 4*, Journal of Pyrotechnic, Inc., **2014**.

[8] a)D. Lundy, J. Eaton, *Occupational Health Hazards Posed by Inventory US Army Smoke/Obscurant Munitions*, US Army Medical Research Detachment, Wright-Patterson Air Force Base, for Walter Reed Army Institute of Research, Washington, DC, USA, **1994**; b)I. B. Rubin, M. V. Buchanan, J. H. Moneyhun, *Chemical Characterization and Toxicologic Evaluation of Airborne Mixtures: Chemical Characterization of Combusted Inventory Red and Violet Smoke Mixes*, ORNL/TM-8810, AD A131527, Oak Ridge, TN, USA, **1982**.

[9] a)G. D. Chen, S. Showalter, G. Raibeck, J. Wejsa, *Environmentally Benign Battlefield Effects Black Smoke Simulator*, ADA481520, NJ, USA, **2006**; b)J. D. Moretti, J. J. Sabatini, A. P. Shaw, G. R. Chen, A. J. Gilbert, K. D. Oyler, *ACS Sustainable Chem. Eng.* **2013**, *1*, 673-678; c)J. D. Moretti, J. J. Sabatini, A. P. Shaw, R. Gilbert, *ACS Sustainable Chem. Eng.* **2014**, *2*, 1325-1330; d)A. P. Shaw, J. C. Poret, R. A. Gilbert, J. A. Domanico, E. L. Black, *Propellants, Explos., Pyrotech.* **2013**, *38*, 622-628; e)N. J. Caldwell, N. E. Hutslar, T. W. Clements, *20th Int.*

Pyrotech. Sem., Proc., IPSUSA Sem. Inc., Colorado Springs, Colorado, USA, July 25-29, **1994**, 139-151; f)A. P. Shaw, J. S. Brusnahan, J. C. Poret, L. A. Morris, *ACS Sustainable Chem. Eng.* **2016**, *4*, 2309-2315.

[10] G. Raibeck, G. Chen, *35th Int. Pyrotech. Semin., Proc.*, IPSUSA Seminars Inc., Fort Collins, Colorado, USA, July 13-18, **2008**, 103-112.

[11] a)J. Glück, T. M. Klapötke, M. Rusan, A. P. Shaw, *Propellants, Explos., Pyrotech.* **2017**, *42*, 131-141; b)J. Glück, T. M. Klapötke, A. P. Shaw, *Cent. Eur. J. Energ. Mater.* **2017**, *14*, 489-500.

[12] S. V. Levchik, O. A. Ivashkevich, A. I. Balabanovich, A. I. Lesnikovich, P. N. Gaponik, L. Costa, *Thermochim. Acta* **1992**, *207*, 115-130.

[13] National Research Council (US) Subcommittee on Military Smokes and Obscurants, *Toxicity of Military Smokes and Obscurants, Vol. 3*, National Academies Press (US), Washington DC, **1999**.

[14] a)G. S. Bondy, C. L. Armstrong, B. A. Dawson, C. Héroux-Metcalf, G. A. Neville, C. G. Rogers, *Toxicol. In Vitro* **1994**, *8*, 329-335; b)M. Hemmilä, M. Hihkiö, K. Linnainmaa, *Propellants, Explos., Pyrotech.* **2007**, *32*, 415-422; c)T. C. Marrs, H. F. Colgrave, P. Rice, J. A. G. Edginton, B. Morris, *J. Hazard. Mater.* **1989**, *21*, 73-88; d)M. van Hulst, J. P. Langenberg, W. P. C. de Klerk, M. J. Alblas, *Propellants, Explos., Pyrotech.* **2016**, *42*, 17-23.

[15] R. K. Wharton and A. J. Barratt, *Propellants, Explos., Pyrotech.*, **1993**, *18*, 77-80.

[16] BAM Bundesanstalt für Materialforschung und -prüfung, *BAM standards, Vol. 5*, BAM Bundesanstalt für Materialforschung und -prüfung, Berlin, Germany, **2015**.

Supporting Information

1. Explanation of Triangle Diagrams

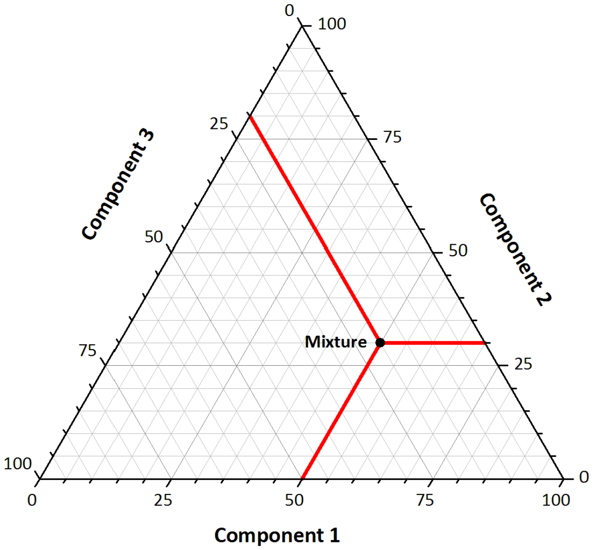

Figure 1: Triangle diagram and how to read it.

The illustration within a triangle diagram (Fig. 1/Fig. 2) is a powerful tool to summarize the results of all kind of pyrotechnical formulations. In detail, this diagram includes three axes representing three different components from 0 to 100 %. Every point defines an unique ratio of the components applied. Since the reading direction is unintuitive for diagrams with three axes, it is marked with red lines in (Fig. 1) for a mixture containing 50 % of component 1, 30 % of component 2 and 20 % of component 3. Therefore, it is mandatory that the percentages of all three components results in 100 %. The artificial lines at the scale of every axe additionally support the given reading direction. Triangle diagrams offer promising advantages for pyrotechnics. They can discover hidden trends and relationships between different ratios of components, and for this reason, lead quickly to an optimum pyrotechnical formulation. A more detailed explanation and study exercises is given by Kosanke (K. L. Kosanke, B. J. Kosanke, *Selected pyrotechnic publications of K. L. and B. J. Kosanke*, Journal of Pyrotechnics, Whitewater, CO, USA, **1995**).

2. Testing Protocol

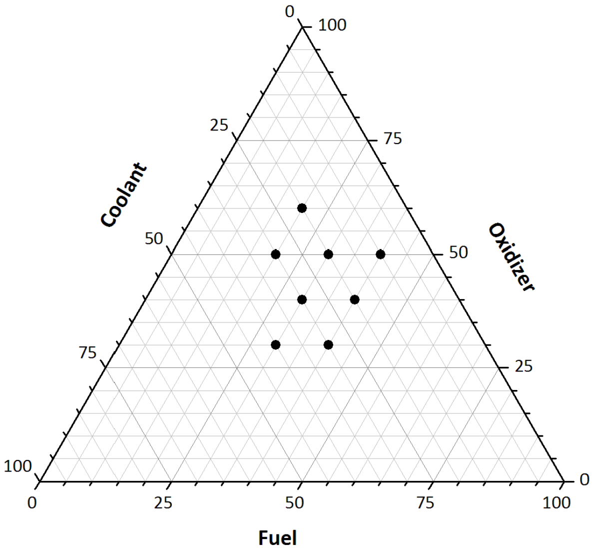

Figure 2: Triangle diagram of initial burning tests.

The testing protocol includes eight preliminary fuel mixes for initial burning tests. Therefore, the resulting smoke formulations have a fixed amount of 30 % dye, while the remaining 70 % is one of the specific fuel mixes consisting of various ratios of oxidizer, fuel and coolant (Fig. 2). A more detailed explanation and study exercises is given by Domanico (J. A. Domanico, *Using a Standard Testing Protocol to Qualify Candidate Low Toxicity Colored Smoke Dyes*, 35th International Pyrotechnics Seminar, Fort Collins, CO, USA, **2008**).

3. Aerosol Determination

The arising aerosol of four pellets (2.0 g) per formulation was collected and averaged.

Table 1: Aerosol of yellow-, green, red- and violet-colored smoke formulations based on fuel mixes **FM1**, **FM2**, **FM3** and **Ref-FM**.

	Y1	**Y2**	**Y3**	**G1**	**G2**	**G3**	**Ref-Y**	**Ref-G**
Aerosol /g	0.584	0.418	0.593	0.720	0.486	0.636	0.670	0.642
	R1	**R2**	**R3**	**V1**	**V2**	**V3**	**Ref-R**	**Ref-V**
Aerosol /g	0.499	0.590	0.574	0.575	0.522	0.578	0.729	0.652

4. Smoke Characterization

Table 2: Properties of yellow-, green, red- and violet-colored smoke formulations based on fuel mixes **FM1**, **FM2**, **FM3** and **Ref-FM**.

	BT /s	**BR** /g s^{-1}	**Y** /%	**RH** /%	**T%** /%	$\mathbf{m_{HPLC}}$ /mg	**IS** /J	**FS** /N	**ESD** /J	$\mathbf{T_{onset}}$ /°C
Y1	15	0.34	29	26	59	354	40	360	1.0	184
Y2	26	0.10	21	23	56	233	40	360	0.4	189
Y3	29	0.10	30	33	49	292	40	360	0.5	187
Ref-Y	13	0.43	33	29	73	435	40	360	0.3	178
G1	20	0.32	36	33	–	–	40	360	0.4	192
G2	45	0.08	24	34	–	–	40	360	0.2	198
G3	31	0.12	31	33	–	–	40	360	0.5	194
Ref-G	19	0.41	32	28	–	–	30	360	0.2	172
R1	20	0.29	29	29	76	457	40	360	0.5	184
R2	75	0.07	25	28	58	351	40	360	0.7	182
R3	41	0.07	28	29	72	432	40	360	0.5	189
Ref-R	21	0.29	36	28	86	514	40	360	0.6	172
V1	23	0.28	29	28	–	–	40	360	0.2	182
V2	27	0.07	26	26	–	–	40	360	0.3	186
V3	27	0.08	29	29	–	–	40	360	0.3	180
Ref-V	15	0.43	32	28	–	–	30	360	0.7	178

Annotation: measured for 2.0 g pellet; BT = burn time; BR = burn rate (10.0 g pellet); Y = yield; RH = relative humidity; T% = transfer rate; m_{HPLC} *= dye content present in aerosol; IS = impact sensitivity; FS = friction sensitivity; ESD = electric discharge sensitivity;* T_{onset} *= onset temperature of decomposition.*

The solution of violet smoke dye mix in acetonitrile already degraded during measurement. A change of the coloured solution was observed within a few hours. The green formulations applying two dyes will be addressed in the future.

5. Aerosol Determination

The arising aerosol of four pellets (2.0 g) per formulation was collected and averaged.

Table 3: Aerosol of yellow-, green, red- and violet-colored smoke formulations based on fuel mixes **FM1**, **FM2**, **FM3** and **Ref-FM**.

	Y1	**Y2**	**Y3**	**G1**	**G2**	**G3**	**Ref-Y**	**Ref-G**
Aerosol /g	0.584	0.418	0.593	0.720	0.486	0.636	0.670	0.642

	R1	**R2**	**R3**	**V1**	**V2**	**V3**	**Ref-R**	**Ref-V**
Aerosol /g	0.499	0.590	0.574	0.575	0.522	0.578	0.729	0.652

6. HPLC strategy

A Thermo Scientific™ DIONEX™ UltiMate™ 3000 HPLC System (accucore RP-MS column (3.0 x 150.0 mm, particle size 2.6 µm) with a DAD-3000 photometer and Chromeleon® 7.2 Chromatography Management Software was used to quantify the amount of dye. The single component devices were: SRD-3400 4-channel Degaser Eluenten-Rack, HPG-3400SD Gradient Pump, WPS-3000TSL (Analytical) Autosampler, TCC-3000SD Column oven.

Mobile Phase: Eluent A = water/acetonitrile (95/5), eluent B = water/acetonitrile (5/95).
Gradient: 0 min (50 % A), 5 min (0 % A), 8 min (0 % A), 14 min (50 % A).
Flow rate: 0.3 mL min^{-1}
Injection volume: 5 µL
DAD: 220 nm, 250 nm, 3D-area: 190–800 nm
Column temperature: 30 °C
Sample temperature: 20 °C

7. Burn rate

Compositions were pressed into cardboard tube for burn rate studies. The cardboard rolls, cylindrical and open on both ends, had a 2.5 cm inner diameter, 3.0 cm height, and a 1.6 mm wall thickness. The compositions (10.0 g) were pressed with a consolidation dead load of 3.0 t for 10.0 s. The pellets were ignited at the top using a resistance heating Kanthal® A1 wire (FeCrAl, 0.8 mm diameter, 2.9 Ω m^{-1}). Upon testing of formulations with 3 g pyrotechnical payload and cylindrical pellet sizes of 1 cm diameter and 2.8 cm height, some of those formulations burned with an open flame and produced no smoke anymore. The so obtained values should be treated with care, since a lot of factors such as the surface, pressure, humidity and the pellet size influence the observed burn rate. Large deviations are obtained for different pellet sizes/payloads (Table 4).

Table 4: Burn rate of yellow-, green, red- and violet-colored smoke formulations based on fuel mixes **FM1**, **FM2**, **FM3** and **Ref-FM**.

	BT /s 10 g pellets	**BR** /g s^{-1} 10 g pellets	**BR** /g s^{-1} 3 g pellets	**BT** /s 3 g pellets
Y1	15	0.34	0.10	25
Y2	26	0.10	flame	n.d.
Y3	29	0.10	flame	n.d.
Ref-Y	13	0.43	0.08	37
G1	20	0.32	0.09	38
G2	45	0.08	n.d.	n.d.
G3	31	0.12	n.d.	n.d.
Ref-G	19	0.41	n.d.	n.d.
R1	20	0.29	n.d.	n.d.
R2	75	0.07	n.d.	n.d.
R3	41	0.07	n.d.	n.d.
Ref-R	21	0.29	n.d.	n.d.
V1	23	0.28	n.d.	n.d.
V2	27	0.07	n.d.	n.d.
V3	27	0.08	n.d.	n.d.
Ref-V	15	0.43	n.d.	n.d.

Annotation: BT = burn time; BR = burn rate, n.d. = not determined, flame = no smoke formation was observed, instead the pellet burned with an open flame.

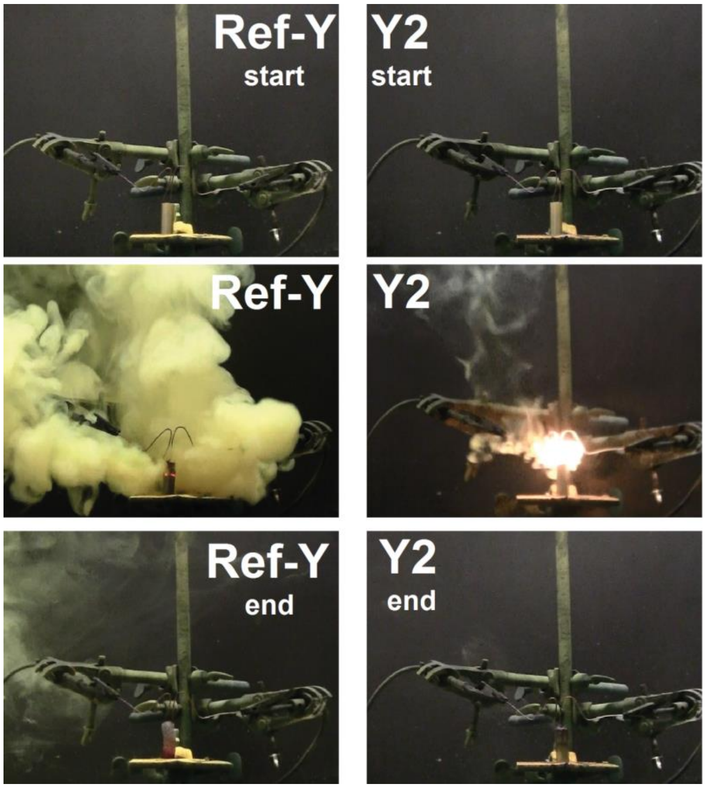

Figure 3: Burning of Ref-Y and Y2 with a pellet size of 3 g.

8. DTA of tested formulations

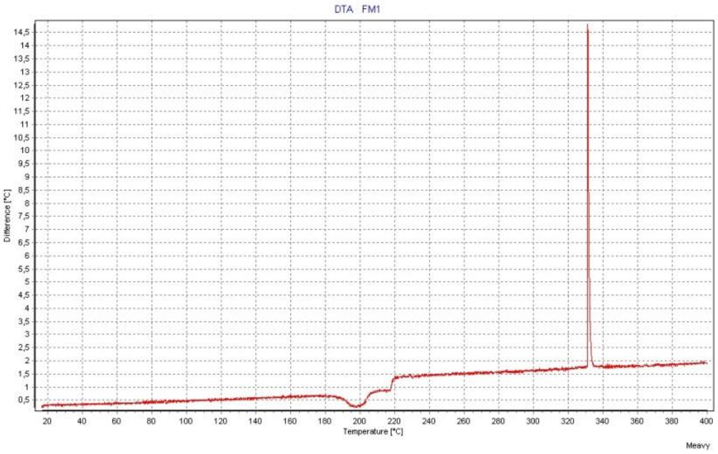

Figure 4: DTA of FM1.

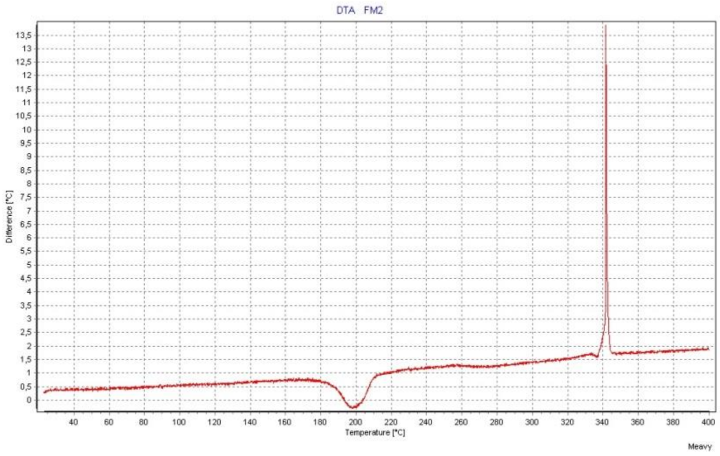

Figure 5: DTA of FM2.

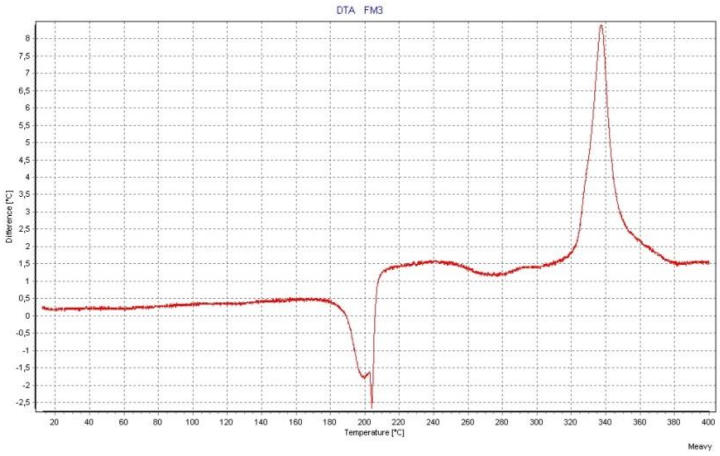

Figure 6: DTA of FM3.

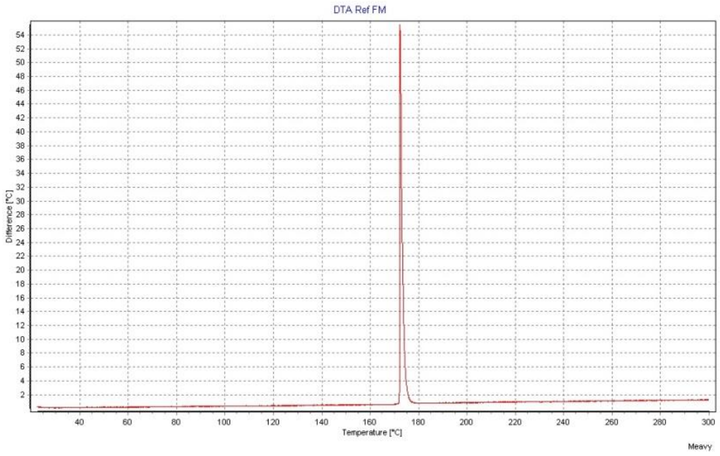

Figure 7: DTA of Ref-FM.

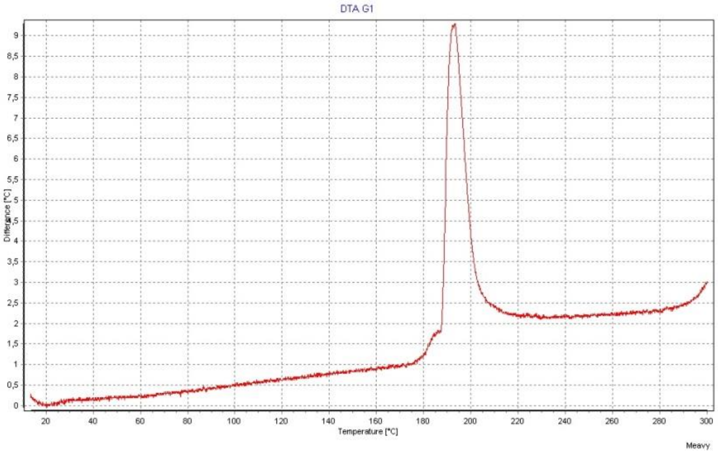

Figure 8: DTA of G1.

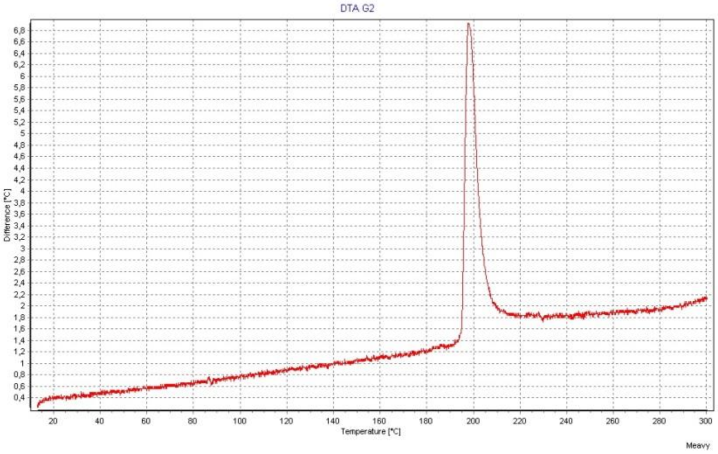

Figure 9: DTA of G2.

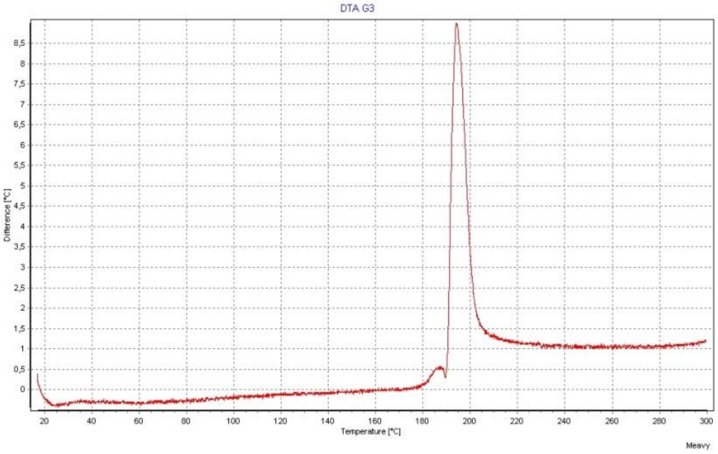

Figure 10: DTA of G3.

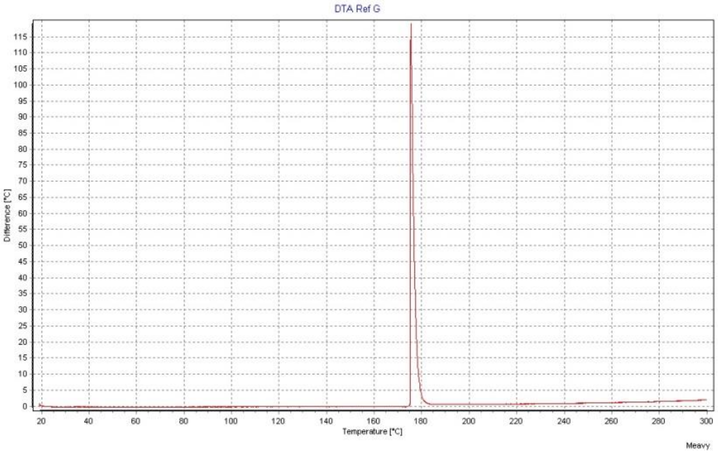

Figure 11: DTA of Ref-G.

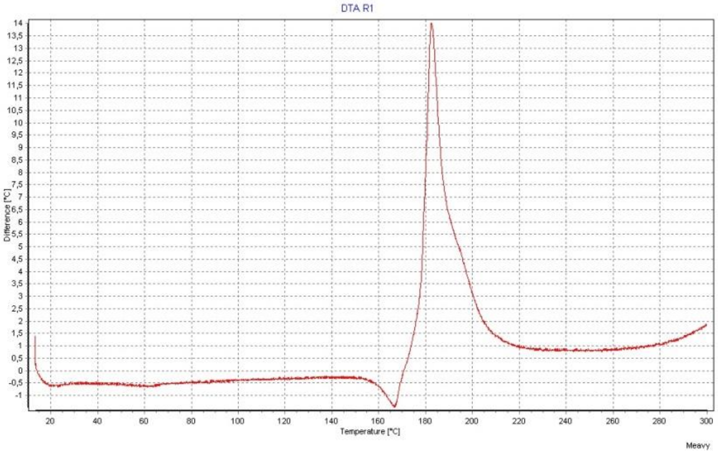

Figure 12: DTA of R1.

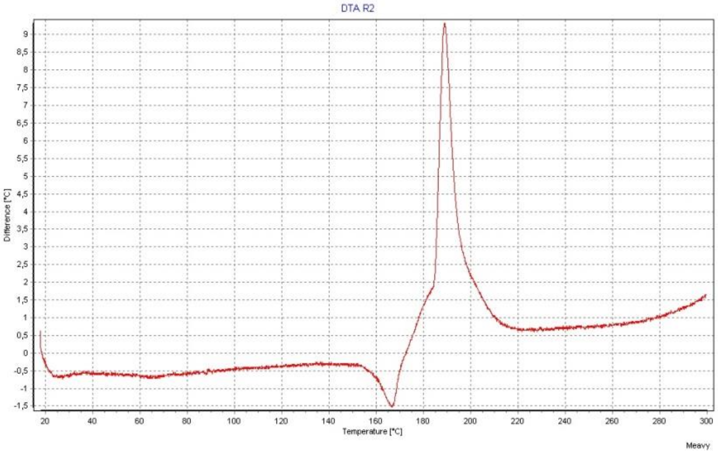

Figure 13: DTA of R2.

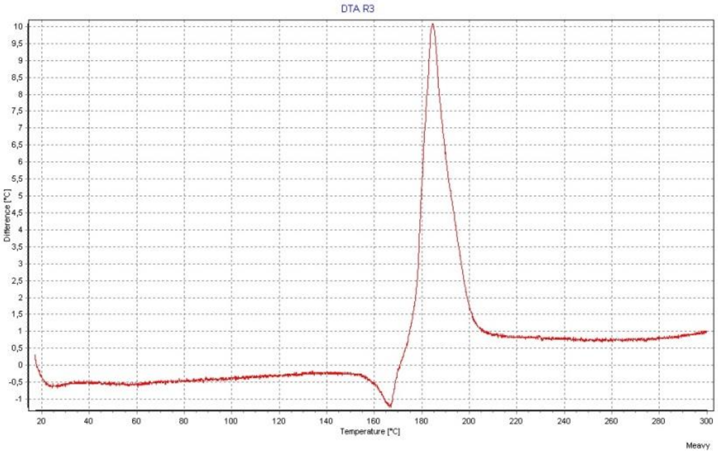

Figure 14: DTA of R3.

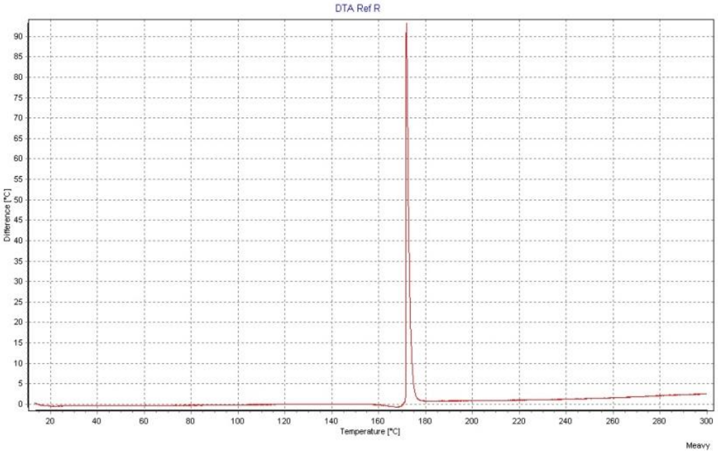

Figure 15: DTA of Ref-R.

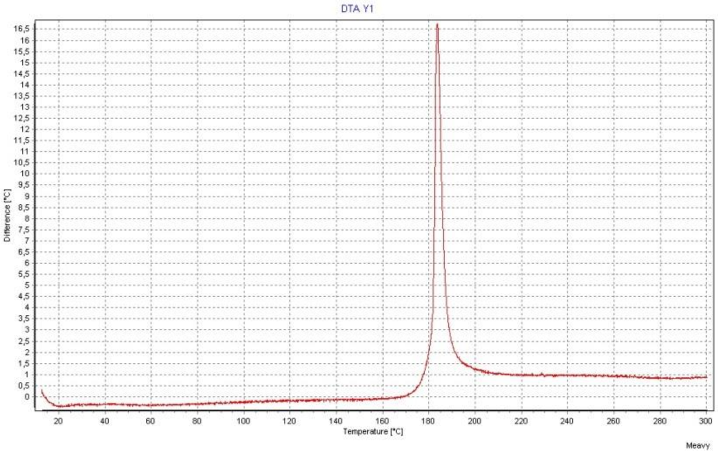

Figure 16: DTA of Y1.

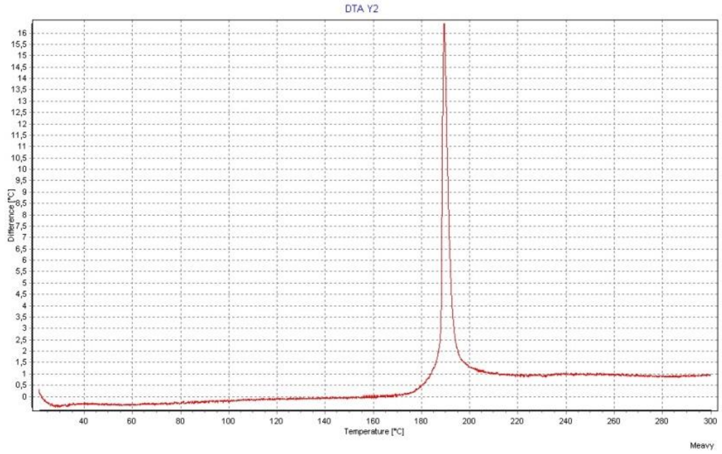

Figure 17: DTA of Y2.

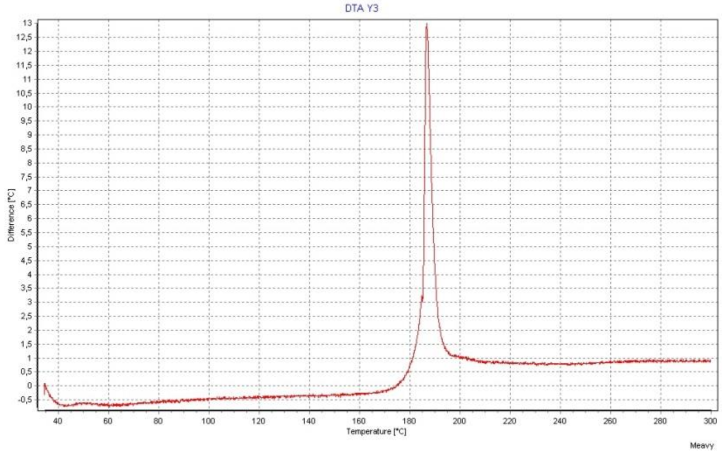

Figure 18: DTA of Y3.

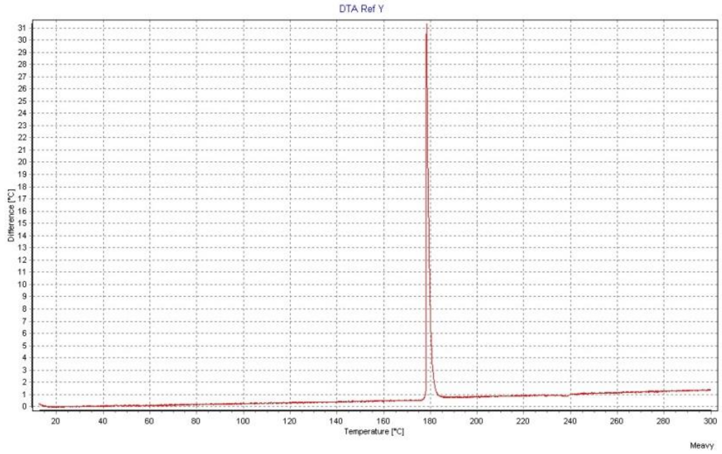

Figure 19: DTA of Ref-Y.

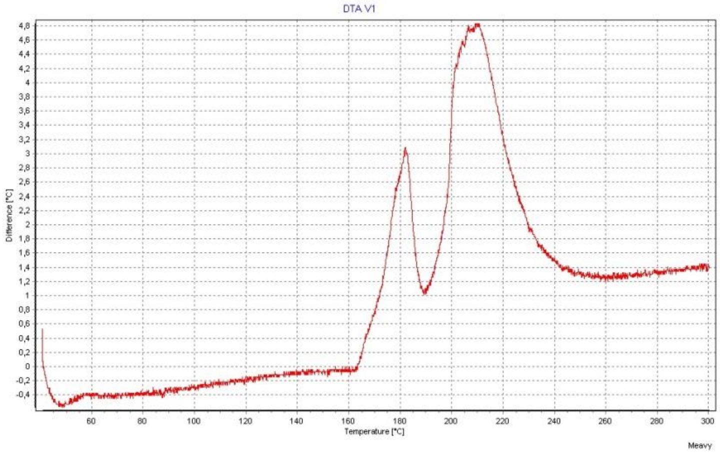

Figure 20: DTA of V1.

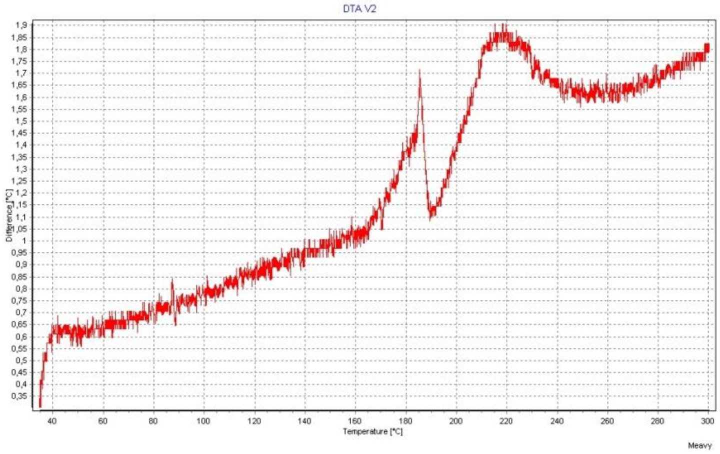

Figure 21: DTA of V2.

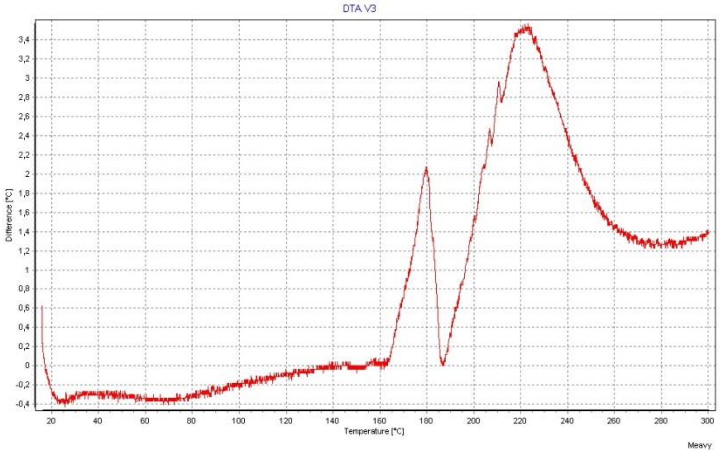

Figure 22: DTA of V3.

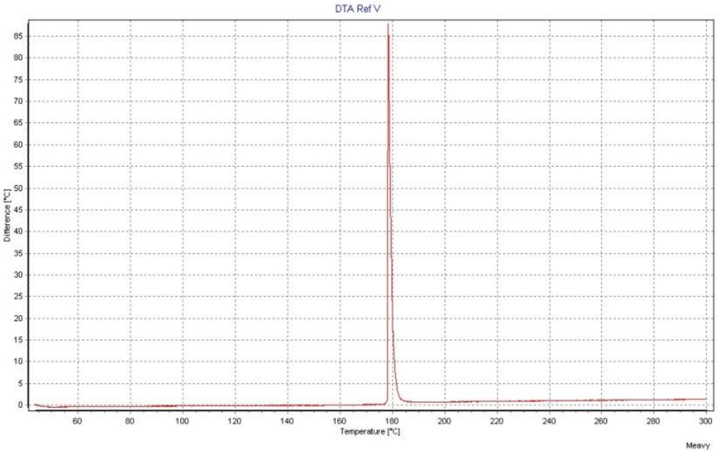

Figure 23: DTA of Ref-V.

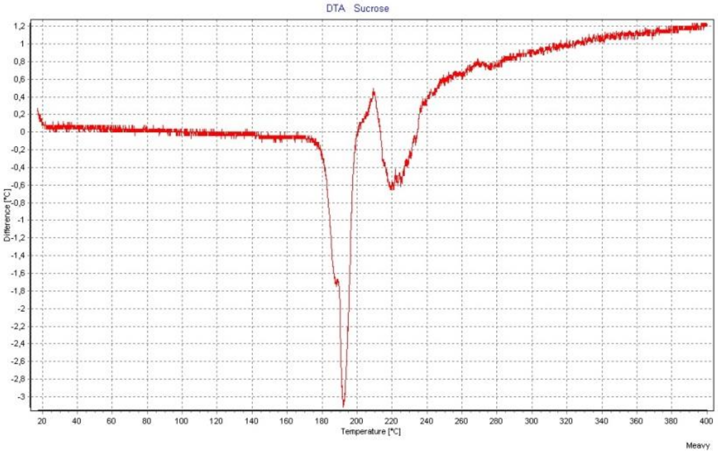

Figure 24: DTA of sucrose.

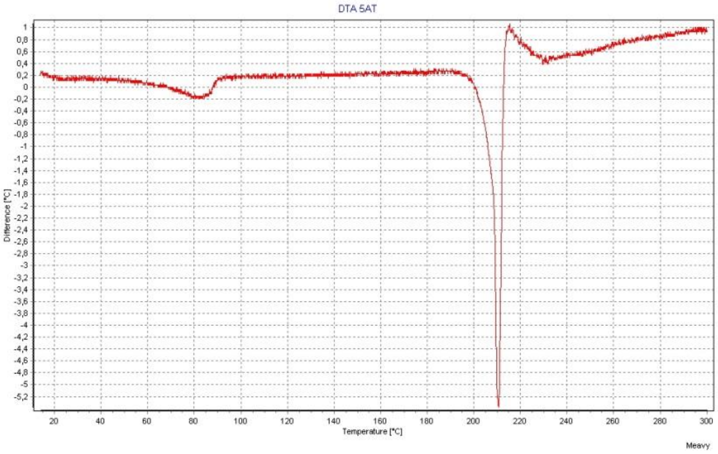

Figure 25: DTA of 5-AT.

4. Light-Generating Pyrotechnics

4.1 Metal Salts of 3,3'-Diamino-4,4'-Dinitramino-5,5'-Bi-1,2,4-Triazole in Pyrotechnic Compositions

Published in Z. anorg. allg. Chem. ***2018****, Accepted Author Manuscript.*
(DOI: 10.1002/zaac.201800179)

Abstract: The synthesis of alkali and alkaline earth salts of 3,3'-diamino-4,4'-dinitramino-5,5'-bi-1,2,4-triazole (H_2ANAT) is reported. The fast and convenient three steps reaction toward the target compounds does not require any organic solvents. In addition to an intensive characterization of all synthesized metal salts, the focus was on developing chlorine and nitrate-free red-light-generating pyrotechnical formulations. Strontium 3,3'-diamino-4,4'-dinitramino-5,5'-bitriazolate hexahydrate served as colorant and oxidizer in one molecule. The energetic properties of all developed pyrotechnical formulations assure safe handling and manufacturing.

Introduction

In recent years the development of environmental friendly pyrotechnics for both military and civilian application became more and more important.[1] This affected all ingredients of a typical light-producing pyrotechnical formulation such as the oxidizer, fuel, colorant, and additives.[2] One of the first steps toward this goal is correlated with the commonly used oxidizers ammonium perchlorate (NH_4ClO_4) and potassium perchlorate ($KClO_4$). Next to their advantageous properties, like a high oxygen balance, stability, low cost and low hygroscopicity, both were identified as environmental and human health hazards.[3] The high solubility makes them a successful groundwater contaminant, which is addressed by American authorities resulting in increasing regulations regarding the permissible concentration in the water supply.[3,4] In the case of red-light-emitting pyrotechnics, additional chlorine sources like PVC are usually combined with strontium salts, typically strontium nitrate (colorant) to produce the metastable red light emitter Sr(I)Cl.[5] During the combustion of chlorine-containing pyrotechnic formulations, highly carcinogenic polychlorinated biphenyls, polychlorinated dibenzofurans, and polychlorinated dibenzo-*p*-dioxins are formed.[6] In 2015, Sabatini *et al.* reported first about a chlorine-free red light composition based on strontium nitrate, which meets the U.S. Army performance requirements for red light (dominant wavelength (DW) = 620±20 nm; spectral purity (SP) ≥ 76%) and at the same time prevents the formation of toxic chlorine-containing compounds (Figure 1).[7]

In addition to the perchlorate issue, a new environmental issue may arise. In November 2016, the European Union sued Germany for too high nitrate concentrations in the groundwater. According to the new regulations, the groundwater concentration of nitrates between 2012–2014 exceeded the threshold value of 50 mg/L in 28% of the checkpoints. Further 8.5 % were already in between 40–50 mg/L. Such a high value may harm expectant mothers and young children. Even though the candidate to blame is clearly identified as the intensive agriculture, military practice grounds and civilian fireworks are a source of environmental pollution, too.[5d, 8] A possible solution for "greener" pyrotechnics is the application of high-nitrogen compounds.[5a, 5b, 9] High-nitrogen energetic salts derive their energy from their high positive heat of formation upon release of non-toxic dinitrogen gas as a main combustion product.[10] This is beneficial to achieve brilliant colors and a good color performance.[11]

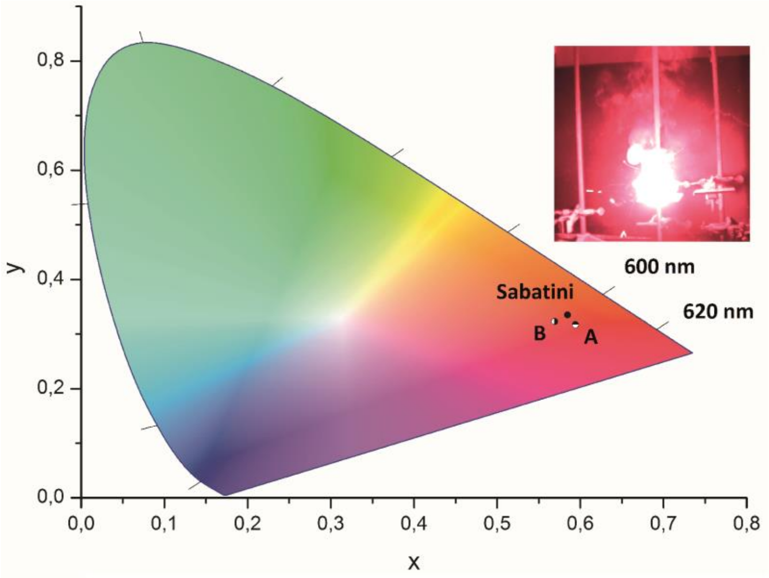

Figure 1. CIE 1931 chromaticity diagram of **A**, **B** and the reference formulation by Sabatini.

Introducing additional nitro, nitramino or N-oxide moieties to high-nitrogen compounds such as tetrazoles or triazoles may optimize the energetic performance and the oxygen balance of the target molecule.[12] As a consequence, no further oxidizers like nitrates would be needed. Since future applications of new environmentally more friendly compounds in the pyrotechnic sector are often cost forbidden, we focused on the recently reported 3,3'-diamino-4,4'-dinitramino-5,5'-bi-1,2,4-triazole and the corresponding alkali/alkaline earth metal salts thereof.[13] The target metal salts can be synthesized in a simple three steps synthesis starting from commercially available compounds. No organic solvents are needed. The new developed chlorine/nitrate free red-light-emitting pyrotechnical formulations based on the newly synthesized strontium salt achieve a dominant wavelength (DW) = 616 nm and a spectral purity (SP) = 75%. The present paper discusses the syntheses of the corresponding metal salts and the results of DW and SP for the developed strontium-containing formulations. In addition, sensitivity measurements have been carried out to secure safe handling.

Results and Discussion

Syntheses

The starting material 3,3'-diamino-4,4'-dinitramino-5,5'-bi-1,2,4-triazole (**2**) was synthesized according to a literature procedure by stepwise condensation of 1,3-diamino-guanidine monohydrochloride with oxalic acid and further selective N-amino nitration (Figure 2).[13a] The preparation of **2** and its energetic salts **3**–**9** is displayed in Figure 2. 1,3-Diaminoguanidine hydrochloride and oxalic acid were dissolved in polyphosphoric acid and heated to give 4,4',5,5'-tetraamino-3,3'-bi-1,2,4-triazole (**1**). **1** was slowly added to ice-cooled 100% HNO_3 and stirred at 0 °C for 1.5 h. Afterward the solution was quenched with ice-water and the formed precipitate was filtered off yielding pure **2**. Compound **2** can be used as obtained and does not require further purification such as chromatography, or recrystallization.

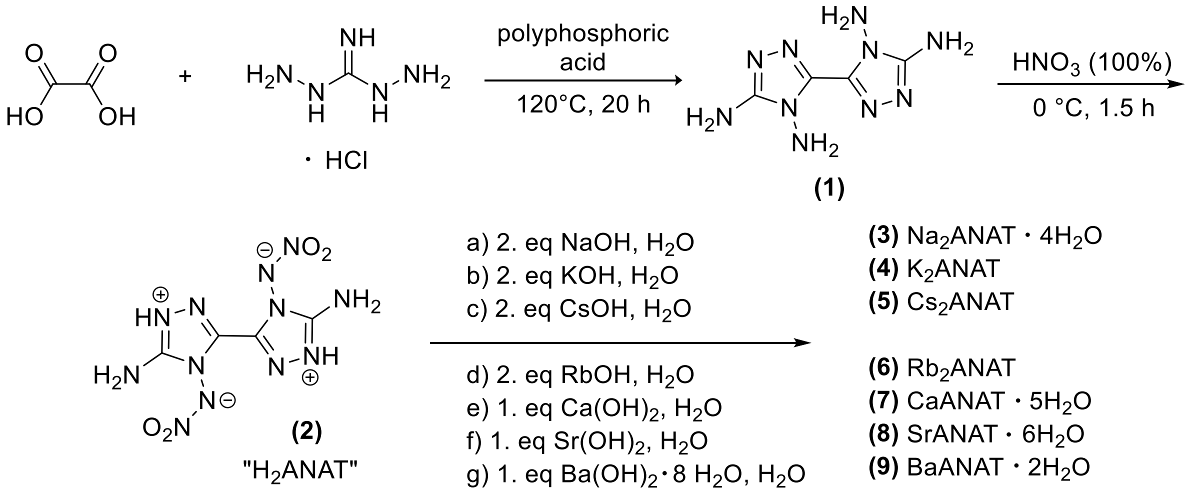

Figure 2. Synthetic route toward compound **1**–**9**.

The alkali and alkaline earth salts of **2** were obtained by the reaction of compound **2** with the corresponding metal hydroxides. Therefore **2** was suspended in water and the corresponding base was added. The suspension was heated until a clear solution appeared and then left for crystallization to obtain compounds **3**–**9.** Compound **9** was obtained as a brown powder. The corresponding lithium salt was reported earlier.[13b]

Crystal Structures

The crystal structures of compounds **3**–**8** were determined. The crystal structures were uploaded to the CSD database[14] and can be obtained free of charge with the CCDC nos. 1837414 (**3**), 1837411 (**4**), 1837410 (**5**), 1837413 (**6**), 1837409 (**7**), and 1837412 (**8**). In addition, selected data and parameters of the X-ray measurement can be found in the Supporting Information.

The molecular structures of compounds **3**–**8** are similar to the neutral compound **1**. All bond lengths and angles are similar to the neutral compound. Also, the anion of **3**–**8** is in plane except for the two nitramino groups. The two nitramino groups are tilted out of the plane by 70–73°. Only compound **5** slightly differ from the neutral compound.

Disodium 3,3'-diamino-4,4'-dinitramino-5,5'-bitriazolate tetrahydrate (**3**) crystallizes from water in the triclinic space group *P-1* with two molecules per unit cell and a density of 1.716 g cm^{-3} at 293 K.

The molecular unit of **3** is illustrated in Figure 3. The sphere of atom Na1 is characterized by distorted tetrahedral coordination of four atoms (O3i, O3ii, N1, N5i). A dimeric motif is formed by two bridging water molecules O3^{ii}/O3 and the atoms Na1/Na1^{ii} (Figure 3). The dimeric motif is in plane and revealed a distance between the atoms Na1-O3 of approximately 2.45 Å. The observed angles between the atoms Na1-O3^{ii}-Na1^{ii} and O3^{ii}-Na1-O3 are approximately 90 °. The coordination distance between the atoms Na1-O3 (2.43 Å) is in good agreement with the literature reported values (2.37 Å).[15]

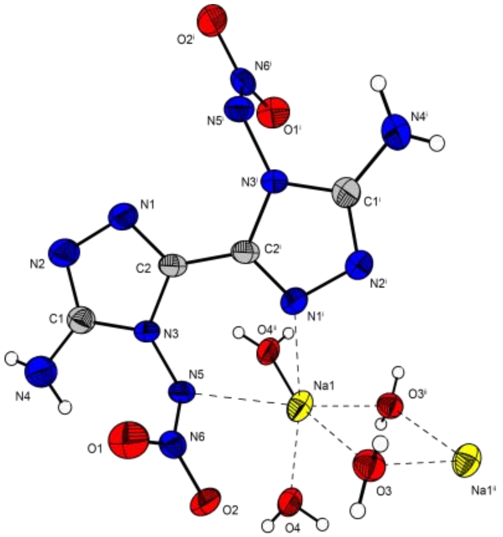

Figure 3. Molecular unit of **3** showing the atom-labeling scheme. Ellipsoids represent the 50% probability level. Symmetry codes: (i = -x, -y, 1 – z; ii = -x, -y, 2–z). Selected bond length (Å): Na1-O3^{ii} 2.4525(2), Na1-O3 2.2525(2). Selected bond angles (°): O3^{ii}-Na1-O3 90.300(6), Na1-O3-Na1^{ii} 89.700(6).

Dipotassium 5,5'-diamino-4,4'-dinitramino-3,3'-bitriazolate (**4**) crystallizes from water in the monoclinic space group *P21/n* with four molecules per unit cell and a density of 2.001 g cm^{-3} at 294 K. The structure of **4** is illustrated in Figure 4. The view of multiple unit cells along the *b* axis indicates a stacking of both the anions and the potassium atoms. Two potassium atoms (K^{i}, Ki^{ii}) are connected to each other via the oxygen atom O2^{vi} of the nitramino group and form alternating potassium-oxygen chains. The observed coordination distance between the atoms K1^{ii}-O2^{vi} is approximately 2.78 Å.

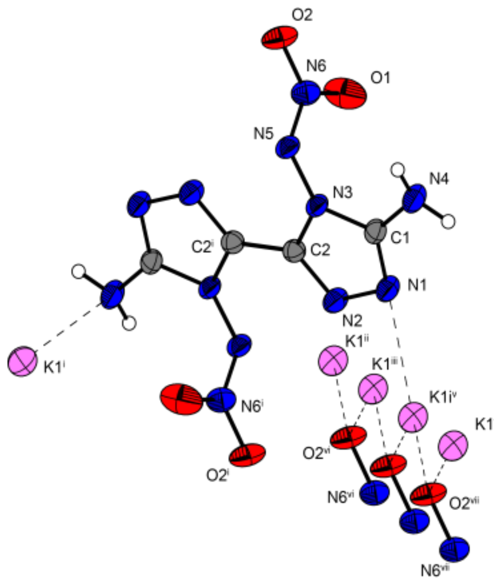

Figure 4. View on the structure of **4** showing the atom-labeling scheme. Ellipsoids represent the 50% probability level. Symmetry codes: (i = 1–x, 2–y, -z; ii = 1.5–x, -0.5 + y, 0.5–z; iii = 1.5–x, 0.5 + y, 0.5–z; iv = 1.5–x, -1.5 + y, 0. –z, v = 1.5–x, 1.5+y, 0.5–z; vi = 1+x, -1+y, vii = 1+x, -1+y, z). Selected bond length (Å): K1^{i} – N4^{i} 3.0536(1), K1^{iv}-N1 3.0664(1), K1^{ii}-O2^{vi} 2.7388(1), O2^{vi}-K1^{iii} 2.17812(1), O2^{vi}-N6^{vi} 1.2675(1). Selected bond angles (°): K1^{ii}-O2^{vi}-K1^{iii} 126.962(3).

Dicesium 3,3'-diamino-4,4'-dinitramino-5,5'-bitriazolate (**5**) crystallizes from water in the orthorhombic space group *Pca2₁* with four molecules per unit cell and a density of 2.670 g cm^{-3} at 296 K. The molecular unit of **5** is illustrated in Figure 5. The molecular structure slightly differs from the corresponding structures, *e.g.* the neutral and guanidinium salt. The aromatic triazole rings are not coplanar and twisted approximately 2 ° (N3-C2-C3-N9) to each other. The observed bond length of the atoms C1-C3 is in the range of the neutral and the guanidinium compound (1.45 Å). The nitramino moiety is twisted out of plane (N3-N5-N6-O1 = 71 °).

The cesium atom (Cs1) is coordinated by one oxygen atom (O1). The observed distance between the atoms Cs1-O1 is 3.20 Å and is in good agreement with literature reported values.[16]

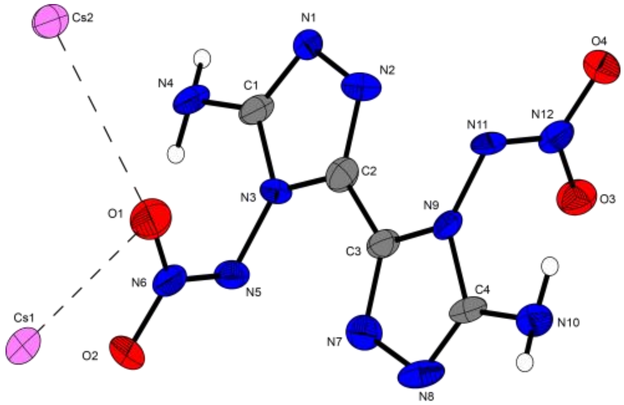

Figure 5. Molecular unit of **5** showing the atom-labeling scheme. Ellipsoids represent the 50% probability level. Selected bond length (Å): Cs1-O1 3.292(9), Cs2-O1 3.375(8). Selected torsion angles (°): N2-C2-N3-N5 2.275(9), N3-N5-N6 108.521(1).

Dirubidium 3,3'-diamino-4,4'-dinitramino-5,5'-bitriazolate (**6**) crystallizes from water in the monoclinic space group *P21/n* with two molecules per unit cell and a density of 2.424 g cm^{-3} at 173 K. The molecular unit of **6** is illustrated in Figure 6. The rubidium atom is distorted coordinated by one oxygen atom of the nitro group. The observed distance between the atoms Rb1-O2 is approximately 2.85 Å.

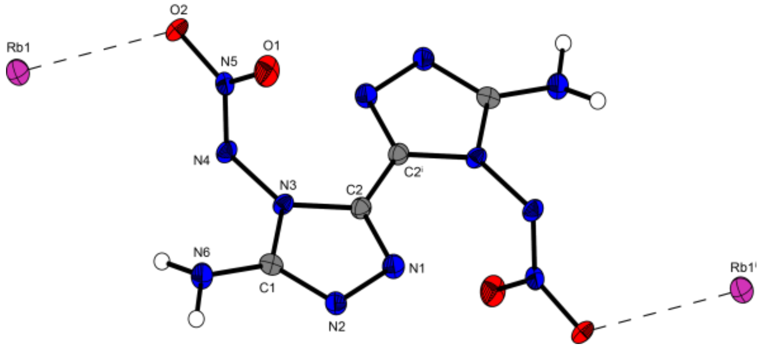

Figure 6. Molecular unit of **6** showing the atom-labeling scheme. Ellipsoids represent the 50% probability level. (i =1-x,1-y, 2-z). Selected bond length (Å): Rb1-O2 2.8519(1).

Calcium 3,3'-diamino-4,4'-dinitramino-5,5'-bitriazolate pentahydrate (**7**) crystallizes from water in the monoclinic space group *C2/c* with five molecules per unit cell and a density of 1.737 g cm^{-3} at 173 K. The molecular unit of **7** is illustrated in Figure 7. The calcium atom (Ca1) is distorted coordinated by four water molecules (O3, O3i, O4, O4i) and two times by one oxygen atom (O2) and one nitrogen atom (N5) of the nitramino group. The observed coordination distance between the atoms Ca1-O3, Ca1-O3i, Ca1-O4, Ca1-O4i is approximately 2.37 Å. The distance between the atoms Ca1-O2, Ca1-O2i, and Ca1-N5, Ca1-N5i is 2.48 Å and 2.58 Å respectively. The view of multiple unit cells along the *a* axis indicates a stacking of both the anions and the calcium atoms.

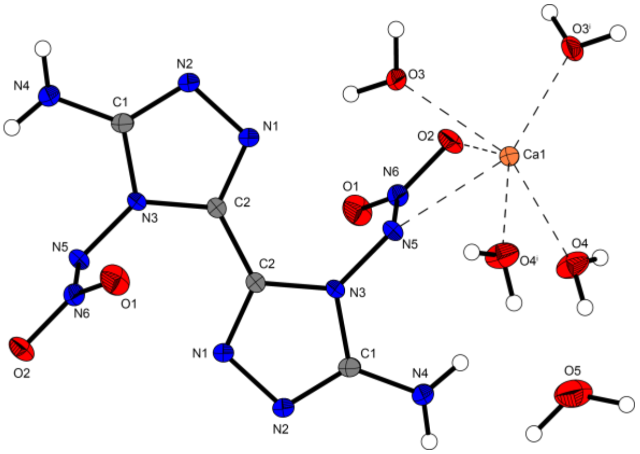

Figure 7. Molecular unit of **7** showing the atom-labeling scheme. Ellipsoids represent the 50% probability level. Symmetry codes: (i = 0.5+x, 0.5+y, z). Selected bond length (Å): Ca1-O2 2.4801(14), Ca1-O3 2.3797(14), Ca1-O4 2.3614(1), Ca1-N5 2.5785(1).

Strontium 3,3'-diamino-4,4'-dinitramino-5,5'-bitriazolate hexahydrate (**8**) crystallizes from water in the monoclinic space group *P2₁/m* with two molecules per unit cell and a density of 1.908 g cm^{-3} at 295 K. The molecular unit of **8** is illustrated in Figure 8. The bond lengths between all the atoms in the triazole ring are in the range of the reported guanidinium salt.[13a] The observed bond length of the ring nitrogen atoms are between the values for a N-N single bond (1.47 Å) and a N=N double bond (1.25 Å).[17]

The strontium atom (Sr1) is distorted septahedral coordinated by five water molecules (O2, O3, O6, O5i, O5, O4), as well as by one oxygen atom (O2) and one nitrogen atom (N5) of the nitramino group. The observed distances between the atoms Sr1-O2, Sr-O3, Sr1-O4, Sr1-O5 is in the range of 2.53–2.66 Å. The coordination distance between the atoms Sr1-O2 and Sr1-N5 is 2.77 Å.

The view of multiple unit cells along the *a* axis indicates a stacking of both the anions and the strontium atoms. Two strontium atoms are connected to each other via two hydrogen bridges Sr1-O6-H7a (2.76 Å) and O7-H7b-O4 (2.25 Å).

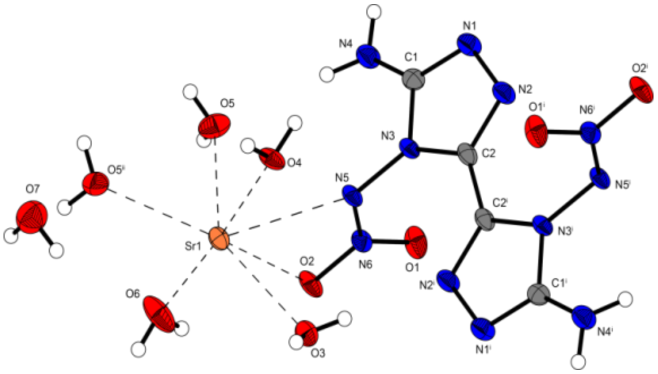

Figure 8. Molecular unit of **8** showing the atom-labeling scheme. Ellipsoids represent the 50% probability level. Symmetry codes: (i = 1+x, 0.5-y, z). Selected bond length (Å): Sr1-O2 2.7687(18), Sr1-O3 2.582(3), Sr1-O4 2.531(3), Sr1-O5 2.601(2), Sr1-O6 2.624(3), Sr1-N5 2.765(2).

Thermal and energetic properties

The decomposition temperatures T_{dec} of compounds **2**–**9** was determined by means of differential thermal analysis (DTA) with a heating rate of 5 °C min^{-1}. The decomposition temperatures are given as onset temperatures (Table 1/Table 2).

Table 1. Thermal and energetic properties of compounds **2**–**5**.

	2	**3**	**4**	**5**
***FS* [N]**	120	360	360	360
***IS* [J]**	9	40	3	8
T_{onset} [°C]	259	287	250	220

Annotation: BAM standard; FS = friction sensitivity; IS = impact sensitivity; T_{onset} = decomposition temperature (heating rate of 5 °C min^{-1}).

All tested metal salts are completely insensitive toward friction. Compounds **3**, **7**, **8** and **9** contain at least two water molecules per unit cell and are insensitive toward impact. In contrast, the crystal water-free compounds **4**, **5** and **6** are categorized as impact sensitive. Compound **4** is very sensitive toward impact (Table 1/Table 2).

Table 2. Thermal and energetic properties of compounds **6**–**9**.

	6	**7**	**8**	**9**
***FS* [N]**	360	360	360	360
***IS* [J]**	10	40	40	40
T_{onset} [°C]	250	$150_{\text{dehdyr.-dec.}}$	$160_{\text{dehdyr.-dec}}$	280

Annotation: BAM standard; FS = friction sensitivity; IS = impact sensitivity; T_{onset} = decomposition temperature (heating rate of 5 °C min^{-1}).

All tested metal salts show high decomposition temperatures in the range from 250 °C to 287 °C. Only compound **7** and **8** showed an earlier dehydration-decomposition transition at 150 °C and 160 °C (Table 1/Table 2).

Pyrotechnic formulations

In this project, we focused on the use of strontium salt **8** as a colorant for red-light-producing signal flares. The obtained formulations were compared to a chlorine-free strontium containing formulation published by Sabatini *et al.* in 2015 which meets the US Army requirement for the spectral purity (SP) and dominant wavelength (DW) (Table 3). A major goal was to achieve comparable good red light applying no chlorine and nitrate compounds in our formulations to meet potential future regulations.

Table 3. Reference formulation by Sabatini.[7]

Mixture/ wt%	**$Sr(NO_3)_2$**	**Mg 50/100 Mesh**	**5-AT**	**Epoxy Binder[a]**
Sabatini	48.0	33.0	12.0	7.0

[a] = Epon 813/Versamid 140 (80:20).

The current US Army in-service M158 red star cluster formulation consists of strontium nitrate (48 wt%), Mg (30/50 Mesh, 33 wt%), PVC (15 wt%) and Laminac 4116 /Lupersol (4 wt%). Starting from this formulation, Sabatini *et al.* replaced the Laminac 4116/Lupersol binder system with a simple "drop-in" of Epon 813/Versamid 140 for environmental reasons.[7]

Table 4. New formulations based on **8**.

Mixture/ wt%	**Mg 30/50 Mesh**	**8**	**5-AT**	**Epoxy Binder[a]**	**NC[b]**
A	35.3	47.1	11.7	3.9	2.0
B	33.0	50.0	13.0	–	4.0

[a] = Epon 813/Versamid 140 (50:50); [b] = Nitrocellulose solution (4–8%) in ethanol/diethyl ether (2 wt% = 1 mL on 1 g scale).

Compound **8** served as an oxidizer and colorant in one molecule. Mg and 5-AT act as fuel (Table 4). Formulation **A** applied a mixture of two binders (NC and epoxy binder); however, NC may also act as fuel in this formulation. In contrast, only the epoxy binder system was applied in formulation **B**.

Table 5. Performance values of tested formulations.

	BT **[s]**	***DW*** **[nm]**	***SP*** **[%]**
US Army requirement[7]	–	620±20	≥76
Sabatini	5	607	79
A	8	616	75
B	8	612	71

[a] = Epon 813/Versamid 140 (50:50); [b] = Nitrocellulose solution (4-8%) in ethanol/diethylether (2 wt% = 1 mL on 1 g scale).

Testing the new developed formulations **A** and **B** on a 1 g scale revealed an increased DW compared to the reference formulation (Table 5). However, both formulations failed to meet the SP requirement.

Table 6. Sensitivities of the tested formulations.

	IS [J]	*FS* [N]	T_{onset} [°C]
Sabatini	9	240	231
A	30	360	156
B	30	360	156

Annotation: BAM standard; FS = friction sensitivity; IS = impact sensitivity; T_{onset} = decomposition temperature (heating rate of 5 °C min^{-1}).

The safe handling of formulations **A** and **B** can be guaranteed by low sensitivities compared to Sabatini´s formulation (Table 5). Applying a binder mixture of NC and an epoxy binder system in **A** resulted in the same sensitivity toward mechanical stimuli as measured for formulation **B**. Formulation **A** and **B** displayed identical decomposition temperatures at 156 °C which is close to the decomposition temperature of the pure compound **8**.

Conclusions

Several alkali and alkaline earth salts of 3,3'-diamino-4,4'-dinitramino-5,5'-bi-1,2,4-triazole (H_2ANAT) were synthesized and intensively characterized. Crystal structures with the exception of the barium salt were determined and discussed. The herein presented synthesis is free of organic solvents, which helps to reduce solvent and other wastes in flare manufacturing. The energetic and thermal investigations revealed low sensitivities toward mechanical stimuli and high decomposition temperatures of the corresponding metals salts. Future investigations will focus on improving the spectral purities while maintaining the high dominant wavelengths of the developed red-light-emitting pyrotechnical formulations. Since all pyrotechnical formulations are to some extent scale-sensitive, the investigation of the luminous intensity is postponed to full-scale test, which will also show the compatibility with other requirements such as burn time and ignition reliability of the prototype device.

Experimental Section

CAUTION! The compounds described in this work are potential explosives, which are sensitive to external stimuli such as impact, friction, heat or electrostatic discharge. While no issues in the handling of these materials were encountered, appropriate precautions and proper protective measures (safety glasses, face shields, leather coat, Kevlar gloves and ear protectors) should be taken when preparing and manipulating these materials.

General: All reagents and solvents were purchased from Sigma-Aldrich, Fluka, and Acros Organics. Decomposition temperatures were measured with a OZM Research DTA 552-Ex Differential Thermal Analyzer using heating rates of 5 °C min^{-1}. ^{1}H and ^{13}C NMR spectra were measured with a JEOL Eclipse 400, JEOL Eclipse 270 or JEOL EX400 instrument at an ambient temperature. All chemical shifts are quoted in ppm relative to TMS (^{1}H, ^{13}C) as external standards. Infrared spectra were measured using a Perkin-Elmer Spectrum One FT-IR spectrometer. Elemental analyses were performed with an Elementar Vario EL or an Elementar Vario EL micro cube. The impact and friction sensitivities were determined using a BAM drophammer and a BAM friction tester. The sensitivities of the compounds were indicated according to the UN Recommendations on the Transport of Dangerous Goods. (+): impact: insensitive >40 J, less sensitive >35 J, sensitive >4 J, very sensitive <4 J; friction: insensitive >360 N, less sensitive=360 N, sensitive <360 N, very sensitive <80 N, extreme sensitive <10 N.[19] The values represent the lowest impact energy at which the result "explosion or deflagration" is obtained from at least one out of at least six trials. The controlled burn down of the pyrotechnic formulations was filmed with a digital video camera recorder (SONY, DCR-HC37E). Spectrometric measurements of the formulations were performed with a HR2000+ES spectrometer with an ILX511B linear silicon CCD-array detector and included software from Ocean Optics with a detector-sample distance of 1 meter. The dominant wavelength and spectral purity were measured based on the 1931 CIE method using illuminant C as the white reference point. Four samples were measured for each formulation.

Preparation of pyrotechnic formulations: The samples were weighed out according to their weight percentages (max. 1 g total) into a mortar. After grinding by hand for 3 min, both the Epon 813 (20 mg/mL) and the Versamid 140 solution (10 mg/mL) in ethyl acetate were added using a syringe. The mixture was blended with a spatula every 10 min until the solvent was evaporated. The solid material was stored over night at 70 °C in the drying oven for curing. Before consolidation, the pyrotechnic material was ground again by hand for 3 min. The formulations were pressed with the aid of a tooling die (inner diameter 12.9 mm) into a cylindrical shape. The formulation powders were pressed at a consolidation dead load of 2 t with a dwell time of 3 s.

Metal 3,3'-Diamino-4,4'-dinitramino-5,5'-bi-1,2,4-triazole Salts: The 3,3´-diamino-4,4´-dinitramino-5,5´-bi-1,2,4-triazole (**2**) salts were synthesized by suspending **2** (300 mg, 1.05 mmol) in water. The corresponding metal bases were added in stoichiometric amounts and heated until a clear solution appeared. After cooling to ambient temperatures, the solution was left for crystallization. The obtained solids were recrystallized from a solvent mixture of ethanol/water (1:2).

Disodium 3,3'-Diamino-4,4'-dinitramino-5,5'-bitriazolate tetrahydrate (3)

3 was obtained as a brown powder. Recrystallization leads to yellow crystals. **Yield:** 363 mg (0.902 mmol, 86 %). **^{1}H NMR** ([D6]DMSO): δ = 5.26 (s, 4 H, -NH_2) ppm. **^{13}C NMR** ([D6]DMSO): δ = 138.1 (2C, CC), 153.4 (2C, -CNO_2) ppm. $C_4H_4N_{12}O_4Na_2 \cdot 4H_2O$ (402.19): calcd. C 11.95, H 3.01, N 41.79%; found C 12.13, H 2.99, N 41.29%. **IR** (ATR): $\tilde{v}$ = 3455 (m), 3390 (m), 3292 (m), 3225 (m), 1687 (w), 1618 (s), 1558 (m), 1465 (m), 1393 (s), 1286 (s), 1221 (s), 1093 (w), 1031 (m), 972 (m), 887 (m), 738 (w), 707 (w) cm^{-1}. **IS** (grain size <100µm): 40 J. **FS** (grain size <100µm): 360 N. **DTA**: 287 °C (onset.).

Dipotassium 3,3'-Diamino-4,4'-dinitramino-5,5'-bitriazolate (4)

4 was obtained as a brown powder. Recrystallization leads yellow crystals. **Yield:** 353 mg (0.973 mmol, 93 %). **^{1}H NMR** ([D6]D_2O): δ = 9.55 (s, 4 H, -NH_2) ppm. **^{13}C NMR** ([D6]DMSO): δ = 137.6 (2C, CC), 153.7 (2C, -CNO_2) ppm. $C_4H_4N_{12}O_4K_2$ (362.35): calcd. C 13.26, H 1.11, N 46.93%; found C 13.36, H 1.47, N 45.36%. **IR** (ATR): $\tilde{v}$ = 3373 (m), 3291 (w), 3218 (w), 3079 (m), 1639 (s), 1561 (m), 1467 (m), 1426 (w), 1372 (s), 1286 (s), 1101 (m), 1030 (m), 1004 (w), 965 (m), 879 (m), 782 (m), 717 (m), 653 (w) cm^{-1}. **IS** (grain size <100µm): 3 J. **FS** (grain size <100µm): 360 N. **DTA**: 250 °C (onset.).

Dicesium 3,3'-Diamino-4,4'-dinitramino-5,5'-bitriazolate (5)

5 was obtained as yellow crystals. **Yield:** 541 mg (0.983 mmol, 94 %). **^{1}H NMR** ([D6] D_2O): δ = 9.57 (s, 4 H, $-NH_2$) ppm. **^{13}C NMR** ([D6]D_2O): δ = 137.7 (2C, CC), 154.0 (2C, $-CNO_2$) ppm. $C_4H_4N_{12}O_4Cs_2$ (549.96): calcd. C 8.74, H 0.73, N 30.56%; found C 8.73, H 0.91, N 29.51%. **IR** (ATR): ν˜ = 3343 (w), 3291 (w), 3080 (w), 1636 (m), 1554 (m), 1465 (m), 1367 (s), 1281 (s), 1219 (m), 1119 (w), 1029 (m), 997 (w), 964 (w), 876 (m), 833 (w), 779 (w), 715 (m), 696 (m), 653 (w) cm^{-1}. **IS** (grain size <100µm): 8 J. **FS** (grain size <100µm): 360 N. **DTA**: 220 °C (onset.).

Dirubidium 3,3'-Diamino-4,4'-dinitramino-5,5'-bitriazolate (6)

6 was obtained as a brown powder. Recrystallization leads to colorless crystals. **Yield:** 430 mg (0.945 mmol, 90 %). **^{1}H NMR** ([D6]D_2O): δ = 9.55 (s, 4 H, $-NH_2$) ppm. **^{13}C NMR** ([D6]DMSO): δ = 138.37 (2C, CC), 154.6 (2C, $-CNO_2$) ppm. $C_4H_4N_{12}O_4Rb_2$ (455.09): calcd. C 10.65, H 0.89, N 36.93%; found C 10.94, H 1.28, N 37.40%. **IR** (ATR): ν˜ = 3376 (m), 3289 (w), 3215 (s), 3096 (m), 1740 (w), 1635 (s), 1559 (m), 1465 (m), 1374 (s), 1283 (s), 1220 (s), 1105 (m), 1026 (m), 1105 (w), 1026 (m), 964 (m), 877 (m), 782 (w), 717 (w), 650 (w) cm^{-1}. **IS** (grain size <100µm): 10 J. **FS** (grain size <100µm): 360 N. **DTA**: 250 °C (onset.).

Calcium 3,3'-Diamino-4,4'-dinitramino-5,5'-bitriazolate pentahydrate (7)

7 was obtained as a brown powder. Recrystallization leads to yellow crystals. **Yield:** 383 g (924 mmol, 88 %). **^{1}H NMR** ([D6]DMSO): δ = 5.33 (s, 4 H, $-NH_2$) ppm. **^{13}C NMR** ([D6]DMSO): δ = 138.0 (2C, CC), 153.4 (2C, $-CNO_2$) ppm. $C_4H_4N_{12}O_4Ca \cdot 5H_2O$ (414.31): calcd. C 11.60, H 3.41, N 40.57%; found C 11.93, H 3.42, N 40.39%. **IR** (ATR): ν˜ = 3435 (m), 3346 (m), 1739 (w), 1616 (s), 1554 (m), 1470 (m), 1435 (m), 1418 (m), 1283 (s), 1247 (m), 1102 (w), 1035 (w), 1017 (m), 973 (m), 904 (m),776 (w), 756 (w), 719 (w), 677 (w), 653 (w) cm^{-1}. **IS** (grain size <100µm): 40 J. **FS** (grain size <100µm): 360 N. **DTA**: 150 °C (onset.).

Strontium 3,3'-Diamino-4,4'-dinitramino-5,5'-bitriazolate hexahydrate (8)

8 was obtained as an orange powder. Recrystallization leads to colorless crystals. **Yield:** 459 mg (0.957 mmol, 91 %). **^{1}H NMR** ([D6]DMSO): δ = 6.00 (s, 4 H, $-NH_2$) ppm. **^{13}C NMR** ([D6]DMSO): δ = 138.1 (2C, CC), 153.0 (2C, $-CNO_2$) ppm. $C_4H_4N_{12}O_4Sr \cdot 6H_2O$ (479.86): calcd. C 10.01, H 3.31, N

35.03%; found C 9.94, H 3.19, N 34.62%. **IR** (ATR): ṽ = 3549 (m), 3292 (s), 3229 (s), 3176 (s), 17139 (w), 1621 (s), 1566 (s), 1472 (m), 1412 (s), 1299 (s), 1234 (s), 1130 (m), 1050 (m), 1024 (w), 976 (m), 900 (m), 779 (w), 714 8w), 658 (w) cm^{-1}. **IS** (grain size <100µm): 40 J. **FS** (grain size <100µm): 360 N. **DTA**: 250 °C (onset.).

Barium 3,3'-Diamino-4,4'-dinitramino-5,5'-bitriazolate dihydrate (9)

9 already precipitated in boiling water and was obtained as a brown powder. Due to solubility issues, no further NMR analysis or recrystallization was possible since even boiling DMSO (Reflux 170 °C / 2h) failed to dissolve the crude product. **Yield:** 355 mg (0.770 mmol, 73 %). $C_4H_4N_{12}O_4Ba \cdot 2H_2O$ (461.54): calcd. C 10.41, H 2.62, N 36.42%; found C 10.55, H 1.92, N 36.22%. **IR** (ATR): ṽ = 3608 (w), 3410 (m), 3316 (m), 3252 (m), 3187 (m), 3000 (m), 2190 (w), 1629 (s), 1566 (s) 1472 (m)1442 (s), 1417 (s), 1291 (s) 1229 (s) 1092 (m) 1034 (m), 966 (m), 898 (s), 772 (m), 721 (w), (667 (w), 637 (w) cm^{-1}. **IS** (grain size <100µm): 40 J. **FS** (grain size <100µm): 360 N. **DTA**: 280 °C (onset.).

Literature

[1] a)J. D. Moretti, C. M. Csernica, J. C. Poret, A. P. Shaw, N. E. Carlucci, M. G. Seiz, J. D. Conway, *ACS Sustainable Chem. Eng.* **2017**, 10.1021/acssuschemeng.7b02623; b)J. T. Koenig, A. P. Shaw, J. C. Poret, W. S. Eck, L. J. Groven, *ACS Sustainable Chem. Eng.* **2017**, 10.1021/acssuschemeng.7b02579; c)J. S. Brusnahan, A. P. Shaw, J. D. Moretti, W. S. Eck, *Propellants, Explos., Pyrotech.* **2017**, *42*, 62-70; d)J. S. Brusnahan, J. C. Poret, J. D. Moretti, A. P. Shaw, R. K. Sadangi, *ACS Sustainable Chem. Eng.* **2016**, *4*, 1827-1833; e); f)J. D. Moretti, J. J. Sabatini, A. P. Shaw, R. Gilbert, *ACS Sustainable Chem. Eng.* **2014**, *2*, 1325-1330; g)E. J. Miklaszewski, A. P. Shaw, J. C. Poret, S. F. Son, L. J. Groven, *ACS Sustainable Chem. Eng.* **2014**, *2*, 1312-1317.

[2] a)P. Yin, J. Zhang, C. He, D. A. Parrish, J. n. M. Shreeve, *J. Mater. Chem. A* **2014**, *2*, 3200-3208; b)C. K. Wilharm, A. Chin, S. K. Pliskin, *Propellants, Explos., Pyrotech.* **2014**, *39*, 173-179; c)J. D. Moretti, J. J. Sabatini, G. Chen, *Angew. Chem. Int. Ed.* **2012**, *51*, 6981-6983.

[3] K. Sellers, K. Weeks, W. R. Alsop, S. R. Clough, M. Hoyt, B. Pugh, *Perchlorate Environmental Problems and Solutions*, Taylor & Francis, Boca Raton, FL (USA), **2007**.

[4] Health and Ecological Criteria Division, Office of Science and Technology, Office of Water, U.S. Environmental Protection Agency, *Interim Drinking Water Health Advisory for Perchlorate,*, EPA 822-R-08-025*,* Washington, DC, **2008**.

[5] a)T. M. Klapötke, T. G. Müller, M. Rusan, J. Stierstorfer, *Z. Anorg. Allg. Chem.* **2014**, *640*, 1347-1354; b)I. E. Drukenmüller, T. M. Klapötke, Y. Morgenstern, M. Rusan, J. Stierstorfer, *Z. Anorg. Allg. Chem.* **2014**, *640*, 2139-2148; c)I. M. Tuukkanen, E. L. Charsley, P. G. Laye, J. J. Rooney, T. T. Griffiths, H. Lemmetyinen, *Propellants, Explos., Pyrotech.* **2006**, *31*, 110-115; d)J. J. Sabatini, J. D. Moretti, *Chem. - Eur. J.* **2013**, *19*, 12839-12845; e)B. E. Douda, *Theory of Colored Flame Production, ADA951815,* , RDTN No. 71*,* NSWC Crane, Indiana, USA, **1964**; f)J. A. Conkling;, C. Mocella, *Chemistry of Pyrotechnics: Basic Principles and Theory*, CRC Press, Boca Raton **2010**.

[6] W. Christmann, D. Kasiske, K. D. Klöppel, H. Partscht, W. Rotard, *Chemosphere* **1989**, 387-392.

[7] J. J. Sabatini, E.-C. Koch, J. C. Poret, J. D. Moretti, S. M. Harbol, *Angew. Chem. Int. Ed.* **2015**, *54*, 10968-10970.

[8] G. Steinhauser, T. M. Klapötke, *Angew. Chem., Int. Ed.* **2008**, *47*, 3330-3347.

[9] a)J. Glück, T. M. Klapötke, M. Rusan, J. Stierstorfer, *Chem. - Eur. J.* **2014**, *20*, 15947-15960; b)N. Fischer, M. Feller, T. M. Klapötke, M. Kowalewski, S. Scheutzow, J. Stierstorfer, *Propellants, Explos., Pyrotech.* **2014**, *39*, 166-172; c)N. Fischer, T. M. Klapötke, S. Marchner, M. Rusan, S. Scheutzow, J. Stierstorfer, *Propellants, Explos., Pyrotech.* **2013**, *38*, 448-459; d)N. Fischer, T. M. Klapötke, K. Peters, M. Rusan, J. Stierstorfer, *Z. Anorg. Allg. Chem.* **2011**, *637*, 1693-1701; e)T. M. Klapötke, J. Stierstorfer, K. R. Tarantik, I. D. Thoma, *Z. Anorg. Allg. Chem.* **2008**, *634*, 2777-2784; f)V. Ernst, T. M. Klapötke, J. Stierstorfer, *Z. Anorg. Allg. Chem.* **2007**, *633*, 879-887; g)D. E. Chavez, M. A. Hiskey, D. L. Naud, *J. Pyrotech.* **1999**, *10*, 17-36; h)D. E. Chavez, M. A. Hiskey, *J. Pyrotech.* **1998**, *7*, 11-14; i)T. M. Klapötke, H. Radies, J. Stierstorfer, K. R. Tarantik, G. Chen, A. Nagori, *Propellants, Explos., Pyrotech.* **2010**, *35*, 213-219; j)L. H. Finger, F. G. Schröder, J. Sundermeyer, *Z. Anorg. Allg. Chem.* **2013**, *639*, 1140-1152.

[10] T. M. Klapötke, *Chemistry of High-Energy Materials*, 4th ed., De Gruyter, Berlin, Boston, **2017**.

[11] J. J. Sabatini, in *Green Energetic Materials* (Ed.: T. Brinck), John Wiley & Sons, Ltd, West Sussex, United Kingdom, **2014**, pp. 63-102.

[12] P. Yin, Q. Zhang, J. M. Shreeve, *Acc. Chem. Res.* **2016**, *49*, 4-16.

[13] a)T. M. Klapötke, M. Leroux, P. C. Schmid, J. Stierstorfer, *Chem. - Asian J.* **2016**, *11*, 844-851; b)J. Glück, T. M. Klapötke, M. Rusan, J. J. Sabatini, J. Stierstorfer, *Angew. Chem., Int. Ed.* **2017**, *56*, 16507.

[14] Crystallographic data for the structures have been deposited with the Cambridge Crystallographic Data Centre. Copies of the data can be obtained free of charge on application to The Director, CCDC, 12 Union Road, Cambridge CB2 1EZ, UK (Fax: int.code_(1223)336-033; e-mail for inquiry: fileserv@ccdc.cam.ac.uk; e-mail for deposition: (deposit@ccdc.cam.ac.uk).

[15] L. E. Tønnesen, B. F. Pedersen, J. Klaveness, *Acta Chem. Scand.* **1996**, *50*, 603-608.

[16] J. Mähler, I. Persson, *Inorg. Chem.* **2012**, *51*, 425-438.

[17] A. Bondi, *J. Phys. Chem.* **1964**, *68*, 441-451.

[18] J. C. Cackett, *Monograph on pyrotechnic compositions,* (Ed.: Royal Armament Research and Development Establishment), Ministry of Defence (Army), Fort Halstead, Seven Oaks, United Kingdom, **1965**, 53-54.

[19] United Nations, *Recommendations on the Transport of Dangerous Goods: Manual of Tests and Criteria - Amendment 1 of the 5th Revised Edition,*5th ed., **2011**, doi:http://dx.doi.org/10.18356/fbc2c205-en.

Supporting Information

Crystallographic data

The crystal structures were uploaded to the CSD database[1] and can be obtained free of charge with the CCDC nos. 1837414 (**3**), 1837411 (**4**), 1837410 (**5**), 1837413 (**6**), 1837409 (**7**), and 1837412 (**8**).

Table 1. Crystallographic data of **3**–**5**.

Compound	**3**	**4**	**5**
Formula	$C_4H_4N_{12}O_4Na_2 \cdot 4H_2O$	$C_4H_4N_{12}O_4K_2$	$C_4H_4N_{12}O_4Cs_2$
Form. Mass [g/mol]	201.12	181.20	550.01
Crystal system	triclinic	monoclinic	orthorhombic
Space Group	*P-1* (No. 2)	*P21/n* (No. 14)	*Pca2₁* (No. 29)
Color / Habit	yellow block	yellow block	yellow needle
Size [mm]	0.10 × 0.20 × 0.25	0.10 × 0.10 × 0.35	0.05 × 0.06 × 0.40
a [Å]	5.7190(7)	8.7758(4)	15.4025(9)
b [Å]	8.0939(10)	4.9394(2)	4.9514(3)
c [Å]	9.4531(10)	14.3239(7)	17.9392(9)
α [°]	111.276(11)	90	90
β [°]	103.533(10)	104.426(5)	90
γ [°]	94.954(10)	90	90
V [$Å^3$]	389.28(9)	601.32(5)	1368.11(13)
Z	2	4	4
$\rho_{calc.}$ [g cm^{-3}]	1.716	2.001	2.670
μ [mm^{-1}]	0.201	0.836	5.372
F(000)	206	364	1016
$\lambda_{MoK\alpha}$[Å]	0.71073	0.71073	0.71073
T [K]	293	294	296
ϑ min-max [°]	4.2, 26.0	4.4, 26.0	4.1, 26.0
Dataset h; k; l	-6:7; -7:9; -11:11	-10:10; -6:6; -17:17	-19:13; -6:5; -9:22
Reflect. coll.	2812	8041	3419
Independ. refl.	1516	1178	1820
R_{int}	0.024	0.026	0.024
Reflection obs.	1157	1178	1857
No. parameters	142	108	200
R_1 (obs)	0.0394	0.0254	0.0327

wR_2 (all data)	0.1099	0.0683	0.0854
S	1.03	1.06	1.09
Resd. Dens. [e Å^{-3}]	-0.20, 0.41	-0.22, 0.35	-1.24, 1.87
Device type	Oxford Xcalibur3 CCD	Oxford Xcalibur3 CCD	Oxford Xcalibur3 CCD
Solution	SIR-92	SIR-92	SIR-92
Refinement	SHELXL-97	SHELXL-97	SHELXL-97
Absorpt. corr.	multi-scan	multi-scan	multi-scan
CCDC	1837414	1837411	1837410

Table 2. Crystallographic data of **6**–**8**.

Compound	**6**	**7**	**8**
Formula	$C_4H_4N_{12}O_4Rb_2$	$C_4H_4N_{12}O_4Ca \cdot 5H_2O$	$C_4H_4N_{12}O_4Sr \cdot 6H_2O$
Form. Mass [g/mol]	455.13	414.31	479.91
Crystal system	monoclinic	monoclinic	monoclinic
Space Group	*P21/n* (No. 14)	*C2/c* (No. 15)	$P2_1/m$ (No. 11)
Color / Habit	colorless needle	yellow crystals	colorless block
Size [mm]	0.08 × 0.08 × 0.18	0.4 x 0.4 x 0.4	0.10 × 0.16 × 0.20
a [Å]	8.8652(4)	11.4009(8)	6.3002(5)
b [Å]	5.1322(2)	13.7933(5)	13.4566(9)
c [Å]	14.1922(6)	11.5508(7)	10.1845(7)
α [°]	90	90	90
β [°]	105.030(4)	119.273(9)	104.650(8)
γ [°]	90	90	90
V [Å^3]	623.63(5)	1584.5(2)	835.36(11)
Z	2	4	2
$\rho_{calc.}$ [g cm^{-3}]	2.424	1.737	1.908
μ [mm^{-1}]	7.894	0.473	3.308
F(000)	436	856	484
$\lambda_{MoK\alpha}$[Å]	0.71073	0.71073	0.71073

T [K]	173	173	295
ϑ min-max [°]	4.2, 26.0	4.6, 26.0	4.3, 27.0
Dataset h; k; l	-8:10; -6:6; -17:17	-12:14; -16:15 ; -14:14	-7:8; -17:16; -13:5
Reflect. coll.	4270	5873	3577
Independ. refl.	1226	1546	1880
R_{int}	0.025	0.021	0.030
Reflection obs.	1226	1366	1880
No. parameters	108	147	164
R_1 (obs)	0.0223	0.0286	0.0315
wR_2 (all data)	0.0557	0.0767	0.0694
S	1.08	1.05	1.04
Resd. Dens. [e Å^{-3}]	-0.89, 0.37	-0.21, 0.43	-0.38, 0.72
Device type	Oxford Xcalibur3 CCD	Oxford Xcalibur3 CCD	Oxford Xcalibur3 CCD
Solution	SIR-92	SIR-92	SIR-92
Refinement	SHELXL-97	SHELXL-97	SHELXL-97
Absorpt. corr.	multi-scan	multi-scan	multi-scan
CCDC	1837413	1837409	1837412

CIE 1931 chromaticity diagram

An easy way to show or compare the spectral purity and dominant wavelength of various formulations is CIE 1931 chromaticity diagram (Figure 1). The color purity of a visible flare with the chromaticity (x, y) is its difference from the illuminant´s white point (WP) relative to the furthest point on the chromaticity diagram with the same hue (dominant wavelength for monochromatic sources). The color purity can be calculated by dividing the distance WP to A (x, y) = d(WP, A) by the distance WP to B = d(WP, B). B is the point with the maximum purity of 100% for the dominant wavelength of formulation A.[2] The higher the spectral purity of A, the more the point moves to the right until it ends up having the coordinates of B.

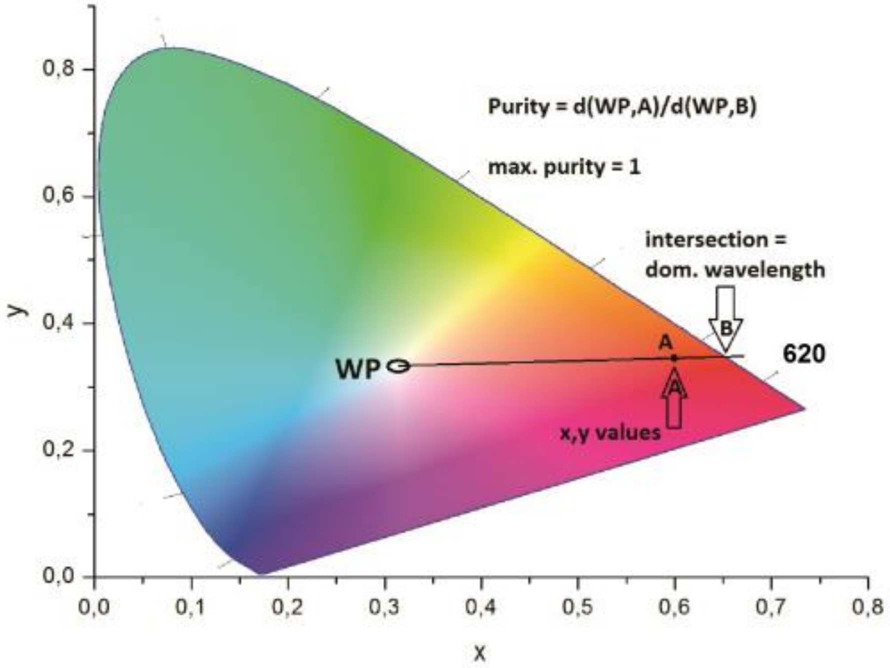

Figure 1. CIE 1931 chromaticity diagram

References

[1] Crystallographic data for the structures have been deposited with the Cambridge Crystallographic Data Centre. Copies of the data can be obtained free of charge on application to The Director, CCDC, 12 Union Road, Cambridge CB2 1EZ, UK (Fax: int.code_(1223)336-033; e-mail for inquiry: fileserv@ccdc.cam.ac.uk; e-mail for deposition: (deposit@ccdc.cam.ac.uk).

[2] T. M. Klapötke, *Chemistry of High-Energy Materials*, 4th ed., De Gruyter, Berlin, Boston, **2017**.

4.2 A Strontium- and Chlorine-Free Pyrotechnic Illuminant of High Color Purity

Published in *Angew. Chem., Int. Ed.* **2017**, *56,* 16507. (DOI: 10.1002/anie.201710746)

Abstract: The need to develop a red-light-emitting pyrotechnic illuminant has garnered interest from the pyrotechnics community due to potential United States Environmental Protection Agency (U.S. EPA) regulations of strontium and chlorinated organic materials. To address these environmental regulatory concerns, the development of lithium-based red-light-emitting pyrotechnic compositions of high purity and color quality is described. These formulations do not contain strontium or chlorinated organic materials. Rather, the disclosed formulations are based on a non-hygroscopic dilithium high-nitrogen salt which serves as both the oxidizer and red colorant. These formulations are likely to draw interest from the civilian fireworks and military pyrotechnics communities for further development; both of whom have a vested interest in the development of environmentally conscious formulations.

For many, firework displays are an integral component of national or religious holidays or New Year´s Eve. In the military sector, the production of colored light finds common usage for the purposes of signaling or to illuminate a specified area to accomplish a mission. Due to the ubiquitous nature of colored light-emitting-pyrotechnics, it is imperative that health and environmental issues be considered when developing illuminating compositions of high performance and high color quality. Colored flames are produced mostly by burning alkali and alkaline earth metal salts. Traditional red-light-emitting pyrotechnic formulations are based on strontium and chlorinated organic materials to achieve a suitable red-light-emitting species.[1] These mixtures mostly contain strontium nitrate in combination with a chlorine donor such as polyvinyl chloride (PVC) to form metastable strontium(I) chloride as the red-light-emitting specie.

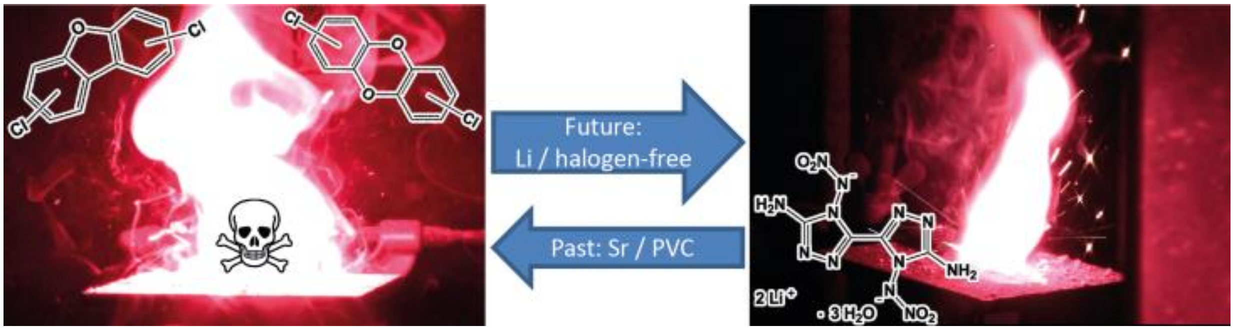

Figure 1. Comparison of Sr/PVC containing and Li/chlorine-free **B**.

Although the bright red light of strontium- and chlorine-containing mixtures seem innocuous, their use is a cause for concern. During the combustion of chlorine-containing pyrotechnic formulations, highly carcinogenic polychlorinated biphenyls, polychlorinated dibenzofurans and polychlorinated dibenzo-*p*-dioxins are formed (Figure 1).[2] Although contradictory opinions concerning the amount of these polychlorinated decomposition products are reported in literature[3, 4], chlorine-free pyrotechnic formulations are desired nevertheless. Chlorine-free pyrotechnic formulations yielding green[5], blue[6] and red light[7] have been reported in recent years, achieving good color qualities and high intensities.

According to a recent U.S. EPA (United States Environmental Protection Agency) report, strontium is potentially harmful to human health.[8] The U.S. EPA states that strontium replaces calcium in the bone, interferes with bone strength, and thus affects the skeletal development of children and adolescents. In 2014, the U.S. EPA has made a preliminary decision to start regulating strontium.[8, 9] Strontium has been detected in 99 percent of public water systems and at levels of concern in 7 percent of public water systems in the USA (U.S. EPA).[10] Although U.S. military training grounds were not included in the study, these facilities may show elevated concentrations of strontium as well, given the presence of strontium in currently used red-light-illuminating signaling pyrotechnic compositions.

Given these newfound concerns associated with strontium, a new method of generating red light of a deep color purity was needed. As an alternative to strontium, lithium-based formulations were considered as a means to generate red light. Although lithium-based formulations have been investigated in the past, these formulations have been plagued by high hygroscopicity and low color purity.[11] Instead of red light, these prior lithium-based formulations yielded pink- or orange-colored flames. Furthermore, past lithium-based formulations utilized perchlorates as the oxidizer, and this oxidizer is no longer viewed as being environmentally acceptable.[11, 12] Certain parameters have to be complied with in order to obtain optimal color properties when using lithium as a red-light emitter. The principle emitter in lithium-based red flames is atomic lithium, and its concentration should be kept as a low as possible to avoid a broadening of the lithium line width.[12c, 13, 14] In contrast to Sr-containing formulations, a reductive flame atmosphere is essential to achieve red light with lithium.

A practical red-light-emitting formulation based on lithium must possess a deep color purity, and a lithium-based material that is not moisture sensitive. To achieve a reductive flame atmosphere, it is important to prevent oxidation processes in the outer part of the flame that are accompanied by the formation of unwanted LiOH, LiO and condensed compounds such as Li_2O. These species lower the amount of atomic lithium present, and serve to lower red-light-emitting color purity. The release of high amounts of nitrogen was believed to be beneficial due to its favorable energy release, and its metal-free combustion.

One suitable candidate, the lithium salt of 3,3'-diamino-4,4'-dinitramino-5,5'-bi-1,2,4-triazolate $\cdot$ 3 H_2O - Li_2ANAT (**3**) (Scheme 1), was synthesized. Compound **3** was found to have a high decomposition temperature, as well as a non-hygroscopic behavior. Thus, it was investigated in pyrotechnic formulations. Colorant **3** was synthesized in a simple three-step reaction (Scheme 1). 4,4',5,5'-Tetraamino-3,3'-bi-1,2,4-triazole (**1**) and 5,5'-diamino-4,4'-dinitramino-3,3'-bi-1,2,4-triazole (**2**) were synthesized previously.[1] Deprotonation of **2** with LiOH gave the dilithium salt **3**.

Scheme 1. Synthesis of dilithium 3,3'-diamino-4,4'-dinitramino-5,5'-bi-1,2,4-triazolate trihydrate (**3**).

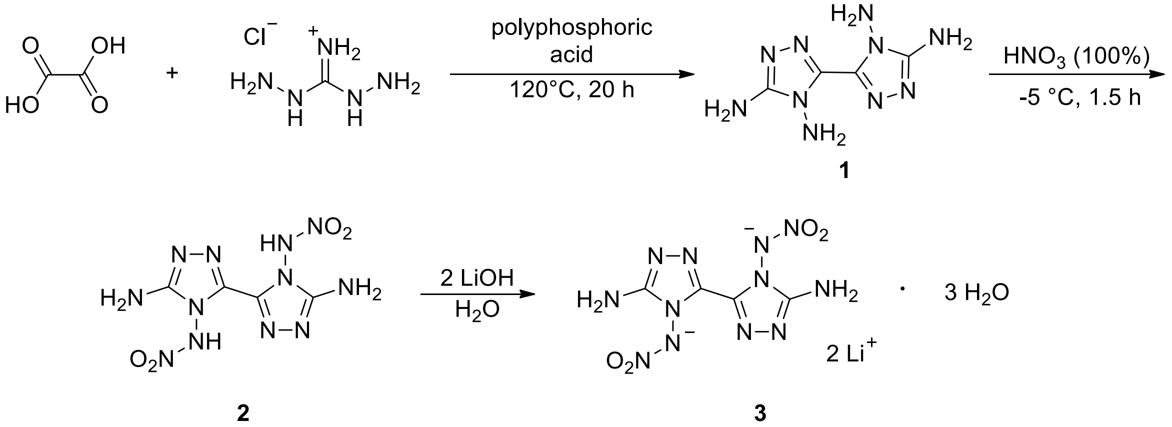

The dilithium salt **3** was extensively characterized by multinuclear NMR and vibrational spectroscopy as well as by X-ray techniques (supporting information). **3** reveals oxidizing and coloring properties at the same time, which is beneficial to reduce the amount of components in pyrotechnic mixtures and was tested for its suitability in pyrotechnic formulations and compared to a chlorine-free Sr-based formulation on a 1 g scale.[7] Two formulations **A** and **B** (Table 1) were investigated. Both formulations consisting of **3**, magnesium, hexamine and nitrocellulose as fuels were prepared with the Epon 813/Versamid 140 (1:1) binder system (Table 1). Although the lithium salt contained crystal water, there were no problems related to hygroscopicity.

Table 1. Formulations **A** and **B** containing Li_2ANAT (**3**) and the Sr-containing control.

Components	Weight %		
Formulation	**Control**	**A**	**B**
Sr(NO3)2	48	-	-
Li_2ANAT (3)	-	51	48
Mg 50/100 mesh	33	31	15
Nitrocellulose	-	2	4
Hexamine	-	12	26
5-AT	12	-	-
Epoxy binder	7	4	7

As the control, the chlorine-free strontium-containing formulation containing strontium nitrate, magnesium, 5-aminotetrazole (5-AT) and the binder system Epon 813/Versamid 140 (4:1) was employed (Table 1).[7] The burn time (BT), dominant wavelength (DW), luminous intensity (LI), spectral purity (SP), friction (FS)-/impact (IS)-/electrostatic discharge sensitivity (ESD) as well as the decomposition temperature (T_{onset}) were measured.

Table 2. Performances of the Strontium-containing control and lithium-based formulations **A** and **B**.

Formulation	BT[a] [s]	LI[b] [cd]	DW[c] [nm]	SP[d] [%]
Control	5	35400	607	79
A	9	2130	605	70
B	16	820	606	88

[a] BT = burn time. [b] LI = luminous intensity. [c] DW = dominant wavelength. [d] SP = spectral purity.

Formulations **A** and **B** burned with a red colored flame and no smoke could be observed. The performance of both formulations is summarized in Table 2. The two formulations exhibited longer burn times than the control, and dominant wavelengths of 605 and 606 nm, which are both within the 620±20 nm region of the required dominant wavelength for red color.[7] Although formulation **A** fell below the minimum spectral purity threshold of 76%, formulation **B** had a significantly improved spectral purity of 88%, which was also significantly greater than the control. The higher magnesium content in **A** compared to **B**, leads to higher luminosity but lower spectral purity owing to the increased incandescence caused by a greater amount of condensed $MgO_{(s, l)}$.

Table 3. Sensitivities of the control and formulations **A** and **B**.

Formulation	IS[a] [J]	FS[b] [N]	ESD[c] [J]	T_{onset} [d] [°C]
Control	9	240	>0.25	231
A	25	360	1.5	198
B	40	360	1	217

[a] IS = impact sensitivity. [b] FS = friction sensitivity. [c] ESD = electrostatic discharge sensitivity. [d] T_{onset} = onset temperature of decomposition.

Relative to the control both formulations **A** and **B** are less sensitive to impact, friction and ESD (Table 3). Additionally, the decomposition temperature of the more optimal formulation **B** was measured to be higher than 200 °C. These properties allow the safe handling of the material. In Figure 2 the CIE 1931 chromaticity diagram of formulations **A**, **B** and the Sr-control is illustrated, thus illustrating that it is possible to develop a suitable red-light-emitter that is free of halogens and strontium.

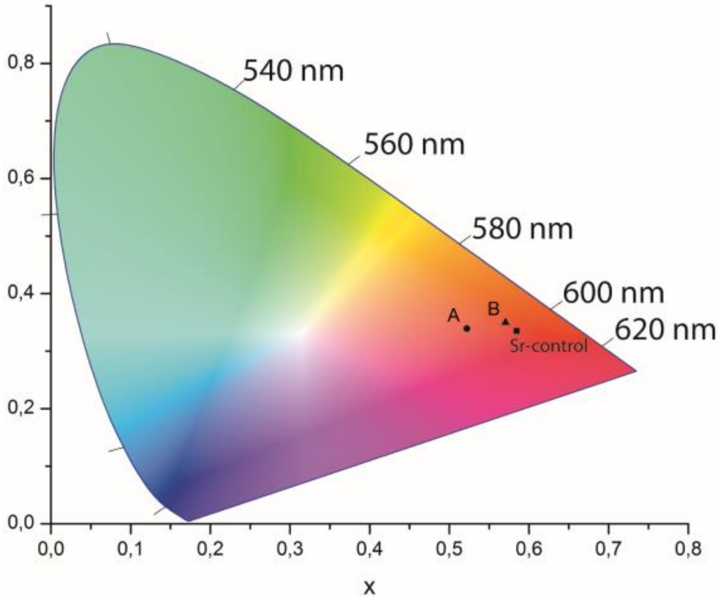

Figure 2. CIE 1931 chromaticity diagram of red formulations**.**

As can be seen, the Li-based colorants reveal color points, which are in close proximity to the red Sr-control formulation (see supporting information for explanation). The emission spectra of composition **B** is depicted below (Figure 3). Both atomic emission lines of lithium can be seen at 670 nm and 610 nm respectively. Like in all pyrotechnic formulations, the sodium emission at 589 nm is present.

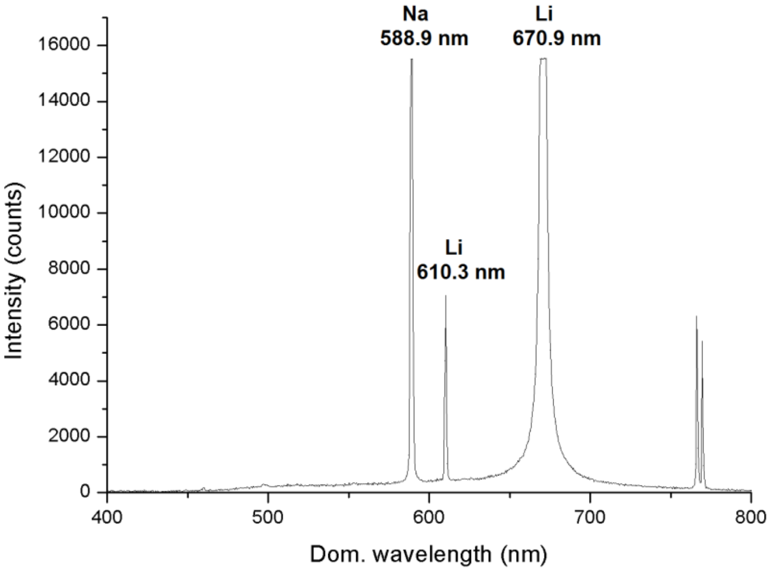

Figure 3. Emission spectrum of formulation **B.**

The use of the lithium-based high-nitrogen compound **3** in pyrotechnic formulations serving as both an oxidizing agent and red colorant yielded red color qualities. The color quality of lithium-based formulation **B** was comparable to those of chlorine-free Sr-based compositions. While further optimization is still needed to improve the luminosity of Li-based red-light-emitting flares, this represents the first known example of a successful red-light-emitting formulation of high color quality and purity that does not contain halogenated- or strontium-based materials.

References

[1] J. A. Conkling, *Chemistry of Pyrotechnics: Basic Principles and Theory 2nd Ed.* Taylor & Francis, New York, **1985**.

[2] W. Christmann, D. Kasiske, K. D. Klöppel, H. Partscht, W. Rotard, *Chemosphere* **1989,** *19,* 387–392.

[3] O. Fleischer, H. Wichmann, W. Lorenz, *Chemosphere* **1999,** *39*, 925–932.

[4] D. Dyke, P. Coleman, *Organohalogen Compd.* **1995**, *24,* 213.

[5] a) J. J. Sabatini, J. C. Poret, R. N. Broad, *Angew. Chem. Int. Ed.* **2011**, *50*, 4624–4626; *Angew. Chem.* **2011**, *123,* 4720–4722; b) T. M. Klapötke, B. Krumm, M. Rusan, J. J. Sabatini, *Chem. Commun.* **2014,** *50,* 9581–9583; c) J. J. Sabatini in *Green Energetic Materials* (Ed.: T. Brinck), Wiley-VCH, Weinheim, **2014**, pp. 76–78.

[6] a) D. Junknelivicius, E. Karvinen, T. M. Klapötke, R. Kubilius, R. Ramanavicius, M. Rusan, *Chem. Eur. J.* **2015,** *21,* 15354–15359; b) T. M. Klapötke, M. Rusan, J. J. Sabatini, *Angew. Chem. Int. Ed.* **2014**, *53,* 9665–9668; *Angew. Chem.* **2014**, *126,* 9820–9823.

[7] J. J. Sabatini, E.-C. Koch, J. C. Poret, J. D. Moretti, S. M. Harbol, *Angew. Chem. Int. Ed.* **2015**, *54,* 10968–10970.

[8] https://archive.epa.gov/epapages/newsroom_archive/newsreleases/ 327f339e63facb5a85257d77005f4bf9.html, access date: November 10, 2017.

[9] http://wisconsinwatch.org/2016/03/wisconsin-strontium-levels-among-highest-in-u-s-drinking-water-supplies/, access date: October 12, 2017.

[10] A. J. O'Donnell, D. A. Lytle, S. Harmon, K. Vu, H. Chait, D. D. Dionysiou, *Water Res.* **2016**, *103*, 319–333.

[11] a) C. Jennings-White, *Pyrotechnica XIII,* **1990**, 26; b) C. Jennings-White, Blue Strobe Light Pyrotechnic Composition, *Pyrotechnica XIV* **1992**, 33; c) E.-C. Koch, *J. Pyro. 13,* **2001**, 1 g) D. E. Chavez, M. A. Hiskey, D. L. Naud, *J. Pyro.* **1999,** *10,* 17–37.

[12] R. Webb, Searching for Environmentally-Friendly Coloured Fireworks, *4th International Symposium on Fireworks*, 9–13 October **1998**, Halifax, Canada, 405; b) C. Jennings-White, *Pyrotechnica XVII,* **1997**, 12; c) E.-C. Koch, C. Jennings-White, *36th Int. Pyro. Semin.* 23–28 August **2009,** Rotterdam, Netherlands, 105.

[13] a) R. Mavrodineanu, H. Boiteux, *Flame Spectroscopy*, John Wiley & Sons, New York, **1965**, 368; b) B. E. Douda, Prediction of Line Shapes in Pyrotechnic Flares Containing Lithium, 5th *Int. Pyrotech. Semin.*, **1976**, Vail Colorado, USA, p. 212; c) D. R. Dillehay, Resonance Line Broadening of the Alkali Metal, 9th *Int. Pyrotech. Semin.*, Colorado Springs, **1984,** Colorado, USA, p. 85.

[14] a) B. E. Douda, Theory of Colored Flame Production, *RDTN Report No. 71,* **1964,** U.S. Naval Ammunition Depot, Crane, IN, USA, 1-68; b) E.-C. Koch, *J. Pyro.* **2002,** *15,* 9.

[15] a) T. M. Klapötke, P. C. Schmid, S. Schnell, J. Stierstorfer, *J. Mater. Chem. A* **2015**, *3*, 2658–2668; b) T. M. Klapötke, M. Leroux, P. C. Schmid, J. Stierstorfer, *Chem. Asian J.* **2016**, *11*, 844–851.

Supporting Information

Experimental Procedures

CAUTION! The mixtures described here are potential explosives, which are sensitive to environmental stimuli such as impact, friction, heat, and electrostatic discharge. While we encountered no problems in handling of these materials, appropriate precautions and proper protective measures (safety glasses, face shields, leather coats, Kevlar gloves, and ear protectors) should be taken when preparing and manipulating these materials.

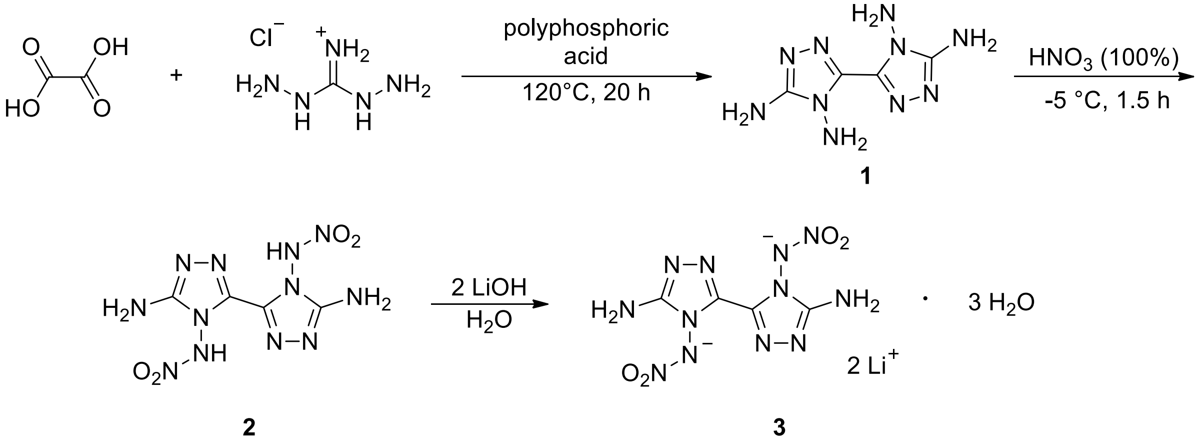

S1. Synthesis of dilithium 3,3'-diamino-4,4'-dinitramino-5,5'-bi-1,2,4-triazolate trihydrate (**3**).

Compound **1** was slowly added to ice-cooled 100% HNO_3 and stirred at -5 °C for 1.5 h. Afterwards the solution was quenched with ice-water and the formed precipitate was filtered off yielding pure 3,3'-diamino-4,4'-dinitramino-5,5'-bi-1,2,4-triazolate (**2**).[[1a]Compound **2** can be used as obtained and does not require further purification. The Li salt **3** was prepared by simple deprotonation reaction. Therefore **2** was suspended in water and lithium hydroxide was added. The suspension was heated until a clear solution appeared and filtrated. The solvent was removed in vacuum to give dilithium 3,3'-diamino-4,4'-dinitramino-5,5'-bi-1,2,4-triazolate trihydrate (**3**) as an orange powder. Recrystallization from water/ethanol yielded colorless crystals (87%) suitable for X-Ray diffraction. DTA (5 °C min^{-1}) onset: 240 °C (dec.); IR (ATR): 3485, 3358, 3299, 3229, 3173, 2179, 2104, 2088, 1648, 1580, 1460, 1421, 1394, 1301, 1237, 1108, 1044, 1016, 971, 896, 826, 768, 716, 656, 586, 538, 489, 467; Raman (1064 nm, 300 mW, 25 °C, cm^{-1}): $\tilde{\nu}$ = 1006 (13), 3365 (1), 1605 (100), 1581 (15), 1550 (5), 1504 (2), 1409 (2), 1398 (2), 1309 (1), 1262 (6), 1094 (5), 1056 (5), 898 (2), 797 (3), 699 (1), 718 (1), 729 (1), 146 (3), 113 (8); ^{1}H NMR ([D_6]DMSO): δ = 5.18 (s, 2H); ^{13}C NMR ([D_6]DMSO): δ = 138.10, 153.40; EA ($C_4H_{10}O_7N_{12}Li_2$, 352.08): C 13.65, H 2.86, N 47.74; found: C 13.87, H 2.88, N 47.44; BAM impact: 35 J; BAM friction: 360 N; ESD: 1.5 J.

Chemicals. Magnesium (98%) volume-based particle size in the range of 0.30 – 0.15 mm, hexamine (99.5%), 1,3-diaminoguanidine monohydrochloride (98%), and collodion solution (nitrocellulose solution 4-8% in ethanol/ether), *Sigma-Aldrich*; lithium hydroxide (98%), *Merck*; oxalic acid anhydrous (98%) and 5-amino-1H-tetrazole (98 %), *abcr*; Epon 813, *Hexion*; Versamid 140, *BASF*. A binder system (50 wt.-% Epon 813/ 50 wt.-% Versamid 140) was applied. All chemicals were used as provided without further purification.

Sample preparation. The samples were weighed out according to their weight percentages (max. 1 g total) into a mortar. After mixing by hand for 3 min, the nitrocellulose solution, both the Epon 813 (20 mg/mL) and the Versamid 140 solution (10 mg/mL) in ethyl acetate were added using a syringe. The mixture was blended with a spatula every 10 min until the solvent was evaporated. The solid material was stored over night at 70 °C in the drying oven for curing. Before consolidation, the pyrotechnic material was mixed again by hand for 3 min.

The formulations were pressed with the aid of a tooling die (inner diameter 12.9 mm) into a cylindrical shape. The formulation powders were pressed at a consolidation dead load of 2 t with a dwell time of 3 s.

Optical measurement. Optical emissive properties were characterized using both an Ocean optics HR2000+ES spectrometer with an ILX511B linear silicon CCD-array detector (range 190 – 1100 nm) and included software from Ocean Optics. Spectra were recorded with a detector-sample distance of 1.00 m and an acquisition time of 20 ms. The dominant wavelength (DW) and spectral purity (SP) were measured based on the 1931 CIE method using illuminant C as the white reference point. Five samples were measured for each formulation and all given values are averaged based on the full burn of the mixture. The controlled burn was filmed with a digital video camera recorder (SONY, DCR-HC37E).

Energetic properties. The impact and friction sensitivities were determined using a BAM drophammer and a BAM friction tester. The sensitivities of the compounds are indicated according to the U.N. Recommendations on the Transport of Dangerous Goods (+): impact: insensitive >40 J, less sensitive >35 J, sensitive >4 J, very sensitive 4 J; friction: insensitive>360 N, less sensitive=360 N, sensitive <360 N >80 N, very sensitive <80 N, extreme sensitive <10 N. Additionally all formulations were tested for sensitivity towards electrical discharge using an Electric Spark Tester ESD 2010 EN. Decomposition points were measured with an OZM Research DTA 552-Ex Differential Thermal Analyzer. Measurements were performed at a heating rate of 5 °C/min.

X-Ray structure and Discussion

3 crystallizes from water in the monoclinic space group $P2_1/n$ with four molecules per unit cell and a density of 1.839 g cm^{-3} (@173 K). The molecular unit of **3** is illustrated in S2. The box on the left shows the observed dimeric motif. The molecular structure slightly differs from corresponding structures, e.g. the guanidinium salt.[1a] Also the neutral parent compound shows a comparable structure.[1a] The aromatic triazole rings are not coplanar and twisted approximately 30° (torsion angle N3–C1–C3–N9) to each other. The observed bond length of the atoms C1–C3 (1.45 Å) is between those of typical C–C single and C=C double bonds and in the range of the neutral and the guanidinium compound.[A1] The triazole rings are aromatic, therefore the observed bond length of the ring nitrogen atoms are between the values for a N–N single bond (1.48 Å) and a N=N double bond (1.20 Å). The observed bond lengths between the atoms C2–N4 and C4–N10, respectively, are again in the range of the reported guanidinium salt but shorter than the common single bond length between the atoms C–N.[1a] The nitramino moiety is twisted out of plane (torsion angle N3–N5–N6–O1 = 72 °). The unit cell contains two different coordinated lithium atoms. Taking into account only interactions smaller than the sum of van-der-Waals radii of Li+N (3.37 Å) and Li+O

(3.34 Å), Li1 is coordinated distorted by five different atoms (N5^{iii}, N7^{iii}, O5, O6, O6^{i}).[2]A dimeric motif is formed by two bridging water molecules O6/O6^{i} and the atoms Li1/Li1^{i}.

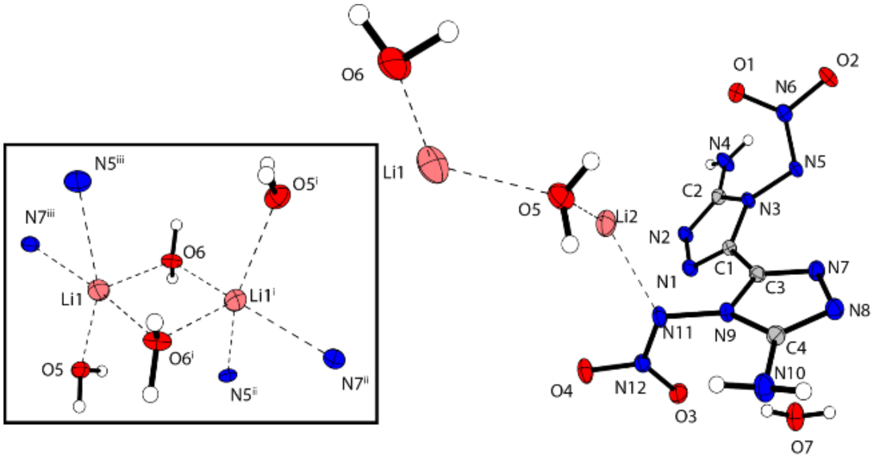

S2. Molecular unit of **3** showing the atom-labeling scheme. Ellipsoids represent the 50% probability level. (i = 2−x, −y, −z; ii = 2−x, −y, 1−z; iii = x, y, −1+z; iv = 0.5+x, 0.5−y, 0.5+z; v = 0.5+x, 0.5−y, −0.5+z).

The dimeric motif is in plane with a bond length between the atoms Li1–O6 of approximately 2.00 Å. The observed angles between the atoms Li1–O6–Li1^{i} and the atoms O6–Li1–O6^{i} are nearly 90 °. The distance between the atoms Li1–O6 is smaller than the sum of the van-der-Waals radii.[2-3] In contrast, the bond length between the atoms Li1–O5 is closer to the observed bond lengths in octahedral coordinated Li-O structures (2.16 Å).[4] The observed bond lengths between the atoms Li1–N5^{iii}/Li1–N7^{iii} are 2.35 Å/2.13 Å, respectively. The atom Li2 is slightly distorted coordinated tetrahedrally by one water molecule O5 and the atoms O4^{iv}/N8^{v}/N11 of two 3,3‘-diamino-4,4‘-dinitramino-5,5‘-bi-1,2,4-triazolate anions. The observed bond lengths between the atoms of Li2–O4/Li–O5 are longer than the reported bond lengths for tetrahedral coordination (~1.96 Å).[5]This might be due to the oxygen-oxygen edge distortions when lithium tetrahedral share edges with other tetrahedra or octahedra.[5]

Crystallographic data. CCDC 1580533 contain the supplementary crystallographic data for **3**. These data are provided free of charge by The Cambridge Crystallographic Data Centre.

CIE 1931 chromaticity diagram

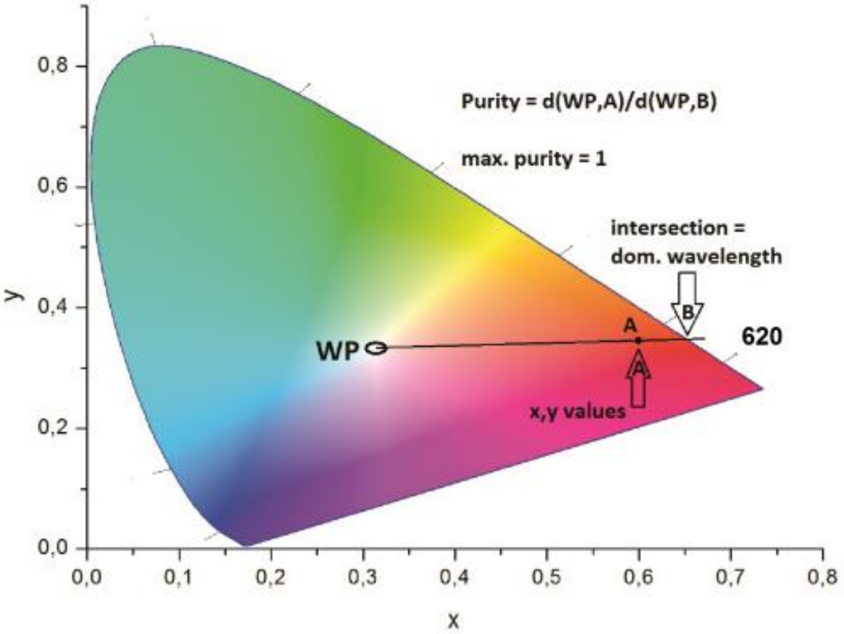

S3. CIE 1931 chromaticity diagram.

An easy way to show or compare the spectral purity and dominant wavelength of various formulations is CIE 1931 chromaticity diagram. The color purity of a visible flare with the chromaticity (x, y) is its difference from the illuminant´s white point (WP) relative to the furthest point on the chromaticity diagram with the same hue (dominant wavelength for monochromatic sources). The color purity can be calculated by dividing the distance WP to A (x, y) = d(WP, A) by the distance WP to B = d(WP, B). B is the point with the maximum purity of 100% for the dominant wavelength of formulation A.[6]The higher the spectral purity of A, the more the point moves to the right until it ends up having the coordinates of B.

References

[1] a)T. M. Klapötke, M. Leroux, P. C. Schmid, J. Stierstorfer, *Chem. - Asian J.* **2016**, *11*, 844-851; b)T. M. Klapötke, P. C. Schmid, S. Schnell, J. Stierstorfer, *J. Mater. Chem. A* **2015**, *3*, 2658-2668.

[2] A. Kirfel, G. Will, R. F. Stewart, *Acta Crystallographica Section B* **1983**, *39*, 175-185.

[3] A. Bondi, *J. Phys. Chem.* **1964**, *68*, 441-451.

[4] a)R. Shannon, *Acta Crystallographica Section A* **1976**, *32*, 751-767; b)C. T. Li, *Z. Krist.* **1968**, *127*, 327-348.

[5] M. Wenger, T. Armbruster, *Eur. J. Mineral.* **1991**, *3*, 387-399.

[6] T. M. Klapötke, *Chemistry of High-Energy Materials*, 4th ed., De Gruyter, Berlin, Boston, **2017**.

4.3 Flare or Strobe: A Tunable Chlorine-Free Pyrotechnic System Based on Lithium Nitrate

Reproduced from *Chem. Commun.* **2018***, 54,* 821-824. (DOI: 10.1039/C7CC09721B) with permission from The Royal Society of Chemistry

Abstract: The development of a red, chlorine-/strontium-free pyrotechnic composition which serves as either strobe or flare is reported. The observed strobing behaviour of a red-light emitting composition of Mg/$LiNO_3$/hexamine/binder was investigated. Additives like 5-amino-1H-tetrazole and nitrocellulose were used to increase the strobing frequency and achieve constant burning.

Red-burning pyrotechnic formulations showing the phenomena of oscillatory combustion are called strobes (Figure 1), whereas constant burning compositions are referred to as flares.[1],[2] Since these formulations are widely used in the military (tracer, tactical signal) and civilian sector (fireworks, twinklers pots, hand-held signals) the environmental impact should be kept at a minimum.[3] Besides the toxicity of the formulation compounds and the resulting combustion products, the produced light is hazardous to human health. Bright red light of a certain frequency (illuminant signals or even TV screens) among other colours and patterns, like parallel lines and stripes can cause epileptic seizures. According to the US epilepsy foundation, about 3 % of people with epilepsy (1.8 % of the population in the USA) suffer from this condition also known as photosensitive epilepsy.[4] It is more common in children and adolescents and becomes less frequent with age. T

ypical flare formulations consist of a metallic fuel (Mg, Al or magnalium), strontium nitrate ($Sr(NO_3)_2$) as an oxidizer, a binder and chlorinated compound like poly(vinyl chloride) (PVC) which serve as a chlorine source.[5] Upon combustion, these compositions produce magnesium oxide ($MgO(s)$), strontium(I) chloride ($SrCl(g)$), and strontium(I) hydroxide ($SrOH(g)$). The last two species both yield a distinct emission pattern in the red spectral wavelength range, while condensed MgO greatly assists in obtaining a high luminous intensity LI.[6] In contrast to two recently published chlorine-free red flare compositions,[2, 7] which prevents the formation of highly carcinogenic polychlorinated aromatic compounds such as polychlorinated dibenzodioxins (PCDDs), polychlorinated dibenzofuranes (PCDFs), and polychlorinated biphenyls (PCBs) most strobe formulations still rely on the use of chlorinated compounds.[1, 8] Ammonium- or potassium perchlorate (NH_4ClO_4/$KClO_4$) are commonly used as oxidizers, potassium dichromate ($K_2Cr_2O_7$) and additives like copper-chrome oxide and hexachlorobenzene are sometimes applied as a frequency stabilizer, alkaline earth metal nitrates or sulfates as a colorant agent and sulfur as the fuel.[1, 9] The European Chemicals Agency (ECHA) hazard classification of potassium dichromate refers to it as a substance of very high concern (SVHC) and was therefore assigned as a major threat in strobe formulations.[10]

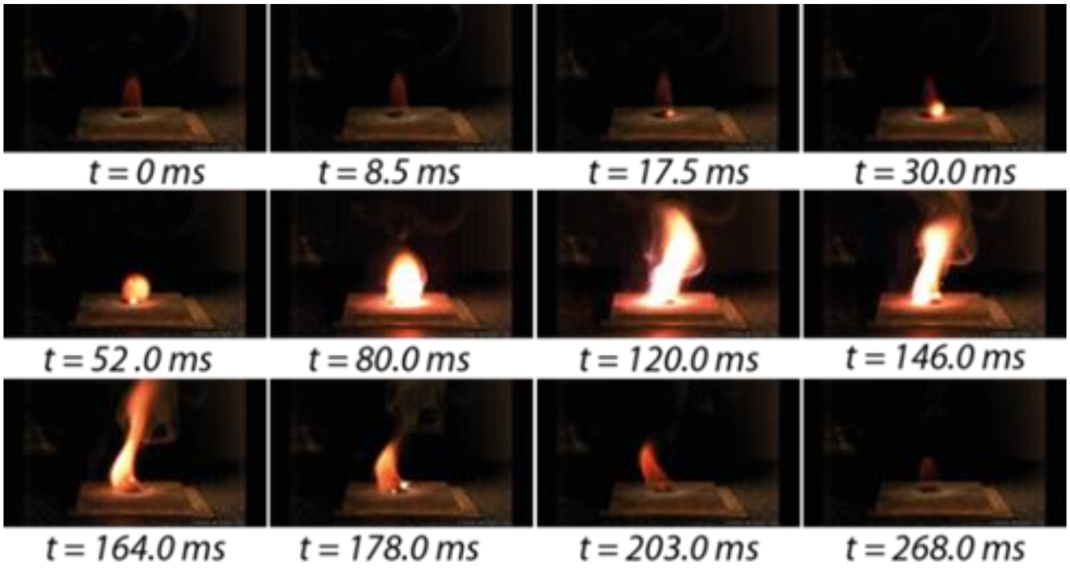

Figure 1: High-speed video recording of **6**.

The compound is known to be toxic, potential carcinogenic and highly toxic to aquatic life to quote only a few. Encouraged by the work done in the past to develop a red-burning flare based on the atomic emission of atomic lithium,[11] the authors decided to take advantage of Sabatini's chlorine-free red composition (**1**) (Table 1) and use it as a starting point for a drop-in of lithium nitrate ($LiNO_3$).[2]

It has to be stated, that the studied health effects of lithium to humans have always been focused on bipolar patients facing the high dose lithium therapy so far.[12] In a recent study by Figueroa *et al.*, it was outlined that those obtained results are not applicable to the normal population.[13] Instead, the focus of the presented study was on the population living on a northern territory in Chile which shows the highest levels of lithium in surface waters in the world. Figuero *et al.* and monitored the lithium concentration in blood, urine and breast milk.[13-14] According to Figueroa *et al.* and Usada *et al.*, further research to obtain reliable health based guidelines values to assess the risks potentially posed by environmental exposure is necessary.[13, 15] Aral and Vecchio-Sadus claims, that lithium is not expected to bioaccumulate and its human and environmental toxicity are low, however the maximum recommended daily intake varies a lot in the literature.[16] For future application purposes of new designed flare and strobe formulations, only commercially available and non-toxic chemicals were considered for further investigations. The authors started with a fixed amount of $LiNO_3$ (51 wt%), Epon 813/Versamid 140 (4 wt%, 1:1), Mg (33 wt%) and 5-AT (12 wt%). In 2009, Koch and Jennings-White concluded a dark red color based on Li requires low LiOH(g), low Li(g) and low temperature.[11c]

Table 1: Sabatini's chlorine-free red composition (**1**)[2]

Component	Sabatini's chlorine-free red (1)[2]
$Sr(NO_3)_2$	48
Mg 50/100 mesh	33
5-AT	12
Epon 813/ Versamid 140	7

To address the need for lower combustion temperatures, the amount of Mg was stepwise reduced by 3 wt% with respect to 5-aminio-1*H*-tetrazole (5-AT). Hexamine and 5-AT are both reported to give lower combustion temperatures.[2] Next to the very hygroscopic behaviour and a pink flame color (sum of red light generated by Li and white light generated by MgO emission), only formulation **2** showed a constant burning (Table 2) (see electronic supplementary information (ESI)).

Table 2: Formulations based on $LiNO_3$, 5-AT or hexamine.

Component	2	3	4	5	6	7	8
$LiNO_3$	51	51	51	51	51	51	51
Mg	30	30	24	18	15	15	15
5-AT	15	-	-	-	-	9	-
hexamine	-	15	21	27	30	21	24
Epon 813/ Versamid 140	4	4	4	4	4	4	4
NC	-	-	-	-	-	-	6

Repeating the experiments with hexamine instead of 5-AT surprisingly resulted in the four strobing formulations **3**, **4**, **5**, **6**. The emission spectra of all strobe formulations look similar. Next to the atomic emission of lithium (610 nm, 670 nm) the spectrum of **6** shows the typical sodium and potassium (Figure 2) impurities. This oscillatory combustion was literature known for a few binary compositions containing perchlorate salts and hexamine but was not reported for $LiNO_3$/hexamine formulations yet.[17]

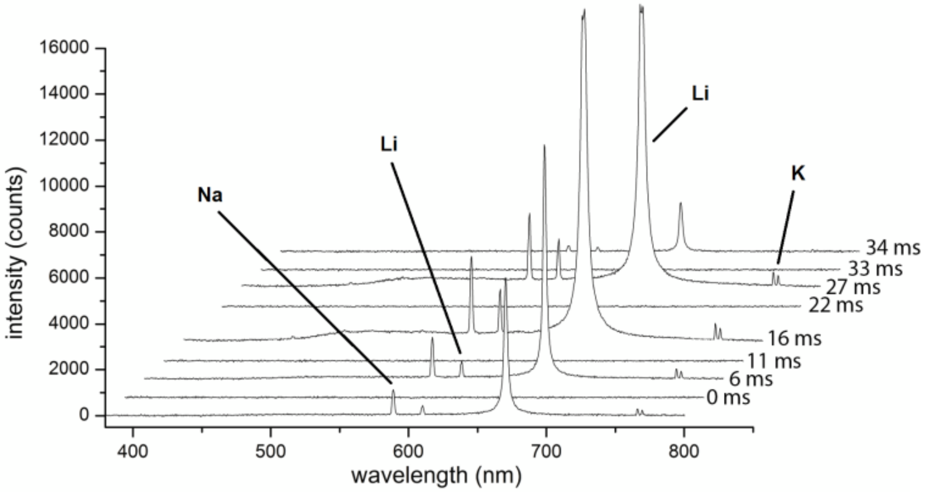

Figure 2. Time dependent high-speed measurement of formulation **6** (see supporting information).

The current hypothesis to explain this oscillating burning behaviour by Shimizu suggested the consideration of a strobe composition as two couples of reaction. The dark reaction (small or no flame) accumulates heat to trigger the flash reaction (high-intensity flame) which emits the characteristic colored flame.[1] The recorded data (see ESI) supports this assumption since the alternating dominant wavelengths range of approximately 604–580 nm fits the timeline of the flash/dark phase reaction respectively (ESI for spectra and calculation of dominant wavelength). For this reason, the dominant wavelength λ_d of strobe formulations (Table 2) presents the range of observed dominant wavelength λ_d for the flash reaction only. However, these unexpected results gave reason to believe in the possibility of achieving a lithium-based red flare with a dominant wavelength $\lambda_d \geq 600$ nm.

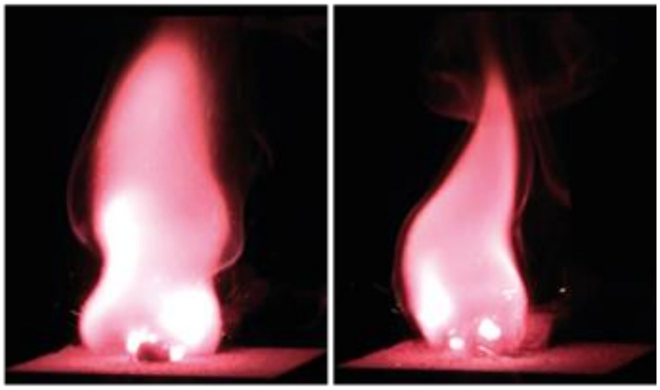
Formulation 8 Formulation 7

Figure 3: Constant burning of formulation **7** and **8.**

The recorded frequencies of formulations **3**, **4**, **5** and **6** were in the range of approximately 3 – 12 Hz (Table 3). The next step was to perform the transition starting from a certain strobe frequency to constant burning. We pursued two possible strategies with regards to the environmental impact. Based on our observations of the different behaviour of 5-AT or hexamine containing formulations, we decided to investigate the effect of applying a mixture of both fuels. Starting from composition **6**, the amount of hexamine was stepwise reduced in 3 wt% steps to 21 wt% and 5-AT (9 wt%) was added (Table 3). Unlike the formulations with less than 9 wt% of 5-AT, which suffered from inconstant burning, **7** showed constant burning and a high averaged strobe frequency of approximately 21.6 Hz (Figure 3). Keeping the human eye maximum sample rate of about 20 Hz in mind, our eyes cannot further distinguish between the single flashes and **7** can be therefore considered as a flare (= constant burning) composition.[18] Additionally, we observed that at the beginning of the burning, the strobe frequency was at its highest and decreased towards the end of the burning time which allowed us to detect single flashes at the very end. The second approach was to apply nitrocellulose (NC) to our strobe formulations. NC can act in many different ways, e. g. as a burning rate modifier, gas generator, fuel and as a binder.[9b, 19] For the desired goal of a constant burning formulation, a higher burning rate and more gaseous combustion products were considered to be important. Whereas a high burning rate is quite obvious, the need for more gaseous combustion products seems not to be that clear at first.

Table 3: Properties of formulations **1** – **8**.

	BT [s]	DW [nm]	SP [%]	LI [cd]	f [1/s]	IS [J]	FS [N]	ESD [J]	T_{onset} [°C]
1	4[a]	607	79	35400	-	9	240	>0.25	231
2	5[a]	563	55	-	-	15	>360	1.25	155
3	5[b]	586 - 602	-	-	11.7	8	>324	>1.5	170
4	26[b]	579 - 604	-	-	3.1	9	>360	>1.5	160
5	25	576 - 610	-	-	3.5	10	>360	>1.5	180
6	34	582 - 605	-	-	4.1	>25	>360	1.25	165
7	30	597	70	4850	21.6	30	>360	>1.5	152
8	27	598	75	1820	21.9	9	>360	1.5	132

Annotation: a = measured for 1g pellet; b = pellet was reignited a few times, burning time is the sum of burning intervals; all other pellets were prepared on a 2g scale; BT = burning time; DW = dominant wavelength; SP = spectral purity; LI = luminous intensity; f = frequency; IS = impact sensitivity; FS = friction sensitivity; ESD = electric discharge sensitivity; T_{onset} = onset temperature of decomposition.

Krone observed two important properties which affect our studies.[19] First, the addition of gas generating compounds like guanidine nitrate or NC, provide a better flash separation and an improved sharpness in the case of earth alkaline metal nitrates.[17c, 19] Second, the strobe effect of compositions containing alkaline nitrates is poor compared to earth alkaline metals. According to Krone, the low melting point of the alkaline nitrates generate extra flashes which results in uncontrolled burning and explosions with many flying sparks. [17c, 19] We decided to apply this strategy to our discovered strobe formulations. The idea was to achieve either constant burning by a dominating (= higher) NC content or to generate as many gaseous combustion products which produce a maximum of flashes and cannot be further detected as single flashes.

Again, formulation **6** served as the starting point of our investigations. The amount of hexamine was stepwise reduced with respect to the NC content with **8** showing the best performance. The measured frequency was 21.9 Hz and well above the maximum sample rate of the human eye. High-speed video recording showed a qualitatively higher number of glowing sparks evolving from the pellet surface which constantly ignited the evolving gases resulting in a higher flash frequency compared to non-NC containing formulations. All developed formulations show at least similar or better sensitivity values (IS, FS, ESD) compared to the reference formulation **1**. Only formulation **3** is slightly more sensitive towards impact. With respect to the onset temperatures, **1** showed the highest temperature whereas **8** had the lowest (100 °C difference). All other formulations were in between 132 – 231 °C. Grain sizes of the formulations as well as the Mg fuel and frequency measurements are reported in the electronic supplementary information (ESI).

The present study on lithium-based flares surprisingly not only resulted in the discovery of a perchlorate-free formulation but also a completely chlorine-free environmentally benign strobe system. There is no further need for applying substances as $K_2Cr_2O_7$ or hexachlorobenzene as a frequency catalyst. Finally, the observed flash separation is comparable to the earth-alkaline metals based compositions. The obtained frequencies are in the range of 3 – 12 Hz, as well as above 20 Hz. Through the use of either NC or a combination of hexamine and 5-AT, constant burning was achieved and formulations **7** and **8** might be better referred to as flare compositions. Especially **8** suffered less from the hygroscopicity issues due to the higher binder content. From a practical point of view, it is now possible to adopt the burning behaviour of pre-mixed solid materials for pyrotechnical formulations (flare or strobe) until the final steps of adding the epoxy binder system and waiting for the curing process. Moreover, the discovery of a chlorine-free strobe system might serve as a starting point for further colored strobe systems. Current research in our group is focused on yellow strobes since both emitters (Li, Na) need a reductive flame atmosphere. Regarding the already existing and increasing environmental regulations with pyrotechnics, the discovered strobe systems, as well as the red flare compositions are in accordance with the common goal to provide "greener" pyrotechnic formulations which might be interesting for both military and civilian (e.g. indoor firework) applications.

References

[1] J. M. L. Corbel, J. N. J. van Lingen, J. F. Zevenbergen, O. L. J. Gijzeman, A. Meijerink, *Angew. Chem. Int. Ed.* **2013**, *52*, 290-303.

[2] J. J. Sabatini, E.-C. Koch, J. C. Poret, J. D. Moretti, S. M. Harbol, *Angew. Chem. Int. Ed.* **2015**, *54*, 10968-10970.

[3] a)J. D. Moretti, J. J. Sabatini, J. C. Poret, *Chem. - Eur. J.* **2014**, *20*, 8800-8804; b)C. M. Csernica, *42nd Int. Pyrotech. Sem., Proc.*, IPSUSA Seminars, Inc., Grand Junction, Colorado, USA, July 10-15, **2016**; c)T. Shimizu, *Fireworks-The Art Science and Technique*, Pyrotechnica Publications, Austin, Texas (USA), **1996**.

[4] a)Photosensitivity and Seizures, https://www.epilepsy.com/learn/triggers-seizures/photosensitivity-and-seizures, Dec 2017; b)Why Do Flashing Images Cause Seizures?, https://www.smithsonianmag.com/smart-news/why-do-flashing-images-cause-seizures-180961504/, Dec 2017.

[5] J. A. Conkling, C. Mocella, *Chemistry of Pyrotechnics: Basic Principles and Theory*, 2nd ed., Taylor & Francis, **2010**.

[6] R. W. B. Pearse, A. G. Gaydon, *The Identification of Molecular Spectra*, Chapman and Hall, **1975**.

[7] J. Glück, T. M. Klapötke, M. Rusan, J. J. Sabatini, J. Stierstorfer, *Angew. Chem., Int. Ed.* **2017**, *56*, 16507.

[8] a)W. Christmann, D. Kasiske, K. D. Klöppel, H. Partscht, W. Rotard, *Chemosphere* **1989**, pp. 387-392; b)G. Steinhauser, T. M. Klapötke, *Angew. Chem., Int. Ed.* **2008**, *47*, 3330-3347.

[9] a)T. Shimizu, *Studies on Strobe Light Pyrotechnics*, Austin, Texas, USA, **1982**; b)R. G. Cardwell, *Pyrotechnica V* **1979**, 6-24.

[10] Hazard classification and labelling of potassium dichromate, https://echa.europa.eu/substance-information/-/substanceinfo/100.029.005, Sept 13, 2017.

[11] a)E.-C. Koch, *Propellants, Explos., Pyrotech.* **2004**, *29*, 67-80; b)E.-C. Koch, *J. Pyrotech.* **2001**, *13*, 1-8; c)E.-C. Koch, C. Jennings-White, *36th Int. Pyrotech. Sem., Proc.*, IPSUSA Seminars, Inc., Estes Park, Rotterdam, Netherlands, Aug 18-23, **2009**, 105-110.

[12] R. F. McKnight, M. Adida, K. Budge, S. Stockton, G. M. Goodwin, J. R. Geddes, *The Lancet* **2012**, *379*, 721-728.

[13] L. T. Figueroa, B. S. Ann, W. J. Schull, A. H. Young, Y. M. Kamiya, J. A. Hoskins, E. B. Ilgren, *Epidemiology Biostatics and Public Health* **2014**, *11*, 1-15.

[14] a)L. Figueroa, S. Barton, W. Schull, B. Razmilic, O. Zumaeta, A. Young, Y. Kamiya, J. Hoskins, E. Ilgren, *Biol. Trace Elem. Res.* **2012**, *149*, 280-290; b)L. T. Figueroa, B. Razmillic, O. Zumeata, G. N. Aranda, S. A. Barton, W. J. Schull, A. H. Young, Y. M. Kamiya, J. A. Hoskins, E. B. Ilgren, *Biol. Trace Elem. Res.* **2013**, *151*, 122-131.

[15] K. Usuda, K. Kono, T. Dote, M. Watanabe, H. Shimizu, Y. Tanimoto, E. Yamadori, *Environ. Health Prevent. Med.* **2007**, *12*, 231.

[16] a)H. Aral, A. Vecchio-Sadus, *Ecotoxicol. Environ. Saf.* **2008**, *70*, 349-356; b)http://www.water-research.net/index.php/lithium, Dec 2017.

[17] a)C. Jennings-White, *Pyrotechnica* **1992**, *14*, 33-45; b)C. Jennings-White, *J. Pyrotech.* **2004**, *20*, 7-16; c)F.-W. Wasman, *5th Int. Pyrotech. Sem., Proc.*, IPSUSA Seminars, Inc., Vail, CO, USA, July 12-16, **1976**, 643-651; d)E. Lohmann, Pyro-Chemie Hermann Weber & Co GmbH, Germany, **1985**, *GB 2153809A*.

[18] A. Hahma, M. Welte, O. Pham, *47th International Annual Conference of the Fraunhofer ICT*, Diehl BGT Defence, Röthenbach, Karlsruhe, Germany, June 28 – July 1, **2016**.

[19] U. Krone, *Nico Pyrotechnic*, Nico Pyrotechnic, Germany, **1973**, *DE000002164437A*.

Supporting Information

1. Chemicals

Table 1: Chemicals.

Chemicals	Supplier	Purity
$Sr(NO_3)_2$	Grüssing GmbH	98 %
$LiNO_3$	Sigma Aldrich	Reagent Plus
Mg 50/100 mesh	Sigma Aldrich	Reagent Grade 98 %
Mg	Grüssing GmbH	97 %
5-Amino-1*H*-tetrazole	abcr	98%
Hexamine	Acros organics	99 %
Epon 813	Hexion	-
Versamid 140	Miller-Stephenson	-
Nitrocellulose	Sigma Aldrich	Collodion solution (4 - 8 % ethanol/diethylether)

2. Grain size/particle size of formulations and Mg

We discovered that the grain size after grinding was mainly influenced by the applied magnesium. The supplier of Mg (Grüssing GmbH, 99%) reported the grain size in the range of 60 – 300 µm. This Mg was applied in formulations **2** – **8**. However, manually sieving revealed that even smaller grain sizes were present. For this reason we quantitatively determined the grain size distribution of a 10g Mg sample applying different sieves. In addition, we used REM measurements (Figure 1, 2) to determine the particle shape of the applied Mg. In formulation **1,** Mg (Sigma Aldrich, Reagent Grade 98%, 50/100 mesh) and a binder ratio of Epon 813/Versamid 140 (4:1) were applied.

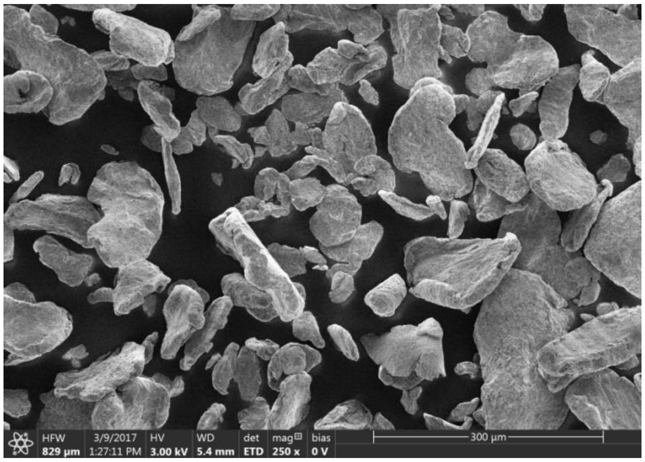

Figure 1. SEM of Mg (Grüssing GmbH, 99%).

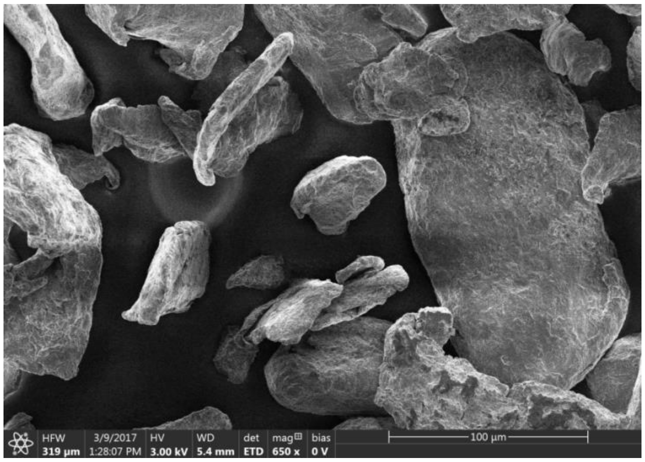

Figure 2. SEM_2 of Mg (Grüssing GmbH, 99%).

3. Sample preparation

The samples were weighed out according to their weight percentages (max. 1 g total) into a mortar. After grinding by hand for 3 min, both the Epon 813 (20 mg/mL) and the Versamid 140 solution (10 mg/mL) in ethyl acetate were added using a syringe. For nitrocellulose, we applied Colloidon solution (4-8 % in ethanol/diethylether) to the pre-grinded solid materials. The mixture was blended with a spatula every 10 min until the solvent was evaporated. The solid material was stored over night at 70 °C in the drying oven for curing. Before consolidation, the pyrotechnic material was grinded again by hand for 3 min. The formulations were pressed with the aid of a tooling die (inner diameter 12.9 mm) into a cylindrical shape. The formulation powders were pressed at a consolidation dead load of 2 t with a dwell time of 3 s. A torch was used to ignite the pellets.

4. Optical emission spectroscopy

Dominant wavelength/spectral purity/luminous intensity:

Optical emissive properties were characterized using both a Ocean optics HR2000+ES spectrometer with an ILX511B linear silicon CCD-array detector (range 190–1100 nm) and included software/calibration files from Ocean Optics. Spectra were recorded with a detector-sample distance of 1.00 m. The acquisition time for the flare formulations was 20 ms/scan. The dominant wavelength (DW) and spectral purity (SP) were measured based on the 1931 CIE method using illuminant C as the white reference point. Four samples were measured for each formulation and all given values are averaged based on the full burn of the mixture. The controlled burn was filmed with a digital video camera recorder (SONY, DCR-HC37E).

Frequency measurement:

Frequency measurements were performed using an acquisition time of 5 ms/scan or 1 ms/scan. Dominant wavelengths were measured based on the 1931 CIE method using illuminant C as the white reference point. The range selection for recording a signal was set the range from 580.11 nm – 680.14 nm covering all previously recorded dominant wavelengths as well as the red light part in the visible spectrum. Calculation of the frequency was done by detecting the single peaks applying the Origin Pro 9.0 software and calculating the period of time between the single peaks (= flash reactions).

5. High-speed camera

Setup:

Highspeed video recording was performed applying the “SpeedCam Visario G2 1500” by Weinberger AG with the accompanied “Visart 2.2” software package. Following data is taken from the supplier data sheet:

Sensor: High-Speed APS-CMOS Sensor

Active Sensor area: 16.89 x 11.26 mm (W x H)

Active pixel size: 11 µm Square

Image formats: 768 x 512 pixel: up to 4000 frames per seconds

Shutter: Electronic shutter down to 10 µsec.

Dynamic range: color depth to 30 Bit

The applied camera lens was purchased from Sigma (24-70 mm, 2.8 EX DG, Macro, diameter 82 mm). In addition, a Heliopan Filter UV SH-PMC 82mm was applied.

High-speed video recording procedure:

The bare pellet was placed in the fume hood and ignited by applying a torch. No prime composition was applied. The distance between the camera and the pellet (same height) was approximately 1 m. Due to the camera settings and applied lense/filter, additional halogen lamps to illuminate the fume hood were applied. A sequence of several seconds was recorded for selected formulations.

6. Emission spectra of formulations **2**, **6** and **8**.

Li emits two sharp lines in the red region at 671 nm and 610 nm with decreasing intensity.[1] Unfortunately, the human eye´s capability to detect light is limited by the so-called *cone cells*. These 3 different types of photoreceptor cells show their own distinctive sensitivities to different wavelengths. The overlap of the single cones results in the human eye´s response to light.[2] The highest sensitivity to detect light also referred to as the peak of photopic response is at 555 nm (green region, 100 %). In the case of higher wavelengths, the sensitivity decreases below 10 % at 670 nm.[2] As a consequence, the emission line at 610 nm (approximately 50 %) is far better detected by the human eyes though being less intense and contributing to the red light performance.[2] A look at the emission spectra of formulation **2** reveals a strong background emission (incandescence produced by condensed MgO, LiO, LiOH and Li_2O) (Figure 3). As a result, the spectral purity drops and the dominant wavelength is given as 563 nm. Due to illuminant C as the white reference point, the contribution of the green emission (part of background emission) is weighted higher compared to red light and results in a calculated dominant wavelength (averaged over the entire burning for each single scan) of 563 nm. Formulation **8** (Figure 4) showed less background radiation and results in a higher spectral purity as well as dominant wavelength.

Literature:

[1] a)T. M. Klapötke, *Chemistry of High-Energy Materials*, 4th ed., De Gruyter, Berlin, Boston, **2017**; b)H. A. Webster III, *Alkali Metal Emitters. I. Analysis of Visible Spectra,MWSC/CR/RDTR-16*, NTIS-AD-A019367*,* Crane, Indiana, **1975**.

[2] S. J. Robinson, J. T. Schmidt, *Mater. Eval.* **1984**, *42*, 1029-1034.

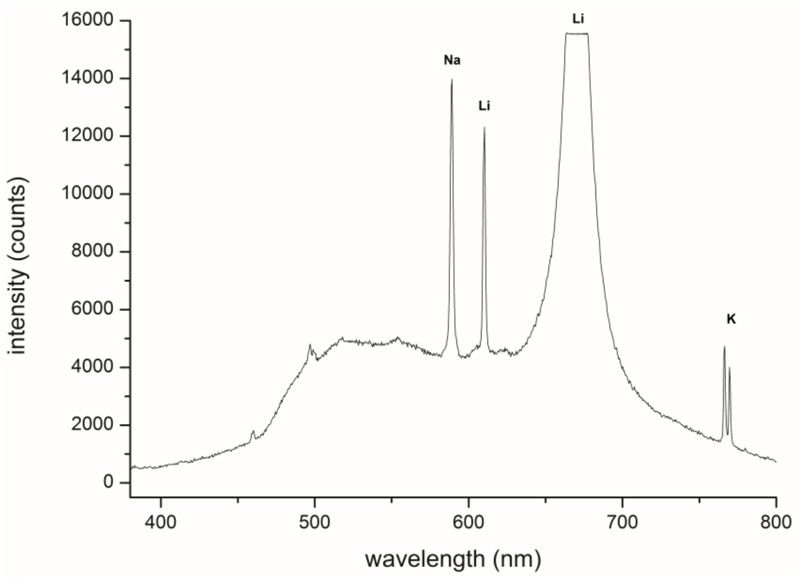

Figure 3. Burning of formulation **2**.

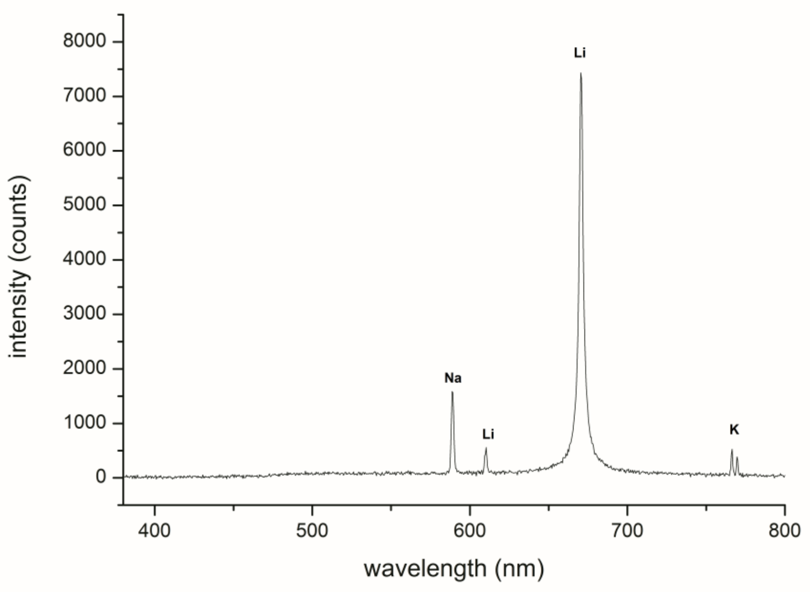

Figure 4**.** Constant burning of formulation **8**.

Figure 5 shows a recorded sequence of formulation **6**. Starting from the second recorded spectrum (dark reaction, t = 0 ms), a spectrum was recorded every 1 ms for 34 ms in total. As can be, the background radiation increases with increased intensity of the formulation (= highest value for Li emission at 670 nm). No unidentified light-emitting species was detected in the recorded spectra.

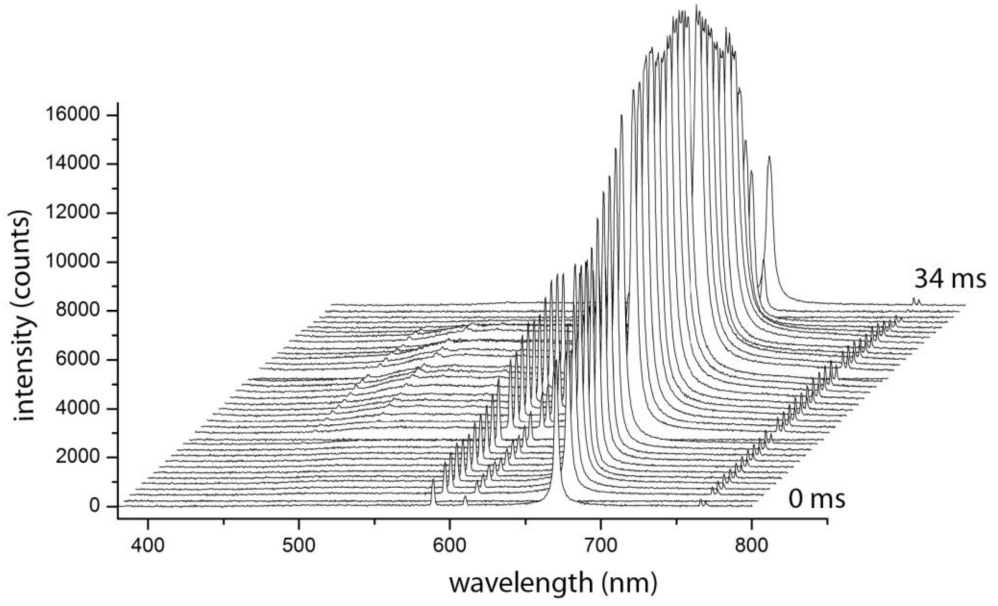

Figure 5. Time dependent high-speed measurement of formulation **6** (1 ms/scan).

7. Frequency spectra

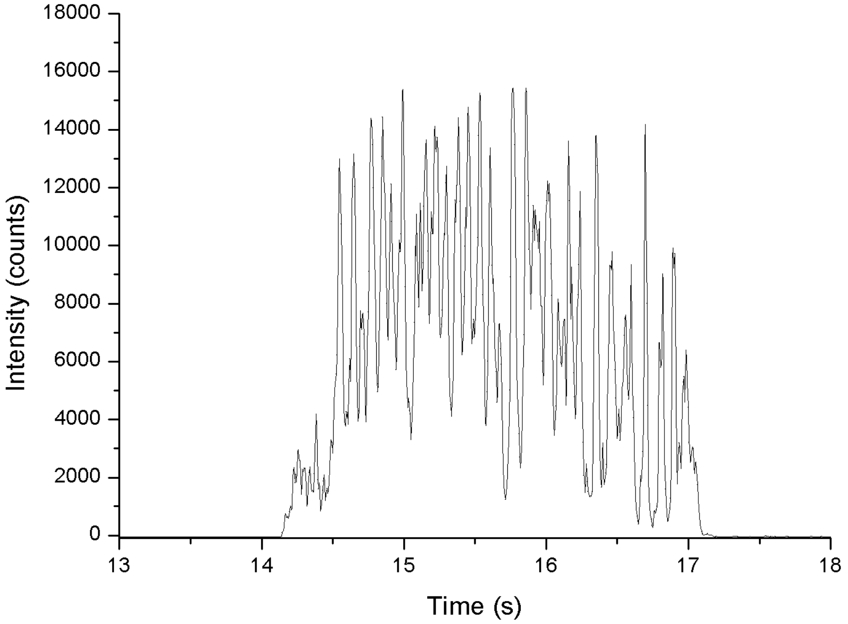

Figure 6. Frequency measurement of formulation **3** with 5 ms/scan.

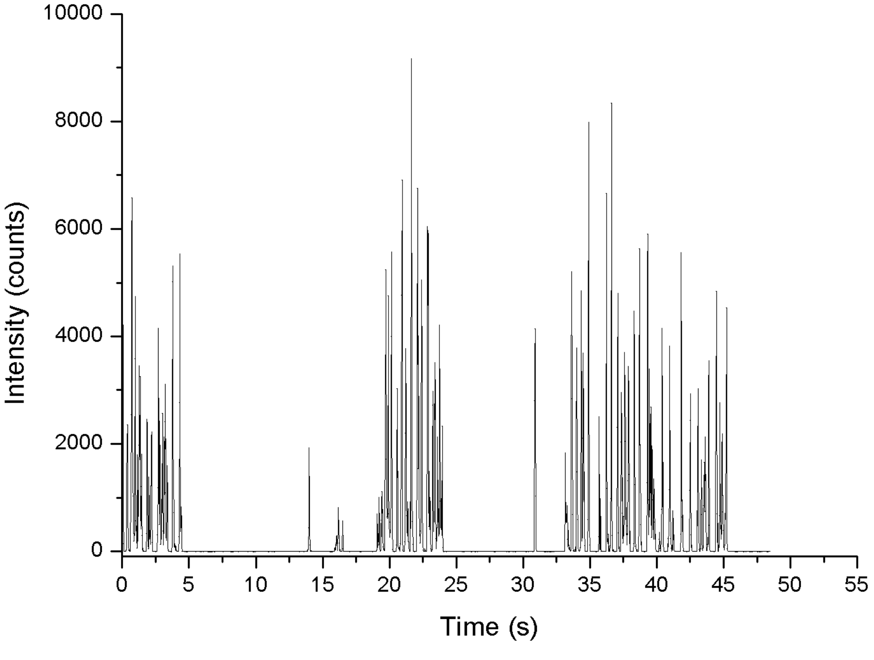

Figure 7. Frequency measurement of formulation **4** with 5 ms/scan.

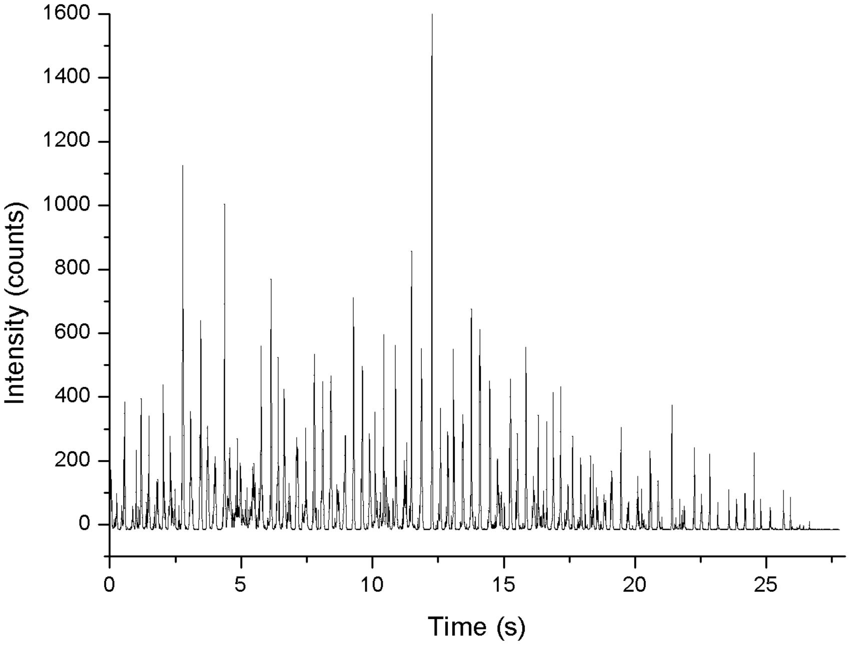

Figure 8. Frequency measurement of formulation **5** with 5 ms/scan.

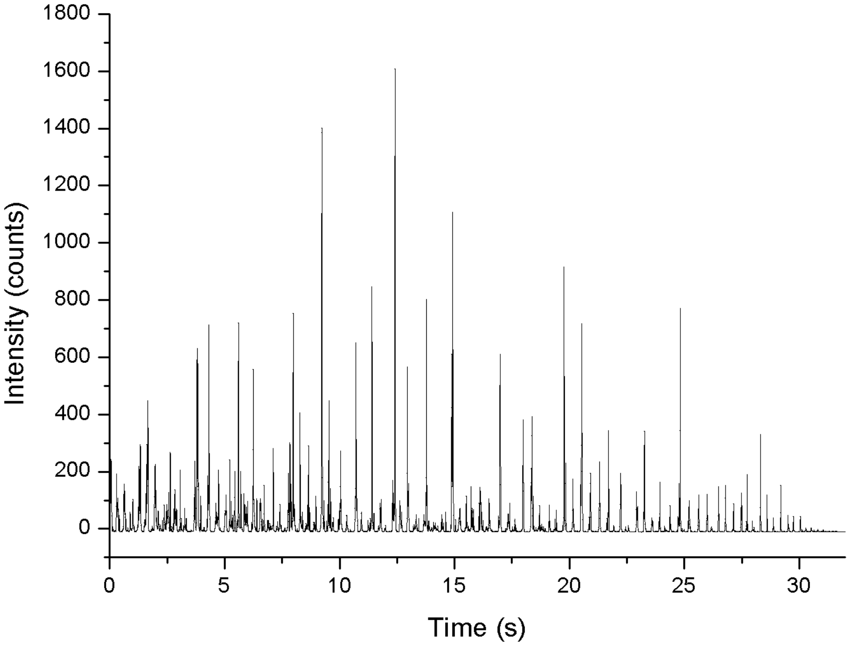

Figure 9. Frequency measurement of **6** with 5 ms/scan.

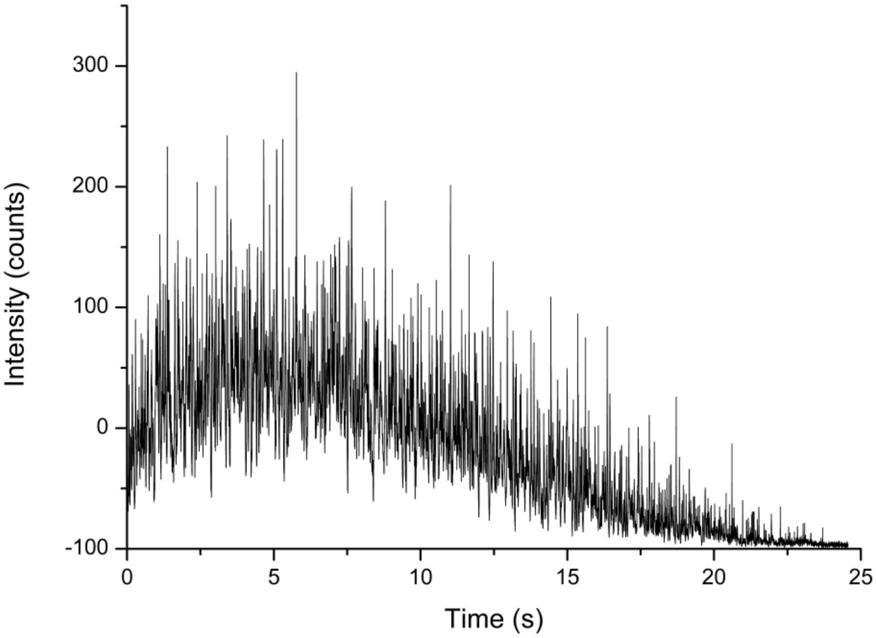

Figure 10. Frequency measurement of **7** with 1 ms/scan.

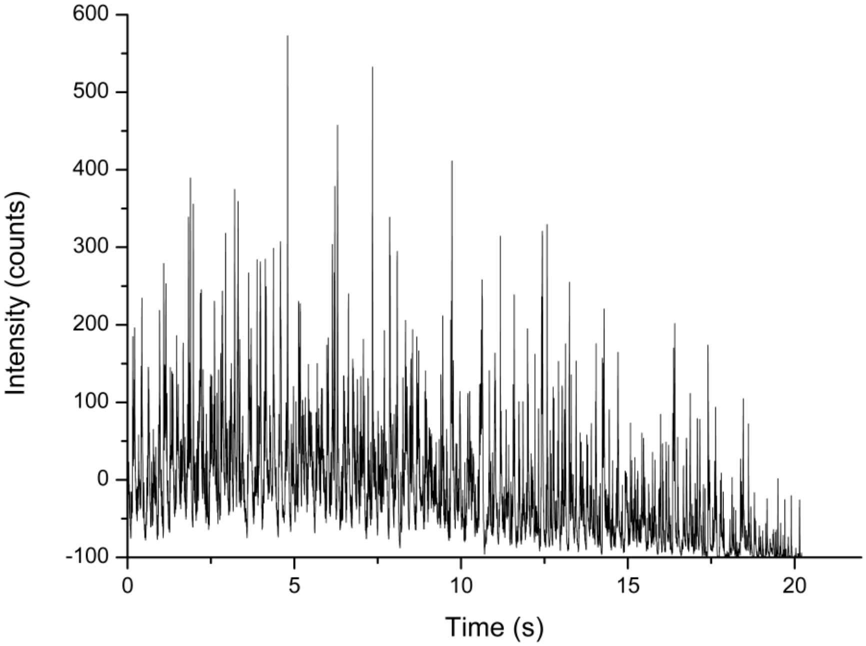

Figure 11. Frequency of **8** with 1 ms/scan.

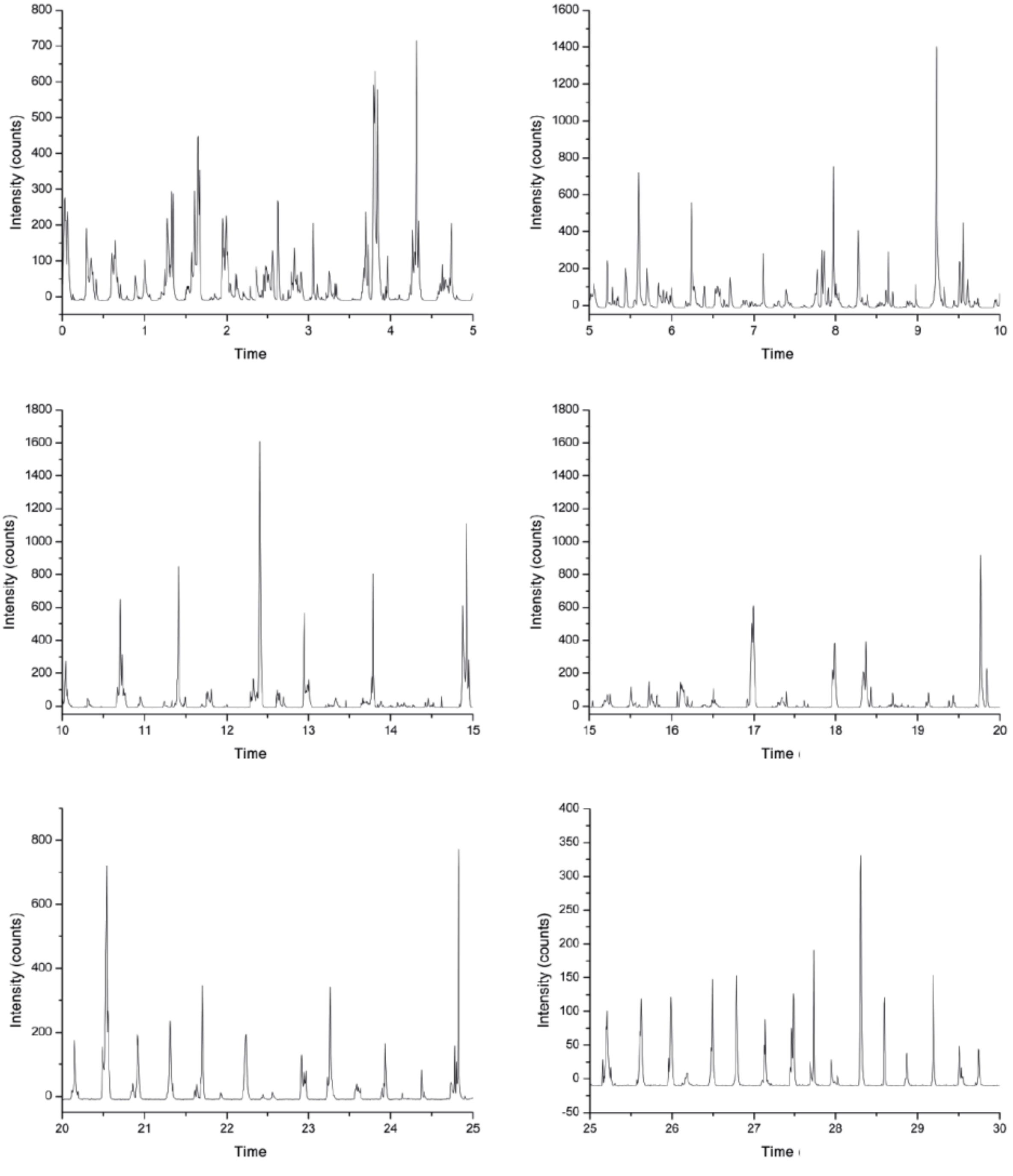

Figure 12. Frequency measurement of **6** in 5 s intervalls (1ms/scan).

4.4 Development of a Sustainable Perchlorate-Free Yellow Pyrotechnical Strobe Formulation

Reprinted with permission from *ACS Sustainable Chem. Eng.* **2018***, 6*, 4400-4404.
(DOI: 10.1021/acssuschemeng.8b00105) Copyright 2018 American Chemical Society

Novel yellow-light-emitting pyrotechnical strobe formulations absent of any chlorine sources were developed. The five yellow strobe formulations cover a frequency range of 7 Hz < x < 20 Hz and do not use potassium dichromate, which is frequently applied as a stabilizer. Frequency measurements and a comparison to a literature-known state-of-the-art red reference strobe formulation revealed a comparable flash separation. In addition, the newly developed formulations meet the requirements of the U.S. Environmental Protection Agency and European regulation law REACH (Registration, Evaluation, Authorization and Restriction of Chemicals), as they do not contain any substances of very high concern, heavy metals, or chlorine atoms (*Interim Drinking Water Health Advisory for Perchlorate; Office of Science and Technology, Office of Water, Health and Ecological Criteria Division, U.S. Environmental Protection Agency: Washington DC, 2008*). Potential resulting synergies with a proposed replacement candidate for the Mk 144 yellow marine smoke and illumination signal might combine commercial and environmental sustainability, which enhances the chances for future application in both the military and civilian sectors.

Introduction

Firework displays are commonly used to celebrate national holidays or public events, such as New Year`s Eve, the Fourth of July in the United States or big sports events. Starting from early childhood, many people are attracted to fireworks due to characteristic special effects, the colorful lights, whistling sounds, and loud cracks. These impressive effects often outshine the negative concomitants such as the bad smell and smoke clouds. These smoke clouds consist of burned as well as unburned materials, which are capable to of affecting human health even on a one-time exposure. In contrast to public opinion, the impact of a single event might not be neglectable. For example, Kulshrestra *et al.* showed that barium concentrations in air increased by more than a factor of 1000 over the course of the Indian Diwali festival.[1] Barium salts are the traditional colorants that produce the green color in pyrotechnical displays. Upon combustion, very poisonous water-soluble Ba^{II} compounds, such as $BaCl_2$, BaO, and $Ba(OH)_2$, are formed. For the colors red and yellow, strontium and sodium salts are used, respectively. It is obvious that environmental risk increases with a higher frequency of events. In the United States, amusement parks such as Disney World and the U.S. Army training grounds show a high consumption of pyrotechnical formulations.[2] In 1997, the critical concentration of the perchlorate anion in groundwater exceeded the maximum permissible level advised by the U.S. Environmental Protection Agency (EPA), which resulted in an all live fire training stop at Camp Edwards. [3] The main health threat of perchlorate oxidizers arises from the similar ionic radius compared to that of iodine, which results in an interference with iodine uptake in the thyroid gland.[4] For decades, perchlorates have been used as the oxidizer of choice, but with increasing environmental regulations, the need for alternatives has increased.[5]

In contrast to the field of constant burning (i.e. flare) formulations, where perchlorate was already successfully replaced for the colors blue, green, red, and yellow to name only a few, there is a lack of perchlorate-, chlorine- and heavy-metal-free options for strobe formulations.[3b, 6] Recently, we reported the development of a red strobe system based on lithium nitrate fulfilling the preset requirements.[7] Strobe formulations are characterized by a periodically alternating flash (big flame, bright light) and dark phase (small or no visible flame) reaction.[8] The first literature reported strobe formulations, the so-called *"Orion flashing guns"* (green light: mixture of sulfur, fine magnesium/aluminium pyroflakes, and barium nitrate) date back to 1898, the mechanisms involved have remained unclear until today.[9] A short historical review of developed formulations as well as a summary of the assumed underlying phenomena is given by Corbel *et al*.[8] Wasmann, Krone, and Shimizu did a lot of work trying to explain and solve the mechanism in the past, whereas our focus was on replacing toxic materials.[10] In addition to the previously mentioned environmentally critical compounds, potassium dichromate is often applied to coat magnesium (the fuel in such formulations) and prevent the reaction with ammonium perchlorate.[10c, 11] It is also hypothesized that there is a regulating power on the flash frequency and improvement to their sharpness.[12] According to the European regulation law REACH (Registration, Evaluation, Authorization and Restriction of Chemicals), potassium dichromate is a substance of very high concern due to the high toxicity and correlated long-term effects.[13] It may cause genetic defects and cancer, damage fertility/unborn children, damage organs through prolonged or repeated exposure and is very toxic to aquatic life.

To tackle the above-described environmental and health concerns arising from the use of perchlorates, heavy metals, and potassium dichromate, we developed several new environmentally benign yellow strobe formulations based on sodium nitrate. We took the previously reported red strobe formulations based on lithium nitrate by Glück *et al.* as a starting point.[7] These new formulations contain no halogen source, which eliminates the risk of highly carcinogenic polychlorinated aromatic compounds such as polychlorinated dibenzodioxins (PCDDs), polychlorinated dibenzofurans (PCDFs), and polychlorinated biphenyls (PCBs).[14] We determined the frequencies of the flash reactions and compared the regularity of the flashes to that of a literature-known red strobe formulation based on strontium salts, perchlorate, and potassium dichromate.

In this paper, we present selected literature-known strobe formulations and compare them to the newly developed yellow strobe formulations in terms of components (known toxicity issues of the starting material) and performance values (e.g., frequency range, energetic properties). The potential application in both the military and civilian sectors will be discussed.

Experimental Section

CAUTION! The mixtures described here are potential explosives which are sensitive to environmental stimuli such as impact, friction, heat, and electrostatic discharge. While we encountered no problems in the handling of these materials, appropriate precautions and proper protective measures (safety glasses, face shields, leather coats, Kevlar gloves, and ear protectors) should be taken when preparing and manipulating these materials.

Chemicals. The following materials were used: Mg (99%), volume-based particle size in the range of 0.3 > x > 0.0 mm, *Grüssing GmbH*; hexamethylenetetramin (hexamine) (99.5%), *abcr*; NH_4ClO_4 (reagent grade), *Alfa Aesar*; $SrSO_4$ (98%), $K_2Cr_2O_7$, colloidon solution (nitrocellulose solution in Et_2O/EtOH, 4 – 8 wt%), *Sigma-Aldrich*; MgAl (1:1), *Omikron GmbH*; $NaNO_3$ (98%), *Appli Chem*; Epon

813, *Hexion*; Versamid 140, *BASF*. A binder system (50 wt% Epon 813/ 50 wt% Versamid 140) was applied. All chemicals were used as provided without further purification. The literature states a maximum grain size of approximately 100 µm to observe the strobe effect.[10b] However, we observed the strobe effect in our formulations by applying a mixture of different grain sizes covering the range of 300 µm and smaller.

Sample Preparation. All solid materials were weighed out into a mortar. After grinding, the binder solutions were added followed by a curing step. Before the powder was pressed into a cylindrical shape, the powder was ground again. For details regarding the sample preparation, chemicals and Mg grain sizes/shapes, see the Supporting Information (Table S1, Figures S1 – S3).

Results and Discussion

Ingredients of Existing and New Yellow Strobe Formulations. A pyrotechnical formulation consists of an oxidizer, fuel, colorant (e.g., $Ba(NO_3)_2$, $SrSO_4$, Na_2SO_4), and sometimes additives to adjust the burning behavior. Typical applied oxidizers are potassium and ammonium perchlorate as well as nitrates (Table 1). The choice of fuel has a big influence on the resulting burning temperature. For this reason, metal fuels such as magnesium or magnalium are applied if high burning temperatures are desired. Other options for lower burning temperatures are compounds such as sulfur, sugar, hexamine, 5-aminotetrazole, or nitrocellulose. Antimony sulfide (Sb_2S_3) may also act as a fuel; however, it is often used in flash formulations to promote the detonation inclination.[10d] The application of Sb_2S_3 is alarming. There is limited evidence for the carcinogenity of this compound, which makes it a suitable candidate for replacement.[15]

Table 1. Selected Literature-Known Strobe Compositions.[10d]

	ingredient (wt%)		
component	***A***	***B***^{a}	***C***^{a}
Mg (60 mesh, coated with $K_2Cr_2O_7$***)***		*40*	*30*
MgAl (coated with linseed oil)	*12*		
NH_4ClO_4		*50*	*50*
$Ba(NO_3)_2$	*33*		
KNO_3	*7*		

$SrSO_4$				*20*
Na_2SO_4		*10*		
BHC[b]	*11*			
sulfur	*27*			
Sb_2S_3	*5*			
sodium oxalate	*5*			
$K_2Cr_2O_7$ (act as stabilizer)		*5*		*5*

Annotation: a: total amount = 100 wt% + 5 wt% stabilizer = 105 wt%; b: BHC = benzene hexachloride.

The corresponding metal sulfates and sodium oxalate are used as the colorant agent. Benzene hexachloride (BHC) is applied as a HCl source upon ignition. According to Shimizu, it is not as effective as the more commonly used poly (vinyl chloride) (PVC). The benefit of BHC is that it does not disturb the flickering of the flame.[10d] The toxicological effects are immense, since BHC is bioaccumulative and is classified by the International Research Agency on Cancer (IARC) and the EPA as a probable human carcinogen.[16] The toxicological and environmental effects of potassium dichromate were already explained in the Introduction. A combination of Epon 813/Versamid 140 was applied as the chlorine-free two-component binder system (Table 2). Sodium nitrate might be used as both an oxidizer and a colorant agent for yellow light.

Table 2. Formulations-Based on $NaNO_3$.

	ingredient (wt%)						
component	**1[a]**	**2**	**3**	**4**	**5**	**6**	**7**
$NaNO_3$	51	51	51	51	51	51	47
Mg	12	23	15	12	15	12	21
hexamine	33	22	30	33	30	33	28
Epon 813/ Versamid 140 (1:1)	4	4					
NC (mL)			1	1	2	2	2

Annotation: measured for 1g pellet; a = no constant burning, NC solution = 4 – 8 wt% in Et_2O/EtOH.

Comparison of the Observed Regularity and Sharpness of the Flashes. Corbel *et al.* reported that the strobe effect of formulation **C** was good with regard to the regularity and sharpness of the flashes.[17] The recorded frequency measurement is shown in Figure 1. The spectrum was recorded with a spectrometer maximum scan rate of 1 scan/ms (for details regarding the experimental setup, measurement procedure, and optical emission spectroscopy, please see the Supporting Information). In general, we observed a good separation of the flashes, which is indicated by an intensity value of 0 before the flash reaction (local intensity maximum) and after each local maximum for a series of events. Of the tested formulations by Corbel et al., formulation **C** was reported to be within the best series. Examples of worse peak separation are given in the Supporting Information (Figures S2 and S4).

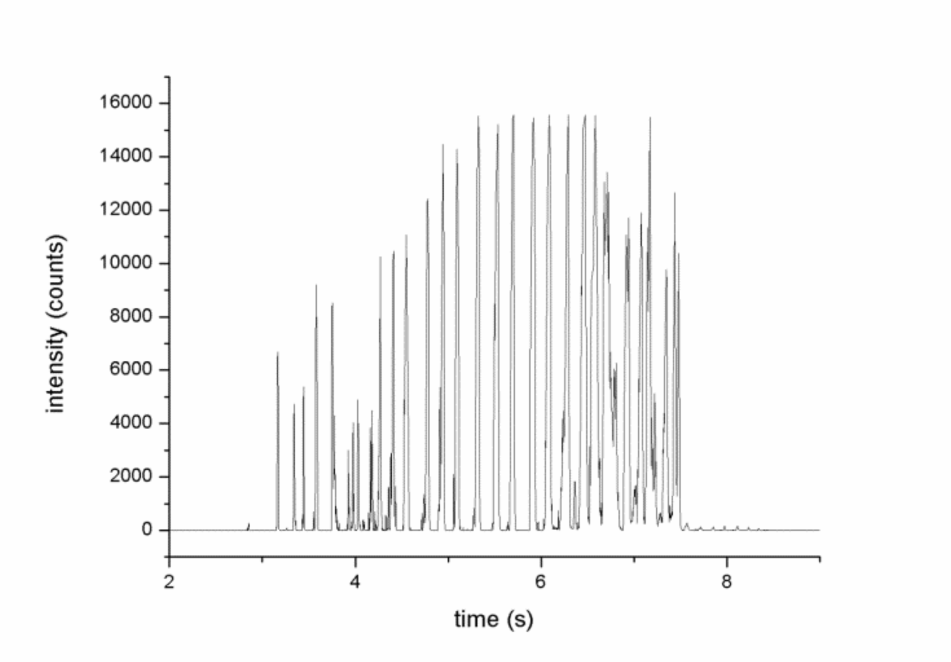

Figure 1. Frequency measurement (1 ms/scan) of formulation **C**.

The recorded frequency spectrum of formulation **4** (Figure 2) looks similar when compared to that of formulation **C**. The regularity of the single flash`s maximum intensity looks similar, whereas a difference is observed for the peak separation. Approximately halfway through the burning, we were able to observe smaller, broad peaks between two peaks with high intensity (between 27 and 35 s). The number of these small peaks is significantly higher in formulation **4** compared to formulation **C**. A high scan rate (5 ms/scan or lower) is essential to reveal the true time period of the flash reaction. Otherwise, two separate flashes might be mistaken for just one broad signal. At the same time, a fast flash reaction (Figure 1) results in a sharp signal which also contributes to a good peak separation. The peaks in formulation **4** are broadened, which provides us more information about the speed of the flash reaction. Since we did not observe the same behavior in formulation **C**, we conclude that the flash reaction of formulation **4** is slower than that of the reference formulation. High-speed video recording (Figure 3) proved this hypothesis. The time period of the bright flash of formulation **4** lasted approximately 290 ms, whereas it was 53 ms in the case of formulation **C** (see the Supporting Information, Figure S9). Another big difference is that formulation **C** shows a dark-phase reaction with absolutely no light output, whereas formulation **4** changes between a small flame (dark phase) and a bigger and brighter flame (flash reaction).

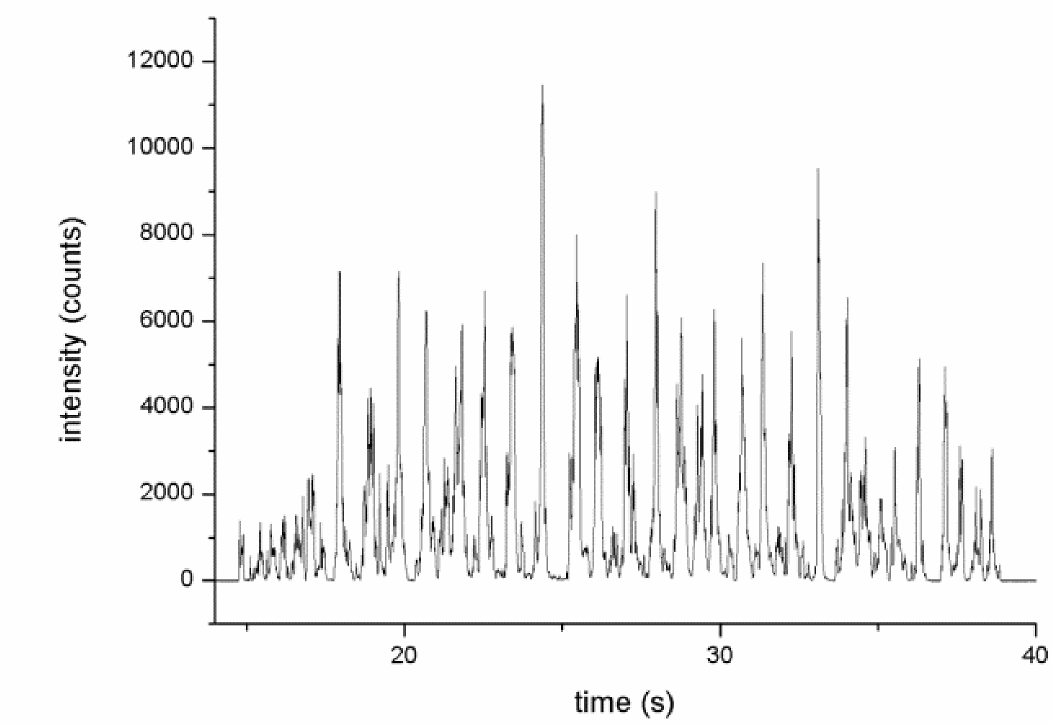

Figure 2. Frequency measurement (1 ms/scan) of formulation **4**.

Our results indicate that the magnesium content directly affects both the burning time and the strobe frequency. Higher magnesium content resulted in a shorter burning time and a higher frequency (Table 3). The effect on the burning time is literature-known and can be easily explained by the heat-conducting properties of metals in general. A higher metal content promotes heat transfer and results in shorter burning times. Within the series of strobe formulations, formulation **2** had the shortest burning time, whereas formulations **4** and **6** had the longest.

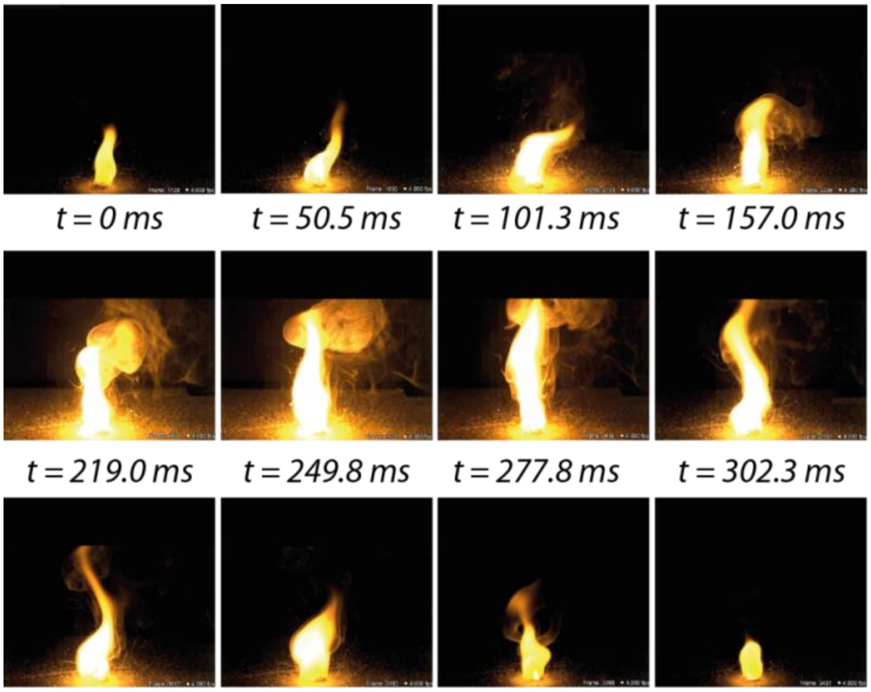
$t = 0$ ms $t = 50.5$ ms $t = 101.3$ ms $t = 157.0$ ms
$t = 219.0$ ms $t = 249.8$ ms $t = 277.8$ ms $t = 302.3$ ms
$t = 322.3$ ms $t = 343.8$ ms $t = 395.0$ ms $t = 425.8$ ms

Figure 3. Time-resolved images of the burning of a strobe pellet (composition **4** in Table 2).

The obtained flare (i.e., constant burning, spectral purity 77 %) formulation **7** had an even shorter burning time, which can be explained by the lack of dark-phase reactions to generate the necessary heat for combustion. At the same time, a faster heat transfer from the top layer of the pellet to the next layer results in shorter dark phases. Since the dark-phase reaction is always followed by a flash-phase reaction in a strobe formulation, the overall flash frequency increases with shorter dark-phase reactions.

Table 3. Properties of Formulations **C** and **1** – **7**.

	BT (s)	DW (nm)	f (1/s)	IS (J)	FS (N)	ESD (J)	T_{onset} (°C)
C	6.0	589-618	5.4				
1	n.d.	583-589		40	>360	1.5	358
2	10.3	583-589	20>x>15	30	>360	1.5	338
3	13.4	583-589	12.1	15	>360	1.0	139
4	19.7	583-589	6.6	15	>360	0.75	137
5	10.3	583-589	11.4	15	>360	0.75	139
6	19.9	583-589	9.7	15	>360	0.65	138
7	7.4	588		10	>360	0.65	139

Annotation: Measured for 1g pellet; n.d. = not determined, pellet showed no constant burning; The spectral purity (SP) of formulation **7** was 77%; BT = burning time; DW = dominant wavelength; f = frequency; IS = impact sensitivity; FS = friction sensitivity; ESD = electric spark discharge sensitivity.

Energetic Properties of Newly Developed Formulations. All newly developed formulations were tested toward their energetic properties regarding impact, friction and shock sensitivity. According to the Bundesanstalt für Materialforschung (BAM) and the U.N. recommendations on the transport of dangerous goods, none of them were sensitive toward friction, which is crucial for both safe manufacturing and handling (see the Supporting Information for the classification ranges). The impact sensitivities of formulations **2** – **7** are categorized as sensitive. Formulation **1** is less sensitive toward impact. The ESD values are in the range of 1.5 – 0.65 J.

Conclusion

An environmentally benign yellow strobe formulation was presented, which according to REACH and the EPA does not contain any substances of very high concern and can therefore serve as a greener alternative to existing formulations. The frequency range covered by these formulations starts at 7 Hz and goes up to more than 15 Hz. We assume that, in the military sector, for training purposes as well as combat actions, the newly developed formulations can remedy the environmental impact while still providing a reliable signal formulation. Smaller variations or inconsistencies in the flash regularity might be neglectable since strobe formulations are not expected to be as accurate as the Morse code. To our knowledge, small deviations in the frequency of the same colored strobe formulation do not transmit different information to the observer. Almost all ingredients involved are applied by a recently published alternative yellow flare formulation by Miklaszewski *et al.*, which might promote synergies in the future, e.g., the same supply chains and application of the same materials.[3b] For the application in the civilian sector, the reduced regularity of flashes might be an issue in big organized fireworks, which are often accompanied by music. Irregular flashing would impede the correct timing from an esthetic point of view. One remaining question is whether it is also possible to change the frequency by changing the magnesium grain size instead of changing the ratio of ingredients. A better understanding of the mechanism involved, in this yellow system and the recently published red strobe system by our group, would strongly reduce the amount of extensive trial and error procedures.

REFERENCES

[1] U. C. Kulshrestha, T. Nageswara Rao, S. Azhaguvel, M. J. Kulshrestha, *Atmos. Environ.* **2004**, *38*, 4421-4425.

[2] Along with beauty, fireworks create a beastly mix of pollutants, http://www.latimes.com/local/la-me-fireworks4-2008jul04-story.html, July 6, 2017.

[3] a)Headquarters, *Field manual 21-60, Visual Signals* (Ed.: Department of the Army), Washington, DC, USA, **1987**; b)E. J. Miklaszewski, J. M. Dilger, C. M. Yamamoto, *ACS Sustainable Chem. Eng.* **2017**, *5*, 936-941.

[4] Health and Ecological Criteria Division, Office of Science and Technology, Office of Water, U.S. Environmental Protection Agency, *Interim Drinking Water Health Advisory for Perchlorate,*, EPA 822-R-08-025*,* Washington, DC, **2008**.

[5] J. S. Brusnahan, A. P. Shaw, J. D. Moretti, W. S. Eck, *Propellants, Explos., Pyrotech.* **2017**, *42*, 62-70.

[6] a)T. M. Klapötke, M. Rusan, J. J. Sabatini, *Angew. Chem., Int. Ed.* **2014**, *53*, 9665-9668; b)J. Glück, T. M. Klapötke, M. Rusan, J. Stierstorfer, *Chem. - Eur. J.* **2014**, *20*, 15947-15960; c)J. J. Sabatini, E.-C. Koch, J. C. Poret, J. D. Moretti, S. M. Harbol, *Angew. Chem. Int. Ed.* **2015**, *54*, 10968-10970; d)D. Juknelevicius, A. Dufter, M. Rusan, T. M. Klapötke, A. Ramanavicius, *Eur.*

J. Inorg. Chem. **2017**, *2017*, 1113-1119; e)J. Glück, T. M. Klapötke, M. Rusan, J. J. Sabatini, J. Stierstorfer, *Angew. Chem., Int. Ed.* **2017**, *56*, 16507.

[7] J. Glück, T. M. Klapötke, J. J. Sabatini, *Chem. Commun.* **2018**, *54*, 821-824.

[8] J. M. L. Corbel, J. N. J. Lingen, J. F. Zevenbergen, O. L. J. Gijzeman, A. Meijerink, *J. Phys. Chem. B* **2012**, *116*, 4967-4975.

[9] A. S. H. Brock, *Pyrotechnics: The History and Art of Fireworks Making*, Daniel O´ Connor, London, UK, **1922**.

[10] a)F.-W. Wasman, *5th Int. Pyrotech. Sem., Proc.*, IPSUSA Seminars, Inc., Vail, CO, USA, July 12-16, **1976**, 643-651; b)U. Krone, *Nico Pyrotechnic*, Nico Pyrotechnic, Germany, **1973**, *DE000002164437A*; c)T. Shimizu, *Pyrotechnica* **1982**, *III*, 5-28; d)T. Shimizu, *Fireworks-The Art Science and Technique*, Pyrotechnica Publications, Austin, Texas (USA), **1996**.

[11] C. Jennings-White, *J. Pyrotech.* **2004**, *20*, 7-16.

[12] M. Davies, *J. Pyrotech.* **2008**, *27*, 42-49.

[13] Hazard classification and labelling of potassium dichromate, https://echa.europa.eu/substance-information/-/substanceinfo/100.029.005, Sept 13, 2017.

[14] W. Christmann, D. Kasiske, K. D. Klöppel, H. Partscht, W. Rotard, *Chemosphere* **1989**, *19*, 387-392.

[15] Toxicity of Antimony Trisulfide, https://toxnet.nlm.nih.gov/cgi-bin/sis/search/a?dbs+hsdb:@term+@DOCNO+1604, Sept 13, 2017.

[16] L. Reed, V. Buchner, P. B. Tchounwou, *Rev. Environ. Health* **2007**, *22*, 213-243.

[17] J. M. L. Corbel, J. N. J. van Lingen, J. F. Zevenbergen, O. L. J. Gijzeman, A. Meijerink, *Angew. Chem. Int. Ed.* **2013**, *52*, 290-303.

Supporting Information

1. Chemicals

Table S1. Chemicals.

Chemicals	Supplier	Purity
$SrSO_4$	Sigma Aldrich	98 %
MgAl (1:1), grain size 100 microns	Omikron GmbH	-
NH_4ClO_4	Alfa Aesar	Reagent grade
Mg	Grüssing GmbH	99 %
Hexamine	Acros organics	99 %
Epon 813	Hexion	-
Versamid 140	Miller-Stephenson	-
Nitrocellulose	Sigma Aldrich	Collodion solution (4 - 8 % ethanol/diethylether)
$K_2Cr_2O_7$	Sigma Aldrich	99 %
$NaNO_3$	AppliChem	98 %

2. Grain size/particle shape of formulations and Mg

We discovered that the grain size after grinding was mainly influenced by the applied magnesium. The supplier of Mg (Grüssing GmbH, 99%) reported the grain size in the range of 60 – 300 µm. This Mg was applied in formulations **1** – **7**. However, manually sieving revealed that even smaller grain sizes were present (Figure S2). For this reason we quantitatively determined the grain size distribution of a 10g Mg sample applying different sieves. In addition, we used REM measurements (Figure S2, S3) to determine the particle shape of the applied Mg. In formulation **C,** Mg (Grüssing GmbH, 99%, 60 mesh) was applied.

a. Mg grain size distribution

The applied Mg was sieved to determine the grain size fractions in the powder.

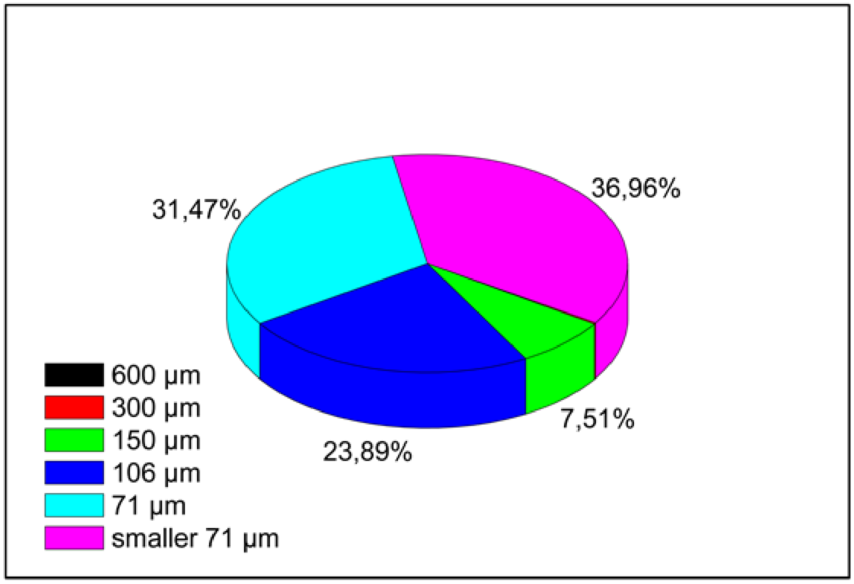

Figure S1. Mg grain size distribution.

Five different sieves with a size of 600 µm, 300 µm, 150 µm, 106 µm, 71 µm were applied (Figure S1). 99.8% of the Mg powder passed through the biggest (600 µm) sieve. The obtained fractions are shown in Figure S1. The color code describes the weight percentage (wt%) of the powder that did not pass through the smaller sieve, e.g. 7.51 wt% are in between 300 – 150 µm. In this case the Mg powder did not pass through the 150 µm sieve. It is notable that 68.43 wt% of the applied Mg powder has a grain size smaller than 106 µm.

b. Mg particle shape

Scanning electron microscopy (SEM) measurements were done to determine the particle size and shape qualitative. The powder can be characterized as a mixture of course ground and fine ground Mg.

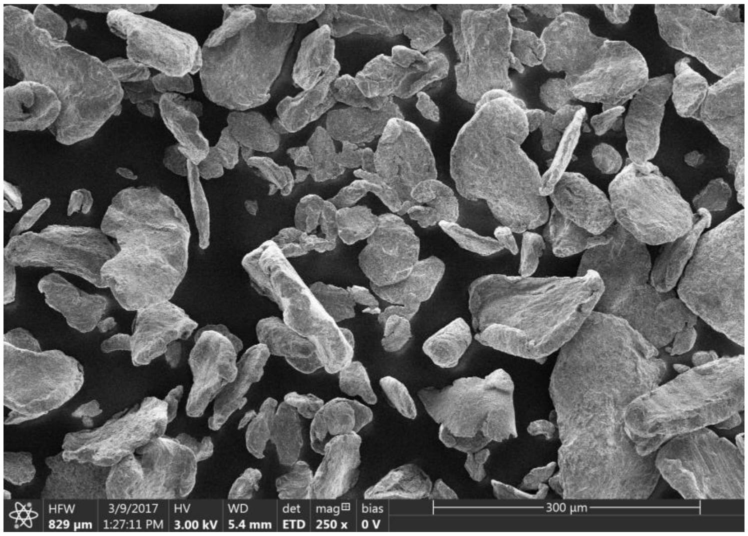

Figure S2. SEM of Mg (Grüssing GmbH, 99%).

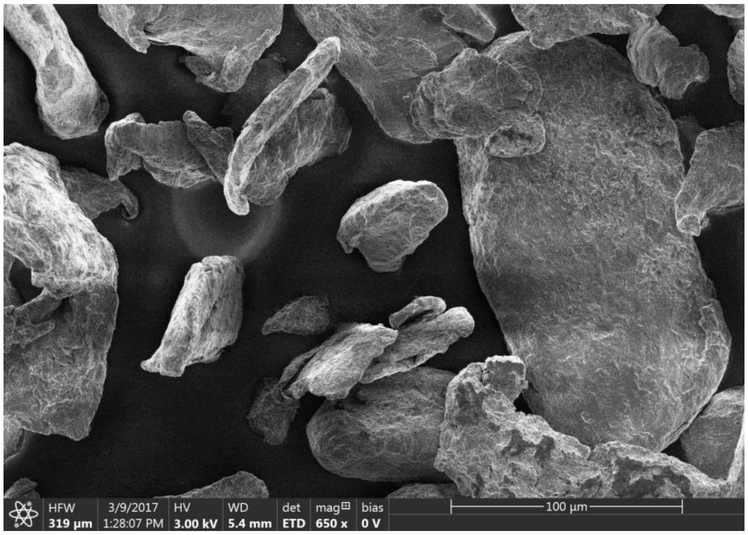

Figure S3. SEM_2 of Mg (Grüssing GmbH, 99%).

3. Sample preparation

The samples were weighed out according to their weight percentages (max. 1 g total) into a mortar. After grinding by hand for 3 min, both the Epon 813 (20 mg/mL) and the Versamid 140 solution (10 mg/mL) in ethyl acetate were added using a syringe. For nitrocellulose, we applied Collodion solution (4 – 8 % in ethanol/diethylether) to the pre-grinded solid materials. The mixture was blended with a spatula every 10 min until the solvent was evaporated. The solid material was stored over night at 70 °C in the drying oven for curing. Before consolidation, the pyrotechnic material was grinded again by hand for 3 min. The formulations were pressed with the aid of a tooling die (inner diameter 12.9 mm) into a cylindrical shape. The formulation powders were pressed at a consolidation dead load of 2 t with a dwell time of 3 s. A torch was used to ignite the pellets.

4. Optical emission spectroscopy

4.1 Dominant wavelength/spectral purity/luminous intensity:

Optical emissive properties were characterized using both an Ocean optics HR2000+ES spectrometer with an ILX511B linear silicon CCD-array detector (range 190 – 1100 nm) and included software/calibration files from Ocean Optics. Spectra were recorded with a detector-sample distance of 1.00 m. The acquisition time for the flare formulation was 20 ms/scan. The dominant wavelength (DW) and spectral purity (SP) were measured based on the 1931 CIE method using illuminant C as the white reference point. Four samples were measured for each formulation and all given values are averaged based on the full burn of the mixture. The controlled burn was filmed with a digital video camera recorder (SONY, DCR-HC37E).

4.2 Frequency measurement:

Frequency measurements were performed using an acquisition time of 1 ms/scan. Dominant wavelengths were measured based on the 1931 CIE method using illuminant C as the white reference point. The range selection for recording a signal was set the range from 560.11 nm – 610.14 nm. Calculation of the frequency was done by detecting the single peaks applying the Origin Pro 9.0 software and calculating the period of time between the single peaks (= flash reactions).

5. High-speed camera

5.1 Setup:

High-speed video recording was performed applying the “SpeedCam Visario G2 1500” by Weinberger AG with the accompanied “Visart 2.2” software package. Following data is taken from the supplier data sheet:

Sensor: High-Speed APS-CMOS Sensor

Active Sensor area: 16.89 x 11.26 mm (W x H)

Active pixel size: 11 µm Square

Image formats: 768 x 512 pixel: up to 4000 frames per seconds

Shutter: Electronic shutter down to 10 µsec.

Dynamic range: color depth to 30 Bit

The applied camera lens was purchased from Sigma (24-70 mm, 2.8 EX DG, Macro, diameter 82 mm). In addition, a Heliopan Filter UV SH-PMC 82 mm was applied.

5.2 High-speed video recording procedure:

The bare pellet was placed in the fume hood and ignited by applying a torch. No prime composition was applied. The distance between the camera and the pellet (same height) was approximately 1 m. Due to the camera settings and applied lense/filter, additional halogen lamps to illuminate the fume hood were applied. A sequence of several seconds was recorded for selected formulations.

6. Energetic properties

The impact and friction sensitivities were determined using a BAM drophammer and a BAM friction tester. The sensitivities of the compounds are indicated according to the U.N. Recommendations on the Transport of Dangerous Goods (+): impact: insensitive >40 J, less sensitive >35 J, sensitive >4 J, very sensitive 4 J; friction: insensitive>360 N, less sensitive=360 N, sensitive >360 N >80 N, very sensitive <80 N, extreme sensitive <10 N. Additionally all formulations were tested for sensitivity towards electrical discharge using an Electric Spark Tester ESD 2010 EN. Decomposition points were measured with an OZM Research DTA 552-Ex Differential Thermal Analyzer. Measurements were performed at a heating rate of 5 °C/min.

7. Recorded spectra

The maximum recorded intensity was set to the value I = 10 (no light emission I = 0). All intenisites are given relative to the highest value I = 10 in following style: **Formulation** (Intensity 1-10).

A comparison of the maximum recorded relative intensities of all constant burning strobe formulations reveals following trend:

C (10.0) > **2** (5.4) > **7** (3.2) > **3** (2.2) > **4** (2.0) > **5** (1.8) > **6** (1.7)

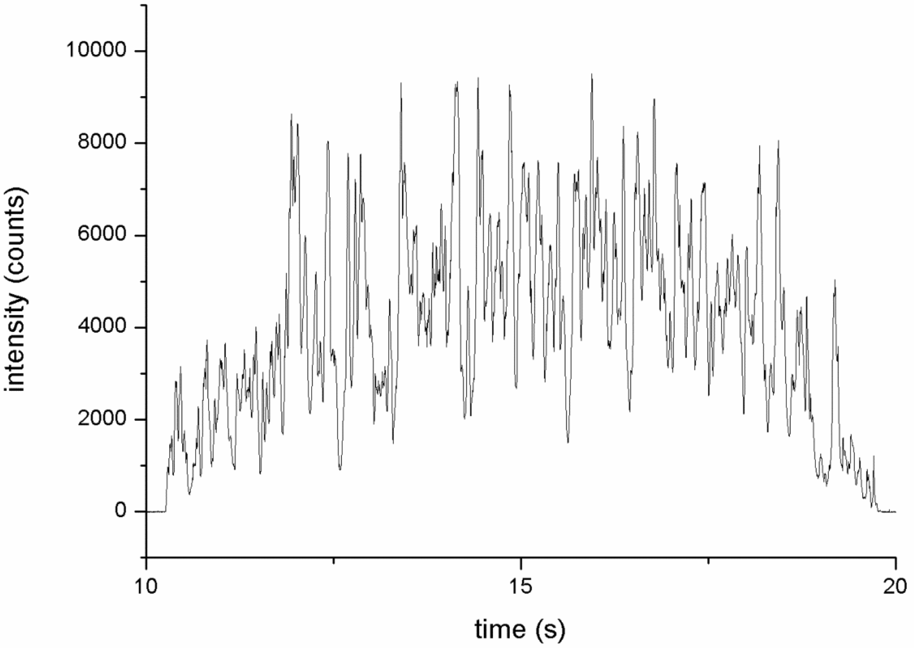

Figure S4. Formulation **3.**

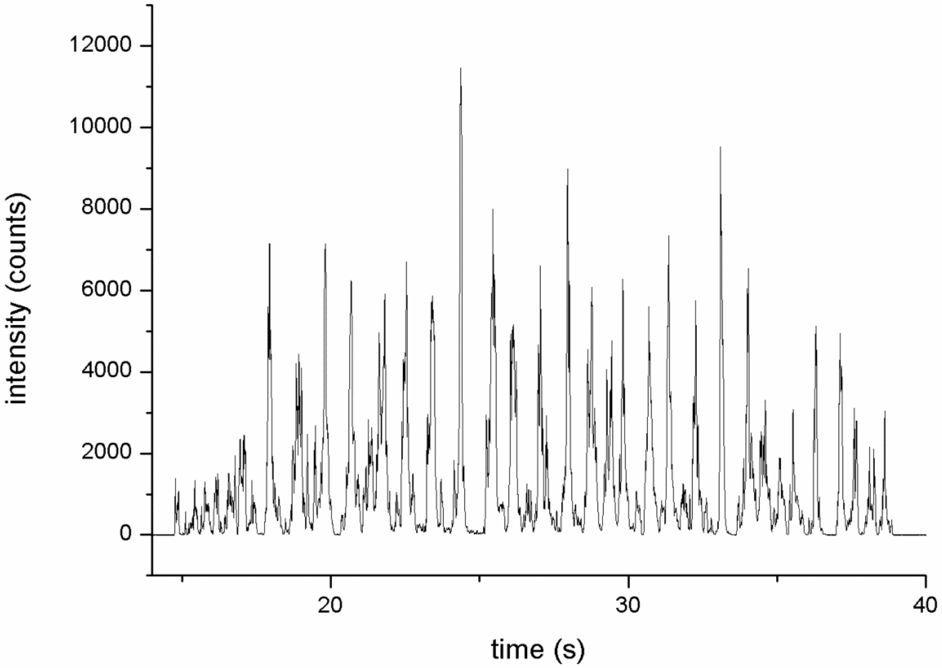

Figure S5. Formulation **4**.

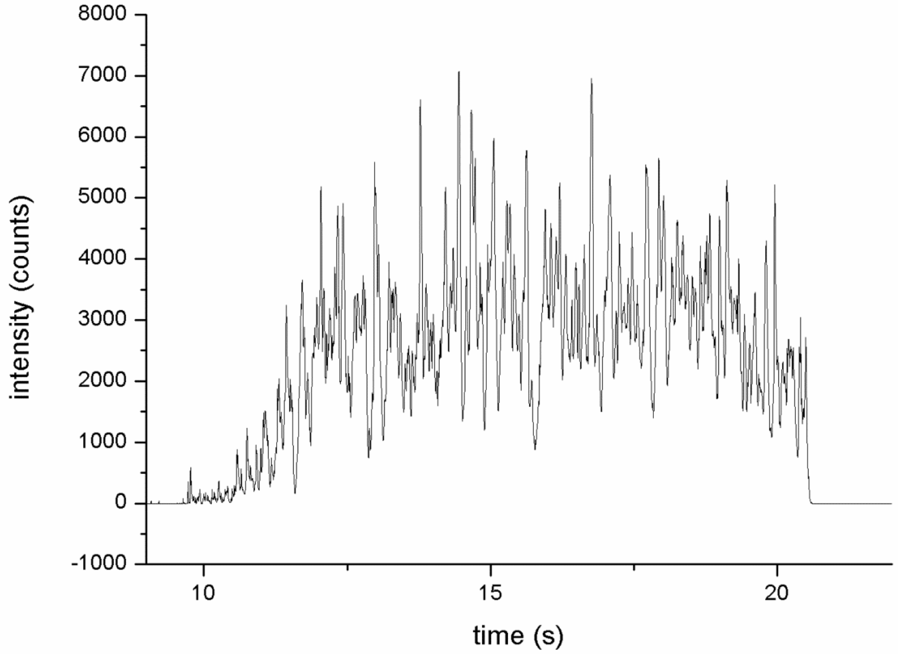

Figure S6. Formulation **5**.

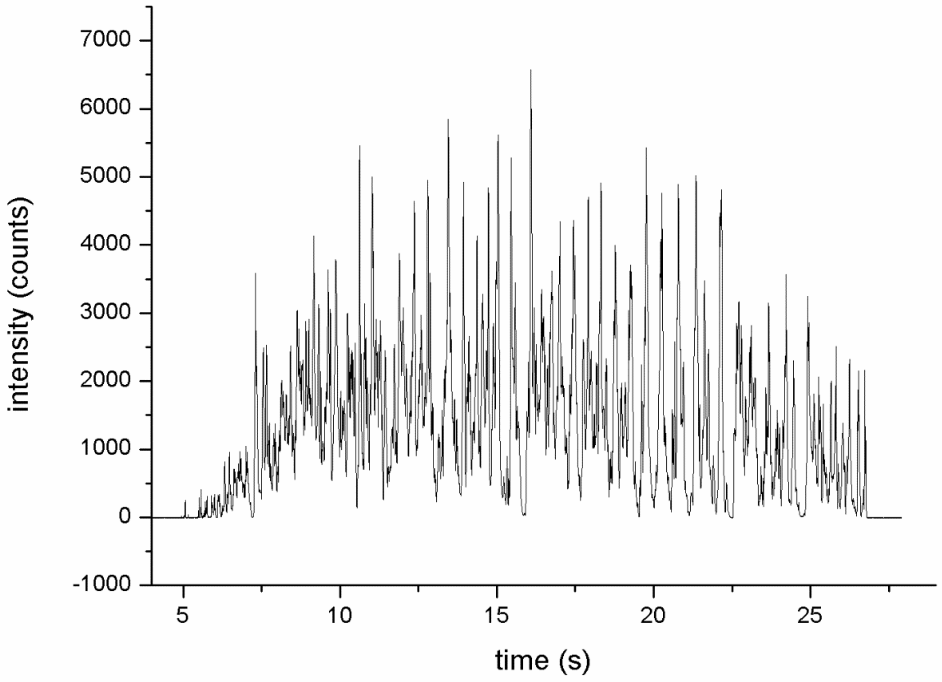

Figure S7. Formulation **6**.

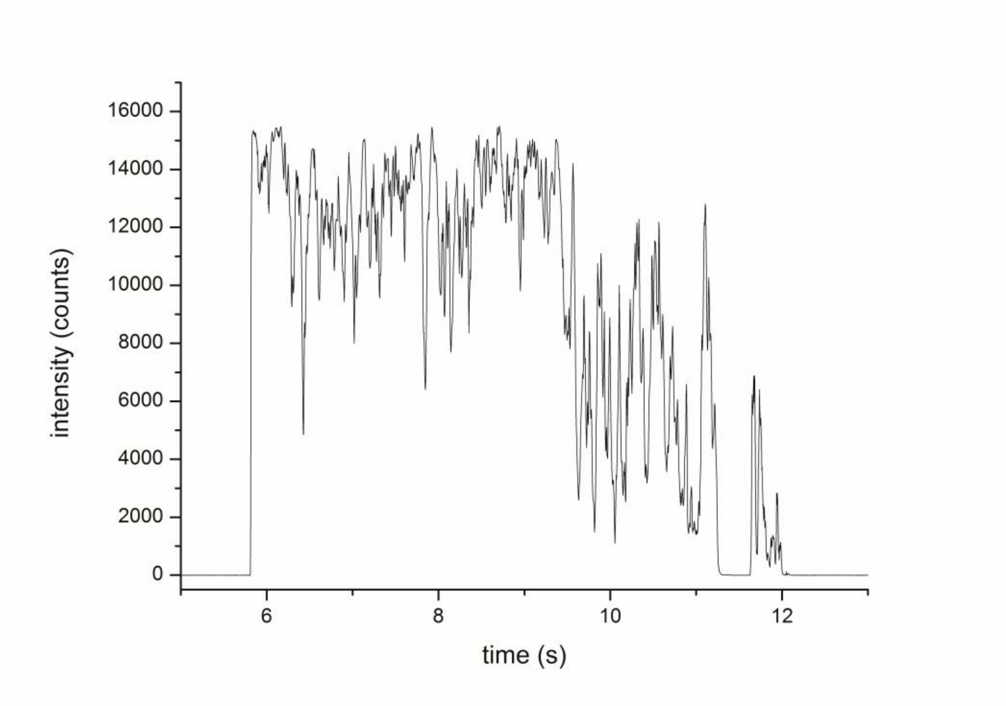

Figure S8. Formulation **2**.

1. Frequency measurement of reference formulation **C**

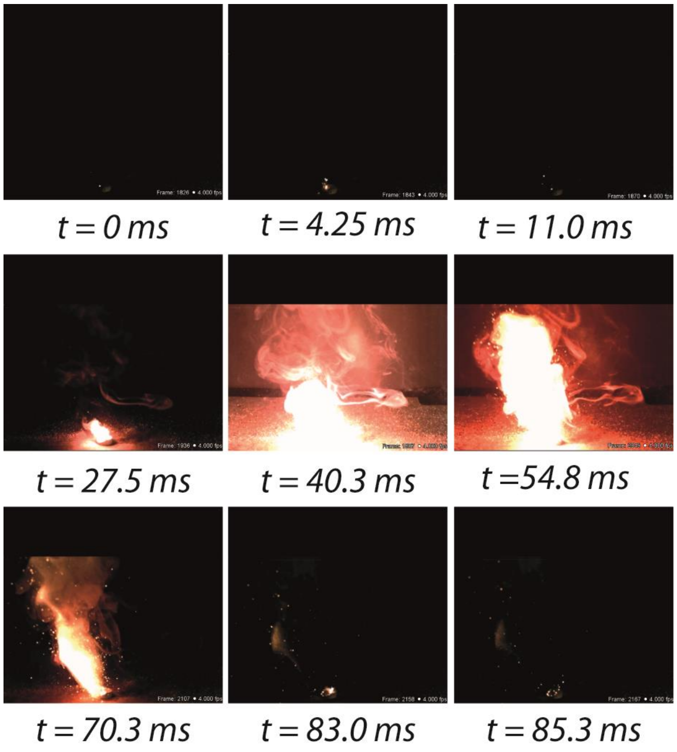

Figure S9. High speed video recording of formulation **C** (4000 frames per seconds).

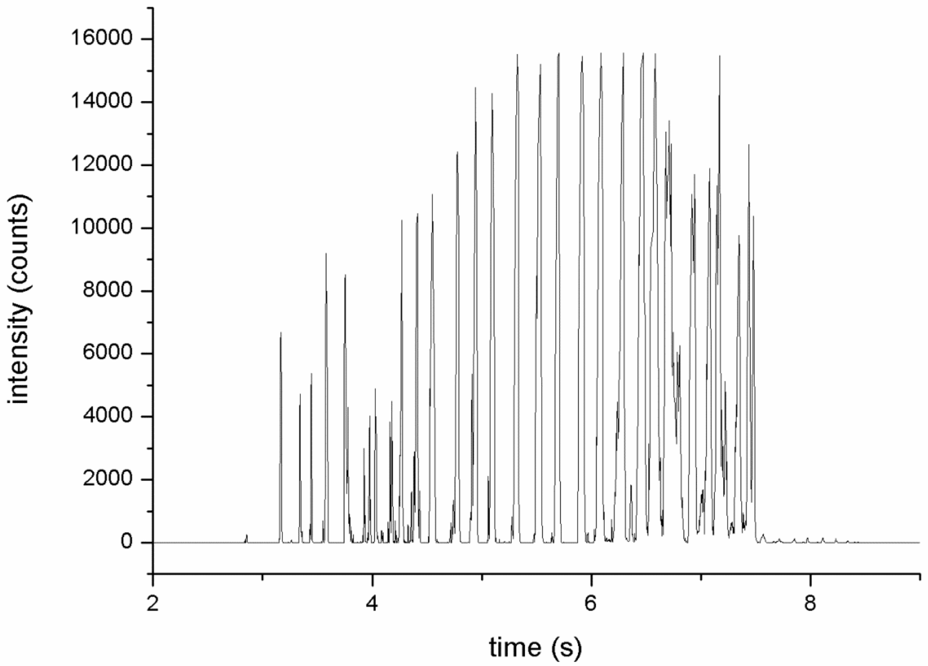

Figure S10. Sr red strobe reference **C**.

Appendix

List of Publications

The contributions are listed chronologically and alphabetically. J. Glück is the first author of all presented contributions.

Publications

[1] J. Glück, T. M. Klapötke, M. Rusan, A. P. Shaw, Improved Efficiency by Adding 5-Aminotetrazole to Anthraquinone-Free New Blue and Green Colored Pyrotechnical Smoke Formulations, *Propellants*, *Explos.*, *Pyrotech*. **2017**, *42*, 131-141.

[2] J. Glück, T. M. Klapötke, A. P. Shaw, Effect of Adding 5-Aminotetrazole to a Modified U.S. Army Terephthalic Acid White Smoke Composition, *Cent. Eur. J. Energ. Mater.* **2017**, *14*, 489-500.

[3] J. Glück, T. M. Klapötke, M. Rusan, J. J. Sabatini, J. Stierstorfer, A Strontium- and Chlorine-Free Pyrotechnic Illuminant of High Color Purity, *Angew. Chemie.*, *Int. Ed.* **2017**, *56*, 16507.

[4] J. Glück, T. M. Klapötke, J. J. Sabatini, A Tunable Chlorine-Free Pyrotechnic System Based on Lithium Nitrate, *Chem. Commun.* **2018**, *54*, 821-824.

[5] J. Glück, T. M. Klapötke, T. Küblböck, Development of a Sustainable Perchlorate-Free Yellow Pyrotechnical Strobe Formulation, *ACS Sustainable Chem. Eng.* **2018**, *6*, 4400-4404.

[6] J. Glück, T. M. Klapötke, T. Küblböck, 5-Amino-1H-Tetrazole-Based Multi-Coloured Smoke Signals Applying the Concept of Fuel Mixes, *New. J. Chem*. **2018**, *42*, 10670-10675.

[7] J. Glück, I. Gospodinov, T. M. Klapötke, J. Stierstorfer, Metal Salts of 3,3'-Diamino-4,4'-Dinitramino-5,5'-Bi-1,2,4-Triazole in Pyrotechnic Compositions, *Published in Z. anorg. allg. Chem.* ***2018,*** Accepted Author Manuscript. DOI: 10.1002/zaac.201800179

Oral Presentations and/or Conference Papers

[1] J. Glück, T. M. Klapötke, M. Rusan, A. P. Shaw, Improved Blue and Green Colored Pyrotechnical Smoke Formulations, *42nd Int. Pyrotech. Sem., Proc.*, IPSUSA Seminars, Inc., Grand Junction, Colorado, USA, July 10–15, **2016**, 143-155.

[2] J. Glück, T. M. Klapötke, M. Rusan, A. P. Shaw, Effect of Adding 5-aminotetrazole to Anthraquinone-Free New Green Colored Pyrotechnical Smoke Formulations, *20th Seminar on New Trends in Research of Energetic Materials (NTREM)*, Pardubice, Czech Republic, April 26–18, **2017**, 144-151.

[3] J. Glück, T. M. Klapötke, J. J. Sabatini, Novel Heavy-Metal and Chlorine-Free Lithium-Based Red-Light-Emitting Pyrotechnics, *4th International Symposium on High Energy Materials (KISHEM-4) & 2017 International Autumn Seminar on Propellants, Explosives and Pyrotechnics (2017-IASPEP)*, Seoul, South Korea, Aug 29–Sept 2, **2017**. Presentation only.

[4] J. Glück, T. M. Klapötke, T. Küblböck, Chlorine-Free Yellow and Red Strobe Formulations, *21st Seminar on New Trends in Research of Energetic Materials (NTREM)*, Pardubice, Czech Republic, April 18–20, **2018**, 134-139.

[5] J. Glück, T. M. Klapötke, T. Küblböck, Multi-Coloured Smoke Signals Applying the Concept of Fuel Mixes, *21st Seminar on New Trends in Research of Energetic Materials (NTREM)*, Pardubice, Czech Republic, April 18–20, **2018**, 183-187. Conference paper only.

[6] J. Glück, T. M. Klapötke, J. J. Sabatini, The Investigation of Lithium-Based Flare and Strobe Formulations, *49th International ICT-Conference,* Karlsruhe, Germany, June 26–29, **2018**, in press. Conference paper only.

[7] J. Glück, T. M. Klapötke, J. J. Sabatini, The Development of Strontium-/Chlorine-Free Flare and Strobe Formulations Based on Lithium, *43rd Int. Pyrotech. Sem., Proc.*, IPSUSA Seminars, Inc., Fort Collins, Colorado, USA, July 8–13, **2018**, in press.

Poster Presentations

[1] J. Glück, T. M. Klapötke, A. P. Shaw, Effect of Adding 5-Aminotetrazole to a Modified U.S. Army Terephthalic Acid White Smoke Composition, *4th International Symposium on High Energy Materials (KISHEM-4) & 2017 International Autumn Seminar on Propellants, Explosives and Pyrotechnics (2017-IASPEP)*, Seoul, South Korea, Aug 29–Sept 2, **2017**.

[2] J. Glück, T. M. Klapötke, J. J. Sabatini, Novel Heavy-Metal and Chlorine-Free Lithium-Based Red-Light-Emitting Pyrotechnics, *4th International Symposium on High Energy Materials (KISHEM-4) & 2017 International Autumn Seminar on Propellants, Explosives and Pyrotechnics (2017-IASPEP)*, Seoul, South Korea, Aug 29–Sept 2, **2017**.

[3] J. Glück, T. M. Klapötke, J. J. Sabatini, The Investigation of Lithium-Based Flare and Strobe Formulations, *49th International ICT-Conference,* Karlsruhe, Germany, June 26–29, **2018**.

Award and Scholarships

[1] *Frank Carver Bursary Award* 2018 sponsored by the International Pyrotechnics Society

[2+3] GDCh Travel Scholarship 2017 and 2018

[4] DAAD Travel Scholarship 2016